© 2019 by Yifan Song. All rights reserved.

# COLD, DENSE QUARK MATTER

BY

YIFAN SONG

DISSERTATION

Submitted in partial fulfillment of the requirements
for the degree of Doctor of Philosophy in Physics
in the Graduate College of the
University of Illinois at Urbana-Champaign, 2019

Urbana, Illinois

Doctoral Committee:

Professor Jessie Shelton, Chair
Professor Gordon Baym, Director of Research
Professor Michael Stone
Professor Douglas H Beck

# Abstract

This thesis discusses the properties of cold quark matter as exists in the core of massive neutron stars, with baryon densities several times of nuclear saturation density, $n_0 \approx 0.16$ fm$^{-3}$, at zero temperature. Specifically, we study effective quark models, the symmetry pattern of different quark matter phases, the collective modes associated with spontaneous chiral symmetry breaking, a possible realization of quark-hadron continuity in the color-flavor locked (CFL) quark superfluid, and the implications of these issues to quark matter equations of state, and thus to neutron star structure including the mass-radius ($M$-$R$) relation.

In Chapter 1, we present a general overview of quark matter described by quantum chromodynamics (QCD) in the context of dense neutron star cores. We discuss the physical motivation for studying quark matter, and how the fundamental symmetry and symmetry breaking patterns of QCD guide the construction of phenomenological quark models – in particular, the Nambu–Jona-Lasinio (NJL) model. We briefly review the modern understanding of the QCD phase diagram studied via such effective quark models, and give an overview of recent progress in constructing quark-hadron crossover equation of states using quark model and nuclear matter models, and how neutron star observations constrain the parameter spaces, thus providing insight into quark matter.

After the introduction, we next focus on details of the NJL model and how it can be made to reflect the QCD symmetries in Chapter 2. We describe quark matter using effective local interactions, and demonstrate how the spontaneous breaking of chiral symmetry is realized through such interactions. We work through a Hubbard-Stratonovich transformation and derive the effective quark-meson theory in a vacuum with chiral condensate, and note its structural connection to the sigma model. We then describe diquark pairing in the NJL model, which breaks chiral symmetry at high density as well. Lastly we explore the problem of meson condensation in quark matter, which is relevant to the both neutron star $M$-$R$ relation and the cooling process; we show that the physics of quark matter meson condensation is very tightly connected to hadronic meson condensation studies, and discuss the criteria of condensation instability caused by quark-meson interactions.

The next part of this thesis, Chapter 3, turns to the issue of connecting the

chiral symmetry breaking in the vacuum and in high density color superconductors – the interplay of chiral and diquark condensates in the effective quark model. By using a schematic NJL model, we solve the phase diagram at zero temperature, and demonstrate a continuous evolution of the Goldstone bosons, i.e., the pions, from their vacuum $\bar{q}q$ form to their diquark $qq$ form. We identify all the collective modes associated with the chiral and diquark condensates and calculate the pion self-energy, deriving a generalized Gell-Mann–Oakes–Renner (GMOR) relation. We thus establish a picture of continuous chiral symmetry breaking from vacuum to high density quark matter, and discuss its implications and connection to the quark-hadron continuity conjecture.

In Chapter 4 we focus on a possible realization of quark-hadron continuity in the color-flavor-locked (CFL) superfluid phase, where the CFL diquark condensates screen color charges of elementary excitations, a novel feature of the $SU(3)$ color-flavor structure. We construct the dressing scheme inspired by the non-linear sigma model, and derive an effective theory in terms of baryons and mesons, a gauge-invariant theory that originally started with quarks and gluons. Such a mapping is a direct realization of the quark hadron continuity in both the fermion sector and the boson sector, suggesting that we may study the properties of CFL quark matter in an entirely gauge-invariant manner at lower energies. The mapping scheme also brings up the relation between the effective baryon-meson Lagrangian's couplings, elementary excitations and collective modes, and those of quark and nuclear matter as a potential research topic, which contributes to our further understanding of the ground state of dense matter at several times $n_0$.

Finally, in Chapter 5 we turn back to the effective quark model and try to connect it to both nuclear matter and the more fundamental QCD. We demonstrate that the explicit single gluon exchange energy can help understanding the magnitude and density dependence of the constrained value of the phenomenological vector repulsion necessary to support massive neutron stars, with a moderate strong coupling constant and gluon mass at some $5n_0$. We also estimate the effect of higher order effects of introducing quark chiral masses and CFL pairing into the quark Green's functions. Our calculation yields an approximately flavor-symmetric vector repulsion that is a monotonous decreasing function of density, which we parametrize for use in future studies of neutron star equations of state. We also discuss the potential connections of this calculation to the concept of quark-hadron continuity, based on the similarity of the quark model to chiral baryon models.

# Acknowledgement

I am indebted to many people for their help and support throughout the years, without which this thesis could not be possible. I must thank Professor Gordon Baym, my thesis advisor, who has provided me with countless guidance, wisdom and inspirations during the years I have spent in Urbana. Gordon is the best teacher I have ever met, not only in terms of physics, but also on many different aspects of life. I am deeply grateful to my families for their continuous support. My parents always make me feel loved and cared about, giving me strength and determination to carry through any hard times I have experienced.

I am grateful to Dr. Phillip Powell and Dr. Toru Kojo, who were once postdocs in Gordon's group; they helped me tremendously in my early years of graduate study. I had many memorable and instructive discussion with them, during which I was exposed to both impressive enthusiasm and extensive knowledge of physics.

I am also very thankful to Professor Tetsuo Hatsuda, who invited me to visit RIKEN in Japan for a wonderful month during which he had several delightful and educational discussions with me.

The research presented in the thesis was supported in part by Natural Science Foundation Grants PHY1305891 and PHY1714042.

# Contents



[1] This section's material is primarily based on the author's published work [8].

# List of Tables

# List of Figures

# Chapter 1

# Introduction

In this thesis we study the properties of cold, dense QCD matter beyond several times nuclear saturation density, $n_0 \sim 0.16\,\mathrm{fm}^{-3}$, where the description of nuclear matter with its rich collections of hadrons is no longer valid. The system should be described in terms of quarks and gluons instead. We focus on four major topics. After introducing quark matter in dense QCD in the context of neutron stars, we first study the Nambu-Jona-Lasinio (NJL) [1, 2] effective quark model, its predicted phases of QCD, and the associated low energy collective modes. Secondly, we study the possibility of a smooth crossover with continuous chiral symmetry breaking from low to high density at zero temperature, and construct a continuous spectrum of generalized Nambu-Goldstone bosons. Thirdly, we discuss a potential realization of the quark-hadron continuity: a possibility of a smooth transition from hadronic matter to quark matter, with the help of the color-flavor-locked (CFL) diquark condensate, and the mapping of QCD into an effective low energy gauge-invariant theory. Finally, we consider the connections of the energy density from effective fermion-fermion vector repulsions between nuclear matter, NJL quark matter and QCD matter, which improves our understanding of the effective NJL quark model via gluon exchange.

We devote this Chapter to introducing the general background relevant to the research topics presented in this thesis. The principal research reported throughout Chapters 2 to 5 is organized as follows.

Chapter 2 includes a instructive review of spontaneous chiral symmetry breaking realized in the NJL model via local quark interactions at mean field in the absence of diquark pairing, and the identification of the Nambu-Goldstone (NG) bosons as emergent collective modes. This review contains the chiral condensation in NJL at mean field and the mapping of the Hubbard-Stratonovich transformed NJL model into a linear sigma model via renormalization, after which the NG bosons appear as elementary degrees of freedom coupled to the quarks. From this coupling we calculate the self-energy of the pions; in particular, we find that the pion self-energy match the form of s- and p-wave interaction energies of pions and nucleons, suggesting that the NG boson sector of chirally broken quark matter is qualitatively identical to the nuclear matter. If no first-order phase transition exists between hadronic matter and quark matter, one

can expect the possible meson condensates from both phases to smoothly connect. At the end of the Chapter we show, in the context of quark matter, the identification of pionic modes from the meson inverse propagator dressed by pion-quark self-energies and the onset condition of a meson condensation, using methods from similar studies of nuclear matter pion condensation [3].

Chapter 3 addresses the physics of diquark pairing introduced at high density, which plays a major role in quark matter chiral symmetry breaking. A brief review of diquark pairing described by NJL at mean field is given in Sec. 3.1. In Sec. 3.2, we apply a single color, single flavor $N_f = N_c = 1$ schematic NJL model to study the chiral symmetry breaking due to the simultaneous existence of chiral and diquark condensates, and how their interplay determines the mass, decay constant and coupling with the quarks of the NG boson – the generalized pion. After identifying the collective modes of the system, we demonstrate how the vacuum pion, resulting from $\bar{q}q$ chiral condensate, and the diquark pion, resulting from $qq$ diquark condensate, form linearly independent combinations, yielding the generalized pion and its unstable massive partner. We then derive a generalized matrix form of the Gell-Mann–Oakes–Renner (GMOR) [4] relation, expressing the pion mass matrix in powers of the current (bare) quark mass $m_q$. A continuous chiral symmetry breaking picture is obtained: as the system smoothly transforms from the chirally broken vacuum to a high density color superfluid, the generalized pion exhibits a continuous variation of its masses, decay constants and coupling with the quarks. We conclude that the NG boson sector in quark matter can well support the quark-hadron continuity.

Afterwards, in Sec. 3.3 and 3.4, we address the problem of calculating more complicated GMOR relations in realistic quark models with $N_f, N_c > 1$. Firstly in Sec. 3.4, we study the problem of calculating the inverse propagators of the mesons self-consistently, using the method developed in Ref. [5] and [6]. Then in Sec. 3.4, we develop a formalism of perturbing the meson's inverse propagators by vertex insertions into quark loop diagrams in order to derive the desired GMOR relations, illustrated with a simple $N_f = N_c = 1$ example; the detailed procedure of applying this formalism to realistic models is summarized at the end of the section.

We turn to the general theory of quarks and gluons in color-flavor-locked (CFL) superfluid phase in Chapter 4, and consider the quark-hadron continuity from a more elementary QCD perspective. Based on the observation that the CFL diquark condensates can screen color charges of elementary excitations (a novel feature of the $SU(3)$ color-flavor structure), we generalize a diquark-dressing scheme from Ref. [7] to transform both quarks and gluons into color-singlet "baryons" and "mesons," mapping QCD into an effective gauge-invariant theory. The construction of this mapping is similar to that of baryon-meson chiral Lagrangians in the study of hadrons. We argue that such a mapping is a direct realization of the quark hadron continuity in both the fermion sector and the boson sector, suggesting that we may study the properties of CFL

quark matter in an entirely gauge-invariant manner at some energy scale. We then open questions regarding the relation between the effective baryon-meson Lagrangian's couplings, elementary excitations and collective modes, and those of quark and nuclear matter; such research topics may help to advance our understanding of how hadrons turn into quark matter at neutron star core density.

In Chapter 5 we return to the NJL quark model, and try to understand the effective quark-quark interactions from the underlying QCD. In particular, we calculate explicit single gluon exchange between quarks in the vector channel, and find that with non-perturbative massive gluon propagators and a moderate strong coupling $\alpha_s$, an effective vector repulsion between quarks strong enough to support two-solar-mass neutron stars can be obtained. We then estimate the effect of higher order effects of introducing quark chiral masses and CFL pairing into the quark Green's functions, and arrive at a flavor-symmetric (to a good approximation) vector repulsion which is a monotonous decreasing function of density. We then propose a specific parametrization of a density dependent vector repulsion for use in future studies of neutron star equations of state. Finally, we discuss the potential connections of this calculation to quark-hadron continuity, based on the similarity of the quark model to chiral baryon-meson models.

Section 3.2 of Chapter 3 and the entire Chapter 5 are based on the author's published work [8] and [9], the latter yet to be published at the time of submission of this thesis.

## 1.1 Cold, dense quark matter: low energy QCD beyond hadrons

QCD is the fundamental theory underlying the strong interaction, which governs the behavior and interactions of the rich collection of hadrons such as protons, neutrons, hyperons, and mesons found in nature. One of its great discoveries is the fact that hadrons are not elementary particles, but composite states made of more basic degrees of freedom – quarks, which come in different flavors, colors and fractional charges, and gluons, which are non-abelian gauge bosons coupled to the $SU(3)$ color charges of quarks. However, due to confinement, one can never isolate colored quarks out of color-neutral nuclear matter; all hadrons are strictly color singlets, and any attempt to isolate color charges will only result in pair production of quarks and antiquarks that immediately neutralize the colors of both the isolated target and the mother medium. This confinement phenomenon forces us to study strong interactions only as many-body systems.

Hadronic matter, being the phase of QCD at low energy scales, can be well described in terms of hadronic degrees of freedom; interactions between baryons are mediated by meson exchanges. The theory of hadrons is an effective theory

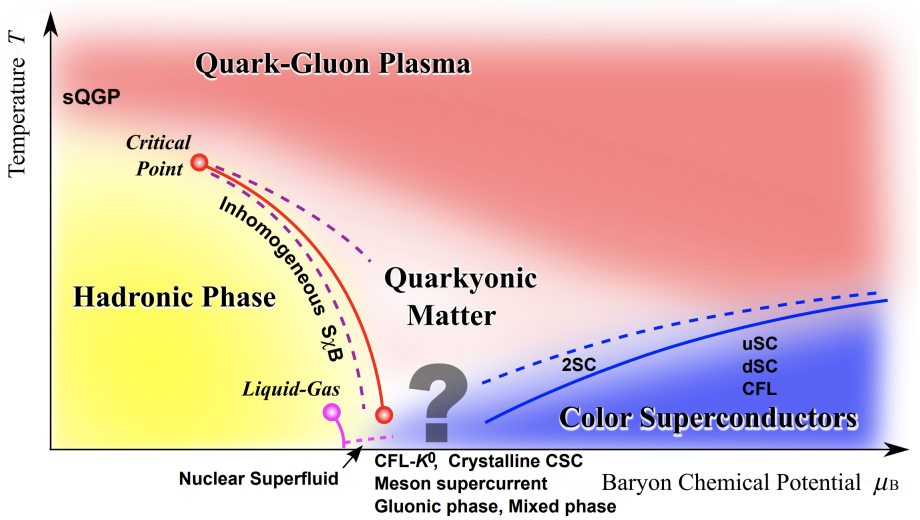


Figure 1.1: Conjectured QCD phase diagram in the temperature ($T$) – baryon chemical potential ($\mu_B$) plane, adopted from Reference [51]. In the high-$T$ limit, the matter is a hot, deconfined quark-gluon plasma (QGP), which can be studied in heavy ion collisions and lattice simulations. In the high-$\mu_B$ direction, i.e., dense quark matter, there is great uncertainty in the intermediate (gray) density region, with many different possible color superfluid and meson condensation phases. In ultrahigh density, the quark matter forms a color-flavor locked (CFL) superconductor via diquark pairing, a unique feature for $N_f = N_c = 3$.

of QCD, where the dynamics of quarks and gluons (and in particular, how they determine the QCD ground state properties) are not manifestly visible. The situation changes as the density rises above $\sim 2n_0$: nucleons begin to severely overlap and percolate, and there is no spatial separation inhibiting quarks from hopping from one nucleon into another. At this point, the hadronic description faces not only the issue of three or larger N-body forces becoming more important – which makes the system untraceable in terms of its interactions – but also loses its basic validity, since the quark and gluon wave functions are no longer constrained within individual hadrons [10]. In such a case, the proper degrees of freedom change to quarks and gluons, and their many-body properties become manifest.

The phases of QCD in terms of quarks and gluons are extremely rich and extensive in the temperature-baryon chemical potential ($T-\mu_B$) plane, schematically shown in Fig. 1.1. Since QCD likely becomes weakly coupling only after $\sim 100n_0$, the quark matter that forms at a few times of $n_0$ (corresponding to the area with gray question mark in Fig. 1.1) is still strongly correlated, non-perturbative and highly non-trivial. Understanding this regime has remained very challenging in modern physics, both theoretically and experimentally.

From the theory perspective, the coupling constant for the strong interaction, $\alpha_s$, is likely at least of order unity at such densities, making perturbation theories powerless in resolving the low energy excitations [11]; many fundamental char-

acteristics of the QCD ground state, such as confinement, spontaneous chiral symmetry breaking and color superconductivity are inherently non-perturbative phenomena. Only at very high energy scale, where the strong coupling $\alpha_s$ becomes weak due to asymptotic freedom, can one study QCD perturbatively, using techniques similar to those from perturbative quantum electrodynamics (QED). Computation-wise, the simulations of QCD on a discretized space-time grid, known as the lattice QCD, can only be employed at high temperature and zero density regime; the (in)famous fermion sign problem [12, 13], which prohibits the application of lattice QCD to dense quark matter. At present, only some reduced models of QCD (such as two-color, commonly denoted "$QC_2D$") support lattice calculations at finite density [11], but their results are at most suggestive for three colors.

From the experiment perspective, it is only possible to recreate high temperature QCD in a controlled laboratory environment at the moment, in the form of ultrarelativistic heavy ion collisions [14]. Such collisions involves the smashing of two counter-propagating heavy ion beams accelerated to near the speed of light, provoking high momentum transfer between quarks and gluons forming the traveling nucleons, which provides important information on high temperature QCD. However, despite nucleons being naturally part of the QCD ground state at finite density, the probe of ground state itself from these collision experiments is very limited, since the process is not under strict thermodynamic equilibrium; the temporarily dense region in the collision center expands rapidly, and the debris quickly turns back into hadrons again while escaping.

As a result, the only realistic access to cold, dense quark matter is from compact astrophysical objects – neutron stars. Neutron stars are supernova remnants from one to above two solar masses and with typical radii of a dozen kilometers; their compactness suggests a core density that can reach beyond several $n_0$, where nucleons would be squeezed deeply into each other, forming matter positively beyond a hadronic description. Such a large density, combined with the relatively low temperature resulting from cooling, makes neutron stars excellent probes of cold, dense QCD; observations of e.g., the neutron star mass-radius relationship, the cooling history and the maximum neutron star mass before collapse into blackholes provide constraints on both the ground state and the transport properties. In particular, modern observation of neutron stars with masses close to or even exceeding two solar masses (e.g. J1614-2230 [15] at $1.928 \pm 0.017 M_\odot$, J0348+0432 [16] at $1.97 \pm 0.04 M_\odot$, and more recently PSR J0740+6620 [17] at $2.17 \pm 0.1 M_\odot$) indicates the existence of stiff, dense cores beyond $\sim 5 n_0$, which can be explained by quark matter with reasonably strong repulsive forces, even with strangeness.[1]

[1] The appearance of strangeness in nuclear matter in the form of hyperons, on the other hand, faces severe softening issues due to the development of additional degrees of freedom, making nuclear matter unlikely to support two solar mass neutron stars on their own, known as the hyperon puzzle [18].

## 1.2 Phenomenological quark models

Effective quark models without gluons – the NJL model in particular – are popular methods to study dense quark matter. Due to the complication of the non-abelian nature of the color $SU(3)$ gauge, gluons are particularly hard to understand at such density due to their self-interactions and thus anti-screening; it is thus instructive to inspect the quark sector alone, since many important symmetries other than the gauge symmetry only involve transformations of the quark field (e.g., chiral symmetry). Such effective quark models are reasonably expected to capture at least the major characteristics of the QCD ground state; the gluon sector is kept implicit, and its physics is supposed to be contained in effective quark-quark interactions and a "bag constant" in the vacuum.

### 1.2.1 Symmetries and symmetry breaking in QCD

The QCD symmetries and their breaking guides the construction of effective quark models. We begin with the QCD Lagrangian,

$$\mathcal{L} = \bar{q}(i\partial\!\!\!/ - \hat{m}_q)q - g\bar{q}\gamma^\mu \frac{\lambda_\alpha}{2} A^\alpha_\mu q - \frac{1}{4} G^\alpha_{\mu\nu} G^{\mu\nu}_\alpha, \tag{1.1}$$

where $q$ is the quark field, $\hat{m}_q$ is the current (bare) quark mass matrix, $\lambda_{\alpha=1,\ldots,8}$ are the $SU(3)$ Gell-Mann matrices normalized to $\mathrm{tr}(\lambda_\alpha \lambda_\beta) = 2\delta_{\alpha\beta}$, $g$ is the gauge coupling (related to strong coupling $\alpha_s$ by $g^2 = 4\pi\alpha_s$), $A^\alpha_\mu$ are the gluon fields, and

$$G^\alpha_{\mu\nu} = \partial_\mu A^\alpha_\nu - \partial_\nu A^\alpha_\mu - g f_{\alpha\beta\gamma} A^\beta_\mu A^\gamma_\nu \tag{1.2}$$

is the gluon field tensor, with $f_{\alpha\beta\gamma}$ being the $SU(3)$ structure constants defined by

$$[\lambda_\alpha, \lambda_\beta] = 2 f_{\alpha\beta\gamma} \lambda_\gamma. \tag{1.3}$$

Aside from local gauge and Lorentz invariance, the Lagrangian (1.1) possesses four additional global symmetries – flavor $SU(3)_{L,R}$ (if in the chiral limit $\hat{m}_q = 0$), baryon number $U(1)_B$, and axial $U(1)_A$, making a total symmetry group

$$SU(3)_L \otimes SU(3)_R \otimes SU(3)_C \otimes U(1)_B \otimes U(1)_A. \tag{1.4}$$

If we include electromagnetic interactions, the additional $U(1)_{EM}$ local gauge invariance plus the photon field are there as well.

The (approximate, due to realistic $\hat{m}_q \neq 0$) chiral symmetry, corresponding to the axial transformations of $SU(3)_{L,R}$, is found to be spontaneously broken in the vacuum by a chiral condensate, $\langle \bar{q}q \rangle \approx -245\ \mathrm{MeV}^3$, confirmed by hadron spectroscopy and lattice QCD [19], and is believed to generate a major part of the effective masses of the quarks (and thus the nucleons). This symmetry

breaking can be summarized as

$$SU(3)_L \otimes SU(3)_R \to SU(3)_V. \tag{1.5}$$

According to Goldstone's theorem, a total of $3^2-1 = 8$ (nearly) massless Nambu-Goldstone (NG) bosons exist in the spectrum, corresponding to the fluctuations of the ground state towards nearby equivalent ground states via transformation of the broken symmetry. These are the pseudoscalar mesons (the pions, kaons, etc.), and are present in hadronic matter as well. In quark matter, they are collective $\bar{q}q$ states similar to physical hadronic mesons, but they couple to quarks manifestly instead of to baryons.

Chiral symmetry can also be spontaneously broken by diquarks, which are BCS pairs of quarks formed by attractions in the color antisymmetric channel [101]. In particular, a special type of diquark pairing, known as the color-flavor-locking (CFL) [20], likely appears in $N_f = N_c = 3$ quark matter at very high density. The CFL pairing is described by the diquark condensate

$$\langle q_a^i q_b^j \rangle = \kappa_{\rm S}(\delta_a^i \delta_b^j + \delta_b^i \delta_a^j) + \kappa_{\rm A}(\delta_a^i \delta_b^j - \delta_b^i \delta_a^j), \tag{1.6}$$

where S and A are shorts for "symmetric" and "antisymmetric." The CFL condensate is not invariant under individual vectorial flavor $SU(3)$ nor color $SU(3)$ global transformations, but under a simultaneous vectorial $SU(3)$ rotation of flavor and color, thus the name. It is also not invariant under axial $SU(3)$ flavor rotations, thus breaking chiral symmetry as well. Overall, the CFL condensate breaks the symmetry to

$$SU(3)_L \otimes SU(3)_R \otimes SU(3)_C \to SU(3)_{\rm CFL}. \tag{1.7}$$

The breaking of the color $SU(3)$ does not generate any NG bosons, but instead gives the gluons effective masses via the Meissner mechanism. As a result, one still ends up with 8 NG bosons, and since it is the axial part of $SU(3)$ that is broken, the eight NG bosons are still pseudoscalar. Thus, in the high density quark matter, chiral symmetry is broken similarly to the vacuum; however, the nature of these NG bosons depends on the specific condensates that break the symmetries, which are $\langle \bar{q}q \rangle$ and/or $\langle qq \rangle$, as we will study in details in Chapter 2 and 3.

The axial $U(1)_A$ symmetry, despite being respected at the classic level, is explicitly broken by quantum (instanton) effects [21, 22]; this breaking is commonly known as the axial anomaly.

### 1.2.2 The NJL model: a brief overview

The general NJL Lagrangian, based on the symmetries of QCD, is schematically [23]

$$\mathcal{L}_{\rm NJL} = \bar{q}(i\partial\!\!\!/ - \hat{m}_q)q + \mathcal{L}_4 + \mathcal{L}_6 \tag{1.8}$$

which describes quarks with effective local four- and six- quark interactions $\mathcal{L}_4$ and $\mathcal{L}_6$. The most straightforward way of constructing an $\mathcal{L}_4$ that respects QCD symmetries is through single-gluon exchange, which yields a color current-current interaction $\sim (\bar{q}\gamma^\mu\lambda_\alpha q)^2$. Then, a re-arrangement of the fermion operators (known as a Fierz transformation) decomposes this interaction into specific Dirac, flavor and color channels. The $\mathcal{L}_6$ interactions are specific to $N_f \geq 3$, and are constructed to explicit break the $U(1)_A$ symmetry in place of the instantons.[2]

The NJL model study of quark matter usually proceeds in the following manner [23]. Taking advantage of the Fierz decomposition, the NJL model is then studied at mean field which realizes different symmetry-breaking condensates $\langle\bar{q}\Gamma q\rangle$ where $\Gamma$ is some Dirac, flavor or color matrix. After a mean field approximation, the Lagrangian reduces to quadratic form in terms of quark fields, which can then be used to compute the thermodynamic potential density $\Omega$ in terms of the mean fields; by minimizing $\Omega$, a set of self-consistent gap equations are obtained, which are then used to determine the values of the mean fields. As the condensates represented by the mean fields characterize different symmetry breaking, this procedure yields the NJL quark matter phase diagram in the $T-\mu$ plane. For a homogeneous system, $\Omega$ is the negative of pressure $\Omega = -P$, giving the equation of state.

In general, the three basic schematic channels considered in $\mathcal{L}_4$ are: $G(\bar{q}q)^2$, the attractive color-singlet scalar-isoscalar channel, describing spontaneous chiral symmetry breaking via the chiral condensate $\langle\bar{q}q\rangle$; $H(qq)(\bar{q}\bar{q})$, the attractive scalar channel of completely flavor-color-antisymmetric diquark pairing; and $g_V(\bar{q}\gamma^\mu q)^2$, the repulsive color-single, vector-isovector channel, necessary to stiffen the equation of state to support massive neutron stars. The coupling constants in the models, $G, H$ and $g_V$, together with the current (bare) quark mass matrix $\hat{m}_q$ and an ultraviolet cutoff $\Lambda_{\rm NJL}$ are the parameters of the model. Among them, $G, \hat{m}_q$ and $\Lambda_{\rm NJL}$ are fixed by fitting to vacuum pion phenomenology. The diquark pairing coupling $H$ and the vector repulsion $g_V$ are kept as variables constrained by neutron star models via their appearances in the equation of state.

[2] Confinement can also be included in the NJL model in the form of a Polyakov loop [24, 25, 26] as the order parameter, which is out of the scope of our current discussion. In general, including the Polyakov loop is unlikely to have significant effects on the the low temperature phase diagram, since lattice simulation indicates a vanishing effective potential for the Polyakov loop at zero temperature [27, 28].

## 1.3 From quark matter to neutron stars: QHC19

At $N_f = N_c = 3$ the NJL model has been recently employed in the construction of a robust state-of-the-art *Q*uark-*H*adron *C*rossover equation of state (QHC19) [10, 29], which can successfully explain over-two-solar-mass neutron stars within reasonable parameter ranges, while also satisfying a number of physical constraints (to be discussed below). This achievement provides profound insight into the effective couplings between quarks, and the results are very useful in future studies of neutron star modeling and quark matter in general.

The NJL model used in QHC19 features the following four-quark interactions in quark-antiquark and quark-quark channels:

$$\begin{aligned}\mathcal{L}_4 &= G\sum_{a=1}^{8}\left[\frac{2}{3}\left(\bar{q}q\right)^2+\left(\bar{q}\tau_a q\right)^2+\frac{2}{3}\left(\bar{q}i\gamma_5 q\right)^2+\left(\bar{q}i\gamma_5\tau_a q\right)^2\right] \\ &\quad +H\sum_{a,A=2,5,7}\left[\left|q^T C i\gamma_5\tau_a\lambda_A q\right|^2+\left|q^T C\tau_a\lambda_A q\right|^2\right]-g_V(\bar{q}\gamma^\mu q)^2; \quad (1.9)\end{aligned}$$

here, $\tau_a, \lambda_A$ are the Gell-Mann matrices corresponding to the $SU(3)$ flavor and color, $\gamma^5 = i\gamma^0\gamma^1\gamma^2\gamma^3$, and $C = i\gamma^2\gamma^0$ is the charge conjugate matrix. These four-quark interactions describe spontaneous chiral symmetry breaking via the $G$ terms and diquark pairing via the $H$ terms, plus a vector repulsion $g_V$. The six-quark interactions $\mathcal{L}_6$ are given by the Kobayashi-Maskawa-'t Hooft (KMT) interactions [30, 22], which described axial anomaly by instanton effects:

$$\begin{aligned}\mathcal{L}_6 &= -K\left[\det\left(\bar{q}(1+\gamma_5)q\right)+\det\left(\bar{q}(1-\gamma_q)q\right)\right] \\ &\quad +K'\left\{\mathrm{tr}\left[\left(d_R^\dagger d_L\right)\phi\right]+h.c.\right\}, \quad (1.10)\end{aligned}$$

where both the trace and the determinant are taken over the flavor indices; here, the composite left/right diquark operators are defined by $d^\dagger_{L,R} = \varepsilon_{ijk}\varepsilon_{abc}q_L^{iaT}Cq_L^{jb}$, and $\phi_{ij} = q^\dagger_{Rj}q_{Li}$. Although the KMT interaction is important in the phase diagram, its effect on the equation of state is very limited, thus does not receive strong constraints from neutron star observations. In the QHC19 study, the following Hatsuda-Kunihiro (HK) [32] parameter set for the NJL model is used:

$$\begin{aligned}&\Lambda_{\mathrm{NJL}} = 631.4\mathrm{MeV},\ m_{u,d} = 5.5\mathrm{MeV},\ m_s = 135.7\mathrm{MeV}, \\ &G = 1.835\Lambda_{\mathrm{NJL}}^{-2},\ K = 9.29\Lambda_{\mathrm{NJL}}^{-5}; \quad (1.11)\end{aligned}$$

the diquark coupling $H$ and vector repulsion $g_V$ are free parameters; $K'$, whose impact on the equation of state is tightly correlated to $H$ and $g_V$. As a result, it is very difficult to constrain the value of $K'$, since there exists a small null space where one can simultaneously vary $H, g_V$ and $K'$ but the resulting equation of state remains almost the same. Furthermore, at several $n_0$ the suppression

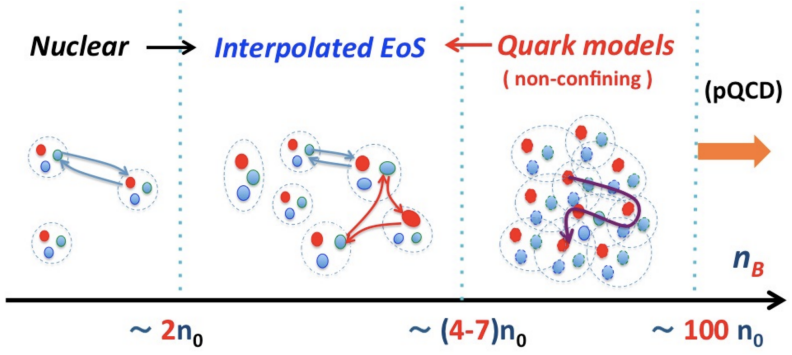


Figure 1.2: Schematic description of a crossover from nuclear (hadronic) matter to quark matter near neutron star core densities $\gtrsim 2n_0$ used in QHC19, adopted from [10]. Below $2n_0$, a nuclear matter equation of state (EoS) is used. Above $\sim 4-7n_0$, the NJL model is used. In between, a polynomial interpolation between the two model EoS is performed, which is made to satisfy thermodynamic and causality constraints.

of instanton effect comes into play, which will likely decrease $K'$ significantly. Considering these factors, the $K'$ interaction is often not manifestly considered in such studies.

In addition to $\mathcal{L}_4$ and $\mathcal{L}_6$, electric and color neutrality are enforced by introducing electric $\mu_Q$ and color $\mu_{3,8}$ chemical potentials,[3] with charged leptons also added to the Lagrangian:

$$\begin{aligned} \mathcal{L}_{\text{neutrality}} &= \mu_Q \left( q^\dagger \hat{Q} q - \sum_{l=e,\mu} \psi_l^\dagger \psi_l \right) + \mu_3 q^\dagger \lambda_3 + \mu_8 q^\dagger \lambda_8 q, \\ \mathcal{L}_{\text{lepton}} &= \bar{\psi}_e (i\partial\!\!\!/ - m_e)\psi_e + \bar{\psi}_\mu (i\partial\!\!\!/ - m_\mu)\psi_\mu. \end{aligned} \tag{1.12}$$

The practical application of the NJL quark matter in QHC19 is schematically summarized in Fig. 1.2. Below $2n_0$, the matter is reliably described by a nuclear matter Togashi et al. equation of state [33]. At densities $\gtrsim 5-7n_0$, the NJL model is used. Acknowledging the uncertainties in the transition from nuclear matter to quark matter, the equation of state in between is given by a polynomial interpolation to $N$-th order in pressure $P$ as a function of baryon chemical potential $\mu$:

$$P(\mu) = \sum_{n=0}^{N} C_n \mu^n, \tag{1.13}$$

where $C_n$ are interpolation constants that depend on equations of state of both nuclear matter and NJL quark matter. Achieving continuity in $P(\mu)$ and its 1st and 2nd order derivative requires $N = 5$ which ensures both baryon number continuity and baryon number compressibility continuity, and is used in practice.

[3] By a proper selection of the color basis in the presence of diquark pairing, only 3 and 8 components of the color density remain possibly non-zero.

In addition, $P(\mu)$ must also satisfy the thermodynamic stability condition

$$\frac{\partial^2 P}{\partial \mu^2} = \frac{\partial n}{\partial \mu} > 0, \tag{1.14}$$

as well as the causality condition where the sound speed $c_s$ cannot exceed the speed of light

$$\frac{c_s^2}{c^2} = \frac{\partial P}{\partial \varepsilon} = \frac{1}{c^2}\frac{\partial \ln \mu}{\partial \ln n} \leq 1; \tag{1.15}$$

here, $\varepsilon = \mu n - P$ is the energy density (assuming zero temperature). Since the $C_n$ depend naturally on the NJL model parameters while the nuclear matter end of the equation of state is well known, these two conditions restricts the NJL free parameters $H$ and $g_V$. After interpolation, a QHC19 equation of state $P(\varepsilon)$ over the whole range up to $\sim 10 n_0$ is obtained, and is ready to be used in neutron star modeling.

To obtain the mass-radius relationship and the density distribution of the neutron stars, one starts with the Tolman-Oppenheimer-Volkov (TOV) [34, 35], which is the static, spherically symmetric solution to Einstein's field equation in general relativity:

$$\frac{\partial P(r)}{\partial r} = -G_N \frac{\rho(r) + P(r)/c^2}{[r - 2G_N m(r)/c^2]r}[m(r) + 4\pi r^3 P(r)/c^2], \tag{1.16}$$

where $G_N$ is Newton's gravitational constant, $m(r) = \int_0^r 4\pi r' \rho(r') dr'$ is the mass within radius $r$, and $\rho(r) = \varepsilon(r)/c^2$ is the mass density. Integrating the TOV equation with the center pressure as the boundary condition yields the mass distribution of the neutron star as a function of $r$, as well as the maximum possible mass of a neutron star.

The QHC equation of state aligns well with the equation of state constraint from neutron star observational data, as shown in Fig. 1.3, with a strong diquark pairing $H = 1.5G$ and a vector repulsion strength $g_V = 0.8G$. In general, $H \sim 1.35 - 1.65G$ and $g_V \sim 0.6 - 1.3G$ can produce neutron stars with above $2M_\odot$, while also satisfying the physical constraints discussed above (see Fig. 1.4 and 1.5). That is, quark matter at $\gtrsim 5n_0$ likely exhibits strong quark-quark correlation and vector repulsion. The phase diagram associated with QHC19 also suggests that quark matter might have already entered the color-flavor-locked phase at $5n_0$ with approximate symmetry in flavor densities, which means $2M_\odot$ neutron stars likely have significant amount of strangeness in their cores. These observations are particularly important to our discussion in all the following Chapters, as we will elaborate with specific contexts in each of them.

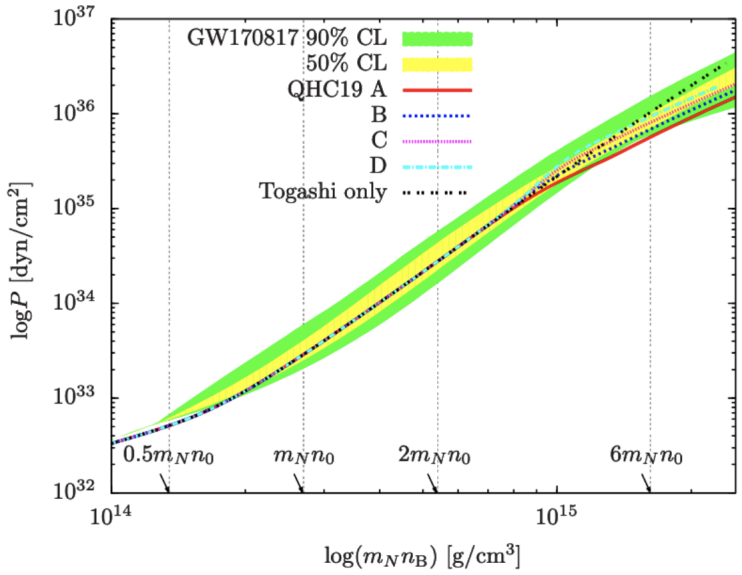


Figure 1.3: The QHC19 compared with $2\sigma$ confidence level in equation of state derived from observed mass-radius relation of neutron stars. The Steiner et. al. region is constructed in Ref. [36], and the Özel et.al. in [37]. Adopted from [29].

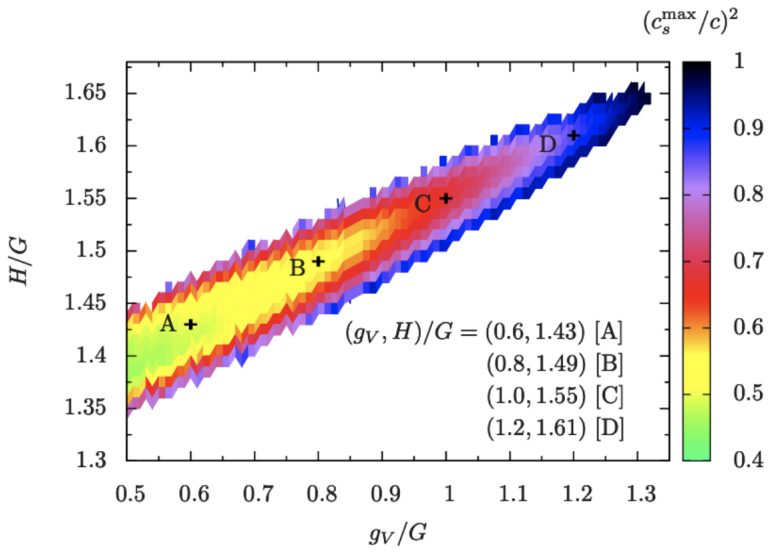


Figure 1.4: The constrained region of $g_V$ and $H$ from maximum neutron star mass. Adopted from [29].

.

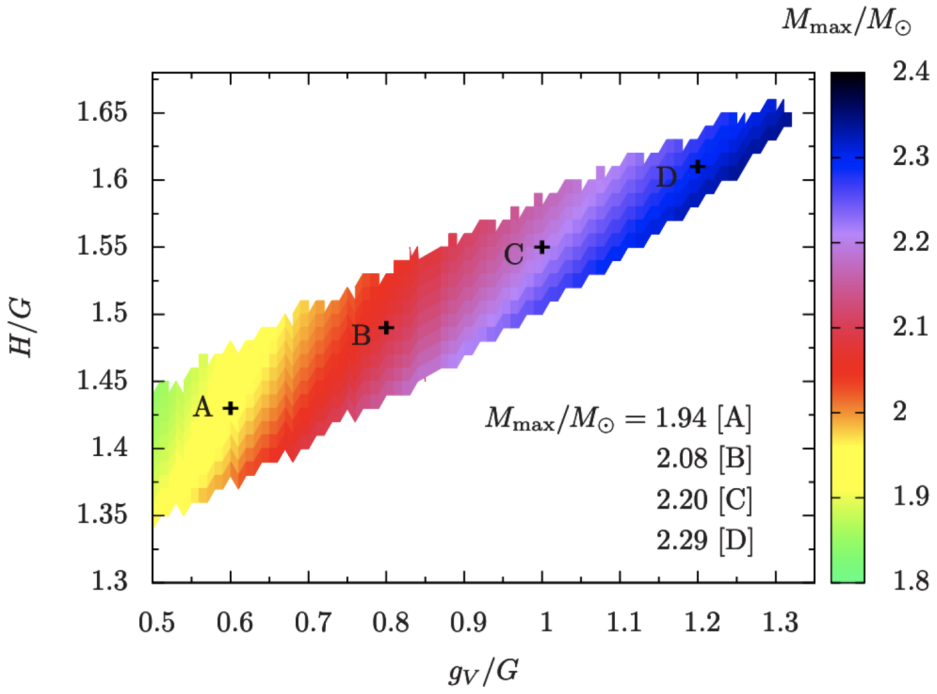


Figure 1.5: The constrained region of $g_V$ and $H$ from causality requirement. Adopted from [29].

.

# Chapter 2

# Chiral symmetry breaking in the NJL model without diquark pairing

In this Chapter we study spontaneous chiral symmetry breaking in the Nambu–Jona-Lasinio (NJL) model in the absence of diquark pairing. We start our discussion with a simple two flavor $N_f = 2$, no-pairing model, demonstrate the realization of chiral symmetry breaking, and compute physical properties of the NG bosons in Sec. 2.1. We demonstrate in Sec. 2.2 that this NJL model, after bosonization with a saddle point expansion, transforms into a linear sigma model, an interacting theory of NG bosons (the pions) with the quarks. We study how these properties may result in Bose-Einstein condensation of the NG bosons, and make the connection to nuclear matter in Sec. 3.3.

## 2.1 $N_f = 2$ NJL model with spontaneous chiral symmetry breaking

### 2.1.1 The Lagrangian, condensates and mean field approximation

In this section we introduce how spontaneous chiral symmetry breaking is realized in a simple NJL model.[1] The simple $N_f = 2, N_c = 3$ NJL model with only a four-quark interaction in the chiral channel is

$$\mathcal{L} = \bar{q}(i\partial\!\!\!/ - m_q + \gamma^0\mu)q + G\left[(\bar{q}q)^2 + \left(\bar{q}i\gamma^5\tau_a q\right)^2\right], \tag{2.1}$$

where $m_q$ is the current (bare) quark mass matrix, $\mu$ the quark chemical potential, $G$ the attractive four-quark coupling strength, and $\tau_{a=1,2,3}$ are generators of the isospin group $SU(2)$, given by Pauli matrices. The Lagrangian (2.1) respects, in the chiral limit $m_q = 0$, the global symmetry group

$$SU(2)_L \otimes SU(2)_R \otimes SU(3)_C \otimes U(1)_B; \tag{2.2}$$

the axial $U(1)$ is explicitly broken.

To study the formation of symmetry breaking condensates, i.e. the chiral condensate in this case, we use the mean field approximation. For any field

[1] For a more comprehensive discussion, see Ref. [23] and the references therein.

operator $s$ (which can be composite), we separate it into

$$s = (s - \langle s \rangle) + \langle s \rangle; \tag{2.3}$$

the quantity inside the bracket corresponds to the fluctuations around the expectation value. When a condensate first forms, $\langle s \rangle \neq 0$, one may treat the fluctuation as small and expand

$$\begin{aligned} s^2 &= [(s - \langle s \rangle) + \langle s \rangle]^2 \\ &= \langle s \rangle^2 + 2\langle s \rangle (s - \langle s \rangle) + (s - \langle s \rangle)^2 \\ &\approx 2\langle s \rangle s - \langle s \rangle^2. \end{aligned} \tag{2.4}$$

In our case, the chirally broken state is characterized by the chiral condensate $\langle \bar{q} q \rangle$. Denoting the real expectation values

$$\langle \bar{q} q \rangle = \sigma, \ \langle \bar{q} i \gamma^5 \tau_i q \rangle = \pi_i, \ i = 1, 2, 3, \tag{2.5}$$

and $\hat{\sigma}, \hat{\pi}_i$ as their corresponding fluctuations, the NJL Lagrangian in mean field is

$$\mathcal{L} = \bar{q} \left( i \gamma^\mu \partial_\mu + 2G\sigma + 2G i \gamma^5 \vec{\tau} \cdot \vec{\pi} \right) q - G \left( \sigma^2 + \vec{\pi}^2 \right). \tag{2.6}$$

The $\pi_i$ condensates in terms of the charged and neutral pions, $\pi^\pm$ and $\pi_0$, are

$$\begin{aligned} \pi &= \frac{1}{\sqrt{2}} (\pi_1 + i\pi_2) = \sqrt{2} i \langle \bar{u} \gamma^5 d \rangle, \ \pi^-; \\ \pi^\dagger &= \frac{1}{\sqrt{2}} (\pi_1 - i\pi_2) = \sqrt{2} i \langle \bar{d} \gamma^5 u \rangle, \ \pi^+; \\ \pi_0 &= \pi_3, \ \pi^0. \end{aligned} \tag{2.7}$$

The chiral and pion condensates are not invariant under chiral transformation, thus breaking the chiral symmetry. Indeed, under an axial $SU(2)$ rotation,

$$\begin{aligned} q &\rightarrow e^{-\frac{1}{2} i \gamma^5 \vec{\tau} \cdot \vec{\theta}} q = \left[ \cos \frac{\theta}{2} - i \gamma^5 \left( \vec{\tau} \cdot \hat{\theta} \right) \sin \frac{\theta}{2} \right] q, \\ \bar{q} &\rightarrow \bar{q} \left[ \cos \frac{\theta}{2} - i \gamma^5 \left( \vec{\tau} \cdot \hat{\theta} \right) \sin \frac{\theta}{2} \right], \end{aligned} \tag{2.8}$$

so

$$\begin{aligned}
\bar{q}q \quad &\rightarrow \quad \bar{q}\left[\cos\frac{\theta}{2} - i\gamma^5\left(\vec{\tau}\cdot\hat{\theta}\right)\sin\frac{\theta}{2}\right]^2 q = \bar{q}\left[\cos\theta - i\gamma^5\left(\vec{\tau}\cdot\hat{\theta}\right)\sin\theta\right] q \\
&= \bar{q}q\cos\theta - \bar{q}i\gamma^5\vec{\tau}q\cdot\hat{\theta}\sin\theta, \\
\bar{q}i\gamma^5&\left(\vec{\tau}\cdot\hat{\theta}\right) q \\
&\rightarrow \bar{q}\left[\cos\frac{\theta}{2} - i\gamma^5\left(\vec{\tau}\cdot\hat{\theta}\right)\sin\frac{\theta}{2}\right] i\gamma^5\left(\vec{\tau}\cdot\hat{\theta}\right)\left[\cos\frac{\theta}{2} - i\gamma^5\left(\vec{\tau}\cdot\hat{\theta}\right)\sin\frac{\theta}{2}\right] q \\
&= \bar{q}i\gamma^5\vec{\tau}q\cdot\hat{\theta}\cos\theta + \bar{q}q\sin\theta; \qquad (2.9)
\end{aligned}$$

therefore

$$\begin{aligned}
\sigma \quad &\rightarrow \quad \sigma\cos\theta - \vec{\pi}\cdot\hat{\theta}\sin\theta, \\
\vec{\pi}\cdot\hat{\theta} \quad &\rightarrow \quad \vec{\pi}\cdot\hat{\theta}\cos\theta + \sigma\sin\theta. \qquad (2.10)
\end{aligned}$$

However, the combination, $\sigma^2 + \vec{\pi}^2$, is invariant under chiral transformation.

When $\vec{\pi} = 0$, the vacuum is in a scalar state since $\sigma$ has positive parity; other states with the same $\sigma^2 + \vec{\pi}^2$ but different $\sigma, \vec{\pi}$ condensates are related to the scalar state and each other via chiral transformations; states with $\vec{\pi} \neq 0$ have pion condensation, and for now they have identical energies as the scalar state.

The mean field Lagrangian (2.6) is quadratic in quark field and thus can be integrated out analytically in the path integral formalism; the term $2G\sigma$ becomes the effective (chiral) mass of the quarks $M = -2G\sigma$. The dressed quark inverse propagator, $\mathcal{G}^{-1}$, is then

$$\mathcal{G}^{-1} = \mathcal{G}_0^{-1} - 2G\sigma, \;\; \mathcal{G}_0^{-1} = i\partial\!\!\!/ + \gamma^0\mu. \qquad (2.11)$$

Further denoting $V(\sigma, \vec{\pi}) = G(\sigma^2 + \vec{\pi})^2$, the generating functional $\mathcal{Z}$ is now

$$\begin{aligned}
\mathcal{Z} \quad &= \quad \int \mathcal{D}(\bar{q}, q) \exp i \int \mathcal{L} d^4x \\
&= \quad \int \mathcal{D}(\bar{q}, q) \exp\left(i \int d^4x \, \bar{q}\mathcal{G}^{-1}q - V\right), \qquad (2.12)
\end{aligned}$$

where the time $x_0$ is integrated over $(0, -i\beta)$, $\beta = 1/T$ being the inverse temperature. This analytic continuation into the imaginary time of the generating functional $\mathcal{Z}$ is the partition function in quantum statistical mechanics; the Fourier transform in the imaginary time is a sum of Matsubara frequencies:

$$\mathcal{G}(t) = \frac{1}{-i\beta}\sum_\nu e^{-i\omega_\nu t}\mathcal{G}(\omega_\nu), \qquad (2.13)$$

where $\omega_\nu = \pi\nu/(-i\beta)$, and $\nu$ runs over integers for bosons, and odd half-integers for fermions. Throughout this thesis, all integrations over the frequency space,

$\int dp_0$, are understood as Matsubara frequency sums, unless stated otherwise.

For simplicity we consider a homogeneous phase where $\sigma(x) = \langle\bar{q}(x)q(x)\rangle = \sigma(0)$. The grand thermodynamic potential density is then

$$\begin{aligned}\Omega &= -\frac{T}{V}\ln\mathcal{Z} = V - \frac{T}{V}\mathrm{tr}\ln\mathcal{G}^{-1} \\ &= V - 2TN_fN_c\int\frac{d^3k}{(2\pi)^3}\left[\ln\left(1+e^{\beta(\epsilon_k-\mu)}\right)+\ln\left(1+e^{-\beta(\epsilon_k-\mu)}\right)\right], \\ \epsilon_k &= \sqrt{k^2+M^2}. \end{aligned} \tag{2.14}$$

The trace "tr" in this context runs over all space-time and quantum numbers. The chiral condensate $\sigma$ is found by minimizing $\omega$ with respect to $\sigma$, i,e. the minimal energy configuration:

$$\frac{\partial\Omega}{\partial\sigma} = 0. \tag{2.15}$$

Since $\sigma$ is directly related to the effective quark mass, this equation is also called the gap equation; this terminology applies to any mean fields. Evaluating (2.15) with (2.14) we find

$$\sigma = 4N_fN_cG\sigma\int\frac{d^3k}{(2\pi)^3}\frac{1-f(\epsilon_k-\mu)-f(\epsilon_k+\mu)}{\epsilon_k}, \tag{2.16}$$

where $f(x) = (1+\exp\beta x)^{-1}$ is the Fermi-Dirac distribution function.

The gap equation (2.16) always has a trivial solution $\sigma = 0$ which corresponds to a chirally invariant ground state. When the chirally broken state – corresponding to a non-trivial solution $\sigma \neq 0$ – exists, the $\sigma = 0$ state becomes metastable; the effective potential of $\sigma$ takes on the famous "Mexican hat" shape (see Fig. 2.1), and the system will have a chirally broken ground state. Since the only dependence in the integral of (2.16) on $\sigma$ is via $M^2 = 4G\sigma^2$, the solutions $\pm|\sigma|$ are degenerate.

When $m_q \neq 0$ explicitly breaks the chiral symmetry, the gap equation (2.15) still yields (2.16), but with the effective quark mass

$$M = -2G\sigma + m_q; \tag{2.17}$$

we can shift $\sigma \to \sigma + m_q/2G$ to absorb $m_q$ to $\sigma$ in the quark energies, but as a trade-off the gap equation (2.16) becomes

$$\begin{aligned}\sigma + \frac{m_q}{2G} &= 4N_fN_cG\sigma\int\frac{d^3k}{(2\pi)^3}\frac{1-f(\epsilon_k-\mu)-f(\epsilon_k+\mu)}{\epsilon_k}, \\ M &= -2G\sigma. \end{aligned} \tag{2.18}$$

In this case $\sigma = 0$ is no longer a solution; thus, the chiral condensate, however small, will always exist in the presence of bare quark masses. In particular, the original trivial solution $\sigma = 0$ will be deformed into $\sigma \sim m_q$. Also, the shifting

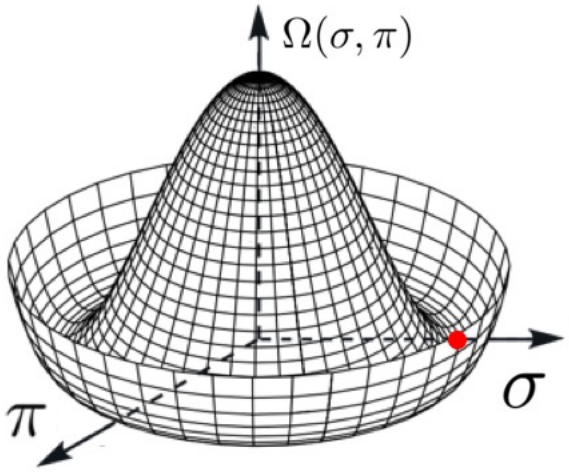


Figure 2.1: The "Mexican hat" potential for the fluctuations in the $\sigma$-$\pi$ plane, typical of systems exhibiting spontaneous symmetry breaking. The red dot corresponds to the scalar state configuration $\pi = 0$.

of the potential term for $\sigma$, $V \sim G\sigma^2 \to G(\sigma + m_q/2G)^2$, implies the negative solution $\sigma < 0$ will be more energetically favorable than the $\sigma > 0$ solution, and is thus the true ground state.

The gap equation (2.15) can be equivalently obtained via a self-consistent equation, where we essentially "re-calculate" the chiral condensate using the mean field quark propagator itself:

$$\langle \bar{q}(0)q(0)\rangle \quad = \quad -i\mathrm{Tr}\ \mathcal{G}(t = 0^+, \boldsymbol{x} = 0) = -i\int_p \mathrm{Tr}\ \mathcal{G}(p), \tag{2.19}$$

and the result is identical. In later Chapters we will use this method to derive gap equations in general, which avoids having to compute the thermodynamic potentials.

### 2.1.2 Pion dispersion relation through quark-antiquark T-matrix

Having reviewed the mean field results of the NJL model in terms of chiral condensates, we now study the spectrum of the pions (the NG bosons) via the quark-antiquark T-matrix.

In the chirally broken state the existence of the pions, the NG bosons, can be demonstrated through the quark-antiquark scattering amplitude. Since the pions are coupled to quark-antiquark pairs, they exist as intermediate states in the T-matrix of quark-antiquark scattering in the right channel. For isospin vector index $a = 1, 2, 3$, the T-matrix corresponding to an incoming state having the same quantum number as $\bar{q}i\gamma_5\tau_a q$ with total momentum $k$ under random

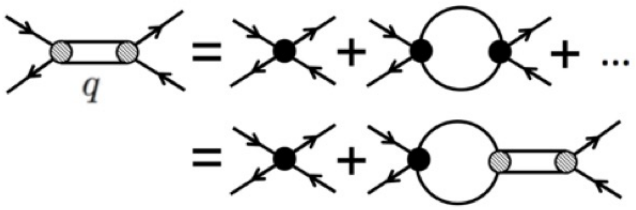


Figure 2.2: Graphical representation of the T-matrix in random phase approximation, corresponding to the bubble chain diagrams: $T_a = 2G + 4GB_aG + \cdots = 2G + 2GB_aT_a$.

phase approximation (RPA) in the NJL model [23] (see Fig. 2.2), is

$$T_a(k^2) = 2G + 2GB_a(k^2)T_a(k^2), \tag{2.20}$$

where the bubble is

$$\begin{aligned} B_a(k^2) &= i\int_p \mathrm{Tr}\left(\mathcal{G}(p)i\gamma_5\tau_a\mathcal{G}(p-k)i\gamma_5\tau_a\right) \\ &= N_fN_c4i\int_p\left(\frac{1}{p^2-M^2} - \frac{\frac{1}{2}k^2}{(p^2-M^2)((p-k)^2-M^2)}\right) \\ &\equiv J_1 + \frac{1}{2}k^2J_2(k^2); \end{aligned} \tag{2.21}$$

here,

$$\begin{aligned} J_1 &= N_fN_c4i\int_p \frac{1}{p^2-M^2}, \\ J_2(k^2) &= -N_fN_c4i\int_p \frac{1}{(p^2-M^2)((p-k)^2-M^2)}; \end{aligned} \tag{2.22}$$

by dimensional arguments one sees that $J_1$ is quadratically ultraviolet divergent, while $J_2$ is logarithmically divergent.

Evaluating the imaginary frequency summation, one can show using the gap equation (2.39) that,

$$J_1 = \frac{1}{2G} - \frac{m_q}{2GM}. \tag{2.23}$$

The poles of $T_a$, equivalently the zeros of

$$T_a^{-1} = \frac{1}{2G} - B_a(k^2) = \frac{1}{2G} - J_1 - \frac{1}{2}k^2 J_2(k^2) \tag{2.24}$$

give the dispersion relations for the pions, as they show up as intermediate bound states. Near the pion poles and in the long wavelength limit, the T-matrix can be parametrized as

$$T_a \approx \frac{-g^2}{k^2 - m_\pi^2}, \tag{2.25}$$

where the residue $g^2$ has the physical meaning of the square of the effective coupling between the pion and the quarks. With this parametrization,

$$\begin{aligned} g^{-2} &= \frac{1}{2}I_2(0) + \mathcal{O}(m_q^2), \\ m_\pi^2 &= \frac{m_q}{GMI_2(0)} + \mathcal{O}(k^2). \end{aligned} \tag{2.26}$$

We have assumed $J_2(k^2)$ only weakly depends on $k$ in the long wavelength limit. In general, $J_2$'s momentum dependence will make $m_\pi^2$ momentum-dependent; such effect corresponds to self-energy modification due to pions interacting with quarks. On the other hand, the pion decay constant $f_\pi$ can be related to the vacuum-to-axial-current transition amplitude of a pion state,

$$ik^\mu f_\pi \delta_{ab} = \langle 0|A_a^\mu|\pi_b(k)\rangle = -ig\int_p \mathrm{Tr}\left[i\gamma_5\tau_a\mathcal{G}(p)\frac{\tau_b}{2}\gamma_\mu\gamma_5\mathcal{G}(p+k)\right], \tag{2.27}$$

where the axial current is $A_\mu^a = \bar{q}\tau_a\gamma_\mu\gamma_5 q/2$. Evaluating the trace, we find

$$f_\pi = \frac{1}{2}MgI_2(k^2); \tag{2.28}$$

combined with Eqs. (2.26), we obtain the Gell-Mann–Oaks–Renner relation at leading order in $m_q$:

$$f_\pi^2 m_\pi^2 = m_q \cdot \frac{M}{2G} + \mathcal{O}(m_q^2) = -m_q\langle\bar{q}q\rangle + \mathcal{O}(m_q^2). \tag{2.29}$$

### 2.1.3 Hubbard-Stratonovich transformation and effective pion theory

We have so far only concerned ourselves with the quarks, and the pions only implicitly through the T-matrix. To derive an effective theory of pions from the quark-only Lagrangian, we need to bosonize the field fluctuations around the chiral condensate and extract them as individual degrees of freedom; this procedure is known as the Hubbard-Stratonovich transformation.

Denoting $\tilde{\sigma}$ as a spin-0 boson field; we have the identity

$$1 = \int D\tilde{\sigma}\, \exp\left[ i \int d^4x\, \left( G\tilde{\sigma}^2 + G\bar{q}q\bar{q}q - 2G\tilde{\sigma}\bar{q}q \right) \right], \tag{2.30}$$

since this is nothing but a shifted Gaussian integral in $\tilde{\sigma}$. Then we can insert this identity into the generating functional of the original NJL Lagrangian (2.1), and note the canceling of the $G(\bar{q}q)^2$ interaction term; the resulting action, as a functional of both the original quark fields and the new boson field, $\tilde{\sigma}$, is

$$S(\tilde{\sigma}, q, \bar{q}) \;=\; \int d^4x\, \left\{ \bar{q}\left( i\gamma^\mu \partial_\mu + 2G\tilde{\sigma} \right) q + G\left( \bar{q} i\gamma^5 \vec{\tau} q \right)^2 - G\tilde{\sigma}^2 \right\}. \tag{2.31}$$

Performing the same procedure to the $G(\bar{q} i\gamma_5 \boldsymbol{\tau} q)^2$ interaction with a new boson field $\tilde{\boldsymbol{\pi}}$, we arrive at

$$S(\tilde{\sigma}, \tilde{\pi}, q, \bar{q}) = \int d^4x\, \left\{ \bar{q}\left( i\gamma^\mu \partial_\mu + 2G\tilde{\sigma} + 2Gi\gamma_5 \boldsymbol{\tau} \cdot \tilde{\boldsymbol{\pi}} \right) q - G\left( \tilde{\sigma}^2 + \tilde{\boldsymbol{\pi}}^2 \right) \right\}; \tag{2.32}$$

the theory now has explicit boson fields, and is equivalent to the original NJL model. When the boson fields are replaced by their vacuum expectation values and become mean fields, we retrieve the mean field NJL Lagrangian.

We now consider the fluctuations of the boson fields, i.e. the sigma particle and the pions, around their vacuum expectation value:

$$\hat{\sigma} \equiv \tilde{\sigma} - \sigma, \;\; \hat{\boldsymbol{\pi}} \equiv \tilde{\boldsymbol{\pi}} - \boldsymbol{\pi}. \tag{2.33}$$

The action is

$$\begin{aligned} S(\tilde{\sigma}, \tilde{\pi}, q, \bar{q}) \;&=\; \int d^4x\, \left\{ \bar{q}\left( \mathcal{G}^{-1} + 2G\hat{\sigma} + 2iG\gamma^5 \boldsymbol{\tau} \cdot \hat{\boldsymbol{\pi}} \right) q - G\left[ (\sigma + \hat{\sigma})^2 + \hat{\boldsymbol{\pi}}^2 \right] \right\} \\ &\equiv\; \int d^4x\, \left\{ \bar{q}\left( \mathcal{G}^{-1} + 2G\hat{\sigma} + 2iG\gamma^5 \boldsymbol{\tau} \cdot \hat{\boldsymbol{\pi}} \right) q - V(\hat{\sigma}, \hat{\boldsymbol{\pi}}, \sigma) \right\} \end{aligned} \tag{2.34}$$

Still quadratic in quark fields, we can perform the Gaussian integral, and then re-exponentiate the determinant to obtain

$$\begin{aligned} S \;&=\; -i \ln \det(\mathcal{G}^{-1} + 2G\hat{\sigma} + 2iG\gamma^5 \boldsymbol{\tau} \cdot \hat{\boldsymbol{\pi}}) - \int d^4x\, V(\hat{\sigma}, \hat{\boldsymbol{\pi}}, \sigma) \\ &=\; -i \mathrm{tr} \ln(\mathcal{G}^{-1} + 2G\hat{\sigma} + 2iG\gamma^5 \boldsymbol{\tau} \cdot \hat{\boldsymbol{\pi}}) - \int d^4x\, V(\hat{\sigma}, \hat{\boldsymbol{\pi}}, \sigma). \end{aligned} \tag{2.35}$$

Denoting the total fluctuation as $\hat{x} = 2G\hat{\sigma} + 2iG\gamma^5 \boldsymbol{\tau} \cdot \hat{\boldsymbol{\pi}}$; then, we can expand the logarithm

$$\begin{aligned} \mathrm{tr} \ln\left( \mathcal{G}^{-1} + \hat{x} \right) \;&=\; \mathrm{tr} \ln \mathcal{G}^{-1} \left( 1 + \mathcal{G}\hat{x} \right) \\ &=\; \mathrm{tr} \ln \mathcal{G}^{-1} + \sum_{n=1}^{\infty} (-1)^{n+1} \frac{\mathrm{tr}(\mathcal{G}\hat{x})^n}{n}. \end{aligned} \tag{2.36}$$

The $\mathrm{tr}\ln\mathcal{G}^{-1}$ corresponds to the mean field quark action; the series expansion corresponds to the action of the bosons, up to infinite order.

Let us calculate the boson action term by term. The linear order term is

$$\begin{aligned} S^{(1)} &= -2iG\mathrm{tr}\left(\mathcal{G}\hat{x}\right) = -2Gi\int\frac{d^4p}{(2\pi)^4}\,\mathrm{Tr}\mathcal{G}_0(p)\left[\hat{\sigma}(p=0)+i\gamma_5\boldsymbol{\tau}\cdot\hat{\boldsymbol{\pi}}(p=0)\right] \\ &= -2Gi\int d^4x\,\hat{\sigma}(x)\int\frac{d^4p}{(2\pi)^4}\,\mathrm{Tr}\frac{4M}{p_0^2-\epsilon_k^2} \\ &= -8GMI_1\int d^4x\,\hat{\sigma}(x), \end{aligned} \tag{2.37}$$

where we denote the four-integrals in momentum space as

$$I_n = (-1)^{n+1}N_fN_ci\int\frac{d^4p}{(2\pi)^4}\frac{1}{(p_0^2-\epsilon_p^2)^n}; \tag{2.38}$$

we recall that the integration over frequency $p_0$ is understood as the imaginary Matsubara frequency summation. In addition, the $V$ contribution to the action at linear order in boson field is $\int dx^4\,(-2G\sigma)\hat{\sigma}$. Thus, the effective action for $\hat{\sigma}$ at linear order is

$$\int dx^4\,\left[-2G\sigma-8GMI_1\right]\hat{\sigma}, \tag{2.39}$$

while there is no contribution at linear order in the pion fields $\hat{\boldsymbol{\pi}}$. On the other hand, using the gap equation (2.16), one can show that

$$\begin{aligned} I_1 &= N_fN_c\int\frac{d^3p}{(2\pi)^3}\,\frac{1-f(\epsilon_k-\mu)-f(\epsilon_k+\mu)}{2\epsilon_k} \\ &= -\frac{\sigma}{4M} = \frac{1}{8G}, \end{aligned} \tag{2.40}$$

thus $2G\sigma+8GMI_1=0$. As a result, the action in linear order in bosons vanishes; this is a consequence of our, by employing the gap equation, expanding the action around the chirally broken phase, which is a local extremum of the potential for $\sigma$ and $\boldsymbol{\pi}$.

The quadratic term will, in addition to producing potential terms for the bosons, yield kinetic energy terms:

$$S^{(2)} = i\tfrac{1}{2}\mathrm{tr}\left[\mathcal{G}\hat{x}\right]^2 = 2iG^2\left[\mathrm{tr}\left(\mathcal{G}\hat{\sigma}\mathcal{G}\hat{\sigma}\right)+\mathrm{tr}\left(\mathcal{G}i\gamma_5\boldsymbol{\tau}\cdot\hat{\boldsymbol{\pi}}\mathcal{G}i\gamma_5\boldsymbol{\tau}\cdot\hat{\boldsymbol{\pi}}\right)\right]. \tag{2.41}$$

We first investigate the $\hat{\sigma}$ part:

$$\begin{aligned} S_\sigma^{(2)} &= 2iG^2\mathrm{tr}\left(\mathcal{G}\hat{\sigma}\mathcal{G}\hat{\sigma}\right) \\ &= 2iG^2\left[\mathrm{Tr}\int\frac{d^4pd^4q}{(2\pi)^8}\mathcal{G}_0(p)\mathcal{G}_0(q+p)\sigma(-q)\sigma(q)\right] \\ &\equiv 2G^2\int\frac{d^4q}{(2\pi)^4}\Pi(q)\sigma(-q)\sigma(q), \end{aligned} \tag{2.42}$$

where

$$\Pi(q) \equiv i \int \frac{d^4p}{(2\pi)^4} \mathrm{Tr}\left[\mathcal{G}(p)\mathcal{G}(p-q)\right] \tag{2.43}$$

is the polarization operator. In the long wavelength limit, we may expand

$$\Pi(q) = \Pi(0) + \frac{1}{2}\frac{\partial^2\Pi(0)}{\partial q^\mu \partial q^\nu} q^\mu q^\nu + \dots \tag{2.44}$$

In the zeroth order in momentum,

$$\begin{aligned} \Pi(0) &= i4\mathrm{Tr}\int \frac{d^4p}{(2\pi)^4} \frac{p_0^2 - \epsilon_p^2 + 2M^2}{\left(p_0^2-\epsilon_p^2\right)^2} = 4i\mathrm{Tr}\int \frac{d^4p}{(2\pi)^4}\left[\frac{1}{p_0^2-\epsilon_p^2} + \frac{2M^2}{\left(p_0^2-\epsilon_p^2\right)^2}\right] \\ &= 4I_1 - 8M^2 I_2. \end{aligned} \tag{2.45}$$

To compute the quadratic term, we first calculate

$$\begin{aligned} \frac{\partial\Pi(q)}{\partial q^\mu} = 4i\mathrm{Tr}\int \frac{d^4p}{(2\pi)^4}\frac{1}{p^2-M^2}\Bigg[&\frac{p^\mu}{(p+q)^2-M^2} \\ &- \frac{p^2+p\cdot q+M^2}{\left[(p+q)^2-M^2\right]^2}\cdot 2(p+q)^\mu\Bigg], \end{aligned} \tag{2.46}$$

and

$$\begin{aligned} &\tfrac{1}{2}\tfrac{\partial^2\Pi(0)}{\partial q^\mu\partial q^\nu}q^\mu q^\nu = i\mathrm{Tr}\int \tfrac{d^4p}{(2\pi)^4}\tfrac{\not{p}+M}{p_0^2-E_p^2}\left[-\tfrac{2\not{q}(p\cdot q)}{(p^2-M^2)^2} + \tfrac{\not{p}+M}{(p^2-M^2)^3}\cdot 4(p\cdot q)^2 - \tfrac{\not{p}+M}{(p^2-M^2)^2}q^2\right] \\ &= 4i\mathrm{tr}_{fc}\int \tfrac{d^4p}{(2\pi)^4}\left[\left[\tfrac{2}{(p^2-M^2)^3} + \tfrac{8M^2}{(p^2-M^2)^4}\right](p\cdot q)^2 - \left(\tfrac{1}{(p^2-M^2)^2} + \tfrac{2M^2}{(p^2-M^2)^3}\right)q^2\right]; \end{aligned} \tag{2.47}$$

as a result[2],

$$\begin{aligned} \frac{1}{2}\frac{\partial^2\Gamma(0)}{\partial q^\mu\partial q^\nu}q^\mu q^\nu &= i\mathrm{Tr}\int\frac{d^4p}{(2\pi)^4}\left[-\frac{2}{(p^2-M^2)^2} + \frac{2M^2}{(p^2-M^2)^3} + \frac{8M^4}{(p^2-M^2)^4}\right] \\ &= \left(2I_2 + 2M^2 I_3 - 8M^4 I_4\right)q^2. \end{aligned} \tag{2.49}$$

The effective Lagrangian in quadratic order of $\hat{\sigma}$, from the calculations (2.41) –

[2]We have used, in Euclidean space,

$$\int d^4p\, g(p^2)(p\cdot q)^2 = \int d^4p\, g(p^2)\frac{p^2q^2}{4} \tag{2.48}$$

for arbitrary function $g(p^2)$.

(2.49), is then

$$\begin{aligned}\mathcal{L}^{(2)}_{\hat{\sigma}} &= -G\hat{\sigma}^2 + 2G^2\left(4I_1 - 8M^2 I_2\right)\hat{\sigma}^2 \\ &\quad +2G^2\left(2I_2 + 2M^2 I_3 - 8M^4 I_4\right)\partial_\mu\hat{\sigma}\partial^\mu\hat{\sigma} \\ &= -16G^2M^2 I_2\hat{\sigma}^2 + 2G^2\left(2I_2 + 2M^2 I_3 - 8M^4 I_4\right)\partial_\mu\hat{\sigma}\partial^\mu\hat{\sigma}. \quad (2.50)\end{aligned}$$

where we have again used the gap equation (2.16).

Similarly for the pion field,

$$\begin{aligned}S^{(2)}_{\hat{\boldsymbol{\pi}}} &= 2G^2 i\int\frac{d^4p}{(2\pi)^4}\frac{d^4q}{(2\pi)^4}\mathrm{Tr}\left[\frac{1}{\not{p}-M}i\gamma_5\boldsymbol{\tau}\cdot\boldsymbol{\pi}(q)\frac{1}{\not{p}+\not{q}-M}i\gamma_5\boldsymbol{\tau}\cdot\boldsymbol{\pi}(-q)\right] \\ &\equiv 2G^2\int\frac{d^4q}{(2\pi)^4}\Pi'(q)\boldsymbol{\pi}(q)\cdot\boldsymbol{\pi}(-q); \quad (2.51)\end{aligned}$$

we have used $\mathrm{tr}\tau_a\tau_b = 2\delta_{ab}$ and the fact that quarks are diagonal in flavor space. The polarization operator in the pseudoscalar channel is

$$\Pi'(q) = i\int\frac{d^4p}{(2\pi)^4}\mathrm{Tr}\left[\mathcal{G}(p)i\gamma_5\mathcal{G}(q-p)i\gamma_5\right]. \quad (2.52)$$

Again expanding in long wavelength limit, using

$$\Pi'(0) = 4I_1 \quad (2.53)$$

and

$$\begin{aligned}\frac{1}{2}\frac{\partial^2\Pi'(q)}{\partial q^\mu\partial q^\nu}q^\mu q^\nu &= 2iN_fN_c\int\frac{d^4p}{(2\pi)^4}\left[-\frac{2q^2}{(p^2-m^2)^2} + \frac{4(p\cdot q)^2}{(p^2-m^2)^3}\right] \\ &= \left(2I_2 + 2M^2 I_3\right)q^2; \quad (2.54)\end{aligned}$$

we find the Lagrangian for the pions at quadratic order is

$$\mathcal{L}^{(2)}_{\hat{\pi}} = 4G^2\left(I_2 + M^2 I_3\right)\partial_\mu\hat{\boldsymbol{\pi}}\cdot\partial^\mu\hat{\boldsymbol{\pi}}, \quad (2.55)$$

where the non-derivative mass term has been cancelled out due to the gap equation again; this confirms the Goldstone theorem which states that the pions as the NG bosons should be massless.

As it turns out, the full structure of the effective action for $\hat{\sigma}$ is only revealed at higher orders. Thus, we compute the 3rd and 4th order terms for the $\sigma$ field:

$$\begin{aligned}S^{(3)}_{\hat{\sigma}} &= -i\frac{1}{3}\mathrm{tr}\left[\mathcal{G}2G\hat{\sigma}\right]^3 = -i\frac{8}{3}G^3\mathrm{tr}\left[\mathcal{G}\hat{\sigma}\right]^3 \\ &= -i\frac{8}{3}G^3\mathrm{Tr}\int\frac{d^4pd^4q_1d^4q_2}{(2\pi)^{12}}\mathcal{G}(p)\mathcal{G}(p-q_1)\mathcal{G}(p+q_2)\hat{\sigma}(q_1)\hat{\sigma}(q_2)\hat{\sigma}(-q_1-q_2); \\ &\quad (2.56)\end{aligned}$$

at the point interaction level, i.e. neglecting momentum dependence from the

quark propagators, we have

$$\begin{aligned} S^{(3)}_{\hat{\sigma}} &\approx -i\frac{8}{3}G^3\mathrm{Tr}\int\frac{d^4p}{(2\pi)^4}\mathcal{G}(p)^3\int\frac{d^4q_1d^4q_2}{(2\pi)^8}\hat{\sigma}(q_1)\hat{\sigma}(q_2)\hat{\sigma}(-q_1-q_2) \\ &= -\frac{8}{3}G^3\int d^4x\,\hat{\sigma}(x)^3 i\mathrm{Tr}\int\frac{d^4p}{(2\pi)^4}\mathcal{G}(p)^3. \end{aligned} \tag{2.57}$$

Using

$$\begin{aligned} i\mathrm{Tr}\int\frac{d^4p}{(2\pi)^4}\mathcal{G}(p)^3 &= i\mathrm{Tr}\int\frac{d^4p}{(2\pi)^4}\left(\frac{\not{p}+M}{p^2-M^2}\right)^3 \\ &= 4iM\int\frac{d^4p}{(2\pi)^4}\left[\frac{3}{(p^2-M^2)^2}+\frac{4M^2}{(p^2-M^2)^3}\right] \\ &= -12MI_2+16M^3I_3, \end{aligned} \tag{2.58}$$

we have

$$\mathcal{L}^{(3)}_{\hat{\sigma}} = G^3M\left(32I_2-\frac{128}{3}M^2I_3\right)\hat{\sigma}^3. \tag{2.59}$$

In the 4th order,

$$\begin{aligned} S^{(4)}_{\hat{\sigma}} &= i\frac{1}{4}\mathrm{tr}\left[\mathcal{G}2G\hat{\sigma}\right]^4 \\ &= 4G^4\int d^4x\,\sigma^4(x) i\mathrm{Tr}\int\frac{d^4p}{(2\pi)^4}\mathcal{G}(p)^4+\ldots; \end{aligned} \tag{2.60}$$

using

$$\begin{aligned} &i\mathrm{Tr}\int\frac{d^4p}{(2\pi)^4}\mathcal{G}(p)^4 \\ &= 4i\mathrm{Tr}\int\frac{d^4p}{(2\pi)^4}\left[\frac{1}{(p^2-M^2)^2}+\frac{8M^2}{(p^2-M^2)^3}+\frac{8M^4}{(p^2-M^2)^4}\right] \\ &= -4I_2+32M^2I_3-32M^4I_4 \end{aligned} \tag{2.61}$$

we have

$$\mathcal{L}^{(4)}_{\hat{\sigma}} = 4G^4\cdot\left(-4I_2+32M^2I_3-32M^4I_4\right)\hat{\sigma}^4. \tag{2.62}$$

Summing over all contributions, the effective Lagrangian for the $\hat{\sigma}$ and $\hat{\boldsymbol{\pi}}$ is

$$\begin{aligned}
\mathcal{L}_{\hat{\sigma},\hat{\boldsymbol{\pi}}} &= \sum_{i=1}^{4}\mathcal{L}_{\hat{\sigma}}^{(i)} + \sum_{i=1}^{2}\mathcal{L}_{\hat{\boldsymbol{\pi}}}^{(i)} \\
&= -16G^2M^2I_2\hat{\sigma}^2 + 32G^3MI_2\hat{\sigma}^3 - 16G^4I_2\hat{\sigma}^4 \\
&\quad +4G^2\left(I_2 + M^2I_3 - 4M^4I_4\right)\partial_\mu\hat{\sigma}\partial^\mu\hat{\sigma} \\
&\quad +4G^2\left(I_2 + M^2I_3\right)\partial_\mu\hat{\boldsymbol{\pi}}\cdot\partial^\mu\hat{\boldsymbol{\pi}} \\
&= 4G^2\left(I_2 + M^2I_3 - 4M^4I_4\right)\partial_\mu\hat{\sigma}\partial^\mu\hat{\sigma} + 4G^2\left(I_2 + M^2I_3\right)\partial_\mu\hat{\boldsymbol{\pi}}\cdot\partial^\mu\hat{\boldsymbol{\pi}} \\
&\quad -16I_2G^4\left(\left(\hat{\sigma}+\sigma\right)^2 - \sigma^2\right)^2. \qquad (2.63)
\end{aligned}$$

Intriguingly, the coefficient in front of the kinetic energy terms for $\hat{\sigma}$ and $\hat{\boldsymbol{\pi}}$ are different. This is a result of expanding theory in a chirally broken state, i.e. $\sigma \neq 0$; the isospin space is no longer isotropic in terms of energy cost of space-dependent fluctuations. Nevertheless, the difference $\sim I_4$ is a finite quantity, while in the renormalization of the field operators which we will introduce in later sections involves absorbing the divergent quantity $I_2$; as a result, the renormalized theory still has chirally invariant kinetic energy term. One can show that if we chose a different ground state, e.g. $\pi_3 \neq 0$ while $\sigma = \pi_1 = \pi_2 = 0$, then the kinetic energy coefficient for $\pi_3$ will lose the $I_4$ term, which will be obtained by the $\sigma$ instead.

A pattern of $S^{(n)}_{\hat{\sigma},\hat{\boldsymbol{\pi}}}$ can be observed in terms of the coefficients in front of $I_n$s, if we re-arrange the terms in the Lagrangians according to $I_n$s instead of powers of $\hat{\sigma}$ and $\hat{\boldsymbol{\pi}}$. In fact, if one computes $S^{(n)}_{\hat{\sigma},\hat{\boldsymbol{\pi}}}$ even further, one finds that the coefficient for each $I_n$ will always be proportional to the $n$th power of

$$(\hat{\sigma}+\sigma)^2 + \hat{\boldsymbol{\pi}}^2 - \sigma^2 = \hat{\sigma}(\hat{\sigma}+2\sigma) + \hat{\boldsymbol{\pi}}^2 \equiv \varepsilon; \qquad (2.64)$$

the potential part of the boson Lagrangian is actually an expansion in powers of $\varepsilon$. Computing up to eight power in $\hat{\sigma}$ and $\hat{\boldsymbol{\pi}}$, one can verify that the potential energy term (the point interactions) in the effective Lagrangian for the bosons is

$$\mathcal{L}^{\text{potential}}_{\hat{\sigma},\hat{\boldsymbol{\pi}}} = \left(8G^2I_1 - G\right)\varepsilon - 16G^4I_2\varepsilon^2 + \frac{128}{3}G^6I_3\varepsilon^3 - 128G^8I_4\varepsilon^4 + \ldots \qquad (2.65)$$

where the linear term vanishes if we apply the gap equation. Thus, we are essentially expanding around the extremum point of a Mexican hat potential around the scalar state configuration (see Fig. 2.1) for $\hat{\sigma}$, which grants a $\hat{\sigma}$ mass as expected; meanwhile, the NG boson modes, $\hat{\boldsymbol{\pi}}$, remain massless.

When the chiral symmetry is explicitly broken by a finite bare quark mass $m_q$, additional terms involving the mean fields will appear in the effective theory. One can shift the mean field value $\sigma$ by $m_q/2G$ to absorb it in the quark inverse propagator. This shift will introduce a term linear in $\sigma$ in the mean field

potential term:

$$V = G[(\hat{\sigma}+\sigma)^2 + (\hat{\boldsymbol{\pi}}+\boldsymbol{\pi})^2] \to G[(\hat{\sigma}+\sigma)^2 + (\hat{\boldsymbol{\pi}}+\boldsymbol{\pi})^2] + m_q(\hat{\sigma}+\sigma); \tag{2.66}$$

such a shift will modify the gap equation for $\sigma$ into

$$\sigma + \frac{m_g}{2G} = 8GI_1\sigma. \tag{2.67}$$

As a result, the linear term in $\varepsilon$ will no longer vanish:

$$(8G^2I_1 - G)\varepsilon = \frac{m_q}{2\sigma}\varepsilon. \tag{2.68}$$

Since $\varepsilon$ contains a quadratic term for the pions $\hat{\boldsymbol{\pi}}$, this linear term will grant the pions a mass; this corresponds to the "tilting" of the Mexican hat potential due to explicit chiral symmetry breaking. For $m_q > 0$, the negative solution of $\sigma$ will be favored, since it reduces the extra potential energy caused by the $m_q\sigma$ term.

The effective pion-$\hat{\sigma}$ bosonized theory we have derived in this section is structurally similar to the linear sigma model used in nuclear matter. We next show that through renormalization, our bosonized theory can be exactly transformed into a quark linear sigma model.

## 2.2 Deriving the linear sigma model for quark matter

In this section we demonstrate how to transform the boson Lagrangian (2.63), combined with the quark sector Lagrangian

$$\mathcal{L}_q = \bar{q}\mathcal{G}q, \tag{2.69}$$

into the linear sigma model.[3] So far, the bosonized theory obtained via the Hubbard-Stratonovich transformation,

$$\mathcal{L}_{HS} = \mathcal{L}_{\hat{\sigma},\hat{\boldsymbol{\pi}}} + \mathcal{L}_q, \tag{2.70}$$

is not well-defined without a cutoff $\Lambda$ in the momentum integration; the integrals, $I_n$, appearing in the kinetic and potential energies of the boson fields in $\mathcal{L}_{\hat{\sigma},\hat{\boldsymbol{\pi}}}$, are ultraviolet divergent for $n = 1, 2$. The $I_1$, appearing in the gap equation, is quadratically divergent $\sim \Lambda^2$, and $I_2$ is logarithmically divergent $\sim \ln\Lambda/M$.

By renormalizing the boson fields and boson-quark coupling vertex, one

[3] For a more sophisticated formalism of this transformation in terms of renormalization group, see Ref. [38].

can absorb such divergences into field re-definitions, and arrive at a cutoff-independent theory. To do so, we re-scale the boson fields into renormalized fields $\hat{\sigma}_R$ and $\hat{\boldsymbol{\pi}}_R$:

$$2G\sqrt{2I_2}\hat{\sigma} = -\hat{\sigma}_R,\ 2G\sqrt{2I_2}\hat{\boldsymbol{\pi}} = -\hat{\boldsymbol{\pi}}_R; \tag{2.71}$$

further more, define dimensionless coupling constants

$$g = \frac{1}{\sqrt{2I_2}},\ \lambda = \frac{1}{I_2}, \tag{2.72}$$

and the vacuum expectation value of the rescaled field

$$f_\pi = \sigma_R; \tag{2.73}$$

ignoring all terms of order $I_{n\geq 3}/I_2$, the HS Lagrangian then takes the form

$$\begin{aligned}\mathcal{L} &= \frac{1}{2}\left(\partial\hat{\boldsymbol{\pi}}_R\right)^2 + \frac{1}{2}\left(\partial\hat{\sigma}_R\right)^2 + \bar{q}\left(i\partial\!\!\!/ - g\left(\hat{\sigma}_R + i\gamma_5\boldsymbol{\tau}\cdot\hat{\boldsymbol{\pi}}_R\right) + \gamma_0\mu\right)q \\ &\quad -\frac{\lambda}{4}\left(\hat{\sigma}_R^2 + \hat{\boldsymbol{\pi}}_R^2 - \sigma_{R0}^2\right)^2 + f_\pi m_\pi^2\hat{\sigma}_R.\end{aligned} \tag{2.74}$$

Here, we have shifted a mean field value $\sigma_R$ back to $\hat{\sigma}_R$, and restored an explicit coupling of $\hat{\sigma}_R$ with the quark field; also

$$\begin{aligned}m_\pi^2 &\equiv \frac{gm_q}{2Gf_\pi}, \\ \sigma_{R0} &\equiv f_\pi^2 - \frac{m_\pi^2}{\lambda}.\end{aligned} \tag{2.75}$$

The Lagrangian (2.74) is precisely the linear sigma model for $N_f = 2$ quarks, and contains the same physics as the bosonized NJL quark Lagrangian. The quantities $f_\pi$ and $m_\pi$ are interpreted as the physical pion decay constant and mass; they naturally obey the Gell-Mann–Oaks–Renner (GMOR) relation,

$$f_\pi^2 m_\pi^2 = \frac{gf_\pi m_q}{2G} = -\sigma m_q = -\langle\bar{q}q\rangle m_q; \tag{2.76}$$

that is, the bare quark mass contributes linearly at leading order to the pion mass squared. The nucleon linear sigma model can be obtained by simply replacing the isospin doublet of quarks $(u, d)$ by the nucleons $(p, n)$.

The linear sigma model has been particularly useful in studying the pion condensation in nuclear matter. In the following section, we use both the NJL model and the quark linear sigma model to study possible pion condensation in both the Dirac sea sector and the medium sector, to study the potential connection of pion condensation in nuclear matter to that in quark matter.

## 2.3 Pseudoscalar meson condensation: mean field, self-energy, and connection with nuclear matter pion condensation

The small masses of the pions combined with the fact that they are bosons make them vulnerable to possible Bose-Einstein condensation, a macroscopic occupation of the lowest energy state. The possible presence of such condensates would have profound implications on the neutron star cooling process. In this section we study two particular examples of possible pion condensation: the dual chiral density wave (Sec. 2.3.1) [39] and the running wave charged pion condensation (Sec. 2.3.2) [3] at the mean field level, demonstrating how they effectively reduce the Dirac sea energy, thus becoming energetically favorable compared to scalar state. We go beyond mean field at Sec. 2.3.3 for the running wave charged pion condensate and consider the pion-quark interaction energy; the resulting self-energy for the pions turns out to have the same structure as pion-nucleon s- and p-wave interactions together.

A pion condensation can be characterized by an arbitrary configuration of $\boldsymbol{\pi} \neq 0$; it may point into any direction in the isospin space, and the condensate can be either homogeneous or inhomogeneous. In ultradense matter, it is yet uncertain what realistic condensation phase might appear. We may parametrize the pion condensates on the isospin sphere in general as

$$\begin{aligned} \pi_1 &= \kappa \sin\psi \sin\theta \sin\phi, \\ \pi_2 &= \kappa \sin\psi \sin\theta \cos\phi, \\ \pi_3 &= \kappa \sin\psi \cos\theta, \\ \sigma &= \kappa \cos\psi \end{aligned} \tag{2.77}$$

for $\psi \neq 0$; $\kappa^2 = \sigma^2 + \boldsymbol{\pi}^2$ is a chirally invariant order parameter for chiral symmetry breaking, and simply $\kappa = \sigma$ in the scalar state. Here, $\psi$, $\theta$ and $\phi$ are isospin spherical coordinates that can be spatially dependent; there are many different such possibilities. When $\theta, \phi$ are constants, the pion condensation is spatially homogeneous; the $\theta = 0$ condensate will correspond to neutral $\pi_0$ condensation, and $\theta = \pi, \phi = -\pi/4$ correspond to charged $\pi^-$ condensation, etc. For spatially dependent condensates, we consider two popular possible scenarios in this study. The first is a dual chiral density wave, featuring spatially oscillating neutral pion condensation in the $z$ direction with wave number $g_z$:

$$\sigma(x) = \kappa \cos 2g_z z, \ \pi_3(x) = \kappa \sin 2g_z z, \ \pi_1 = \pi_2 = 0; \tag{2.78}$$

this corresponds to $\psi = 2g_z z$, $\theta = \phi = 0$. The other case, the running wave charged pion condensation with wave number $k$ in $z$ direction, assumes the

condensation of charged pions instead:

$$\sigma(x) = \kappa \cos\psi,\ \pi_1 = \kappa \sin\psi \cos kz,\ \pi_2 = \kappa \sin\psi \sin kz,\ \pi_3 = 0; \tag{2.79}$$

this corresponds to $\psi =$ constant, $\theta = \pi/2$ and $\phi = \pi/2 - kz$. This running wave condensate is still spatially homogeneous, since the magnitude corresponding to the charged pion $\pi_1 + i\pi_2 = \pi^-$ is constant; only its phase is spatially dependent.

The physical arguments for the dual chiral density wave and the charged pion running wave condensates are different. For the dual chiral density wave, the oscillation of $\pi_3$ component of the isospin periodically reduces the effective mass gaps of some states, thus lowering the energy of the Dirac sea. For the charged pion running wave condensate, it is caused by the p-wave attractive interaction between the pions and the nucleons, plus the big isospin asymmetry of the ground state. We discuss these two different possibilities in details in the following sections, using the NJL quark model in mean field. For the running wave condensate, we also connect it to the nuclear matter results, since the NJL quark model is equivalent to a linear sigma model; the latter can be precisely used to study pion condensation in nuclear matter.

### 2.3.1 Dual chiral density wave

The physics of the dual chiral density wave, corresponding to a spatially oscillating neutral pion condensation, can be studied using the mean field NJL Lagrangian

$$\begin{aligned} \mathcal{L} &= \bar{q}\left(i\gamma^\mu \partial_\mu + \gamma^0 \mu + 2G\sigma + 2Gi\gamma^5 \tau_3 \cdot \pi_3\right) q - G\left(\sigma^2 + \pi_3^2\right) \\ &\equiv \bar{q}\mathcal{G}^{-1} q - G\left(\sigma^2 + \pi_3^2\right) \end{aligned} \tag{2.80}$$

where we have set $\pi_1 = \pi_2 = 0$. The quark inverse propagator is diagonal in isospin (flavor) space:

$$\mathcal{G}^{-1} = \begin{pmatrix} \mathcal{G}_u^{-1} & 0 \\ 0 & \mathcal{G}_d^{-1} \end{pmatrix}, \tag{2.81}$$

where, in the Dirac basis,

$$\begin{aligned} \mathcal{G}_u^{-1} &= \begin{pmatrix} \omega + 2G\sigma & -\boldsymbol{\sigma}\cdot\boldsymbol{p} + 2iG\pi_3 \\ \boldsymbol{\sigma}\cdot\boldsymbol{p} + 2iG\pi_3 & -\omega + 2G\sigma \end{pmatrix}, \\ \mathcal{G}_d^{-1} &= \begin{pmatrix} \omega + 2G\sigma & -\boldsymbol{\sigma}\cdot\boldsymbol{p} - 2iG\pi_3 \\ \boldsymbol{\sigma}\cdot\boldsymbol{p} - 2iG\pi_3 & -\omega + 2G\sigma \end{pmatrix}. \end{aligned} \tag{2.82}$$

We first consider the homogeneous case where $\sigma, \pi_3$ are constants. The energy eigenvalues, $\omega(\boldsymbol{p})$, are obtained by solving

$$\det \mathcal{G}^{-1}(\omega(\boldsymbol{p}), \boldsymbol{p}) = 0; \tag{2.83}$$

the up and down quark energies in this case are degenerate:

$$\omega_u(\boldsymbol{p}) = \omega_d(\boldsymbol{p}) = \pm\sqrt{4G^2\left(\sigma^2 + \pi_3^2\right) + \boldsymbol{p}^2}. \tag{2.84}$$

This is expected, since the effective quark mass, a physical observable, can only depend on the chirally invariant quantity $\sigma^2 + \boldsymbol{\pi}^2$.

For a dual chiral density wave in $\hat{\boldsymbol{k}} = \hat{z}$ direction with wave number $\boldsymbol{k} = 2g_z\hat{z}$, $\sigma$ and $\pi_3$ are functions of spatial coordinates as given by (2.78). We can also write the condensate compactly as

$$\sigma(x) + i\pi_3(x) = \kappa e^{i\boldsymbol{k}\cdot\boldsymbol{x}}; \tag{2.85}$$

then the action of this condensate on the quark field in the momentum space is equivalent to a Lorentz boost in $\boldsymbol{k}$ direction. To use this interpretation, we consider the equation of motion of the up quark field in the mean field Lagrangian (we write $q = (u, d)^T$; the down quark case is identical but with opposite sign in the $\gamma_5$ term),

$$\left[i\gamma^\mu\partial_\mu + 2G\sigma(x) + 2Gi\gamma_5\pi_3(x)\right] u(t, \boldsymbol{x}) = 0; \tag{2.86}$$

in momentum space, this equation becomes

$$\begin{aligned} 0 = \int \frac{d^3\boldsymbol{q}}{(2\pi)^3} \Big[ & i\gamma^0\partial_t - \boldsymbol{\gamma}\cdot\boldsymbol{q} + G\kappa\left(e^{i\boldsymbol{k}\cdot\boldsymbol{x}} + e^{-i\boldsymbol{k}\cdot\boldsymbol{x}}\right) \\ & + i\gamma_5 G\kappa\left(e^{i\boldsymbol{k}\cdot\boldsymbol{x}} - e^{-i\boldsymbol{k}\cdot\boldsymbol{x}}\right)\Big] e^{i\boldsymbol{q}\cdot\boldsymbol{x}} u(t, \boldsymbol{q}) \end{aligned} \tag{2.87}$$

which further implies

$$\begin{aligned} \left[i\gamma^0\partial_t - \boldsymbol{\gamma}\cdot\boldsymbol{q}\right] u(t, \boldsymbol{q}) + G\kappa\left[1 + i\gamma_5\right] u\left(t, \boldsymbol{q} - \boldsymbol{k}\right) \\ + G\kappa\left[1 - i\gamma_5\right] u\left(t, \boldsymbol{q} + \boldsymbol{k}\right) = 0. \end{aligned} \tag{2.88}$$

The equation of motion, (2.88), is analogous to lattice solid state physics where sites on the reciprocal lattice $\psi(\boldsymbol{q})$ and $\psi(\boldsymbol{q} + N\boldsymbol{k}), N = 0, \pm 1, \ldots$ are coupled to each other via interactions, and the wave vector $\boldsymbol{k}$ spans the space of the solutions. We can thus use similar techniques to solid state physics to solve the quasiparticle energies by boosting the fields; such a task is easier done in the

chiral basis, where the up quark part of the Lagrangian reads

$$
\begin{aligned}
&\bar{q}\mathcal{G}^{-1}q \\
&= \bar{u}\begin{pmatrix} -2iG\kappa\sin\boldsymbol{k}\cdot\boldsymbol{x}+2G\kappa\cos\boldsymbol{k}\cdot\boldsymbol{x} & \omega+i\boldsymbol{\sigma}\cdot\nabla \\ \omega-i\boldsymbol{\sigma}\cdot\nabla & 2iG\kappa\sin\boldsymbol{k}\cdot\boldsymbol{x}+2G\kappa\cos\boldsymbol{k}\cdot\boldsymbol{x} \end{pmatrix} u \\
&+\bar{d}\begin{pmatrix} -2iG\kappa\sin\boldsymbol{k}\cdot\boldsymbol{x}-2G\kappa\cos\boldsymbol{k}\cdot\boldsymbol{x} & \omega+i\boldsymbol{\sigma}\cdot\nabla \\ \omega-i\boldsymbol{\sigma}\cdot\nabla & 2iG\kappa\sin\boldsymbol{k}\cdot\boldsymbol{x}-2G\kappa\cos\boldsymbol{k}\cdot\boldsymbol{x} \end{pmatrix} d \\
&= \begin{pmatrix} u_L^\dagger & u_R^\dagger \end{pmatrix}\begin{pmatrix} \omega-i\boldsymbol{\sigma}\cdot\nabla & 2G\kappa e^{i\boldsymbol{k}\cdot\boldsymbol{x}} \\ 2G\kappa e^{-i\boldsymbol{k}\cdot\boldsymbol{x}} & \omega+i\boldsymbol{\sigma}\cdot\nabla \end{pmatrix}\begin{pmatrix} u_L \\ u_R \end{pmatrix} \\
&+\begin{pmatrix} d_L^\dagger & d_R\dagger \end{pmatrix}\begin{pmatrix} \omega-i\boldsymbol{\sigma}\cdot\nabla & 2G\kappa e^{-i\boldsymbol{k}\cdot\boldsymbol{x}} \\ 2G\kappa e^{i\boldsymbol{k}\cdot\boldsymbol{x}} & \omega+i\boldsymbol{\sigma}\cdot\nabla \end{pmatrix}\begin{pmatrix} d_L \\ d_R \end{pmatrix}. \qquad (2.89)
\end{aligned}
$$

We apply the following boost to the quark fields,

$$q \to q' = e^{i\frac{1}{2}\gamma_5\tau_3\boldsymbol{k}\cdot\boldsymbol{x}}q; \qquad (2.90)$$

this corresponds to a boost differently to left and right handed fields for up quarks

$$\begin{pmatrix} u_L \\ u_R \end{pmatrix} \to \begin{pmatrix} e^{-i\frac{1}{2}\boldsymbol{k}\cdot\boldsymbol{x}}u_L \\ e^{i\frac{1}{2}\boldsymbol{k}\cdot\boldsymbol{x}}u_R \end{pmatrix} = \begin{pmatrix} e^{-i\frac{1}{2}\boldsymbol{k}\cdot\boldsymbol{x}} & \\ & e^{i\frac{1}{2}\boldsymbol{k}\cdot\boldsymbol{x}} \end{pmatrix}\begin{pmatrix} u_L \\ u_R \end{pmatrix} = \begin{pmatrix} u'_L \\ u'_R \end{pmatrix} \qquad (2.91)$$

and down quarks

$$\begin{pmatrix} d_L \\ d_R \end{pmatrix} \to \begin{pmatrix} e^{i\frac{1}{2}\boldsymbol{k}\cdot\boldsymbol{x}}d_L \\ e^{-i\frac{1}{2}\boldsymbol{k}\cdot\boldsymbol{x}}d_R \end{pmatrix} = \begin{pmatrix} e^{i\frac{1}{2}\boldsymbol{k}\cdot\boldsymbol{x}} & \\ & e^{-i\frac{1}{2}\boldsymbol{k}\cdot\boldsymbol{x}} \end{pmatrix}\begin{pmatrix} d_L \\ d_R \end{pmatrix} = \begin{pmatrix} d'_L \\ d'_R \end{pmatrix}. \qquad (2.92)$$

Under these transformations, since

$$
\begin{aligned}
\sigma &= \langle\bar{q}q\rangle = \langle u_L^\dagger u_R + u_R^\dagger u_L + d_L^\dagger d_R + d_R^\dagger d_L\rangle, \\
\pi_3 &= \langle\bar{q}i\gamma_5\tau_3 q\rangle = i\langle -u_R^\dagger u_L + u_L^\dagger u_R + d_R^\dagger d_L - d_L^\dagger d_R\rangle, \qquad (2.93)
\end{aligned}
$$

we obtain

$$\sigma + i\pi_3 = 2\langle u_R^\dagger u_L + d_L^\dagger d_R\rangle \to e^{-i\boldsymbol{k}\cdot\boldsymbol{x}}\left(\sigma+i\pi_3\right); \qquad (2.94)$$

this implies that the potential term $\sim \sigma^2+\pi_3^2$ is still invariant even under this spatially dependent transformation.

The inverse propagators for the up and down quarks are

$$\mathcal{G}^{-1}_{u,d}(\omega,\boldsymbol{p}) = \begin{pmatrix} \omega+2G\kappa\cos(\boldsymbol{k}\cdot\boldsymbol{x}) & -\boldsymbol{\sigma}\cdot\boldsymbol{p}\pm 2iG\kappa\sin(\boldsymbol{k}\cdot\boldsymbol{x}) \\ \boldsymbol{\sigma}\cdot\boldsymbol{p}\pm 2iG\kappa\sin(\boldsymbol{k}\cdot\boldsymbol{x}) & -\omega+2G\kappa\cos(\boldsymbol{k}\cdot\boldsymbol{x}) \end{pmatrix}, \qquad (2.95)$$

where + is for up quark and − for down quark. The kinetic energy however will produce extra terms due to this boost, as

$$\begin{aligned} u_L^\dagger \nabla u_L &= u_L^{'\dagger} \left(\nabla - \tfrac{i}{2}\boldsymbol{k}\right) u'_L, \\ u_R^\dagger \nabla u_R &= u_R^{'\dagger} \left(\nabla + \tfrac{i}{2}\boldsymbol{k}\right) u'_R. \end{aligned} \tag{2.96}$$

As a result, the final quark inverse propagators for the new fields $q' = (u', d')^T$ are

$$\begin{aligned} \mathcal{G}_u^{-1}(\omega, \boldsymbol{p}) &= \begin{pmatrix} \omega + \boldsymbol{\sigma}\cdot\left(\boldsymbol{p} - \frac{1}{2}\boldsymbol{k}\right) & 2G\kappa \\ 2G\kappa & \omega - \boldsymbol{\sigma}\cdot\left(\boldsymbol{p} + \frac{1}{2}\boldsymbol{k}\right) \end{pmatrix}, \\ \mathcal{G}_d^{-1}(\omega, \boldsymbol{p}) &= \begin{pmatrix} \omega + \boldsymbol{\sigma}\cdot\left(\boldsymbol{p} + \frac{1}{2}\boldsymbol{k}\right) & 2G\kappa \\ 2G\kappa & \omega - \boldsymbol{\sigma}\cdot\left(\boldsymbol{p} - \frac{1}{2}\boldsymbol{k}\right) \end{pmatrix}. \end{aligned} \tag{2.97}$$

The inverse propagator for down quark is simply the same as that of the up quark but with $\boldsymbol{k} \to -\boldsymbol{k}$, so we can focus on the up quark only. After some algebra, $\det \mathcal{G}_u^{-1}(\omega, \boldsymbol{p}) = 0$ is

$$\det\left[\left(\omega + \boldsymbol{\sigma}\cdot\left(\boldsymbol{p} - \frac{1}{2}\boldsymbol{q}\right)\right)\left(\omega - \boldsymbol{\sigma}\cdot\left(\boldsymbol{p} + \frac{1}{2}\boldsymbol{q}\right)\right) - M^2\right] = 0,\ M \equiv -2G\kappa. \tag{2.98}$$

Using

$$\begin{aligned} & \left(\omega + \boldsymbol{\sigma}\cdot\left(\boldsymbol{p} - \frac{1}{2}\boldsymbol{k}\right)\right)\left(\omega - \boldsymbol{\sigma}\cdot\left(\boldsymbol{p} + \frac{1}{2}\boldsymbol{k}\right)\right) \\ = \ & \omega^2 - \omega\boldsymbol{\sigma}\cdot\boldsymbol{k} - \boldsymbol{p}^2 + \frac{1}{4}\boldsymbol{k}^2 - \frac{1}{2}\left[\boldsymbol{\sigma}\cdot\boldsymbol{p}, \boldsymbol{\sigma}\cdot\boldsymbol{k}\right] \\ = \ & \omega^2 - \omega\boldsymbol{\sigma}\cdot\boldsymbol{k} - \boldsymbol{p}^2 + \frac{1}{4}\boldsymbol{k}^2 - i\left(\boldsymbol{p}\times\boldsymbol{k}\right)\cdot\boldsymbol{\sigma}, \end{aligned} \tag{2.99}$$

the determinant equation further reduces to

$$\det\begin{pmatrix} \omega^2 - \omega k_z - \epsilon_{\boldsymbol{p}}^2 + \frac{1}{4}\boldsymbol{k}^2 & -i\left(\boldsymbol{p}\times\boldsymbol{k}\right)_x - \left(\boldsymbol{p}\times\boldsymbol{k}\right)_y \\ -i\left(\boldsymbol{p}\times\boldsymbol{k}\right)_x + \left(\boldsymbol{p}\times\boldsymbol{k}\right)_y & \omega^2 + \omega k_z - \epsilon_{\boldsymbol{p}}^2 + \frac{1}{4}\boldsymbol{k}^2 \end{pmatrix} = 0,$$

where $\epsilon_{\boldsymbol{p}} = (M^2 + \boldsymbol{p}^2)^{1/2}$. Finally, using

$$\begin{aligned} \left[\left(\boldsymbol{p}\times\boldsymbol{k}\right)_y - i\left(\boldsymbol{p}\times\boldsymbol{k}\right)_x\right]\left[-i\left(\boldsymbol{p}\times\boldsymbol{k}\right)_x - \left(\boldsymbol{p}\times\boldsymbol{k}\right)_y\right] &= -\left(\boldsymbol{p}\times\boldsymbol{k}\right)_x^2 - \left(\boldsymbol{p}\times\boldsymbol{k}\right)_y^2 \\ &= -\left(\boldsymbol{p}\times\boldsymbol{k}\right)^2 \\ &= \left(\boldsymbol{p}\cdot\boldsymbol{k}\right)^2 - \boldsymbol{k}^2\boldsymbol{p}^2, \end{aligned} \tag{2.100}$$

we arrive at

$$\left(\omega^2 - \epsilon_{\boldsymbol{p}}^2 + \frac{1}{4}\boldsymbol{k}^2\right)^2 - \omega^2\boldsymbol{k}^2 + \boldsymbol{k}^2\boldsymbol{p}^2 - \left(\boldsymbol{p}\cdot\boldsymbol{k}\right)^2 = 0. \tag{2.101}$$

The solutions to (2.101) are

$$\omega(\boldsymbol{p}) \quad = \pm\sqrt{\epsilon_{\boldsymbol{p}}^2 + \tfrac{1}{4}\boldsymbol{k}^2 \pm \sqrt{\boldsymbol{k}^2 M^2 + (\boldsymbol{p}\cdot\boldsymbol{k})^2}}, \tag{2.102}$$

where the two "±" are independent of each other.

The quasiparticle energies (2.102) help us to understand why the dual chiral density wave is more favorable than a mere homogeneous condensate. In the $z$ direction,

$$\omega(\boldsymbol{p}) \quad = \pm\sqrt{\epsilon_{\boldsymbol{p}}^2 + \tfrac{1}{4}\boldsymbol{k}^2 \pm \sqrt{\boldsymbol{k}^2 M^2 + (\boldsymbol{p}\cdot\boldsymbol{k})^2}}, \tag{2.103}$$

and in the transverse direction to $z$,

$$\omega(p_x) = \pm\sqrt{M^2 + p_x^2 + \frac{1}{4}k_z^2 \pm k_z M} = \pm\sqrt{\left(M \pm \frac{1}{2}k_z\right)^2 + p_x^2}. \tag{2.104}$$

We can see that $k_z$ splits the energy levels, and acts as effective modifications to the chiral mass $M$ of the quasiparticles; such effects lower the energy of the Dirac sea, making this dual chiral density wave state more energetically favorable than the homogeneous scalar state. Indeed, in numerical studies the dual chiral density wave is found to be more favorable than the scalar state at intermediate density [40].

### 2.3.2 Running wave charged pion condensation

We now turn to the running wave charged pion condensate at mean field, characterized by [3]

$$\pi(\boldsymbol{x}) \quad = \quad \frac{1}{\sqrt{2}}\kappa \sin\theta\, e^{i\boldsymbol{k}\cdot\boldsymbol{x}}, \tag{2.105}$$

$$\pi_0(\boldsymbol{x}) \quad = \quad 0, \tag{2.106}$$

$$\sigma(\boldsymbol{x}) \quad = \quad \kappa\cos\theta. \tag{2.107}$$

Like the chiral density wave, we can understand the origin of energy lowering from the quasiparticle excitations; the techniques will be similar. The mean field quark inverse propagator is now

$$\begin{aligned} \mathcal{G}^{-1} \quad &= \quad i\partial\!\!\!/ + 2G\kappa\left(\cos\theta + i\gamma_5\begin{pmatrix} 0 & e^{-i\boldsymbol{k}\cdot\boldsymbol{x}}\sin\theta \\ e^{i\boldsymbol{k}\cdot\boldsymbol{x}}\sin\theta & 0 \end{pmatrix}\right) \\ &= \quad p\!\!\!/ + 2G\kappa\left[\cos\theta + i\gamma_5\left(\tau_+ e^{-i\boldsymbol{k}\cdot\boldsymbol{x}} + \tau_- e^{i\boldsymbol{k}\cdot\boldsymbol{x}}\right)\sin\theta\right], \end{aligned} \tag{2.108}$$

where the rising and lowering operators in isospin space are

$$\tau_\pm = \frac{1}{2}\left(\tau_1 \pm i\tau_2\right). \tag{2.109}$$

To simplify the calculation, we first perform a chiral boost along the $\tau_3$ axis

$$q(\boldsymbol{x}) \to e^{-i\boldsymbol{k}\cdot\boldsymbol{x}\frac{1}{2}\tau_3} q(\boldsymbol{x}) = q'(\boldsymbol{x}); \tag{2.110}$$

together with the properties

$$e^{-i\boldsymbol{k}\cdot\boldsymbol{x}\frac{1}{2}\tau_3}\tau_\pm e^{i\boldsymbol{k}\cdot\boldsymbol{x}\frac{1}{2}\tau_3} = \tau_\pm e^{\mp i\boldsymbol{k}\cdot\boldsymbol{x}}, \tag{2.111}$$

we have

$$\mathcal{G}^{-1} = i\partial\!\!\!/ + \frac{1}{2}\tau_3\boldsymbol{\gamma}\cdot\boldsymbol{k} + 2G\kappa e^{i\gamma_5\tau_1\theta}. \tag{2.112}$$

The axial phase angle along $\tau_1$ direction can be further rotated away by another transformation

$$q \to e^{-\frac{1}{2}i\gamma_5\tau_1\theta} q,\ \ \bar{q} \to \bar{q} e^{-\frac{1}{2}i\gamma_5\tau_1\theta}; \tag{2.113}$$

together with

$$\begin{aligned}
& e^{-\frac{1}{2}i\gamma_5\tau_1\theta}\tau_3\boldsymbol{\gamma}\cdot\boldsymbol{k}e^{-\frac{1}{2}i\gamma_5\tau_1\theta} \\
= & \left(\cos\frac{\theta}{2} - i\gamma_5\tau_1\sin\frac{\theta}{2}\right)\tau_3\boldsymbol{\gamma}\cdot\boldsymbol{k}\left(\cos\frac{\theta}{2} - i\gamma_5\tau_1\sin\frac{\theta}{2}\right) \\
= & \tau_3\boldsymbol{\gamma}\cdot\boldsymbol{k}\cos^2\frac{\theta}{2} + \tau_1\tau_3\tau_1\boldsymbol{\gamma}\cdot\boldsymbol{k}\sin^2\frac{\theta}{2} - \frac{1}{2}i\left(\tau_3\tau_1\boldsymbol{\gamma}\cdot\boldsymbol{k}\gamma_5 + \tau_1\tau_3\gamma_5\boldsymbol{\gamma}\cdot\boldsymbol{k}\right)\sin\theta \\
= & \boldsymbol{\gamma}\cdot\boldsymbol{k}\left(\tau_3\cos\theta + \gamma_5\tau_2\sin\theta\right),
\end{aligned} \tag{2.114}$$

we finally obtain

$$\mathcal{G}^{-1} = \begin{pmatrix} i\partial\!\!\!/ + \frac{1}{2}\boldsymbol{\gamma}\cdot\boldsymbol{k}\cos\theta - M & -\frac{i}{2}\boldsymbol{\gamma}\cdot\boldsymbol{k}\gamma_5\sin\theta \\ \frac{i}{2}\boldsymbol{\gamma}\cdot\boldsymbol{k}\gamma_5\sin\theta & i\partial\!\!\!/ - \frac{1}{2}\boldsymbol{\gamma}\cdot\boldsymbol{k}\cos\theta - M \end{pmatrix}, \tag{2.115}$$

or, in chiral basis $q = (u_L, u_R, d_L, d_R)^T$,

$$\mathcal{G}^{-1} = \begin{pmatrix} \omega + \boldsymbol{\sigma}\cdot\boldsymbol{p}^- & M & -\frac{i}{2}\boldsymbol{\sigma}\cdot\boldsymbol{k}\sin\theta & 0 \\ M & \omega - \boldsymbol{\sigma}\cdot\boldsymbol{p}^- & 0 & -\frac{i}{2}\boldsymbol{\sigma}\cdot\boldsymbol{k}\sin\theta \\ \frac{i}{2}\boldsymbol{\sigma}\cdot\boldsymbol{k}\sin\theta & 0 & \omega + \boldsymbol{\sigma}\cdot\boldsymbol{p}^+ & M \\ 0 & \frac{i}{2}\sigma\cdot\boldsymbol{k}\sin\theta & M & \omega - \sigma\cdot\boldsymbol{p}^+ \end{pmatrix}, \tag{2.116}$$

where $\boldsymbol{p}^\pm \equiv \boldsymbol{p} \pm \frac{1}{2}\boldsymbol{k}\cos\theta$. The energy eigenvalues solved from $\det\mathcal{G}^{-1}$ is then

$$\omega = \pm\sqrt{\epsilon_{\boldsymbol{p}}^2 + \frac{1}{4}\boldsymbol{k}^2 \pm \sqrt{(\boldsymbol{p}\cdot\boldsymbol{k})^2 + M^2\boldsymbol{k}^2\sin^2\theta}}, \tag{2.117}$$

which is similar in form to the quasiparticle energies of the dual chiral density wave (2.102). When $\theta = \pi/2$, the two types of condensation have exactly the same quasiparticle energies. This is a less obvious consequence of chiral

symmetry. For $\theta = \pi/2$, the running wave charged pion condensate moves on a circle of radius $\kappa$ on the 4-sphere in the $(\sigma, \boldsymbol{\pi})$ space; this circle is the intersection of the $\pi_1, \pi_2$ plane with the 4-sphere. The dual chiral density wave also moves on a circle like this, but on the interaction of the $\sigma, \pi_3$ plane with the 4-sphere instead. When isospin symmetry is respected, these two "paths" are equivalent, and one can go from one circle to the other by a rotation in the $(\sigma, \boldsymbol{\pi})$ space. When $\theta \neq \pi/2$, the path of the running wave charged pion condensate on the 4-sphere is a circle with radius $\kappa \sin\theta$, and can no longer be transformed into the other circle (the dual chiral density wave) which has a different radius.

So far we have only considered the reduction in Dirac sea energy due to the condensates. We now consider medium effects. In the nuclear matter or quark matter at low density, isospin symmetry is broken by charge neutrality. Since up quarks carry charge 2/3 and down quarks -1/3, there are in general almost twice many down quarks than up quarks (the amount of leptons in nuclear matter up to $2n_0$ is usually small compared to quark density); the chemical potential for charged pions $\mu_\pi$ is equal to the electric charge chemical potential $\mu_Q$ – the energy change to the system by increasing the total charge by unity. With excessive down quarks, it can become energetically favorable for a down quark to become an up quark via emitting a $\pi^-$ due to the difference in Fermi sea. If such process yields more energy gain from moving a high momentum state to a low momentum state in quark sector than the energy cost of producing a pion, then the system will spontaneously generate pions; a pion condensate will be formed. This energy consideration is a simple but useful criteria for the onset of pion condensation. On the other hand, the neutral pion does not couple to electric charges, and thus does not receive favors from isospin asymmetry.

### 2.3.3 Charged pions in dense matter beyond mean field

Having considered the Dirac sea effect of the dual chiral density wave and charged pion running wave condensates, we now consider, beyond mean field, charged pions $\pi^\pm$ in dense quark matter, and how their self-energy is affected by interaction with the medium. We assume the system to be in a scalar state $\boldsymbol{\pi} = 0$.

In the bosonized theory, the effective action in quadratic order in $\hat{\pi} \equiv \hat{\pi}_1 + i\hat{\pi})2$ as computed in Sec. 2.1.3 yields the charged pion inverse propagator up to a renormalization constant

$$\begin{aligned} \mathcal{G}_\pi^{-1}(k) &= B_\pi(k) - \frac{1}{2G}, \\ B_\pi(k) &= N_f N_c i \int_p \mathrm{tr}[\mathcal{G}_u(p-k) i\gamma_5 \mathcal{G}_d(p) i\gamma_5]. \end{aligned} \tag{2.118}$$

The pion dispersion relation is again $\det \mathcal{G}_\pi^{-1}(\omega, \boldsymbol{p}) = 0$. To solve this equation,

we first compute the bubble (cf. Eq. (4.1))

$$\begin{aligned} B_\pi(k) &= 2N_f N_c i \int_p \left[ \frac{1}{(p_0+\mu_u)^2-\epsilon_p^2} + \frac{1}{(p_0+\mu_d)^2-\epsilon_p^2} \right. \\ &\quad \left. - \frac{(k_0-\mu_u+\mu_d)^2-\boldsymbol{k}^2}{\left[(p_0-k_0+\mu_u)^2-\epsilon_{p-k}^2\right]\left[(p_0+\mu_d)^2-\epsilon_p^2\right]} \right] \\ &= J_1 + \frac{1}{2}k^2 J_2(k^2). \end{aligned} \tag{2.119}$$

Evaluating $J_2(k^2)$, we find

$$\begin{aligned} &\frac{1}{4N_f N_c} J_2(k^2) \\ &= -i \int_p \frac{1}{\left[(p_0-k_0+\mu_u)^2-\epsilon_{p-k}^2\right]\left[(p_0+\mu_d)^2-\epsilon_p^2\right]} \\ &= \int_{\boldsymbol{p}} T \sum_n \left(i\omega_n - k_0 + \mu_u - \epsilon_{p-k}\right)^{-1} \left(i\omega_n - k_0 + \mu_u + \epsilon_{p-k}\right)^{-1} \\ &\times \left(i\omega_n + \mu_d - \epsilon_p\right)^{-1} \left(i\omega_n + \mu_d + \epsilon_p\right)^{-1} \\ &= \int_{\boldsymbol{p}} T \sum_n \frac{1}{4\epsilon_p \epsilon_{p-k}} \left( \frac{1}{i\omega_n - k_0 + \mu_u - \epsilon_{p-k}} - \frac{1}{i\omega_n - k_0 + \mu_u + \epsilon_{p-k}} \right) \\ &\times \left( \frac{1}{i\omega_n + \mu_d - \epsilon_p} - \frac{1}{i\omega_n + \mu_d + \epsilon_p} \right) \\ &= \frac{1}{4N_f N_c} \left( J_{pp} + J_{\bar{p}\bar{p}} + J_{\bar{p}p} \right), \end{aligned} \tag{2.120}$$

where the particle-particle ($pp$), antiparticle-antiparticle ($\bar{p}\bar{p}$), and particle- antiparticle ($\bar{p}p$) contributions are

$$\begin{aligned} J_{pp} &= 4N_f N_c \int_{\boldsymbol{p}} \frac{1}{4\epsilon_p \epsilon_{p-k}} \left[ \frac{f(\epsilon_{p-k}-\mu_u) - f(\epsilon_p - \mu_d)}{k_0 + \mu_\pi + \epsilon_{p-k} - \epsilon_p} \right], \\ J_{\bar{p}\bar{p}} &= 4N_f N_c \int_{\boldsymbol{p}} \frac{1}{4\epsilon_p \epsilon_{p-k}} \left[ \frac{f(\epsilon_p+\mu_d) - f(\epsilon_{p-k}+\mu_u)}{k_0 + \mu_\pi - \epsilon_{p-k} + \epsilon_p} \right], \\ J_{\bar{p}p} &= 4N_f N_c \int_{\boldsymbol{p}} \frac{1}{4\epsilon_p \epsilon_{p-k}} \left[ -\frac{1 - f(\epsilon_{p-k}+\mu_u) - f(\epsilon_p - \mu_d)}{k_0 + \mu_\pi - \epsilon_{p-k} - \epsilon_p} \right. \\ &\quad \left. + \frac{1 - (\epsilon_p+\mu_d) - f(\epsilon_{p-k}-\mu_u)}{k_0 + \mu_\pi + \epsilon_{p-k} + \epsilon_p} \right]; \end{aligned} \tag{2.121}$$

the pion chemical potential is $\mu_\pi = \mu_d - \mu_u$. Together with the gap equation (2.23), we find the dispersion equation

$$0 = k^2 \left[ J_{\bar{p}p}(k) + J_{pp}(k) + J_{\bar{p}\bar{p}}(k) \right] - \frac{2m_q}{GM}, \tag{2.122}$$

The antiparticle term $J_{\bar{q}\bar{q}}$ vanishes at $T = 0$. The particle-antiparticle term, $J_{\bar{p}p}$, is made of a logarithmically divergent piece plus a finite medium term; in

the vacuum, this term is absorbed during field renormalization, and is related to the $I_2$ term in Sec. 2.2 by

$$J_{\bar{p}p}(0) = 4I_2. \tag{2.123}$$

Further more $J_{\bar{p}p}(k)$ only has a weak $k$-dependence, since the correction in powers of $k$ will be at most finite, compared to the logarithmically diverging zeroth order term. Thus, we replace $J_{\bar{p}p}(k)$ by $I_2$, which will be absorbed in the renormalization procedure. Using $g^{-2} = 2I_2$ and the GMOR relation derived earlier, we find that the dispersion relation can be written as

$$\begin{aligned} 0 &= \omega^2 - \boldsymbol{k}^2 - m_\pi^2 - \frac{g^2}{2}\left(\omega^2 - \boldsymbol{k}^2\right) J_{pp}(k) \\ &\equiv \omega^2 - \boldsymbol{k}^2 - m_\pi^2 - \Pi(\omega, \boldsymbol{k}), \end{aligned} \tag{2.124}$$

where we use $\Pi(\omega = k_0 + \mu_\pi, \boldsymbol{k})$ to denote the self-energy, a consequence of the particle-particle term; it corresponds to the interaction between pion and the quarks:

$$\Pi(\omega, \boldsymbol{k}) = \frac{1}{2} N_f N_c \int_{\boldsymbol{p}} \frac{g^2(\omega^2 - \boldsymbol{k}^2)}{\epsilon_p \epsilon_{p-k}} \times \frac{f(\epsilon_p - \mu_d) - f(\epsilon_{p-k} - \mu_u)}{\omega + \epsilon_{p-k} - \epsilon_p}. \tag{2.125}$$

If we consider long wavelength limit $\boldsymbol{k} \ll M$, then

$$\begin{aligned} \Pi(\omega, \boldsymbol{k}) &\approx \frac{1}{2} N_f N_c \int_{\boldsymbol{p}} \frac{g^2(\omega^2 - \boldsymbol{k}^2)}{\epsilon_p^2} \times \frac{f(\epsilon_p - \mu_d) - f(\epsilon_p - \mu_u)}{\omega} \\ &= \omega g^2 \frac{1}{2} N_f N_c \int_{\boldsymbol{p}} \frac{f_d - f_u}{\epsilon_p^2} - \frac{\boldsymbol{k}^2}{\omega} g^2 \frac{1}{2} N_f N_c \int_{\boldsymbol{p}} \frac{f_d - f_u}{\epsilon_p^2} \\ &\equiv \Pi_s(\omega, \boldsymbol{k}) + \Pi_p(\omega, \boldsymbol{k}), \end{aligned} \tag{2.126}$$

where we write $f_{u,d}(p) = f(\epsilon_p - \mu_{u,d})$ for short. In the limit of heavy quarks $M \to \infty$, the two parts of the self-energy become

$$\Pi_s = \frac{\omega}{2 f_\pi^2}(n_d - n_u), \ \Pi_p = -\frac{\boldsymbol{k}^2}{2\omega f_\pi^2}(n_d - n_u). \tag{2.127}$$

The self-energies (2.127) are effectively the repulsive s-wave and attractive p-wave interaction contribution to the pion self-energy in nuclear matter, as we now demonstrate below.

In nuclear matter consisting of neutrons and protons, the p-wave pion-nucleon interaction Hamiltonian is [3]

$$H_{\mathrm{p-wave}} = -\sqrt{2}\frac{f}{m_\pi} \int_{\boldsymbol{r}} \left[\psi_n^+ \boldsymbol{\sigma} \cdot \nabla \pi \psi_p + h.c.\right], \tag{2.128}$$

where $\psi_{n,p}$ are non-relativistic neutron/proton field operators, $\boldsymbol{\sigma}$ the Pauli matrices, $\pi$ the charged pion field, and the rationalized coupling constant $f$,

which is related to the fully renormalized $\pi - N$ coupling constant $g_N$ by $f/m_\pi = g_N/2m_N, m_N$ being the nucleon mass. The dimensionless coupling constant $g_A$ is defined to be $g_A = f_\pi g_N/m_N$, and has a numerical value $\approx 1.36$ after renormalization of the nucleon axial current. The energy shift due to a pion with momentum $\boldsymbol{k}$ added to the medium, $\Delta E(\boldsymbol{k})$ can be evaluated via second-order perturbation theory:

$$\Delta E(\boldsymbol{k}) = \sum_\ell \frac{|\langle \ell | H_{\mathrm{p-wave}} | 0 \rangle|^2}{E_0 - E_\ell}, \tag{2.129}$$

summed over all intermediate states labeled by $\ell$. In the nuclear medium two processes can happen:

$$\begin{aligned} n + \pi^- &\to 2\pi^- + p, \\ p + \pi^- &\to n. \end{aligned} \tag{2.130}$$

For the first process, the matrix element of a neutron decaying into a pion and a proton is

$$\langle \pi^- p | H_{\mathrm{p-wave}} | n \rangle = -\sqrt{2} \frac{f}{m_\pi} s_p^* \left( \boldsymbol{\sigma} \cdot \frac{-i\boldsymbol{k}}{\sqrt{2\omega_k V}} \right) s_n, \tag{2.131}$$

where $s_{n,p}$ are the neutron/proton spinors, $V$ is the 3-volume, and $\omega_k = (m_\pi^2 + \boldsymbol{k}^2)^{1/2}$ is the free pion energy; then the starting state energy is $\omega_k + \boldsymbol{p}^2/2m_N$ ($\boldsymbol{p}$ is the neutron momentum), and the intermediate state energy is $2\omega_k + (\boldsymbol{p} - \boldsymbol{k})^2/2m_N$. Thus the energy shift for this first process is

$$\Delta E_1 = \frac{2}{\omega_k V} \left( \frac{f\boldsymbol{k}}{m_\pi} \right)^2 \sum_{\boldsymbol{p}} \frac{f_n(\boldsymbol{p})(1 - f_p(\boldsymbol{p} - \boldsymbol{k}))}{-\omega_k + \frac{\boldsymbol{p}^2}{2m_N} - \frac{(\boldsymbol{p}-\boldsymbol{k})^2}{2m_N}}. \tag{2.132}$$

Similarly, the contribution from the second process is

$$\Delta E_2 = \frac{2}{\omega_k V} \left( \frac{f\boldsymbol{k}}{m_\pi} \right)^2 \sum_{\boldsymbol{p}} \frac{f_p(\boldsymbol{p})(1 - f_n(\boldsymbol{p} - \boldsymbol{k}))}{\omega_k - \frac{\boldsymbol{p}^2}{2m_N} + \frac{(\boldsymbol{p}-\boldsymbol{k})^2}{2m_N}}. \tag{2.133}$$

The pion energy is then $\omega = \omega_k + \Delta E$, where $\Delta E = \Delta E_1 + \Delta E_2$. At leading order in $\boldsymbol{k}^2$, we find

$$\begin{aligned} \omega^2 &= \omega_k^2 + 2\omega \Delta E + \mathcal{O}(\boldsymbol{k}^2) \\ &= \omega_k^2 - \left( \frac{g_A \boldsymbol{k}}{f_\pi} \right)^2 \int_p \frac{f_n(\boldsymbol{p}) - f_p(\boldsymbol{p} - \boldsymbol{k})}{\omega_k + E_{p-k} - E_p} \\ &\equiv \omega_k^2 + \Pi_p^{(N)}(\omega_k, \boldsymbol{k}). \end{aligned} \tag{2.134}$$

where the non-relativistic nucleon energies are $E_p = \boldsymbol{p}^2/2M_N$ and the nucleon

distribution functions $f_{p,n}(\boldsymbol{p}) = f(E_p - \mu_{p,n})$. The dispersion equation is then

$$0 = \omega^2 - \boldsymbol{k}^2 - m_\pi^2 - \Pi_p^{(N)}(\omega_k, \boldsymbol{k}). \tag{2.135}$$

Equation (2.135) can be improved by using in-medium pion states instead of free pion states. This is done by replacing the free pion energy in the self-energy term $\omega_k$ by the in-medium energy $\omega$, resulting in a self-consistent description.

The s-wave repulsive interaction between nucleons and charged pion is

$$\mathcal{H}_{\mathrm{s-wave}} = \frac{1}{4f_\pi^2}\left(\psi_n^\dagger\psi_n - \psi_p^\dagger\psi_p\right) i\left(\pi^\dagger\partial_0\pi - \partial_0\pi^\dagger\pi\right), \tag{2.136}$$

resulting in additional self-energy

$$\Pi_s^{(N)}(\omega, \boldsymbol{p}) = \frac{\omega}{2f_\pi^2}(n_n - n_p). \tag{2.137}$$

In total, the pion dispersion equation in non-relativistic nucleon medium is

$$0 = \omega^2 - \boldsymbol{k}^2 - m_\pi^2 - \Pi_p^{(N)}(\omega, \boldsymbol{k}) - \Pi_s^{(N)}(\omega, \boldsymbol{k}). \tag{2.138}$$

If we take the heavy nucleon approximation $M_N \to \infty$, then

$$\Pi_p^{(N)}(\omega, \boldsymbol{k}) = -\frac{g_A^2\boldsymbol{k}^2}{2\omega f_\pi^2}(n_n - n_p). \tag{2.139}$$

Compared with the quark matter result (2.127) and noticing $n_d - n_u = n_n - n_p$, we find that the pion self-energy is identical in quark and nuclear matter at fixed baryon and isospin density, up to an axial current renormalization factor $g_A \neq 1$.[4] This suggests that the pions described in nuclear matter are smoothly connected to the quark matter pions across the transition from nuclear matter to quark matter.

We next identify the pionic modes exhibited by the dispersion relation (2.124), which is no longer trivial when the self-energies as functions of $\omega$ are taken into account. Let us first consider the masses of the modes at $\boldsymbol{k} = 0$, given by the solutions of

$$\begin{aligned} m_\pi^2 &= \omega^2\left(1 - \frac{N_f N_c g^2}{\omega}\int_{\boldsymbol{p}} \frac{f(\epsilon_p - \mu_d) - f(\epsilon_p - \mu_u)}{\epsilon_p^2}\right) \equiv \omega^2\left(1 - \frac{A(\mu_u, \mu_d)}{\omega}\right) \\ &= \omega^2 - A(\mu_u, \mu_d)\omega; \end{aligned} \tag{2.140}$$

[4] It remains an open question how the axial current renormalization of the quark-pion coupling will modify $g_A$, and how such renormalization differs in the nuclear matter. We leave this problem to future research.

there are two solutions,

$$\omega = \frac{1}{2}\left(A(\mu_u,\mu_d) \pm \sqrt{A(\mu_u,\mu_d)^2 + 4m_\pi^2}\right) \tag{2.141}$$

$$= \pm m_\pi + \frac{1}{2}A(\mu_u,\mu_d) + \mathcal{O}(A^2); \tag{2.142}$$

thus, we still have two modes, $\pi^-$ and $\pi^+$, but with split masses

$$\begin{aligned} m_{\pi^-} &= m_\pi + A(\mu_u,\mu_d), \\ m_{\pi^+} &= m_\pi - A(\mu_u.\mu_d). \end{aligned} \tag{2.143}$$

In electrically neutral matter and in the heavy quark limit $M \to \infty$, $\mu_d > \mu_u$, and $A(\mu_u,\mu_d) > 0$; in this case the $\pi^-$ mass is increased, while the $\pi^+$ mass is decreased. This is expected, since creating a $\pi^-$ requires changing a $u$ quark into a $d$ quark, which will cost more energy than in the vacuum since the $d$ quark Fermi sphere is significantly larger.

When $\boldsymbol{k} \neq 0$, additional modes will appear. In this case we need to solve

$$\begin{aligned} m_\pi^2 &= \left(\omega^2 - \boldsymbol{k}^2\right)\left(1 - \frac{1}{2}N_f N_c g^2 \int_{\boldsymbol{p}} \frac{1}{\epsilon_p \epsilon_{p-k}} \cdot \frac{f(\epsilon_p - \mu_d) - f(\epsilon_{p-k} - \mu_u)}{\omega - \epsilon_p + \epsilon_{p-k}}\right) \\ &\equiv \left(\omega^2 - \boldsymbol{k}^2\right)\left(1 - \frac{A(\mu_u,\mu_d,\boldsymbol{k})}{\omega}\right), \end{aligned} \tag{2.144}$$

where the momentum dependence of $A$ is now important. The dispersion equation is also now third order in $\omega$, so there are potentially three modes instead of two. This is easier seen by assuming $m_\pi = 0$; then, in addition to the two "free" pion modes $\omega = \pm|\boldsymbol{k}|$, we have another solution

$$\omega = A(\mu_u,\mu_d,\boldsymbol{k}). \tag{2.145}$$

The function $A$ is decreasing as $\boldsymbol{k}$ increases and starts at $A(\boldsymbol{k}=0) > 0$; as a result, two solutions will intersect at $A(\boldsymbol{k}) = |\boldsymbol{k}|$. To identify the modes with the presence of branch crossing, we need to look at the sign of the residues of the pion inverse propagator near the corresponding poles, i.e. zeros of the dispersion equation. At low momentum $|\boldsymbol{k}| < A(\boldsymbol{k})$, the residue for the pole at $\omega = |\boldsymbol{k}|$ is negative, in contrast to a positive residue without medium modification $A = 0$; thus, this solution actually corresponds to a quantum number of $\pi^+$ instead of $\pi^-$, in addition to the already existing "free" $\pi^+$ mode; the energy of such excitation is the negative of the $\omega$, thus $-|\boldsymbol{k}|$. This mode, denoted as $\pi_s^+$, is known as the spin-isospin zero sound mode as in nuclear matter [41], and describes a collective excitation featuring spatial locking of nucleon (quark) spin and isospin. The $\pi^-$ mode in this regime is actually the $\omega = A(\boldsymbol{k})$ solution, describing a $\pi^-$ mode with a mass of $A(0)$. The "free" $\pi^+$ mode remains unchanged and remains massless.

Above the spectrum crossing point $|\boldsymbol{k}| > A(\boldsymbol{k})$, the residues for the original

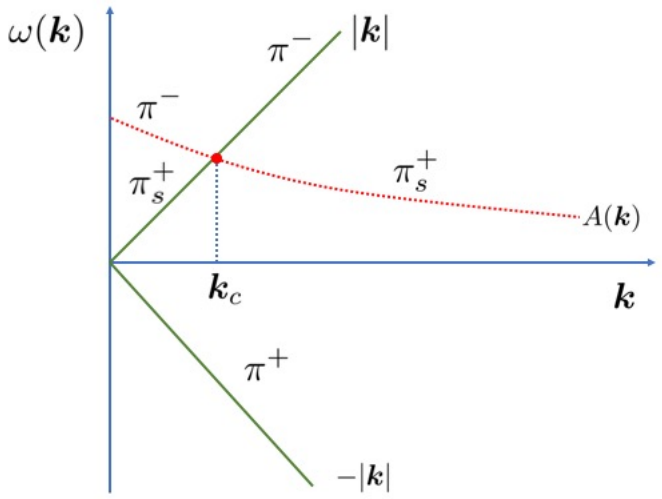


Figure 2.3: Schematic plot of the $\omega(\boldsymbol{k})$ solutions and their corresponding pionic modes. The crossing $|\boldsymbol{k}| = A(\boldsymbol{k})$ happens at some critical momentum $\boldsymbol{k}_c$, where the $\pi^-$ and $\pi_s^+$ modes have exactly opposite energies equal in magnitude. This critical momentum $\boldsymbol{k}_c$ will be the wave vector of the charged pion running wave condensate at onset.

branches of $\pi^-$ and $\pi_s^+$ switche sign; as a result, the $\pi^-$ mode now carries energy $+|\boldsymbol{k}|$, and the $\pi_s^+$ mode has energy $-A(\boldsymbol{k})$. The $\omega(\boldsymbol{k})$ solutions and their corresponding pionic modes are summarized in Fig. 2.3.

At the crossing point, the total energy of producing a pair of $\pi_s^+$ and $\pi^-$ vanishes; it becomes energetically favorable for the system to spontaneously produce such pairs. On the other hand, the system can also produce a $u$ particle and $d$ hole (denoted as $u\bar{d}$), which also costs negative energy; the total energy cost of producing $\pi^-$ plus a $u\bar{d}$ is reduced. These two processes correspond to two possible pathways of $\pi^-$ condensation. When the total energy change of such processes is negative

$$\delta E = E(\pi^- + u\bar{d}) \text{ or } E(\pi^- + \pi_s^+) \leq 0, \tag{2.146}$$

the system becomes unstable against spontaneous production of such pairs, and the $\pi^-$ mode will be generated macroscopically, eventually forming a pion condensate. This is the pion condensation onset criteria from the pion energy perspective. Since $\mu_Q$ by definition is the lowest energy cost of increasing the system's electric charge by unity, we can equivalently state the condensation threshold criteria as $E(\pi^-) - \mu_Q = E(\pi^-) - \mu_\pi \leq 0$.

The strategy outlined in this section is easily generalized to three flavors, even with diquark pairing. By computing the dispersion relation, obtained from the poles of meson propagators, we identify all the mesonic modes, some of them being collective excitations in addition to the NG bosons (e.g., the $\pi_s^+$

mode). By calculating the mode energies, we find whether there are certain quantum-number preserving productions of such modes. If any energetically favorable channels appear, the meson condensation will emerge; this method also suggests the type of meson condensation.

Our demonstration of this method is based on computing meson inverse propagator in the scalar state. However, one can compute the meson inverse propagator at any given mean field state, even those with existing meson condensation. In this way, one can check the stability of any given meson condensation; if the condensation turns out to be unstable, the mode analysis will point out the direction of configuration (e.g., in the chiral $(\sigma, \pi)$ plane) in which the instability develops. Specific application of this method for realistic $N_f = 3$ models can be considered in future studies.

# Chapter 3

# Chiral symmetry breaking at high density: diquark pairing

The discussions of the last Chapter are mostly relevant at lower densities where heavy strange quarks are largely absent. As the baryon chemical potential rises, at some point the energy cost of adding more light quarks surpasses the large strange quark mass, and strange quarks begin to accumulate. At high density, all three quark flavors reach similar Fermi momenta, and diquark pairing begins to develop. The study of chiral symmetry breaking and the Nambu-Goldstone (NG) bosons at such high density must take the strange quarks as well as the diquark condensates into account, as we discuss in this Chapter.

The introduction of diquarks, in addition to leading to gapped quasiparticles (which we discussed in Sec. 3.1), modifies the quark structure of the NG bosons. Specifically, the fluctuations of the diquark condensate result in $\bar{q}\bar{q}qq$-type fluctuations in the NG boson wave function. While the NG bosons have been studied in the limits of low density (non-BCS paired) $\bar{q}q$ condensed matter [42, 43, 44, 45, 46] and high density pure-BCS $qq$ paired matter [47, 48, 49, 50] using the Nambu-Jona-Lasinio (NJL) model [1, 2, 23], a quantitative description of NG mesons at intermediate densities remains an open problem. Such a description requires adopting specific models to describe the changing phase structure with increasing density, itself an unresolved issue [51]. In Sec. 3.2 of this Chapter, we study the chiral structure of a simplified single flavor, single color NJL model that includes both scalar and pseudoscalar condensates. Such a model has a single chiral NG mode, which we refer to as the *generalized pion*,[1] $\pi_G$, corresponding to simultaneous fluctuations of the $\langle\bar{q}q\rangle$ and $\langle qq\rangle$ order parameters. The resulting phase diagram, with properly chosen model interaction parameters, mimics the more realistic QCD phase diagram in terms of chiral symmetry breaking by the low and high density condensates, which are here connected smoothly by a coexistence region (for sophisticated NJL constructions of QCD phase diagram, see e.g., [27, 52, 53, 54, 55, 56, 57, 58, 59, 60, 61, 62, 63]). The generalized pion continuously evolves from the vacuum pion, $\pi$, in the low density chirally broken phase to the diquark-condensate pion, $\pi_d$, in the high density BCS phase; its mass and decay constant are continuous functions of

[1] The name "generalized mesons" was used, e.g., in [64], to describe the $\bar{q}\bar{q}qq$ modes corresponding to fluctuations of the diquark condensates at high density. For clarity, we refer in this paper to the NG modes (a combination of $\bar{q}q$ and $\bar{q}\bar{q}qq$ modes) as "generalized mesons," the $\bar{q}\bar{q}qq$ modes as "diquark-condensate mesons," and the usual $\bar{q}q$ modes as "vacuum mesons."

quark density, and obey a generalized Gell-Mann–Oakes–Renner (GMOR) relation, which we calculate to second order in $m_q$. Its coupling vertex to the quark field also changes continuously with increasing density.

It is remarkable that diquark fluctuations in the form of $\bar{q}\bar{q}qq$ can be smoothly connected with the chiral fluctuations $\bar{q}q$ to form the generalized mesons; this results from the $N_f = N_c = 3$ CFL diquarks, being totally antisymmetric in spin, color and flavor; they form a $\bar{3} \otimes \bar{3}$ representation of flavor and color, and thus, $qq$ behaves like an antiquark $\bar{q}$. In addition, in Chapter 5 we will directly construct a gauge-invariant description of diquark mesons, which are formed by diquark-dressed quarks, screened by the colored condensate; the locking of colors and flavors effectively "transforms" color degrees of freedom into flavors in the dressed theory. The colors carried by the diquark fluctuations, as a result, poses no issues in the construction of eventually gauge-invariant NG bosons.

The study presented in this Chapter is a first step in understanding in detail the density-dependent properties of the pseudoscalar mesons extrapolated into high density quark matter, and is readily generalized to more realistic models with multiple flavors and colors to quantitatively study the meson mass ordering reversal problem [65] (e.g., the kaons, originally heavier than the pions in the vacuum, becomes the lightest meson in the CFL phase; the pion becomes heavier due to strange quarks). In addition to clarifying the QCD phase diagram in terms of generalized meson condensation, the study of the $\pi_G$ mode also contributes to understanding the thermodynamics of dense matter, and thus eventually the interiors and cooling of neutron stars [66].

This Chapter is organized as follows. We first give an introduction to the diquark pairing described in NJL in Sec. 3.1, in particular the color-flavor-locked (CFL) pairing and the two-flavor, two-color partial pairing (2SC), commonly found in quark matter phase diagram studies. Then we use a schematic NJL model to investigate spontaneous chiral symmetry breaking in the presence of both chiral and diquark condensates in Sec. 3.2. We lay down the roadmap to generalization to more realistic models in Sec. 3.3 and 3.4, by presenting a self-consistent formalism of calculating generalized meson correlation functions, and how to perturb those correlation functions by a current (bare) quark mass $m_q$ in order to obtain generalized GMOR relations of NG boson masses expressed in powers of $m_q$, thus determining the spectrum of the low energy mesonic excitations.

## 3.1 Diquark pairing in the NJL model

### 3.1.1 Diquark condensates: CFL and 2SC in the NJL model

We first consider diquark pairing alone in the NJL model, described by

$$\begin{aligned}\mathcal{L} &= \bar{q}(\not{p} - \hat{m}_q + \gamma^0\hat{\mu})q + H\sum_{A,A'}\left[|q^T C i\gamma_5\tau_A\lambda_{A'}q|^2 + |q^T C\tau_A\lambda_{A'}q|^2\right], \\ \hat{\mu} &= \mathrm{diag}(\mu_u,\mu_d,\mu_s),\end{aligned} \tag{3.1}$$

where $A, A' = 2, 5, 7$ correspond to antisymmetric flavor and color Gell-Mann matrices; this model describes quarks with attractive interactions in the totally antisymmetric channel in spin, flavor and color. Such an interaction takes inspiration from magnetic single gluon exchange [23], which is attractive in the color antisymmetric channel. The diquark mean fields in the scalar channels are

$$s_{AA'} = 2H\langle\bar{q}i\gamma_5\tau_A\lambda_{A'}C\bar{q}^T\rangle \equiv 2H\langle\bar{q}i\gamma_5\tau_A\lambda_{A'}q^C\rangle, \tag{3.2}$$

where $q^C \equiv C\bar{q}^T$ is the charge conjugate quark field and $C = i\gamma^2\gamma^0$ is the charge conjugation matrix. The nine different pairing mean fields for different flavors and colors can be transformed into each other by gauge choices. We choose the gauge such that

$$s_{AA'} = \delta_{AA'}s_A, \tag{3.3}$$

a pairing state correlating colors and flavors. In particular, when $s_A = \Delta_{\mathrm{CFL}}$, these condensates are invariant under the locked $SU(3)_{\mathrm{CFL}}$ rotation, where one perform the same $SU(3)$ rotations on the flavor and color simultaneously, corresponding to the CFL state.

The two-color superconductor (2SC) phase, another possibility at densities where strange quarks are significantly less dense than the light quarks, is characterized by $s_{5,7} = 0$, $s_2 = \Delta_{\mathrm{2SC}} \neq 0$; in the 2SC state, only up and down quarks of red and green colors pair, while strange and blue quarks do not participate in the pairing.

The Lagrangian (3.1) respects the full symmetry group

$$U(1)_B \otimes U(1)_A \otimes SU(3)_L \otimes SU(3)_R \otimes SU(3)_C, \tag{3.4}$$

but the diquark condensates spontaneously break some of the symmetries. Under $U(1)_B$ and $U(1)_A$,

$$\begin{aligned} q &\to e^{-i\gamma_5\theta_A/2}e^{-i\theta_B/2}q, \\ q^C &\to e^{-i\gamma_5\theta_A/2}e^{i\theta_B/2}q^C; \end{aligned} \tag{3.5}$$

denoting the pseudoscalar mean fields $p_{AA'} = 2H\langle\bar{q}\tau_A\lambda_{A'}q^C\rangle$ which vanishes in a scalar ground state, we find the scalar mean fields transform as

$$s_{AA'} \to s'_{AA'} = e^{i\phi}\left(s_{AA'}\cos\theta_A + p_{AA'}\sin\theta_A\right). \tag{3.6}$$

Thus diquark condensates spontaneously break both baryon and axial U(1) symmetries. In the chiral and color sectors, the 2SC and CFL condensates differ, since in the former the strange blue quarks for example do not pair. Under a $SU(3)_C$ transformation parametrized by $\phi_a$ and the vector subgroup of $SU(3)_L \otimes SU(3)_R$ parametrized by $\theta_i$,

$$\begin{aligned} q &\to e^{-i\lambda_a\phi_a/2}e^{-i\tau_i\theta_i/2}q, \\ q^C &\to \left(e^{-i\lambda_a\phi_a/2}\right)^T\left(e^{-i\tau_i\theta_i/2}\right)^T q^C. \end{aligned} \tag{3.7}$$

To further find the transformation relations for the condensates, we compute, for an infinitesimal color transformation (the same applies to $SU(3)$ vectorial flavor transformations),

$$\begin{aligned} &e^{-i\lambda_a\phi_a/2}\lambda_A\left(e^{-i\lambda_a\phi_a/2}\right)^T \\ &\approx \begin{cases} \lambda_A - i\frac{\phi_a}{2}[\lambda_a,\lambda_A] = \lambda_A + \phi_a f_{aAb}\lambda_b, & a = 1,3,4,6,8; \\ \lambda_A - i\frac{\phi_a}{2}\{\lambda_a,\lambda_A\} = \lambda_A - i\phi_a d_{aAb}\lambda_b, & a = 2,5,7; \end{cases} \end{aligned} \tag{3.8}$$

here $f_{abc}$ (totally antisymmetric) and $d_{abc}$ (totally symmetric) are $SU(3)$ structure constants, given by

$$[\lambda_a,\lambda_b] = 2if_{abc}\lambda_c,\ \{\lambda_a,\lambda_b\} = \frac{4}{3}\delta_{ab} + 2d_{abc}\lambda_c; \tag{3.9}$$

their values are given in Table 3.1 and 3.2. Similarly, for axial transformations of the flavors (under which the diquark condensates are not invariant),

$$\begin{aligned} &e^{-i\gamma_5\tau_i\theta_i/2}\tau_A\left(e^{-i\gamma_5\tau_i\theta_i/2}\right)^T \\ &\approx \begin{cases} \tau_A - i\gamma_5\frac{\theta_i}{2}[\tau_i,\tau_A] = \tau_A + \gamma_5\theta_i f_{iAj}\tau_j, & i = 1,3,4,6,8; \\ \tau_A - i\gamma_5\frac{\theta_i}{2}\{\tau_i,\tau_A\} = \tau_A - i\gamma_5\theta_i d_{iAj}\tau_j, & i = 2,5,7. \end{cases} \end{aligned} \tag{3.10}$$

Equations (3.8) and (3.10) can be used to calculate how $s_{AA'}$ and $p_{AA'}$ rotate into each other under an arbitrary $SU(3)_C \otimes SU(3)_L \otimes SU(3)_R$ transformation. Table (3.3) summarizes the rotation between diquark condensates induced by those transformations. For axial transformations, scalar and pseudoscalar condensates are rotated into each other, in addition to the rotation of flavors and colors.

| abc | 123 | 147 | 156 | 246 | 257 | 345 | 367 | 458 | 678 |
|---|---|---|---|---|---|---|---|---|---|
| $f_{abc}$ | 1 | 1/2 | -1/2 | 1/2 | 1/2 | 1/2 | -1/2 | $\sqrt{3}/2$ | $\sqrt{3}/2$ |

Table 3.1: Totally anti-symmetric structure constants $f_{abc}$.

| abc | 118 | 146 | 157 | 228 | 247 | 256 | 338 | 344 |
|---|---|---|---|---|---|---|---|---|
| $d_{abc}$ | $1/\sqrt{3}$ | 1/2 | 1/2 | $1/\sqrt{3}$ | -1/2 | 1/2 | $1/\sqrt{3}$ | 1/2 |
| abc | 355 | 366 | 377 | 448 | 558 | 668 | 778 | 888 |
| $d_{abc}$ | 1/2 | -1/2 | -1/2 | $-1/2\sqrt{3}$ | $-1/2\sqrt{3}$ | $-1/2\sqrt{3}$ | $-1/2\sqrt{3}$ | $-1/\sqrt{3}$ |

Table 3.2: Totally symmetric structure constants $d_{abc}$.

In the 2SC phase, only $s_{22} \neq 0$. Using Table (3.3), we find that under a rotation corresponding to the isospin subgroup of the SU(3) chiral symmetry (i.e., $i, a = 1, 2, 3$ as in Eq. (3.8) and (3.10)), $s_{22}$ remains invariant. Therefore, the 2SC phase respects a residue symmetry,

$$SU(2)_C \otimes SU(2)_L \otimes SU(2)_R \otimes U(1)_{\text{Blue}} \otimes U(1)_S; \tag{3.11}$$

here, the $U(1)_S$ corresponds to the phase rotation of the strange quarks, and $U(1)_{\text{Blue}}$ corresponds to a linear combination of baryon number and the $a = 8$ color generator, realizing a conservation of blue color. As a result, only 4 (up, down, red and green) of the 9 quarks are gapped, 5 out of 8 gluons obtain a mass from the Meissner mechanism, and the pions $\pi^{\pm,0}$ cease to be NG bosons due to the isospin symmetry being unbroken. Furthermore, the system does not support baryon $U(1)$ or electromagnetic $U(1)$ supercurrents; the total number of unbroken global $U(1)$ symmetries remains the same [101].

In the CFL phase $s_{22} = s_{55} = s_{77} \neq 0$, the residue symmetry is simply[2]

$$SU(3)_{\text{CFL}}; \tag{3.12}$$

the chiral symmetry is completely broken as in the vacuum by chiral condensates, resulting in the full octet of NG bosons; all gluons acquire a Meissner mass, and all quarks are gapped due to pairing.

### 3.1.2 Diquark pairing at mean field

We study the NJL model description of CFL pairing at mean field in terms of the quasiparticle excitations. The quarks in their original basis are coupled to each other via the diquark condensates. In mean field, the quark inverse propagator is most conveniently written in the Nambu-Gorkov formalism, where we define

$$\psi \equiv (q, q^C)^T/\sqrt{2}; \tag{3.13}$$

[2]There is actually an additional $\mathbb{Z}_2$ residue symmetry, corresponding to changing the sign of the left or right handed quarks [101]; such symmetry is not respected by the chiral condensate. We do not discuss this $\mathbb{Z}_2$ here since it is not relevant to the chiral symmetry breaking.

| $i$ or $a$ | induced rotation between $A$s or $A'$s | associated structure constants |
|---|---|---|
| 1,2 | $5 \leftrightarrow 7$ | $d_{157}, f_{257}$ |
| 3 | $5 \leftrightarrow 5, 7 \leftrightarrow 7$ | $d_{355}, d_{377}$ |
| 4,5 | $2 \leftrightarrow 7$ | $d_{247}, f_{257}$ |
| 6,7 | $2 \leftrightarrow 5$ | $d_{256}, f_{257}$ |
| 8 | $2 \leftrightarrow 2, 5 \leftrightarrow 5, 7 \leftrightarrow 7$ | $d_{822}, d_{855}, d_{877}$ |

Table 3.3: Induced rotation between diquark condensates with flavor index $A$ and color index $A'$. For example, with a color transformation parametrized by $\phi_1$, $s_{55}$ will be rotated into $s_{57}$, $s_{77}$ will be rotated into $s_{75}$, while $s_{22}$ remains invariant. As a second example, an axial chiral transformation parametrized by $\theta_8$ will rotate $s_{22}$ into $p_{22}$, $s_{55}$ into $p_{55}$, and $s_{77}$ into $p_{77}$.

then in terms of the $\psi$ field, the mean field NJL Lagrangian is

$$\begin{aligned} \mathcal{L}_{MF} &= \bar{\psi} \begin{pmatrix} i\partial\!\!\!/ - \hat{m}_q + \gamma^0\hat{\mu} & i\gamma_5 \sum_A \Delta_A^\dagger \tau_A \lambda_A \\ i\gamma_5 \sum_A \Delta_A \tau_A \lambda_A & i\partial\!\!\!/ - \hat{m}_q - \gamma^0\hat{\mu} \end{pmatrix} \psi - \sum_A \frac{|\Delta_A|^2}{4H} \\ &\equiv \bar{\psi}\mathcal{G}_{\rm NG}^{-1}\psi - V(\Delta_A), \end{aligned} \tag{3.14}$$

where $\Delta_A \equiv 2Hs_A$, and $s_{AA'} = \delta_{AA'}s_A$ in our gauge of choice. Since we are formally writing $q^C$ as an independent fermion field, we are effectively doubling the degrees of freedom using the Nambu-Gorkov spinor $\psi$; such degeneracy should be removed in formal calculations involving traces and determinants of the Nambu-Gorkov propagator.

We first focus on CFL pairing. To diagonalize $\mathcal{G}_{\rm NG}^{-1}$, we first write the quark fields in a new basis

$$q^A = \frac{1}{\sqrt{2}} \sum_{i,a} \lambda_{ai}^A q_{ia}, \;\; q_{ia} = \frac{1}{\sqrt{2}} \sum_A \lambda_{ia}^A q^A; \;\; A = 1, \ldots, 9; \tag{3.15}$$

the new quark fields $q^A$ are linear combinations of quarks of different colors and flavors, and we use $\lambda^9 = \mathbf{1}\sqrt{2/3}$ added to the eight Gell-Mann matrices. The conjugate quark fields in the new basis are

$$\bar{q}_{ia} = \frac{1}{\sqrt{2}} \sum_A \lambda_{ia}^{A*} \bar{q}^A. \tag{3.16}$$

It is straightforward to verify that canonical equal-time anti-commutation relations are preserved in the new basis:

$$\begin{aligned} \{q^A(1), q^{B\dagger}(2)\} &= \frac{1}{2}\lambda_{ai}^A \lambda_{bj}^{B*} \{q_{ia}(1), q_{jb}^\dagger(2)\} = \frac{1}{2}\delta(1-2)\lambda_{ai}^A \lambda_{ia}^{B\dagger} \\ &= \delta(1-2)\frac{1}{2}\mathrm{tr}\left(\lambda^A\lambda^B\right) = \delta_{AB}\delta(1-2). \end{aligned} \tag{3.17}$$

In the new basis, the flavor-color structure of the antisymmetric pairing becomes

$$\begin{aligned} q_{ia}\left(\tau_A\right)_{ij}\left(\lambda_B\right)_{ab}q_{jb} &= \frac{1}{2}q^S\left[\lambda^S_{ia}\lambda^A_{ij}\lambda^B_{ab}\lambda^K_{jb}\right]q^K = \frac{1}{2}q^S\left[\left(\lambda^S\lambda^B\right)^T_{bi}\left(\lambda^A\lambda^K\right)_{ib}\right]q^K \\ &= q^S\frac{1}{2}\mathrm{tr}\left[\left(\lambda^S\lambda^B\right)^T\left(\lambda^A\lambda^K\right)\right]q^K \equiv q^S\Gamma^{AB}_{SK}q^K. \end{aligned} \tag{3.18}$$

The vertex matrix in the new basis, $\Gamma^{AB}_{SK}$, is symmetric in $S, K$, but hermitian in $A, B$:

$$\begin{aligned} \Gamma^{AB}_{SK} &= \mathrm{Tr}\left[\left(\lambda^S\lambda^B\right)^T\left(\lambda^A\lambda^K\right)\right] = -\mathrm{Tr}\left[\lambda^B\lambda^{ST}\lambda^A\lambda^K\right] = \mathrm{Tr}\left[\lambda^{KT}\lambda^{AT}\lambda^S\lambda^B\right] \\ &= \mathrm{Tr}\left[\lambda^{BT}\lambda^{KT}\lambda^A\lambda^S\right] = \mathrm{Tr}\left[(\lambda^K\lambda^B)^T\lambda^A\lambda^S\right] = \Gamma^{AB}_{KS}, \end{aligned} \tag{3.19}$$

and

$$\begin{aligned} \Gamma^{AB}_{SK} &= \mathrm{Tr}\left[\left(\lambda^S\lambda^B\right)^T\left(\lambda^A\lambda^K\right)\right] = \left(\mathrm{Tr}\left[\lambda_B\lambda_K\lambda^T_A\lambda^T_S\right]\right)^* \\ &= \left(\mathrm{Tr}\left[\lambda^T_A\lambda^T_S\lambda_B\lambda_K\right]\right)^* = \left(\mathrm{Tr}\left[(\lambda_S\lambda_A)^T\lambda_B\lambda_K\right]\right)^* = (\Gamma^{BA}_{SK})^*. \end{aligned} \tag{3.20}$$

For $\bar{q}\bar{q}$, the vertex matrix is different from $\Gamma^{AB}_{SK}$:

$$\begin{aligned} &\bar{q}_{ia}\left(\tau_A\right)_{ij}\left(\lambda_B\right)_{ab}q^*_{jb} \\ &= \frac{1}{2}\bar{q}^S\left[\lambda^{S*}_{ia}\lambda^A_{ij}\lambda^B_{ab}\lambda^{K*}_{jb}\right]q^{K*} = \frac{1}{2}\bar{q}^S\left[\left(\lambda^{S*}\lambda^B\right)^T_{bi}\left(\lambda^A\lambda^{K*}\right)_{ib}\right]q^{K*} \\ &= \frac{1}{2}\bar{q}^S\mathrm{Tr}\left[\lambda^T_B\lambda^\dagger_S\lambda_A\lambda^*_K\right]q^{K*} \equiv \bar{q}^S\tilde{\Gamma}^{AB}_{SK}q^{K*}. \end{aligned} \tag{3.21}$$

When $A, B = 2, 5, 7$,

$$(\tilde{\Gamma}^{AB}_{SK})^* = \frac{1}{2}\mathrm{Tr}\left[\lambda^T_B\lambda^T_S\lambda_A\lambda_K\right] = \Gamma^{AB}_{SK}. \tag{3.22}$$

In our gauge choice, we only need to consider $A = B = 2, 5, 7$. One can show that the matrices are then real (no summation over $A$):

$$\Gamma^{AA} = \tilde{\Gamma}^{AA} = (\Gamma^{AA})^*, \ A = 2, 5, 7. \tag{3.23}$$

The pairing contribution to the inverse propagator, in the space of the new basis

$A = 1, 2, \ldots, 9$, is then

$$\sum_{A=2,5,7} \Gamma^{AA} i\gamma_5 \Delta_A =$$
$$i\gamma_5 \begin{pmatrix} \Delta_2 \mathbf{1} & . & . & . & . & . \\ . & \Delta_2 & . & . & \frac{\Delta_5-\Delta_7}{\sqrt{3}} & \frac{-\Delta_5+\Delta_7}{\sqrt{6}} \\ . & . & \Delta_5 \mathbf{1} & . & . & . \\ . & . & . & \Delta_7 \mathbf{1} & . & . \\ . & \frac{\Delta_5-\Delta_7}{\sqrt{3}} & . & . & \frac{-\Delta_2+2\Delta_5+2\Delta_7}{3} & \frac{-2\Delta_2+\Delta_5+\Delta_7}{3\sqrt{2}} \\ . & \frac{-\Delta_5+\Delta_7}{\sqrt{6}} & . & . & \frac{-2\Delta_2+\Delta_5+\Delta_7}{3\sqrt{2}} & \frac{-2\Delta_2-2\Delta_5-2\Delta_7}{3} \end{pmatrix}, \tag{3.24}$$

where $\mathbf{1}$ is the two-by-two identity matrix, and "." denotes 0 or $\mathbf{0}_{2\times 2}$. In the CFL phase, $\Delta_{2,5,7} = \Delta_{\rm CFL}$, and the giant matrix above reduces to the diagonal form

$$i\gamma_5 \begin{pmatrix} \mathbf{1}_{8\times 8} & \mathbf{0} \\ \mathbf{0} & -2 \end{pmatrix} \Delta_{\rm CFL}, \tag{3.25}$$

directly indicating that eight quasiparticles resulting from the pairing will have gap $\Delta_{\rm CFL}$, while one quasiparticle will have twice the gap $2\Delta_{\rm CFL}$. Since all quarks in the new basis only pair with themselves in the CFL phase, the quasiparticle energies are directly analogous to the BCS quasiparticle energies, but with relativistic dispersions; assuming $\hat{m}_q \approx 0$ and $\hat{\mu} \approx \mu \mathbf{1}$ at high density, the positive energies are

$$\begin{aligned} E^{(1)}_{k\pm} &= \sqrt{(\pm k - \mu)^2 + \Delta^2_{\rm CFL}} \text{ for quasiparticles } A = 1, \ldots, 8, \\ E^{(9)}_{k\pm} &= \sqrt{(\pm k - \mu)^2 + 4\Delta^2_{\rm CFL}} \text{ for quasiparticle } A = 9. \end{aligned} \tag{3.26}$$

To derive the gap equation for the CFL mean fields, we calculate self-consistently

$$\begin{aligned} \frac{\Delta_{\rm CFL}}{4H} &= \frac{\Delta_{2,5,7}}{4H} = \langle \bar{\psi} \Gamma^{22,55,77} \psi \rangle = -i \int_p {\rm Tr} \left[ \mathcal{G}_{\rm NG}(p) \Gamma^{22,55,77} \right] \\ &= -i \int_p {\rm Tr} \left[ \left( \frac{8}{3} \left( \mathcal{G}_{\rm NG} \right)_{11} (p) - \frac{2}{3} \left( \mathcal{G}_{\rm NG} \right)_{99} (p) \right) \begin{pmatrix} 0 & i\gamma_5 \\ 0 & 0 \end{pmatrix} \right], \end{aligned} \tag{3.27}$$

where the inverses of the propagators for the quasiparticles in the new basis are

$$\begin{aligned} \left( \mathcal{G}^{-1}_{\rm NG} \right)_{11} (p) &= \begin{pmatrix} \not{p} + \gamma_0 \mu & -i\gamma_5 \Delta_{\rm CFL} \\ i\gamma_5 \Delta_{\rm CFL} & \not{p} - \gamma_0 \mu \end{pmatrix}, \\ \left( \mathcal{G}^{-1}_{\rm NG} \right)_{99} (p) &= \begin{pmatrix} \not{p} + \gamma_0 \mu & 2i\gamma_5 \Delta_{\rm CFL} \\ -2i\gamma_5 \Delta_{\rm CFL} & \not{p} - \gamma_0 \mu \end{pmatrix}. \end{aligned} \tag{3.28}$$

The calculation of paired propagators like $(\mathcal{G}_{\rm NG})_{11,99}$ will be presented later in Sec. 3.2.2. Using Eqs. (3.27) and (3.28), we obtain at zero temperature

$$\frac{\Delta_{\rm CFL}}{2H} = \frac{8\Delta_{\rm CFL}}{3}\int_{\boldsymbol{p}}\sum_{\pm}\left[\frac{2}{E^{(1)}_{p\pm}}+\frac{1}{E^{(9)}_{p\pm}}\right]. \tag{3.29}$$

For 2SC pairing, we do not need to resort to a change in the quark basis, since the pairing pattern is already one-to-one.[3] At mean field, the only difference in the 2SC phase is that only 4 quasiparticles are gapped by the same $\Delta_{\rm 2SC}$ (since only two flavors and two colors pair), the rest being free quarks; we thus do not elaborate the details here. The NG modes in the 2SC phase however are very different from the CFL phase, as we have seen from Sec. 3.1.1.

## 3.2 Nambu-Goldstone bosons in the presence of diquark pairing: generalized mesons[4]

After introducing the diquark pairing in the NJL model at mean field, we next study the NG bosons in the presence of diquark pairing in this section. Despite breaking the same chiral symmetry, the diquark condensates $\langle qq\rangle$ contribute very differently to the properties for the associated pseudoscalar NG bosons, compared to the chiral condensate $\langle\bar{q}q\rangle$. Unlike $\langle\bar{q}q\rangle$, the diquark condensates $\langle qq\rangle$ are not gauge-invariant, and as a result the fluctuations of $\langle qq\rangle$ also carry color; the NG bosons parametrized in this way are manifestly gauge-dependent excitations, and are no longer eigenstates of electric charges. However, their color charges can be screened by the diquark condensates themselves, and a generalized charge – a linear combination of 8th color charge and electric charge – remains as a good quantum number that directly matches the original electric charges of the NG bosons in the vacuum, which we will discuss this in details in Chapter 4.

To study the properties such as the masses and decay constants of the NG bosons with diquark pairing, in this section we focus on a $N_f = N_c = 1$ schematic NJL model, emphasizing the core physics of collective modes mixing and continuous chiral symmetry breaking via different condensates (i.e., $\langle\bar{q}q\rangle$ and $\langle qq\rangle$), dodging the algebraic endeavors required to handle multiple $SU(N)$ groups. At high density, $\langle\bar{q}q\rangle$ persists due to axial anomaly, and its contribution to the NG bosons is as important as the $\langle qq\rangle$ condensates. We discuss in detail such NG bosons particularly at the presence of both chiral symmetry breaking condensates, in addition to the model itself.

[3] The CFL pairing in the original color-flavor basis is not manifestly one-to-one, thus requiring using the new basis. Specifically, in the original basis, the CFL pairing pairs up blue up with red down quarks, green up with red strange quarks, green down with blue strange quarks, but the red up quarks pair up with both blue down and green strange quarks, which is not one-to-one. Such a pattern makes it difficult to see the quasiparticle structures.

[4] This section's material is primarily based on the author's published work [8].

This section's material comes primarily from the author's published work [8].

### 3.2.1 Schematic NJL model: Lagrangian, gap equations and dispersion relations

In this subsection we specify the schematic model basics, including the pairing gap equation and quasiparticle dispersions, for later calculations of the NG boson properties. Our schematic model has the Lagrangian

$$\begin{aligned}\mathcal{L} &= \bar{q}\left(i\partial\!\!\!/ - m_q + \gamma_0\mu\right)q + G\left[\left(\bar{q}q\right)^2 + \left(\bar{q}i\gamma_5 q\right)^2\right] \\ &\quad + H\left[\left(q^T i\gamma_5 C q\right)\left(\bar{q}i\gamma_5 C\bar{q}^T\right) + \left(q^T C q\right)\left(\bar{q}C\bar{q}^T\right)\right],\end{aligned} \tag{3.30}$$

where $G$, the coupling strength for the four-quark chiral interaction term, and $H$, the strength of the spin-singlet pairing interaction, are model parameters. Both couplings are attractive, favoring the formation of condensates at mean field. In the chiral limit, the Lagrangian respects a $U(1)_L \otimes U(1)_R$ "chiral" symmetry of the quark field. As the norm of NJL models, which are not renormalizable, we adopt a three-momentum cutoff $\Lambda$ in our calculations, which is also a model parameter.

This "chiral" symmetry in the model does not actually correspond to the chiral symmetry in QCD, but the axial $U(1)$ symmetry; however, the symmetry breaking mechanism via chiral and diquark condensates is the same, and all the arguments presented in this section also apply to the realistic $N_f = N_c = 3$ chiral symmetry breaking and the associated NG bosons, up to a flavor and color group structure. We analogously refer to the single NG boson corresponding to the spontaneous breaking of the axial $U(1)$ in this model as the "pion."

We solve this model at mean field to obtain the phases characterizing the symmetry breaking pattern, which serves as our roadmap to study the NG bosons at different densities. We define the four relevant mean fields,

$$\begin{aligned}\sigma &= 2G\langle\bar{q}q\rangle,\ \pi = 2G\langle\bar{q}i\gamma_5 q\rangle, \\ \Delta_s &= 2H\langle\bar{q}i\gamma_5 C\bar{q}^T\rangle,\ \Delta_{ps} = 2H\langle\bar{q}C\bar{q}^T\rangle,\end{aligned} \tag{3.31}$$

where we have chiral condensate and diquark condensates in both scalar "s" and pseudoscalar "ps" channels; the mean field Lagrangian is

$$\mathcal{L}_{\rm MF} = \bar{\psi}S_{\rm MF}^{-1}\psi - \frac{\sigma^2+\pi^2}{4G} - \frac{|\Delta_s|^2 + |\Delta_{ps}|^2}{4H}, \tag{3.32}$$

with again the Nambu-Gorkov spinor $\psi \equiv (q, q^C)^T/\sqrt{2}$, the mean field inverse propagator for the quarks

$$S_{\rm MF}^{-1} = \begin{pmatrix} i\partial\!\!\!/ - \hat{M} + \gamma^0\mu & i\gamma_5\Delta_s^* + \Delta_{ps}^* \\ i\gamma_5\Delta_s + \Delta_{ps} & i\partial\!\!\!/ - \hat{M} - \gamma^0\mu \end{pmatrix}, \tag{3.33}$$

and the effective quark mass matrix $\hat{M} = m_q - \sigma - i\gamma_5\pi$. The fermionic quasiparticle excitations $\omega(\boldsymbol{p})$ are from solving $\det S_{\rm MF}^{-1}(\omega(\boldsymbol{p}), \boldsymbol{p}) = 0$. After some algebra, we find

$$\begin{aligned} \omega(\boldsymbol{p}) &= \pm\left[(m_q-\sigma)^2 + \pi^2 + \boldsymbol{p}^2 + \mu^2 + |\Delta_s|^2 + |\Delta_{ps}|^2 \pm 2\delta(\boldsymbol{p})\right]^{\frac{1}{2}}; \\ \delta(\boldsymbol{p}) &\equiv \Big[\left(|\boldsymbol{p}|\mu \pm \mathrm{Im}\left[\Delta_s\Delta_{ps}^*\right]\right)^2 + \mu^2\left((m_q-\sigma)^2+\pi^2\right) \\ &\quad + |(m_q-\sigma)\Delta_{ps} - \pi\Delta_s|^2\Big]^{\frac{1}{2}}. \end{aligned} \tag{3.34}$$

The leading "$\pm$" sign in $\omega(\boldsymbol{p})$ corresponds to the Nambu-Gor'kov degeneracy; the second "$\pm$" sign in front of $\delta(\boldsymbol{p})$ corresponds to the particle-hole branches; and the last "$\pm$" sign within $\delta(\boldsymbol{p})$ is a splitting caused by a relative phase between $\Delta_s$ and $\Delta_{ps}$. All three "$\pm$" signs are independent of each other, making a total of eight eigenvalues (or four physical ones, after removing the Nambu-Gor'kov degeneracy and keeping only positive $\omega(\boldsymbol{p})$).

The six gap equations that self-consistently determine the six mean fields are then determined by

$$\frac{\partial\Omega}{\partial\sigma} = \frac{\partial\Omega}{\partial\pi} = \frac{\partial\Omega}{\partial\Delta_s} = \frac{\partial\Omega}{\partial\Delta_s^*} = \frac{\partial\Omega}{\partial\Delta_{ps}} = \frac{\partial\Omega}{\partial\Delta_{ps}^*} = 0, \tag{3.35}$$

where $\Omega$ is the grand thermodynamic potential density, easily calculated using the fermion quasiparticle energies

$$\begin{aligned} \Omega &= -T\sum_{i=1}^{4}\int_{\boldsymbol{p}}\left[\ln\left(1+e^{-\omega_i/T}\right) + \frac{1}{2T}\left(\omega_i - \omega_{i0}\right)\right]. \\ &\quad + \frac{\sigma^2+\pi^2}{4G} + \frac{|\Delta_s|^2+|\Delta_{ps}|^2}{4H}. \end{aligned} \tag{3.36}$$

### 3.2.2 The scalar state

The six gap equations (3.35) admit non-trivial degenerate solutions due to chiral symmetry, corresponding to energetically equivalent ground states spanned by the symmetry group. The following solution in chiral limit $m_q = 0$,

$$\sigma = -M,\ \pi = 0,\ \Delta_s = -i\Delta,\ \Delta_{ps} = 0, \tag{3.37}$$

describes a scalar ground state with positive parity in the absence of pion condensation. In this state, the NG boson corresponding to spontaneous chiral symmetry breaking originates from pseudoscalar fluctuations in $\pi$ and $\Delta_{ps}$, as in realistic chiral symmetry breaking in QCD. At high density, the favored diquark pairing channel is also likely scalar [101]. As in the vacuum NJL, this scalar state is our starting point in studying the NG boson properties.

In the scalar state, the inverse quark propagator becomes

$$S_0^{-1}(\omega, \boldsymbol{p}) = \begin{pmatrix} \not{p} - M + \gamma_0\mu & -\gamma_5\Delta \\ \gamma_5\Delta & \not{p} - M - \gamma_0\mu \end{pmatrix}, \tag{3.38}$$

where we have chosen $\Delta_s = i\Delta$ where $\Delta$ is real. Such a gauge choice results in the eigenstate wave functions to be entirely real, as in the BCS theories. The quasiparticle excitations in the scalar state reduce to

$$\omega_\pm(\boldsymbol{p}) = \sqrt{(\epsilon_\pm(\boldsymbol{p}) - \mu)^2 + \Delta^2},\ \epsilon_\pm(\boldsymbol{p}) = \pm\sqrt{\boldsymbol{p}^2 + M^2}, \tag{3.39}$$

each with spin degeneracy of two, yielding four positive physical eigenvalues in total. The normalized eigenvectors of the inverse propagator are

$$\begin{aligned} \lambda_\pm(\omega_\pm(\boldsymbol{p}), s) &= R_\pm(\boldsymbol{p}) \begin{pmatrix} v_\pm(\boldsymbol{p}) r(\boldsymbol{p}) \\ u_\pm(\boldsymbol{p}) t(\boldsymbol{p}) \end{pmatrix}, \\ r(\boldsymbol{p}) &\equiv \begin{pmatrix} s \\ \hat{P}s \end{pmatrix},\ t(\boldsymbol{p}) \equiv \begin{pmatrix} -\hat{P}s \\ s \end{pmatrix}, \end{aligned} \tag{3.40}$$

where $s = (1,0)^T$ or $(0,1)^T$ are spin-1/2 spinors, $R_\pm^2(\boldsymbol{p}) \equiv (\epsilon_\pm(\boldsymbol{p}) + M)/2\epsilon_\pm(\boldsymbol{p})$ defines the normalization constant, and $\hat{P} \equiv \boldsymbol{\sigma} \cdot \boldsymbol{p}/(\epsilon_\pm(\boldsymbol{p}) + M)$ is a projection operator in spinor space; and the coherence functions $v_\pm(\boldsymbol{p}), u_\pm(\boldsymbol{p})$ are exactly analogous to the non-relativistic BCS results:

$$v_\pm(\boldsymbol{p}) = \sqrt{\frac{\omega_\pm(\boldsymbol{p}) + \epsilon_\pm(\boldsymbol{p}) - \mu}{2\omega_\pm(\boldsymbol{p})}}, u_\pm(\boldsymbol{p}) = \sqrt{\frac{\omega_\pm(\boldsymbol{p}) - \epsilon_\pm(\boldsymbol{p}) + \mu}{2\omega_\pm(\boldsymbol{p})}}, \tag{3.41}$$

which further satisfy

$$v_\pm(\boldsymbol{p})^2 + u_\pm(\boldsymbol{p})^2 = 1;\ v_\pm(\boldsymbol{p}) u_\pm(\boldsymbol{p}) = \frac{\Delta}{2\omega_\pm(\boldsymbol{p})}. \tag{3.42}$$

The negative eigenvalues correspond to the charge conjugate fields in the Nambu-Gorkov formalism; they are given by

$$\tilde{\lambda}_\pm(-\omega_\pm(\boldsymbol{p}), s) = \begin{pmatrix} u_\pm(\boldsymbol{p}) r(\boldsymbol{p}) \\ -v_\pm(\boldsymbol{p}) t(\boldsymbol{p}) \end{pmatrix}. \tag{3.43}$$

The Nambu-Gorkov inverse propagator can be written as a sum over all the eigenvalues and eigenvectors:

$$\begin{aligned} S_0(\omega, \boldsymbol{p}) &= \sum_{\pm,s} \Bigg[ \lambda_\pm(\omega_\pm(\boldsymbol{p}), s) \lambda_\pm^\dagger(\omega_\pm(\boldsymbol{p}), s) \frac{1}{\omega - \omega_\pm(\boldsymbol{p})} \\ &\quad + \tilde{\lambda}_\pm(-\omega_\pm(\boldsymbol{p}), s) \tilde{\lambda}_\pm^\dagger(-\omega_\pm(\boldsymbol{p}), s) \frac{1}{\omega + \omega_\pm(\boldsymbol{p})} \Bigg] \gamma_0, \end{aligned} \tag{3.44}$$

which transforms the calculation of diagrams into products of eigenvector prod-

ucts at each vertices. The gap equations in the scalar state reduce to two independent ones:

$$\frac{M}{2G} = M\sum_{\pm}\int_{\boldsymbol{p}}\frac{1}{\omega_{\pm}(\boldsymbol{p})}\left(1\mp\frac{\mu}{\sqrt{\boldsymbol{p}^2+M^2}}\right), \tag{3.45}$$

$$\frac{\Delta}{2H} = \Delta\sum_{\pm}\int_{\boldsymbol{p}}\frac{1}{\omega_{\pm}(\boldsymbol{p})}. \tag{3.46}$$

The gap equations (3.45) and (3.46) yield the order parameters $\Delta$ and $M$ as functions of $\mu$. Since the procedure of fitting model parameters to vacuum hadron phenomenology does not apply to our $N_c = N_f = 1$ schematic model, we are free to set $G, H$ and $\Lambda$ as long as the resulting phase diagram simulates that of realistic quark matter. To study the particularly interesting region where chiral condensate and diquark condensate coexist, we require the resulting phase diagram to have an extensive coexistence region. We also require the system to be thermodynamically stable as a natural requirement.

### 3.2.3 From model parameters to the phase diagram, and thermodynamic stability

To satisfy the two constraints, we first study $G$ alone in the absence of diquark pairing $\Delta, H = 0$. For $M \neq 0$, the gap equation (3.45) becomes

$$\frac{1}{2G} = \frac{1}{\pi^2}\int_{p_F}^{\Lambda}\frac{p^2dp}{\sqrt{M^2+p^2}}; \tag{3.47}$$

Due to the appearance of $M$ in the denominator the integral on the right hand side is a decreasing function of $G$ and has an upper limit. As a result, for any given $p_F$, there is a minimum value of $G$ below which (3.45) only has trivial solutions $M = 0$, i.e., no spontaneous chiral symmetry breaking. To find out this minimum value, we consider the limit $M \to 0$ in (3.47), which yields

$$G = \frac{\pi^2}{\Lambda^2 - p_F^2}. \tag{3.48}$$

As a result, in the vacuum, $p_F = 0$, the minimum $G > \pi^2/\Lambda^2$ is required to admit a non-trivial solution $M$. We denote this lower bound as $G_{c1} = \pi^2/\Lambda^2$.

On the other hand, the second constraint – the thermodynamic stability requirement – enforces $\partial\mu/\partial n > 0$ where $n = p_F^3/3\pi^2$ is the quark density. This requirement puts an upper bound for $G$. Differentiating $p_F(\mu)^2 = \mu^2 - M(\mu)^2$ with respect to $\mu$, we obtain

$$\frac{\partial n}{\partial\mu} = \frac{p_F}{\pi^2}\left(\mu - M\frac{\partial M}{\partial\mu}\right) \tag{3.49}$$

which must be positive. To relate this to $G$, we plot the solutions $M(\mu)$ as a fam-

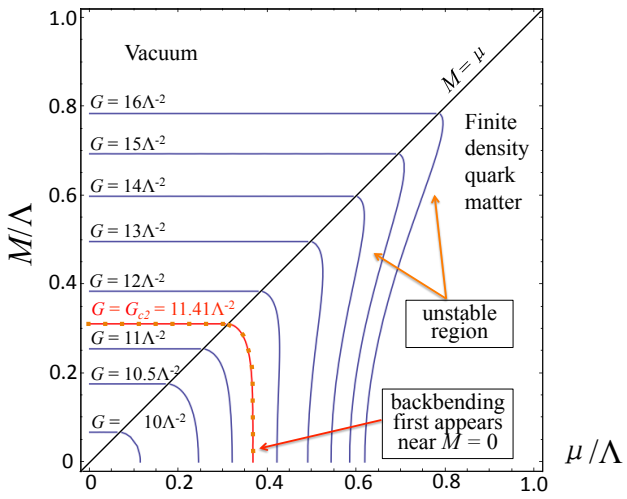


Figure 3.1: Solutions to gap equation $M(\mu)$ for varying $G$. Backbending indicating instability first occurs at $G_{c2}$.

ily of curves given for varying $G$ in Fig. 3.1. Above certain values of $G$, bending back of $M(\mu)$ curve appears[5]: as a result, $\partial M/\partial\mu$ starting finite and negative at the start, turns $-\infty$ and then $+\infty$ before finally settling finite and positive. Such transition means Eq. (3.49) cannot remain positive, implying instability of the system against density fluctuations. The assumption of homogeneous mean fields is not physical if this happens.

To algebraically find $G_{c2}$, we use the fact that $M \to 0$ indicates the first violation of the stability with increasing $G$. In this limit we calculate $\partial M/\partial\mu$ by differentiating the gap equation (3.47):

$$M\frac{\partial M}{\partial \mu} = \left(1 - \ln\frac{\Lambda}{p_F(\mu)}\right)^{-1}\mu. \tag{3.50}$$

At the critical Fermi momentum, $p_{Fc}$, given by $1-\ln\Lambda/p_{Fc}=0$, the divergence of $\partial M/\partial\mu$ related to the backbending appears; thus $p_{Fc} = \Lambda/e$ where $e$ is Napier's constant. We find the critical value $G_{c2}$ by substituting $p_{Fc}$ back into Eq. (3.45) together with $M \to 0$:

$$G_{c2} = \frac{\pi^2}{(1-e^{-2})\Lambda^2}. \tag{3.51}$$

The constraint on $G$ is summarized in Fig. 3.2. With $G_{c1} < G < G_{c2}$, the system exhibits a second order transition from the chirally broken region $M \neq 0$ to the restored region $M = 0$.

We next discuss $H$. In contrast to for $M$ in Eq. (3.47), the integral in the gap equation (3.46) does not have an upper bound as a function of $\Delta$, as a result

[5] A similar instability related to back-bending of $\langle\bar{q}q\rangle(\mu)$ also appears in lattice gauge analyses of chiral restoration, e.g., [67].

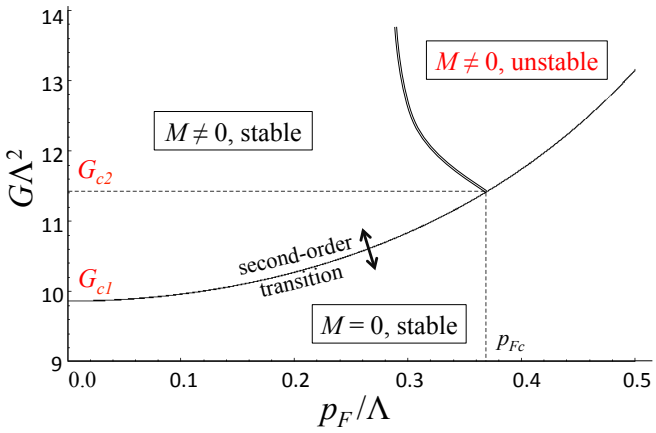


Figure 3.2: Stability of the system at varying Fermi momentum $p_F$ and $G$, in terms of $\Lambda$. In the range $G_{c1} < G < G_{c2}$, the system is stable with a chirally broken vacuum.

of the singularity in $1/\omega_+(\boldsymbol{p})$ at the Fermi surface $|\boldsymbol{p}| = p_F$ when $\Delta \to 0$. At any density, there is always a non-trivial solution $\Delta$, as in non-relativistic BCS theory of superconductors; diquark pairing therefore always happens at finite density in this simple model. As a result, the existence of paired phase alone does not constraint $H$.

The existence of the coexistence phase however does constrain $H$. In the coexistence phase $M, \Delta \neq 0$, one can divide the gap equation (3.45) by $M$ and (3.46) by $\Delta$, and subtract one from the other, to find

$$\frac{1}{2H} - \frac{1}{2G} = \int_{\boldsymbol{p}} \frac{\mu}{\sqrt{\boldsymbol{p}^2 + M^2}} \left( \frac{1}{\omega_+(\boldsymbol{p})} - \frac{1}{\omega_-(\boldsymbol{p})} \right). \tag{3.52}$$

The right side is always positive due to $\omega_+(\boldsymbol{p}) < \omega_-(\boldsymbol{p})$. As a consequence, one must have $H < G$ to have a coexistence phase.

On the other hand, the stability condition becomes subtle and algebraically involving at the simultaneous presence of $H$ and $G$. Numerical calculation suggests that an instability could still develop when $H$ becomes comparable to $G$, but for relatively small $H$, $\lesssim G/2$, a stable coexistence region can be achieved. Figure 3.3 shows the phase structure of the model at varying $p_F$ plotted for a good choice $G = 11\Lambda^{-2}$ and $H = 6\Lambda^{-2}$. When we discuss the collective modes of the system in the following, we assume a phase structure as in Fig. 3.3.

### 3.2.4 Identification of collective modes

The collective modes of the system are given by parametrized mean field fluctuations. In the chiral limit, the spontaneous breaking of $U(1)_L \otimes U(1)_R =$

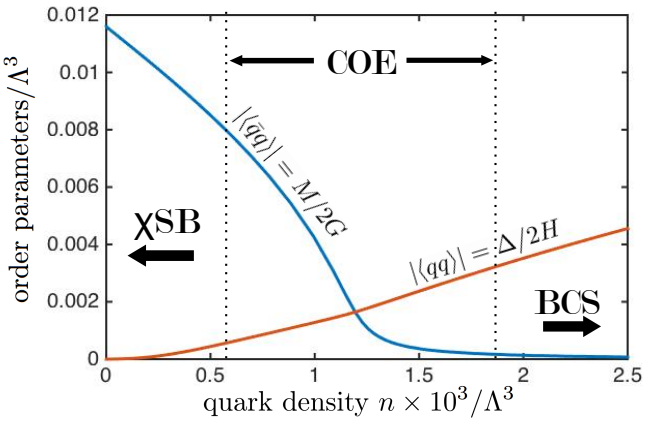


Figure 3.3: The evolution of $|\langle\bar{q}q\rangle| = M/2G$ and $|\langle qq\rangle| = \Delta/2H$ against quark density $n$ with $G = 11\Lambda^{-2}$ and $H = 6\Lambda^{-2}$. The phase diagram can be roughly divided into the chirally broken vacuum ($\chi$SB) with $\Delta \approx 0$, $M \neq 0$, the coexistence (COE) phase where $M$ and $\Delta$ are both finite and comparable, and the high density BCS limit where $\Delta \neq 0$ but $M \approx 0$.

| Mode | Description | Parity |
|---|---|---|
| $\theta_B$ | phonon; NG boson of broken $U(1)_V$ | + |
| $\theta_\pi + \theta_d$ | pionic mode; NG boson of broken $U(1)_A$ | - |
| $\theta_\pi - \theta_d$ | massive chiral oscillation between $\pi$ and $\Delta_{ps}$ | - |
| $M$ | Higgs-like; breaks $U(1)_A$ | + |
| $\Delta$ | Higgs-like; breaks $U(1)_V$ and $U(1)_A$ | + |
| $\phi$ | relative phase oscillation between $\Delta_s$ and $\Delta_{ps}$ | + |

Table 3.4: Six normal collective modes of the system.

$U(1)_V \otimes U(1)_A$ by the coexisting chiral and diquark condensates yield two bosonic modes (denoted as the vacuum $\bar{q}q$ pion $\pi$ and the diquark $qq$ pion $\tilde{\pi}$), whose two independent linear combinations correspond to the NG boson, i.e., the generalized pion $\pi_G$, and a massive pionic excitation $\pi_M$ corresponding to the $\bar{q}q$ and $qq$ fluctuations in the opposite chiral direction. In addition, the overall phase fluctuation of $\Delta_s$ and $\Delta_{ps}$ admits a phonon mode with its massive partner that corresponds to their relative phase fluctuations. The fluctuations of the magnitudes of the chiral and diquark condensates also result in two Higgs-like modes. We summarize these modes in Table 3.4, with the parametrization angles to be defined shortly below.

We choose the following parametrization of the condensate mean fields, in terms of the chiral sector axial $U(1)_A$ angle $\theta_\pi$, the diquark sector $U(1)_A$ angle $\theta_d$, the relative phase angle $\phi$ between $\Delta_s$ and $\Delta_{ps}$, and the overall $U(1)_V$ phase

angle $\theta_B$:

$$\begin{aligned}
\sigma &= -M\cos\theta_\pi, \\
\pi &= -M\sin\theta_\pi, \\
\Delta_s &= -i\Delta e^{i\theta_B}e^{i\phi/2}\cos\theta_d, \\
\Delta_{ps} &= i\Delta e^{i\theta_B}e^{-i\phi/2}\sin\theta_d.
\end{aligned} \tag{3.53}$$

The oscillations of $\theta_\pi$ correspond to the usual pion mode $\pi$, while those of $\theta_d$ correspond to the diquark-condensate pion, $\tilde{\pi}$. We choose a gauge such that $\Delta > 0$, $M > 0$, and thus $\sigma < 0$ at $\theta_\pi = 0$.

Under a $U(1)_V$ transformation, $\Delta_s$ and $\Delta_{ps}$ rotate the same phase $\theta_B \to \theta_B + \theta_V$. Meanwhile, a $U(1)_A$ transformation parametrized by angle $\theta_A$ rotates $\sigma$ and $\pi$ as

$$\left.\begin{aligned}
\sigma &\to \sigma\cos\theta_A - \pi\sin\theta_A \\
\pi &\to \pi\cos\theta_A + \sigma\sin\theta_A
\end{aligned}\right\} \quad \Rightarrow \quad \theta_\pi \to \theta_\pi + \theta_A. \tag{3.54}$$

We also compute the transformation rule of $\Delta_s$ and $\Delta_{ps}$ under $\theta_A$:

$$\begin{aligned}
\Delta_s &\to \Delta_s\cos\theta_A + \Delta_{ps}\sin\theta_A \\
&= -i\Delta\left[\cos\frac{\phi}{2}\cos\left(\theta_d+\theta_A\right) + i\sin\frac{\phi}{2}\sin\left(\theta_d-\theta_A\right)\right] \\
&\equiv -i\Delta e^{i\phi'/2}\cos\theta'_d, \\
\Delta_{ps} &\to \Delta_{ps}\cos\theta_A - \Delta_s\sin\theta_A \\
&= -i\Delta\left[-\cos\frac{\phi}{2}\sin\left(\theta_d+\theta_A\right) + i\sin\frac{\phi}{2}\sin\left(\theta_d-\theta_A\right)\right] \\
&= i\Delta e^{-i\phi'/2}\sin\theta'_d.
\end{aligned} \tag{3.55}$$

The relative phase $\phi$ and the chiral angle $\theta_d$ both rotate under the chiral transformation and thus cannot be treated independently. Only when the two condensates are in phase $\phi = 0$ does the result reduce to $\theta_d \to \theta_d + \theta_A$ and $\theta_\pi \to \theta_\pi + \theta_A$, and the fluctuation in $\phi$ decouples. In this case, the diquark-condensate pion $\tilde{\pi}$ is understood as oscillations of the product of the two diquark terms, $\Delta_s\Delta^*_{ps}$. For general non-zero $\phi$, we have instead

$$\begin{aligned}
\cos\theta_d &\to \cos\theta'_d = \left[\cos^2\frac{\phi}{2}\cos^2\left(\theta_d+\theta_A\right) + \sin^2\frac{\phi}{2}\sin^2\left(\theta_d-\theta_A\right)\right]^{\frac{1}{2}}, \\
\phi &\to \phi' = 2\tan^{-1}\left[\frac{\tan(\phi/2)\sin\left(\theta_d-\theta_A\right)}{\cos\left(\theta_d+\theta_A\right)}\right].
\end{aligned} \tag{3.56}$$

With our choice of parametrization, four invariant quantities under chiral trans-

formations are manifest:

$$\begin{aligned}
&\sigma^2+\pi^2=M^2,\ |\Delta_s|^2+|\Delta_{ps}|^2=\Delta^2,\\
&\mathrm{Im}\left[\Delta_s\Delta_{ps}^*\right]=\frac{\Delta^2}{2}\sin 2\theta_d\sin\phi,\\
&|\sigma\Delta_{ps}+\pi\Delta_s|^2=M^2\Delta^2\left[\sin^2(\theta_\pi-\theta_d)-2\sin\theta_\pi\sin\theta_d\sin^2\frac{\phi}{2}\right];
\end{aligned} \tag{3.57}$$

they are the only allowed terms to appear in the quasiparticle dispersion relations, as in (3.34) in the chiral limit indeed. The now parametrized six independent degrees of freedom, $M,\Delta,\theta_\pi,\theta_d,\theta_B,\phi$, are identified as the six modes we listed earlier:

(1) The massless phonon mode, corresponding to fluctuations of $\theta_B$. This mode is massless since the free energy does not depend on this angle.

(2) The massless pionic mode $\pi_G$ identified with fluctuations of the angle $\theta_G\equiv(\theta_\pi+\theta_d)/2$. Again the free energy does not depend on $\theta_G$. This mode describes the simultaneous chiral rotation of $\sigma$ and $\Delta_s$ in the same direction under chiral transformation and is the NG mode.

(3) A massive pionic mode, denoted as $\pi_M$, identified with fluctuations of $\theta_M\equiv(\theta_\pi-\theta_d)/2$. This mode does not correspond to a $U(1)_A$ rotation of the system and thus must be massive, as seen from its stiffness term:

$$\frac{\partial\Omega}{\partial\sin^2(\theta_\pi-\theta_d)}=-\sum_{\pm}\int_{\boldsymbol{p}}\frac{M^2\Delta^2}{\pm\delta(\boldsymbol{p})\omega_\pm}=\int_{\boldsymbol{p}}\frac{M^2\Delta^2}{\mu\sqrt{\boldsymbol{p}^2+M^2}}\left(\frac{1}{\omega_+}-\frac{1}{\omega_-}\right)>0 \tag{3.58}$$

as long as $M,\Delta\neq 0$ as in the coexistence phase. The proportionality of this stiffness term to $\sim M^2\Delta^2$ originates from the mixing of $\pi$ and $\tilde{\pi}$, even though $\bar{q}q$-$qq$ coupling interactions at mean field level are not present in the original Lagrangian; such mixing phenomenon is discussed from a Ginzburg-Landau perspective in Ref. [64]. We can also trace this term back from the quasiparticle dispersion (3.34), from the appearance of the invariant quantity $|\sigma\Delta_{ps}+\pi\Delta_s|^2$ which appears like a vector product between two "chiral vectors" $(\sigma,\pi)$ and $(\Delta_{ps},\Delta_s)$.

(4) The two massive modes corresponding to fluctuations of $\Delta$ and $M$. These modes can be associated with oscillations in the radial direction of 'Mexican hat' potentials describing the broken symmetry state. In particular, the fluctuations of $M$ are related to the heavy $\sigma$-meson in nuclear matter, but can be removed by going into a non-linear sigma model describing chiral symmetry breaking.

(5) The massive mode associated with fluctuations of the relative phase $\phi$. This mode is generally not discussed in NJL investigations of the phase diagram. If one starts in the scalar state with $\phi=0$, a axial rotation $\theta_A$ will leave this angle untouched, as seen from Eq. (3.56). Note that if either $\Delta_s$ or $\Delta_{ps}$ vanishes,

this mode is not present.

In the following we neglect the phonon mode and the massive modes $M$ and $\Delta$, which have positive parity forbidding them from mixing with the two pionic modes. We assume the scalar ground state with $\phi = 0$ and discuss $\pi$ and $\tilde{\pi}$ in detail.

### 3.2.5 Mass matrix for the pions

We first calculate the mass matrix for the two pionic modes $\pi$ and $\tilde{\pi}$ by expanding the grand thermodynamic potential $\Omega$ to second order in them, and demonstrate how they are related to the NG mode $\pi_G$ and the massive mode $\pi_M$. Starting from

$$\Omega = \Omega_0 + \frac{1}{2}\theta_M^2 \int_{\boldsymbol{p}} \sum_{\pm} \frac{1}{\omega_{\pm}(\boldsymbol{p})\epsilon_{\pm}(\boldsymbol{p})\mu} + \ldots \equiv \Omega_0 + \frac{1}{2}\vec{\theta}^T \Xi \vec{\theta} + \ldots \tag{3.59}$$

where we denote for short the vector $\vec{\theta} \equiv (\theta_\pi, \theta_d)^T$ and $\Omega_0 = \Omega(\theta_\pi = \theta_d = 0)$. Using Eq. (3.59) we obtain the stiffness matrix

$$\Xi = M^2\Delta^2 a \begin{pmatrix} 1 & -1 \\ -1 & 1 \end{pmatrix}, \tag{3.60}$$

where the function $a(\mu) > 0$ is

$$a(\mu) \equiv \int_{\boldsymbol{p}} \sum_{\pm} \frac{1}{\omega_{\pm}(\boldsymbol{p})\epsilon_{\pm}(\boldsymbol{p})\mu}. \tag{3.61}$$

We let $f_\pi$ and $f_{\tilde{\pi}}$ be the decay constants of $\pi$ and $\tilde{\pi}$; since $\pi = f_\pi \theta_\pi$ and $\tilde{\pi} = f_{\tilde{\pi}}\theta_d$, the stiffness matrix $\Xi$ is related to the mass matrix $\Sigma$ by

$$\Sigma = \mathcal{F}^{-1}\Xi\mathcal{F}^{-1} = M^2\Delta^2 a \begin{pmatrix} 1/f_\pi^2 & -1/f_\pi f_{\tilde{\pi}} \\ -1/f_\pi f_{\tilde{\pi}} & 1/f_{\tilde{\pi}}^2 \end{pmatrix}, \tag{3.62}$$

where we denote $\mathcal{F} = \mathrm{diag}(f_\pi,\, f_{\tilde{\pi}})$, a simple invertible matrix relating $\pi$ and $\tilde{\pi}$ to $\theta_\pi$ and $\theta_d$:

$$\vec{\pi} \equiv \begin{pmatrix} \pi \\ \tilde{\pi} \end{pmatrix} = \mathcal{F} \begin{pmatrix} \theta_\pi \\ \theta_d \end{pmatrix}. \tag{3.63}$$

To diagonalize the mass matrix $\Sigma$, we perform the transformation

$$\begin{pmatrix} \pi \\ \tilde{\pi} \end{pmatrix} = \frac{1}{\sqrt{f_\pi^2 + f_{\tilde{\pi}}^2}} \begin{pmatrix} f_\pi & f_{\tilde{\pi}} \\ f_{\tilde{\pi}} & -f_\pi \end{pmatrix} \begin{pmatrix} \pi_G \\ \pi_M \end{pmatrix}, \tag{3.64}$$

which establishes a definition of $\pi_G$ and $\pi_M$ as a linear combination of $\pi$ and $\tilde{\pi}$; the mixing ratios agree with Ref. [64]. The two eigenvalues of $\Sigma$, $m_G^2 = 0$ and $m_M^2 = M^2\Delta^2 a\left(f_\pi^{-2} + f_{\tilde{\pi}}^{-2}\right)$, give the masses of $\pi_G$ and $\pi_M$.

One can understand the off-diagonal terms of $\Sigma$, describing $\pi$-$\tilde{\pi}$ mixing, by perturbing the correlation functions in the chiral and diquark channel. For example,

$$\Xi_{12} = \frac{\partial}{\partial\theta_d}\left(\frac{\partial\Omega}{\partial\theta_\pi}\right) = -iM\frac{\partial\langle\bar{\psi}\Gamma_\pi\psi\rangle}{\partial\theta_d} = M\Delta\frac{\partial\langle\bar{\psi}\Gamma_\pi\psi\rangle}{\partial\langle\bar{\psi}\Gamma_{\Delta_{ps}}\psi\rangle} \sim \frac{\partial\langle\bar{q}i\gamma_5 q\rangle}{\partial\langle qq\rangle}\Big|_{\theta_\pi}, \quad (3.65)$$

where in Nambu-Gor'kov-Dirac space

$$\begin{aligned}\Gamma_\pi &\equiv \frac{1}{M}\frac{\partial S^{-1}}{\partial\theta_\pi} = \begin{pmatrix} i\gamma_5 & 0 \\ 0 & i\gamma_5 \end{pmatrix}, \\ \Gamma_{\Delta_{ps}} &\equiv \frac{1}{i\Delta}\frac{\partial S^{-1}}{\partial\theta_d} = \begin{pmatrix} 0 & 0 \\ \mathbb{1} & 0 \end{pmatrix}; \end{aligned} \quad (3.66)$$

here $\mathbb{1}$ is the $4\times 4$ identity matrix in Dirac space.

The mass matrix and the diagonalization into NG and massive modes can be instructively compared with the Ginzburg-Landau study in Ref. [64], which was based on symmetry principles. The mixing terms in $\Sigma$ naturally result from expanding the thermodynamic potential and do not require direct mixing interactions between $\sigma$ and $\Delta$ at Lagrangian level. We can understand the mode diagonalization as a consequence of Goldstone's theorem, since only the NG mode, corresponding to $\theta_G = (\theta_\pi + \theta_d)/2$, should remain massless. The fluctuations corresponding to the massive mode do not correspond to a global $U(1)_A$ fluctuation of the system, and thus cannot be massless.

### 3.2.6 Decay constant of $\pi_G$

Having extracted $\pi_G$ from the model we next compute its decay constants. In the effective theory of $\pi_G$, the decay constant can be identified from the kinetic energy coefficient of $\theta_G$ in the long wavelength limit. To derive this effective theory we again resort to a Hubbard-Stratonovich transformation and promote $\theta_{\pi,d}$ to spatially dependent fluctuations. We denote the fluctuations of the mean fields by $\hat{\sigma}$, $\hat{\pi}$, $\hat{\Delta}_s$, and $\hat{\Delta}_{ps}$, where the hat distinguishes the bosonic fluctuations from their corresponding mean field values.

We start with the partition function

$$\begin{aligned}\mathcal{Z} &= \int dq\, d\bar{q}\, d\hat{\sigma}\, d\hat{\pi}\, d\hat{\Delta}_s\, d\hat{\Delta}_s^*\, d\hat{\Delta}_{ps}\, d\hat{\Delta}_{ps}^* \\ &\quad \times \exp\left\{ i\int d^4x \left[\bar{q}S^{-1}q - V(\hat{\sigma},\hat{\pi},\hat{\Delta}_s,\hat{\Delta}_{ps})\right]\right\}, \end{aligned} \quad (3.67)$$

where $t = i\tau$, with $0 \le \tau \le \beta$, $\beta$ being the inverse temperature. The inverse quark propagator $S^{-1}$ is perturbed from that in the scalar state $S_0^{-1}$ by the bosonized fields

$$S^{-1} = S_0^{-1} + \hat{x}, \quad (3.68)$$

where

$$\hat{x} \;=\begin{pmatrix} \hat{\sigma}+i\gamma_5\hat{\pi} & i\gamma_5\hat{\Delta}_s^*+\hat{\Delta}_{ps}^* \\ i\gamma_5\hat{\Delta}_s+\hat{\Delta}_{ps} & \hat{\sigma}+i\gamma_5\hat{\pi} \end{pmatrix}, \tag{3.69}$$

and the potential term involving the fluctuations are

$$V(\hat{\sigma},\hat{\pi},\hat{\Delta}_s,\hat{\Delta}_{ps}) = \frac{1}{4G}\left[(\hat{\sigma}-M)^2+\hat{\pi}^2\right]+\frac{1}{4H}\left[|\hat{\Delta}_s-i\Delta|^2+|\hat{\Delta}_p|^2\right]. \tag{3.70}$$

The quark field can again be integrated out, resulting in a fermion determinant to be re-exponentiated to become the effective action of the boson fields:

$$\begin{aligned} \mathcal{A} &= -i\mathrm{Tr}\ln S^{-1}+\int d^4x\, V \\ &= -i\mathrm{Tr}\ln S_0^{-1}-i\mathrm{Tr}\left[S_0\hat{x}-\frac{(S_0\hat{x})^2}{2}\right]+\int d^4x\, V+\ldots, \end{aligned} \tag{3.71}$$

where "Tr" denotes the sum over all indices, including position (or equivalently, momentum). The constant term $-i\mathrm{Tr}\ln S_0^{-1}$ corresponds to the mean field fermion sector and contains no bosonic fluctuations; we set this term aisde. In terms of the spatially dependent real bosonic fields $\hat{\theta}_\pi$ and $\hat{\theta}_d$, we write

$$\begin{aligned} -M\cos\hat{\theta}_\pi &= \hat{\sigma}-M, \\ -M\sin\hat{\theta}_\pi &= \hat{\pi}, \\ -i\Delta\cos\hat{\theta}_d &= \hat{\Delta}_s-i\Delta, \\ i\Delta\sin\hat{\theta}_d &= \hat{\Delta}_{ps}, \end{aligned} \tag{3.72}$$

which further yields to leading order in $\hat{\theta}_\pi$ and $\hat{\theta}_d$,

$$\hat{\sigma}\approx\frac{1}{2}M\hat{\theta}_\pi^2,\ \hat{\pi}\approx -M\hat{\theta}_\pi,\ \hat{\Delta}_s\approx\frac{i}{2}\Delta\hat{\theta}_d^2,\ \hat{\Delta}_{ps}\approx i\Delta\hat{\theta}_d. \tag{3.73}$$

Expanding $\mathcal{A}$ up to second order in $\hat{\theta}_\pi$ and $\hat{\theta}_d$, we obtain

$$\begin{aligned} \hat{x} &\approx M\begin{pmatrix} \frac{1}{2}\hat{\theta}_\pi^2-i\gamma_5\hat{\theta}_\pi & 0 \\ 0 & \frac{1}{2}\hat{\theta}_\pi^2-i\gamma_5\hat{\theta}_\pi \end{pmatrix} \\ &\quad +\Delta\begin{pmatrix} 0 & \frac{1}{2}\gamma_5\hat{\theta}_d^2-i\hat{\theta}_d \\ -\frac{1}{2}\gamma_5\hat{\theta}_d^2+i\hat{\theta}_d & 0 \end{pmatrix} \\ &\equiv M\left(\frac{1}{2}\hat{\theta}_\pi^2\Gamma_\sigma-\hat{\theta}_\pi\Gamma_\pi\right)+\Delta\left(\frac{1}{2}\hat{\theta}_d^2\Gamma_{\sigma_d}-\hat{\theta}_d\Gamma_{\tilde{\pi}}\right). \end{aligned} \tag{3.74}$$

Here, the matrices $\Gamma_\sigma$, $\Gamma_{\sigma_d}$, and $\Gamma_{\tilde{\pi}}$ in Nambu-Gor'kov-Dirac space are

$$\begin{aligned}\Gamma_\sigma &= \begin{pmatrix} \mathbb{1} & 0 \\ 0 & \mathbb{1} \end{pmatrix}, \ \Gamma_{\sigma_d} = \begin{pmatrix} 0 & \gamma_5 \\ -\gamma_5 & 0 \end{pmatrix}, \\ \Gamma_{\tilde{\pi}} &= \begin{pmatrix} 0 & i\mathbb{1} \\ -i\mathbb{1} & 0 \end{pmatrix},\end{aligned} \tag{3.75}$$

where $\Gamma_\pi$ is defined in Eq. (3.66).

Writing the real vector fields $\vec{\theta} \equiv \left(\hat{\theta}_\pi, \hat{\theta}_d\right)^T$, the quadratic effective action becomes

$$\mathcal{A} \approx \frac{1}{2}\beta\mathcal{V}\int \frac{d^4k}{(2\pi)^4}\,\vec{\theta}(-k)^T\mathcal{D}_\theta^{-1}(k)\vec{\theta}(k), \tag{3.76}$$

where

$$\mathcal{D}_\theta^{-1}(k) = \begin{pmatrix} M^2\left(B_{\pi\pi}(k) - 1/2G\right) & M\Delta B_{\pi d}(k) \\ M\Delta B_{\pi d}(k) & \Delta^2\left(B_{dd}(k) - 1/2H\right) \end{pmatrix}; \tag{3.77}$$

here $\mathcal{V}$ is the spatial volume of the system. The bubbles are defined by

$$\begin{aligned} B_{\pi\pi}(k) &= i\int \frac{d^4p}{(2\pi)^4}\mathrm{tr}\left(S_0(p)\Gamma_\pi S_0(p-k)\Gamma_\pi\right), \\ B_{\pi d}(k) &= i\int \frac{d^4p}{(2\pi)^4}\mathrm{tr}\left(S_0(p)\Gamma_\pi S_0(p-k)\Gamma_{\tilde{\pi}}\right), \\ B_{dd}(k) &= i\int \frac{d^4p}{(2\pi)^4}\mathrm{tr}\left(S_0(p)\Gamma_{\tilde{\pi}} S_0(p-k)\Gamma_{\tilde{\pi}}\right). \end{aligned} \tag{3.78}$$

If one replaces the $u$, $d$ quarks by protons and neutrons, the bubble $B_{\pi\pi}$ is simply the self-energy of the conventional in-nuclear medium pion Green's function as calculated in previous sections. We have used "tr" to denote the Dirac and Nambu-Gor'kov trace. By definition, $\mathcal{D}_\theta^{-1}(0)$ simply reduces to $-\Xi$ at zero momentum $k = 0$, which corresponds to a spatially homogeneous variation.

In general, $\mathcal{D}_\theta^{-1}$ is not a function of the Lorentz scalar $k^2$ at finite density due to the violation of Lorentz invariance.[6] As a result, the temporal and spatial decay constants are in general different. We thus write, to second order in $k$,

$$\mathcal{D}_\theta^{-1}(k) \approx -\Xi + \mathcal{Q}k_0^2 - \mathcal{Q}_v\boldsymbol{k}^2. \tag{3.79}$$

The dispersion relations of the modes are given by the eigenvalues of $\mathcal{D}_\theta^{-1}$, the decay constants are contained in the matrix $\mathcal{Q}$, and the mode velocities are included in $\mathcal{Q}_v$. As we show shortly, after keeping only the leading order logarithm divergencies, $\mathcal{Q}$ is related to the matrix $\mathcal{F}$ as defined in Eq. (3.63) by $\mathcal{Q} = \mathcal{F}^2$, while $\mathcal{Q}_v = \mathrm{diag}(v_\pi^2, v_{\tilde{\pi}}^2)\mathcal{Q}$ where $v_\pi$ and $v_{\tilde{\pi}}$ are the mode velocities of $\pi$ and $\tilde{\pi}$.

[6] Even in the vacuum use of a three-momentum cutoff violates Lorentz invariance.

To calculate the bubbles (3.78), we make use of the form (3.44). The decay constant matrix $\mathcal{Q}$ can be obtained from take derivatives of the bubbles with regard to $k_0$ while setting $k = (k_0, \mathbf{0})$. As we are calculating thermodynamic properties, the $p_0$ integrals are Matsubara frequency summations (cf. the explanation in Sec. 2.1.1 below Eq. (2.12)) with $p_0 \to i\omega_\nu = 2\pi i T\nu$ and $\int dp_0 \to 2\pi i T \sum_\nu$, where $\nu = \pm 1/2, \pm 3/2, \ldots$. With the quasiparticle spectrum $\omega_\pm$, the free particle dispersion $\epsilon_\pm$, and the coherence functions $v_\pm$ and $u_\pm$ defined earlier – all functions of the three-momentum integration variable $\boldsymbol{p}$ – the bubbles are

$$\begin{aligned}
B_{\pi\pi}(k_0^2) &= \int_{\boldsymbol{p}} \sum_{j,\ell=\pm} (u_j v_\ell - v_j u_\ell)^2 \left(1 - \frac{M^2 + \boldsymbol{p}^2}{\epsilon_j \epsilon_\ell}\right) A_{j\ell}(k_0), \\
B_{dd}(k_0^2) &= \int_{\boldsymbol{p}} \sum_{j,\ell=\pm} (v_j v_\ell + u_j u_\ell)^2 \left(1 - \frac{M^2 - \boldsymbol{p}^2}{\epsilon_j \epsilon_\ell}\right) A_{j\ell}(k_0), \\
B_{\pi d}(k_0^2) &= \int_{\boldsymbol{p}} \sum_{j,\ell=\pm} (v_j v_\ell + u_j u_\ell)(v_j u_\ell - u_j v_\ell) \times \frac{M(\epsilon_\ell - \epsilon_j)}{\epsilon_\ell \epsilon_j} A_{j\ell}(k_0),
\end{aligned} \tag{3.80}$$

with the factor

$$A_{j\ell}(k_0) = \frac{1}{2}\left(-\frac{1}{k_0 - \omega_j - \omega_\ell} + \frac{1}{k_0 + \omega_j + \omega_\ell}\right). \tag{3.81}$$

The physical meanings of the bubbles and the factor function $A_{j\ell}(k_0)$ are manifest in these forms, summarized as follows:

(1) The pairing part: the first factor sums of products between coherence functions, indicates whether the quark loop connects the quark field with the quark field or with the charge-conjugate quark field.

(2) The Dirac part: the second factor, involving $\epsilon$'s, $M^2$ and $\boldsymbol{p}^2$, depends on whether the quark loop connects particle-antihole states with particle-antihole states, or with antiparticle-hole states.

Both factors are at most of order unity; they result directly from projection operators into different pairing and Dirac components of the eigenvectors. The final factor $A_{j\ell}$ reveals the pole structure of the external frequency $k_0$; it contains a pair of poles located at $\pm(\omega_j + \omega_\ell)$ with opposite signs for the corresponding residues, representing the pion state and anti-pion state described by the bubble. In our model the pion is only neutral, thus they represent the same pion state. In $N_f \geq 2$ models where charged pions are present, the dual poles would represent the $\pi^+$ and the $\pi^-$ state separably.

It is instructive to consider the $B_{\pi\pi}$ bubble as an example to illustrate the physical meanings. The factor $(u_j v_\ell - v_j u_\ell)^2$ involves products between $v$ and $u$, indicating that the quark loop connects the quark field with the charge-conjugate field; the factor $1 - (M^2 + \boldsymbol{p}^2)/\epsilon_j \epsilon_\ell$ vanishes unless $j = -\ell$, indicating that the particle-antihole state is connected to the antiparticle-hole state. Altogether,

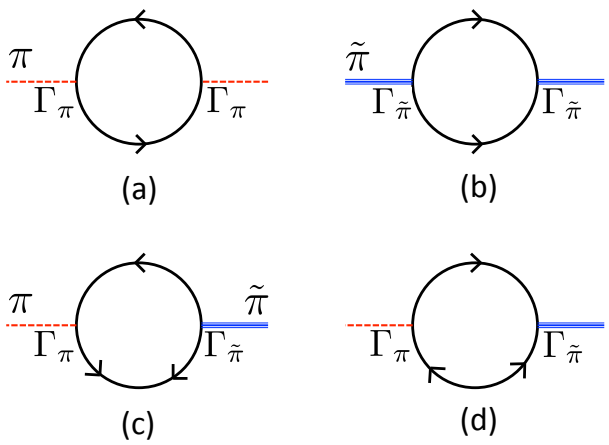


Figure 3.4: Characteristic diagrams corresponding to the bubbles (3.80). The direct (a) $\pi$-$\pi$ and (b) $\tilde{\pi}$-$\tilde{\pi}$ bubbles correspond to $B_{\pi\pi}$ and $B_{dd}$, while the $\pi$-$\tilde{\pi}$ mixing bubbles such as (c) and (d) correspond to $B_{\tilde{\pi}}$. Due to the breaking of $U(1)_V$ by diquark pairing, quark number is not conserved.

the quark field particle-anti-hole state is connected to the charge-conjugate antiparticle-hole state (or equivalently, to the quark field particle-antihole state itself), and the quark field antiparticle-hole state is connected to the charge-conjugate particle-antihole state (or equivalently, to the quark antiparticle-hole state).

We can further simplify the mixing bubble $\Pi_{\pi d}$ by using properties of the BCS coherence functions:

$$B_{\pi d}(k_0^2) = -M\Delta \int_{\boldsymbol{p}} \sum_{j,\ell=\pm} \frac{(\epsilon_j - \epsilon_\ell)^2}{2\epsilon_j \epsilon_\ell \omega_j \omega_\ell} A_{j\ell}(k_0); \tag{3.82}$$

it is non-zero only in the coexistence phase where $M, \Delta \neq 0$. The bubbles are summarized diagrammatically in Fig. 3.4.

In terms of the bubbles, the matrix $\Xi$ is given by $-\mathcal{D}_\theta^{-1}(k = 0)$, as in Eq. (3.77). We find explicitly,

$$\begin{aligned} M^2 \left( B_{\pi\pi}(0) - \frac{1}{2G} \right) &= \Delta^2 \left( B_{dd}(0) - \frac{1}{2H} \right) \\ &= -M\Delta B_{\pi d}(0) = -M^2\Delta^2 a, \end{aligned} \tag{3.83}$$

($a$ is given by Eq. (3.61)) confirming the expected form (3.60) of $\Xi$.

From Eq. (3.80) we calculate the $\mathcal{Q}$ matrix:

$$\begin{aligned}
\mathcal{Q}_{11} &= M^2 \int_{\boldsymbol{p}} \sum_{j,\ell=\pm} (u_j v_\ell - v_j u_\ell)^2 \left(1 - \frac{M^2 + \boldsymbol{p}^2}{\epsilon_j \epsilon_\ell}\right) W_{j\ell}, \\
\mathcal{Q}_{22} &= \Delta^2 \int_{\boldsymbol{p}} \sum_{j,\ell=\pm} (v_j v_\ell + u_j u_\ell)^2 \left(1 - \frac{M^2 - \boldsymbol{p}^2}{\epsilon_j \epsilon_\ell}\right) W_{j\ell}, \\
\mathcal{Q}_{12} &= -2M^2\Delta^2 \int_{\boldsymbol{p}} \frac{1}{\omega_+ \omega_- \left(\omega_+ + \omega_-\right)^3} = \mathcal{Q}_{21},
\end{aligned} \tag{3.84}$$

where

$$W_{j\ell}(\boldsymbol{p}) \equiv \frac{1}{(\omega_j(\boldsymbol{p}) + \omega_\ell(\boldsymbol{p}))^3}. \tag{3.85}$$

The result (3.84) shows that both $\Xi$ and the diagonal elements $\mathcal{Q}_{11}$ and $\mathcal{Q}_{22}$ are logarithmically divergent (of order $\ln \Lambda/M$ or $\ln \Lambda/\Delta$), while the off-diagonal elements $\mathcal{Q}_{12}$ are finite. In the following, we drop the finite off-diagonal terms, following the standard prescription of considering only the ultraviolet-divergent pieces up to logarithmic accuracy of the bubble diagrams in effective bosonized theories (see e.g., [68, 69, 70]). The dropped $Q_{12}$ terms would result in anomalous mixing terms $\sim \partial_\mu \hat{\theta}_\pi \partial^\mu \hat{\theta}_d$ which are absent in general parametrizations of pionic mode kinetic energies (up to second order in the pionic fields) in the literature, e.g., [64]. After this procedure, we identify the remaining diagonal elements of $\mathcal{Q}$ as the squared decay constants for the vacuum pion and the diquark-condensate pion:

$$f_\pi^2 = \mathcal{Q}_{11}, \quad f_{\tilde{\pi}}^2 = \mathcal{Q}_{22}; \tag{3.86}$$

that is, $\mathcal{Q} = \mathcal{F}^2 = \mathrm{diag}(f_\pi^2, f_{\tilde{\pi}}^2)$, where $\mathcal{F} = \mathrm{diag}(f_\pi, f_{\tilde{\pi}})$ as in Eq. (3.63). Similarly dropping the finite off-diagonal terms of the velocity matrix $\mathcal{Q}_v$, we obtain $\mathcal{Q}_v = \mathrm{diag}(v_\pi^2, v_{\tilde{\pi}}^2)\mathcal{Q}$, where the velocities are

$$\begin{aligned}
v_\pi^2 &= \mathcal{Q}_{v11} = f_\pi^{-2} \frac{\partial B_{\pi\pi}(0)}{\partial \boldsymbol{k}^2}, \\
v_{\tilde{\pi}}^2 &= \mathcal{Q}_{v22} = f_{\tilde{\pi}}^{-2} \frac{\partial B_{dd}(0)}{\partial \boldsymbol{k}^2}.
\end{aligned} \tag{3.87}$$

In terms of the pion fields $\pi(x) = f_\pi \hat{\theta}_\pi(x)$ and $\tilde{\pi}(x) = f_{\tilde{\pi}} \hat{\theta}_d(x)$, the effective Lagrangian density is now

$$\frac{1}{2}\vec{\theta}^T \left(-\mathcal{Q}\partial_t^2 + \mathcal{Q}_v \vec{\partial}^2 - \Xi\right) \vec{\theta} \equiv \frac{1}{2}\vec{\pi}^T (-\partial_t^2 + \mathrm{diag}(v_\pi^2, v_{\tilde{\pi}}^2)\vec{\partial}^2 - \Sigma)\vec{\pi}, \tag{3.88}$$

where $\vec{\pi}(x) \equiv (\pi(x), \tilde{\pi}(x))^T = \mathcal{F}\vec{\theta}(x)$. The inverse propagator in Eq. (3.88) is again diagonalized by Eq. (3.64), in terms of the NG mode $\pi_G$ and the massive

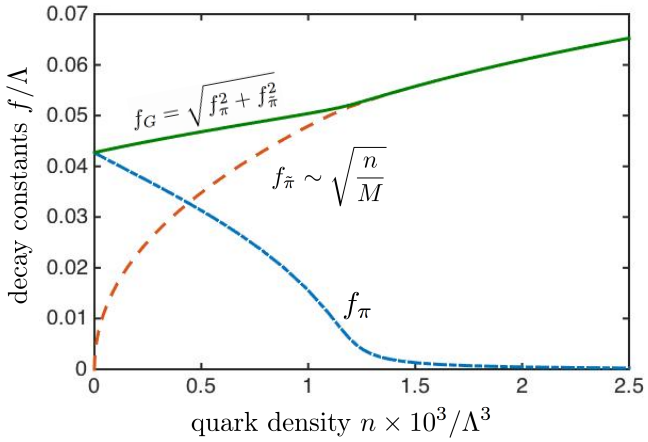


Figure 3.5: ( Decay constants $f_G$, $f_\pi$ and $f_{\tilde{\pi}}$ as functions of quark density $n$, with $G = 11\Lambda^{-2}$ and $H = 6\Lambda^{-2}$.

mode $\pi_M$. Furthermore, in terms of $\hat{\theta}_\pi$ and $\hat{\theta}_d$, we write

$$\pi_G = \frac{f_\pi^2 \hat{\theta}_\pi + f_{\tilde{\pi}}^2 \hat{\theta}_d}{\sqrt{f_\pi^2 + f_{\tilde{\pi}}^2}} \equiv f_G \hat{\theta}_G \tag{3.89}$$

where $\hat{\theta}_G$, the chiral NG boson degree of freedom, is the fluctuation corresponding to the universal axial $U(1)_A$ rotation of the whole system from the scalar state; such rotation corresponds to the simultaneous rotation of $\hat{\theta}_\pi$ and $\hat{\theta}_d$, therefore $\hat{\theta}_G = \hat{\theta}_\pi = \hat{\theta}_d$. As a result,

$$f_G^2 = f_\pi^2 + f_{\tilde{\pi}}^2, \tag{3.90}$$

thus relating the decay constant of the NG boson $f_G$ to the decay constants $f_\pi$ and $f_{\tilde{\pi}}$ for the corresponding chiral rotations of the $\langle \bar{q}q \rangle$ and $\langle qq \rangle$ order parameters. As Eq. (3.89) shows $f_\pi^2$ and $f_{\tilde{\pi}}^2$ can be understood as the "weight functions" of $\pi$ and $\tilde{\pi}$ within the NG mode $\pi_G$.

The plot of $f_G$, $f_\pi$ and $f_{\tilde{\pi}}$ as functions of quark density in Fig. 3.5 shows that the decay constant of the NG pion, $f_G$, always increases with increasing quark density, whereas $f_\pi$ decreases with density; the behavior of $f_\pi$ is in agreement with the prediction of in-medium chiral perturbation theory [71] that to leading order in the density the pion decay constant decreases from its vacuum value linearly.[7] The different behavior of $f_G$ and $f_\pi$ arises from the presence of diquark pairing at all densities in our schematic model; even at low density, the BCS gap causes $f_G$ to increase with increasing density despite $\langle \bar{q}q \rangle$ (and thus $f_\pi$)

[7] Unlike NJL discussions of quark matter, Ref. [71] discusses only a nucleon medium. Although the vacuum cannot be described by deconfined NJL quark matter, the behavior of its chiral NG mode under modification of the density does connect qualitatively well with such nuclear matter models, a similarity suggesting that the transition from nuclear matter to high density quark matter could have continuous dynamic chiral symmetry breaking.

gradually shrinking at the same time.[8]

We now demonstrate how to understand the behavior of $f_\pi$ and $f_{\tilde{\pi}}$ shown by Fig. 3.5 particularly in the low density and the coexistence region. In the low density limit, the behavior of $f_{\tilde{\pi}}$ and $\Delta$ can be derived from the pairing gap equation (3.46) and the bubble results Eq. (3.84). Isolating the divergent part $1/\omega_+$ in the gap equation integral, and approximate near the Fermi surface

$$(\epsilon_p - \mu)^2 \approx \frac{p_F^2}{\mu^2}(p - p_F)^2, \tag{3.91}$$

we obtain

$$\begin{aligned} \frac{1}{2H} &\approx \frac{1}{2\pi^2}\int_0^\Lambda p^2 dp \, \frac{1}{\sqrt{(\epsilon-\mu)^2+\Delta^2}} \\ &\approx \frac{1}{2\pi^2}\int_0^\Lambda p_F^2 dp \, \frac{1}{\Delta\sqrt{\frac{p_F^2}{\mu^2\Delta^2}(p-p_F)^2+1}}. \end{aligned} \tag{3.92}$$

Changing variables to

$$\sinh x = \frac{p_F}{\mu\Delta}(p-p_F),\ \cosh x\, dx = \frac{p_F}{\mu\Delta}dp;\ \sinh x \in \left[-\frac{p_F^2}{\mu\Delta}, \frac{\Lambda p_F}{\mu\Delta}\right], \tag{3.93}$$

then

$$\frac{1}{2H} = \frac{p_F^2}{2\pi^2}\int dx\, \frac{\mu\Delta}{p_F}\frac{\cosh x}{\Delta\sqrt{\sinh^2 x+1}} = \frac{\mu p_F}{2\pi^2}\int dx. \tag{3.94}$$

When $\Delta$ is small, we can approximate $\Lambda p_F/\mu\Delta = \sinh x \approx \frac{1}{2}\exp x$ which yields $x \approx \ln(2\Lambda p_F/\mu\Delta)$. As a result the gap equation becomes

$$\frac{1}{2H} \approx \frac{\mu p_F}{2\pi^2}\left(\ln\frac{2\Lambda p_F}{\mu\Delta} + \ln\frac{2p_F^2}{\mu\Delta}\right) = \frac{\mu p_F}{2\pi^2}\ln\frac{p_F^3\Lambda}{\mu^2\Delta^2} = \frac{\mu p_F}{\pi^2}\ln\frac{p_F}{\mu\Delta}\sqrt{p_F\Lambda}, \tag{3.95}$$

which further yields

$$\Delta \sim \frac{p_F}{\mu}\sqrt{p_F\Lambda}\exp\left(-\frac{\pi^2}{2H\mu p_F}\right) \approx \frac{p_F}{m}\sqrt{p_F\Lambda}\exp\left(-\frac{\pi^2}{2Hmp_F}\right). \tag{3.96}$$

If we assumed $p_F \ll \Lambda$ in evaluating (3.95), we would arrive at

$$\frac{1}{2H} \approx \frac{\mu p_F}{2\pi^2}\ln\frac{2\Lambda p_F}{\mu\Delta} \Rightarrow \Delta \sim \frac{p_F}{m}\Lambda\exp\left(-\frac{\pi^2}{Hmp_F}\right). \tag{3.97}$$

In either case, $\Delta$ is extremely small compared to $p_F$ and vanishes faster than any power of $p_F$. In short, in the limit $n \to 0$, the gap behaves like

$$\frac{\Delta}{\Lambda} \sim \frac{p_F}{M}e^{-\pi^2/HMp_F}, \tag{3.98}$$

[8] Realistically, the homogeneous diquark pairing described in the present model does not appear in the low density QCD phase diagram, owing to the onset of confinement.

and $\Delta/n \to 0$ as $n \to 0$.

We can perform the same analysis to derive the behavior of $f_{\tilde{\pi}}$. We first derive a generalized Goldberger-Treiman relation for the diquark pairing, $g_{\tilde{\pi}} f_{\tilde{\pi}} = \Delta$, where $g_{\tilde{\pi}}$ is the effective diquark pion-quark coupling strength analogous to $g_\pi$ of $g_\pi f_\pi = M$. Let us quickly review the vacuum pion case. The vacuum-to-axial-vector transition parametrizing the decay constant is

$$\begin{aligned} i f_\pi q^\mu = \langle 0 | J_A^\mu | \pi \rangle &= g_{\pi qq} \langle 0 | J_A^\mu \bar{q} i\gamma_5 q | 0 \rangle \\ &= g_\pi i \int_p \mathrm{tr} \left( S(p) \frac{1}{2} \gamma^\mu \gamma_5 S(p-q) i\gamma_5 \right); \end{aligned} \tag{3.99}$$

the coupling $g_\pi$ on the other hand is the $g$ in Sec. 2.1.2, appearing as the residue of the pion pole in the T-matrix; it is related to the bubble $B_{\pi\pi}$ by

$$g_\pi^2 = \left( \frac{dB_{\pi\pi}}{dk_0^2} \right)^{-1}. \tag{3.100}$$

Analogously, for $f_{\tilde{\pi}}$ we write down the amplitude

$$i f_{\tilde{\pi}} q^\mu = g_{\tilde{\pi}} i \int_p \mathrm{tr} \left( S(p) \frac{\gamma^\mu}{2} \gamma_5 S(p-q) \Gamma_d \right), \tag{3.101}$$

where

$$\Gamma_d = \begin{pmatrix} & i \\ -i & \end{pmatrix} \tag{3.102}$$

is the vertex corresponding to the diquark pion. After some algebra and setting $k^\mu = (k_0, \mathbf{0})$, we obtain

$$\begin{aligned} f_{\tilde{\pi}} &= \frac{1}{2} g_{\tilde{\pi}} \int_{\boldsymbol{p}} \sum_{ij} (v_i v_j' + u_i u_j')(u_i v_j' + v u') \left( 1 - \frac{M^2 - \boldsymbol{p}^2}{\epsilon_i \epsilon_j'} \right) \frac{1}{(\omega_i + \omega_j')^2} \\ &= \frac{1}{2} g_{\tilde{\pi}} \Delta \int_{\boldsymbol{p}} \sum_{ij} \left( \frac{1}{2\omega_i} + \frac{1}{2\omega_j'} \right) \left( 1 - \frac{M^2 - \boldsymbol{p}^2}{\epsilon_i \epsilon_j'} \right) \frac{1}{(\omega_i + \omega_j')^2} \equiv g_{\tilde{\pi}} \Delta I_{\tilde{\pi}}, \end{aligned} \tag{3.103}$$

where the sum over $i, j = \pm$ is over all four positive energy eigenvalues as in (3.39), and positive/negative $\epsilon_\pm = \pm(p^2 + M^2)^{-1/2}$, with the corresponding coherence functions $u_\pm$ and $v_\pm$; both $\omega, \epsilon$ and the primed $\omega', \epsilon'$ are evaluated at $\boldsymbol{p} = 0$. Meanwhile,

$$\begin{aligned} g_{\tilde{\pi}}^{-2} = \frac{dB_{dd}}{dk_0^2} &= \int_{\boldsymbol{p}} \sum_{ij} \left( v_i v_j' + u_i u_j' \right)^2 \left( 1 - \frac{M^2 - \boldsymbol{p}^2}{\epsilon_i \epsilon_k'} \right) \frac{1}{(\omega_i + \omega_j')^3} \\ &\equiv J_{\tilde{\pi}}. \end{aligned} \tag{3.104}$$

The terms corresponding to $(i,j) = (+,+)$ or $(-,-)$ are logarithmically divergent, while $(+,-)$ and $(-,+)$ terms are finite; since $J_d$ and $I_d$ eventually undergo the renormalization process as discussed in Sec. 2.1.3, they are identical to logarithmic accuracy; we thus identify $I_{\tilde{\pi}} = J_{\tilde{\pi}}$ at this level, resulting in

$$f_{\tilde{\pi}} = g_{\tilde{\pi}}^{-1}\Delta \to g_{\tilde{\pi}} f_{\tilde{\pi}} = \Delta. \tag{3.105}$$

We are now at a place to calculate the behavior of $f_{\tilde{\pi}}$ as a function of quark density $n$ in the vacuum limit of this model. Isolating the divergent piece of $J_{\tilde{\pi}}$ near the Fermi surface,

$$\begin{aligned} J_{\tilde{\pi}} &\approx \frac{2p_F^4}{8\mu^2} \times \frac{1}{2\pi^2}\int_0^\Lambda dp\ \frac{1}{((\epsilon_p-\mu)^2+\Delta^2)^{3/2}} \\ &\approx \frac{p_F^4}{8\pi^2\mu^2\Delta^3}\int_0^\Lambda dp\ \frac{1}{(\frac{p_F^2}{\mu^2\Delta^2}(p-p_F)^2+1)^{3/2}}; \end{aligned} \tag{3.106}$$

changing the integration variable to $\sinh x = p_F(p-p_F)/\mu\Delta$, we have

$$\begin{aligned} & J_{\tilde{\pi}} \\ & \approx \frac{p_F^4}{8\pi^2\mu^2\Delta^3}\int dx\ \frac{\mu\Delta}{p_F}\frac{\cosh x}{(\sinh^2 x+1)^{3/2}} = \frac{\mu p_F^3}{8\pi^2\mu^2\Delta^2}\int dx\ \frac{1}{\cosh^2 x} \\ & = \frac{\mu p_F^3}{16\pi^2\mu^2\Delta^2}\left(\frac{1}{\left(\frac{\mu\Delta}{2p_F^2}\right)^2+1} - \frac{1}{\left(\frac{2\Lambda p_F}{\mu\Delta}\right)^2+1}\right) \\ & \approx \frac{p_F^3}{16\pi^2 M\Delta^2}, \end{aligned} \tag{3.107}$$

as long as $\Delta$ vanishes faster than any power of $p_F$ (as we already demonstrated) and we have used $\mu \approx M$ in the vacuum limit. As a consequence, we obtain

$$f_{\tilde{\pi}}^2 = J_{\tilde{\pi}}\Delta^2 \sim \frac{p_F^3}{16\pi^2 M} = \frac{3n}{16M}. \tag{3.108}$$

Thus $f_{\tilde{\pi}} \sim \sqrt{n}$.

We can estimate the density in our model at which $f_\pi \sim f_{\tilde{\pi}}$, i.e., the "maximum" mixing where diquark and chiral condensates are equally important. Taking $f_\pi$ to be approximately its vacuum value, we have

$$f_\pi \approx f_{\tilde{\pi}} \to n \approx \frac{16}{3} M f_\pi^2, \tag{3.109}$$

which, with $M = 300$ MeV, gives

$$n \sim M f_\pi^2 \sim 3\times 10^6 \mathrm{MeV}^3 \sim 0.4\mathrm{fm}^{-3} \sim 2n_0 \tag{3.110}$$

where $n_0$ is nuclear matter density. This result suggests that even in realistic

quark models, the chiral and diquark condensates should be equally important at the order of several times $n_0$, thus the study of a coexistence region is highly relevant.

It is preferable to discuss the decay constant of the actual generalized pion $f_G$, since it is the NG boson and thus the directly observable long-lived particle. We can equivalently parametrize $f_G$ as the vector transition amplitude from a state with one generalized pion to the vacuum via the time component of the axial current $J_A^\mu \equiv \bar{\psi} i\gamma^\mu\gamma^5\psi/2$, in the same way as in the vacuum pion treatment [23] in NJL models as discussed above:

$$if_G k^0 = \langle 0|J_A^0|\pi_G\rangle = \frac{1}{f_G}\langle 0|J_A^0|f_\pi\pi + f_{\tilde{\pi}}\tilde{\pi}\rangle\frac{1}{f_G} i(f_\pi^2 + f_{\tilde{\pi}}^2)k^0, \tag{3.111}$$

which indeed confirms Eq. (3.90).

With $f_G$ and the diagonalization (3.64), we can re-write the coupling between quarks and chiral/diquark pions in terms of quarks and NG/massive pions. Using the perturbed quark inverse propagator with the bosonized fields in Eqs. (3.68) and (3.69), and the transformation Eq. (3.64), we have

$$\mathcal{L}_{\text{int}} = \bar{\psi}\left(\frac{M}{f_\pi}\Gamma_\pi\pi + \frac{\Delta}{f_{\tilde{\pi}}}\Gamma_{\tilde{\pi}}\tilde{\pi}\right)\psi = \bar{\psi}\left(\Gamma_G\pi_G + \Gamma_M\pi_M\right)\psi, \tag{3.112}$$

where the interaction vertex with generalized pion $\Gamma_G$ and the massive partner $\Gamma_M$ are

$$\begin{aligned}\Gamma_G(\mu) &\equiv \tfrac{1}{f_G}\left(M\Gamma_\pi + \Delta\Gamma_{\tilde{\pi}}\right), \\ \Gamma_M(\mu) &\equiv \tfrac{1}{f_G}\left(\tfrac{f_{\tilde{\pi}}}{f_\pi}M\Gamma_\pi - \tfrac{f_\pi}{f_{\tilde{\pi}}}\Delta\Gamma_{\tilde{\pi}}\right);\end{aligned} \tag{3.113}$$

they are matrix functions of $\mu$, describing the emerging density-dependent couplings; the graphical summary is presented in Fig. 3.6. The coupling strengths to the chiral sector and the diquark sector are given by the weightings $M/f_G$ and $\Delta/f_G$; in the vacuum limit $\Delta/f_G = 0$, and the former reduces to $g_\pi$, the residue of the pion pole in the $\bar{q}q$-$\bar{q}q$ scattering T-matrix, related to $M$ and $f_\pi$ via the familiar Goldberger-Treimann relation $g_\pi = M/f_\pi$.

In more realistic NJL models where $N_f, N_c > 1$, possible asymmetric chiral and diquark pairings due to the heavy strange quark, and the Kobayahsi-Miskawa-'t Hooft six-quark instanton interaction [21, 22, 72] provide additional $\bar{q}q$-$qq$ mixing, with further modifications of $\Gamma_G$ and $\Gamma_M$. We leave this as a research topic for the future.

### 3.2.7 Explicit chiral symmetry breaking by current (bare) quark mass $m_q \neq 0$

Our discussion so far has focused on the chiral limit, where the NG boson – the generalized pion $\pi_G$ – remains strictly massless. We now generalize to

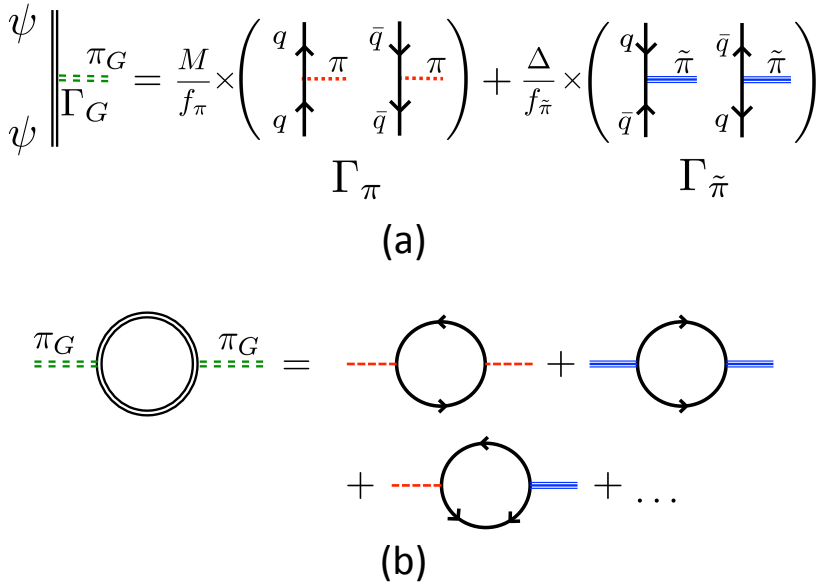


Figure 3.6: (a) Diagrammatic decomposition of quark-$\pi_G$ coupling $\Gamma_G$ into chiral $\Gamma_\pi$ and diquark $\Gamma_{\tilde{\pi}}$ vertices. The (green) dashed double line represents the $\pi_G$ field. The Nambu-Gor'kov field $\psi$ (black, double line) contains both the quark and charge-conjugate quark fields, thus including the quark field (black, solid, arrowed line) propagating in either time direction; $\Gamma_\pi$ is the coupling matrix between vacuum pion $\pi$ (red, dashed line) and the pseudoscalar $\bar{q}q$ quark sector, and $\Gamma_{\tilde{\pi}}$ is the coupling matrix between diquark-condensate pion $\tilde{\pi}$ (blue, double line) and the pseudoscalar $qq$ sector. (b) Characteristic bubble diagrams contributing to the resulting self-energy of $\pi_G$ in the Nambu-Gor'kov formalism, including both direct bubbles, $B_{\pi\pi}$ and $B_{dd}$, and mixing bubbles, $B_{\pi d}$.

$m_q \neq 0$ which explicitly breaks the chiral symmetry, granting the generalized pion mass, while also supposedly modifying the mass of the massive mode $\pi_M$. To investigate the effect of $m_q$ on the pion mass matrix, we directly take second order derivatives of $\Omega$ with respect to $\theta_\pi$ and $\theta_d$, using Eq. (3.36).

We start by briefly reviewing the familiar $\sigma - \pi$ sector alone from this perspective of differentiating the grand thermodynamic potential density $\Omega$. As seen from the quasiparticle spectrum, $\omega_\pm(\boldsymbol{p})$, Eq. (3.34), $m_q$ slightly shifts $\sigma$, causing the system to favor a negative value for $\sigma$ (whence the sign in the parametrization $\sigma = -M\cos\theta_\pi$). In the vacuum scalar state, the eigenvalues expanded to leading order in $m_q$ are:

$$\begin{aligned}\omega_\pm(\boldsymbol{p}) &= \left|\pm\left(\boldsymbol{p}^2 + m_q^2 + \sigma^2 + \pi^2 - 2m_q\sigma\right)^{1/2} - \mu\right| \\ &= \omega_\pm(\boldsymbol{p})_{m_q=0} + \left(\pm\frac{\mu}{\sqrt{\boldsymbol{p}^2+\sigma^2+\pi^2}} - 1\right)\frac{\sigma m_q}{\omega_\pm(\boldsymbol{p})_{m_q=0}}; \quad (3.114)\end{aligned}$$

we can then expand

$$\begin{aligned}\Omega &= \Omega_{m_q=0} + \sigma m_q \sum_\pm \int_{\boldsymbol{p}} \frac{1}{\omega_\pm}\left(1 \mp \frac{\mu}{\sqrt{\boldsymbol{p}^2+\sigma^2+\pi^2}}\right) \\ &\approx \Omega_{m_q=0} + \frac{\sigma m_q}{2G}, \quad (3.115)\end{aligned}$$

where we have used the gap equation Eq. (3.46) in writing the second line, up to linear order in $m_q$. With the parametrization (3.53), this term effectively adds a positive stiffness term for $\theta_\pi^2 \sim \pi^2$, since $\sigma = -M(1 - \theta_\pi^2/2 + \ldots)$. We thus retrieve the well known GMOR result for the vacuum pion mass to leading order in $m_q$,

$$f_\pi^2 m_\pi^2 = \frac{M}{2G} m_q = -\langle\bar{q}q\rangle m_q. \quad (3.116)$$

Next we consider the diquark pairing alone with no chiral condensate, $\sigma = 0$, and choose a gauge where $\Delta_{ps}$ and $\Delta_p$ are in phase. In this case we have the quasiparticle spectrum

$$\omega_\pm^2(\boldsymbol{p}) = \boldsymbol{p}^2 + \mu^2 + \Delta^2 \mp 2\sqrt{(|\boldsymbol{p}|\mu)^2 + m_q^2|\Delta_{ps}|^2}; \quad (3.117)$$

in this case, it is the pseudoscalar diquark NG mode $\tilde{\pi}^2 \sim \theta_d^2 \sim |\Delta_{ps}|^2$ that obtains a mass of

$$f_{\tilde{\pi}}^2 m_{\tilde{\pi}}^2 = a\Delta^2 m_q^2. \quad (3.118)$$

This GMOR relation is second order in $m_q$ and has no linear order contribution, unlike the vacuum GMOR relation for chiral condensate and $\bar{q}q$ pion. The grand

thermodynamic potential then expands as

$$\Omega \quad = \Omega_{m_q=0} + \tfrac{1}{2} a m_q^2 |\Delta_{ps}|^2 + \mathcal{O}\left(m_q^4\right). \tag{3.119}$$

It is interesting that unlike $\sigma$, the diquark mean fields suffer from neither shift in mean field potentials caused by $m_q$, nor any direct coupling to $m_q$ at the Lagrangian level; the key term responsible for such a behavior is $|(m_q - \sigma)\Delta_{ps} - \pi\Delta_s|^2$, one of the chirally invariant quantities (see Eq. 3.57). This term explains why the diquark condensate GMOR relation starts from second instead of first order.

The difference in the leading order dependence on $m_q$ of the GMOR relations in the vacuum phase and the high density BCS phase, which is also present in the more realistic $N_f = 3$, $N_c = 3$ case, can be understood as originating from the $U(1)_A$ axial symmetry. Specifically, when one writes down a general Ginzburg-Landau effective Lagrangian in terms of the chiral and diquark condensates, the term of lowest order in $m_q$ and $\Delta$s that respects $U(1)_A$ symmetry is of order $m_q^2$ [65, 64]. As a result, at high density, where diquark pairing dominates, the chiral NG bosons should obey a GMOR relation $\sim m_q^2$. A subtle complication in more realistic models is that the axial $U(1)_A$ symmetry is explicitly broken by quantum effects (the axial anomaly) at lower densities, which permits an additional mass term for the diquark condensates of order $m_q$. In this case, the chiral NG bosons might still obey a GMOR relation $\sim m_q$ in leading order even with dominating diquark condensates at moderate densities. Nevertheless, it is known that at high density the axial anomaly is heavily suppressed [73, 74] greatly reducing such a $U(1)_A$-violating term; the GMOR relation is then restored to $\sim m_q^2$ in leading order (cf. Eq. (3.118)).[9]

We are in position to calculate the mass matrix when both chiral and diquark condensates are present. When computing the perturbation to the mass matrix by $m_q$, it is necessary to consider up to second order, which as we showed is the leading order in the diquark sector. We start again with the angle fluctuations $\vec{\theta} = (\theta_\pi, \theta_d)^T$, and expand $\Omega$:

$$\Omega(\theta_\pi, \theta_d) = \Omega(0,0) + \frac{1}{2} \vec{\theta}^{\,T} \Xi(m_q) \vec{\theta} + \dots, \tag{3.120}$$

where the stiffness matrix is now

$$\Xi(m_q) = \begin{pmatrix} bMm_q + aM^2\Delta^2 & -aM\Delta^2 (M + m_q) \\ -aM\Delta^2 (M + m_q) & a (M + m_q)^2 \Delta^2 \end{pmatrix}; \tag{3.121}$$

[9] Diquark pairing is not the only known mechanism that can modify the meson mass GMOR relation. The asymmetry in quark flavors could have a similar effect of inducing higher order GMOR relations, such as pions in an isospin-asymmetric medium [75, 76].

here

$$b = \int_{\boldsymbol{p}} \sum_{\pm} \frac{1}{\omega_{\pm}} \left(1 - \frac{\mu}{\epsilon_{\pm}}\right) \tag{3.122}$$

is a function of $M$, $\Delta$, $\mu$, and $m_q$, and is also the integral on the right side of the gap equation (3.45). In the chiral limit $m_q = 0$ in the chirally broken phase with $M \neq 0$, $b$ simply reduces to $1/2G$. In terms of the mass matrix $\Sigma = \mathcal{F}^{-1}\Xi\mathcal{F}^{-1}$ for the pion fields $\vec{\pi}$, we obtain the following matrix generalization of the GMOR relation encompassing both modes:

$$\begin{aligned} \mathcal{F}\Sigma\mathcal{F} &= M^2 a\Delta^2 \begin{pmatrix} 1 & -1 \\ -1 & 1 \end{pmatrix} + M m_q \begin{pmatrix} b & -a\Delta^2 \\ -a\Delta^2 & 2a\Delta^2 \end{pmatrix} \\ &\quad + a\Delta^2 m_q^2 \begin{pmatrix} 0 & 0 \\ 0 & 1 \end{pmatrix} \\ &\equiv \Xi + M m_q \Xi_{\mathrm{I}} + a\Delta^2 m_q^2 \Xi_{\mathrm{II}}, \end{aligned} \tag{3.123}$$

a relation that can be readily generalized to systems with more complex chiral order parameters than $\langle\bar{q}q\rangle$ and $\langle qq\rangle$. Since $a$, $b$, $f_\pi$, $f_{\tilde{\pi}}$, $\Delta$ and $M$ are themselves functions of $m_q$, Eq. (3.123) is not a series expansion in $m_q$ despite its appearance.

To decipher the physical meaning behind Eq. (3.123), we first note that the non-perturbed matrix term $\Xi$ is understood as resulting from Goldstone's theorem as discussed before. The perturbation terms, $\delta\Xi \equiv M m_q \Xi_{\mathrm{I}} + a\Delta^2 m_q^2 \Xi_{\mathrm{II}}$, contains combinations of order parameters that violate the $U(1)_A$ chiral symmetry, such as $\sigma|\Delta_s|^2$ and $\sigma$ (in contrast to the chirally invariant combinations (3.57)); they are caused by $m_q$ which explicitly violates such symmetry.

To leading order in $m_q$, the perturbation to $\Xi$ and thus its eigenvalues (the $\pi_G, \pi_M$ masses) are

$$\begin{aligned} m_G^2 &\approx \frac{bMm_q + a\Delta^2 m_q^2}{f_G^2}, \\ m_M^2 &\approx aM^2\Delta^2 \left(\frac{1}{f_\pi^2} + \frac{1}{f_{\tilde{\pi}}^2}\right) + Mm_q \left(\frac{bf_{\tilde{\pi}}^2}{f_G^2 f_\pi^2} + \frac{2a\Delta^2}{f_{\tilde{\pi}}^2}\right) + m_q^2 \frac{a\Delta^2 f_\pi^2}{f_G^2 f_{\tilde{\pi}}^2}; \end{aligned} \tag{3.124}$$

we plot them as functions of density in Fig. 3.7. In the relatively high density BCS regime, $m_G$ decreases with increasing density as a consequence of the increasing BCS pairing $\langle qq\rangle$ taking on the role of chiral order parameter; $f_{\tilde{\pi}}$ increases while $f_\pi$ vanishes. From the mixing, Eq. (3.64), one sees that the $\pi_G$ mode is mainly composed of $\tilde{\pi}$-like fluctuations, while the massive mode is mainly $\pi$-like, being heavy due to vanishing $\langle\bar{q}q\rangle$. The NG-mode mass obeys the diquark-condensate pion GMOR relation (cf. Eq. (3.118)):

$$f_G^2 m_G^2 \approx a m_q^2 \Delta^2 \tag{3.125}$$

while at low density, the $\pi_G$ mode is primarily $\pi$-like, and one recovers the vacuum pion GMOR relation (cf. Eq. (3.116)):

$$f_G^2 m_G^2 \approx bMm_q \approx \frac{Mm_q}{2G} \approx -\langle\bar{q}q\rangle m_q \tag{3.126}$$

to leading order in $m_q$.

Figure 3.7 also shows a crossing of $m_M$ and $m_G$ at low density, which is actually an artifact of our present schematic model, where diquark pairing persists at arbitrary density. As a result, the $\tilde{\pi}$-like mode, corresponding to chiral fluctuations of pairing amplitude $\langle qq\rangle$ mainly near the Fermi surface, the free energy cost goes to zero as the Fermi surface vanishes. In the vacuum this mode is simply not present. Realistically, this regime should be described by nuclear matter instead, which is beyond the scope of deconfined quark models; one would need include the physics of chiral symmetry breaking in nuclear matter.

The density at which $m_M$ crosses $m_G$ can be roughly estimated using Eq. (3.124) and the fact that $\Delta \ll f_{\tilde{\pi}}$ at low density (see Eq. (3.98) and its comments) to show that when $m_G \sim m_M$, the decay constants are comparable with each other: $f_\pi \sim f_{\tilde{\pi}}$. Since $f_{\tilde{\pi}}^2 \sim n/M$ at low density, $f_\pi \sim f_{\tilde{\pi}}$ implies $n \sim f_\pi^2 M$, a characteristic density scale for chiral symmetry breaking via $\langle\bar{q}q\rangle$. Using values from realistic NJL models where the effective quark mass $M$ is $\sim 300\,\mathrm{MeV}$ and the experimental $f_\pi$ is $\sim 92$ MeV, we find that $n$ is of order nuclear matter density, $n_0 \approx 0.16\,\mathrm{fm}^{-3}$, as we have shown earlier in the decay constant discussion. In this density regime, QCD confinement binds quarks into nucleons, and the homogeneous diquark pairing picture in the schematic model at these densities is no longer physical. Nevertheless, the $\pi_G$ mode does obey the well-known vacuum pion GMOR relation in the low density limit, allowing this pionic mode to be smoothly interpolated between nuclear matter and quark matter at high density, where chiral symmetry remains broken throughout.

### 3.2.8 Physical implications of generalized pion and outlook

We have studied in detail a schematic model in this section of continuous chiral symmetry breaking by chiral and diquark condensates. From the vacuum to high density, the symmetry breaking condensate gradually evolves from the $\bar{q}q$ chiral condensate alone, to a coexistence phase of chiral and diquark $qq$ condensates, and finally a diquark pairing dominated phase. Throughout the same chiral symmetry is broken, and the NG boson, the generalized pion $\pi_G$, smoothly changes from the vacuum pion $\pi$ into a generalized pionic mode as a linear combination of $\pi$ and $\tilde{\pi}$, whose properties such as decay constant, mass and coupling to the quark medium are all continuous functions of density. Our discussion suggests that the NG boson sector in cold, dense quark matter may remain qualitatively the same at varying densities, despite the change in the

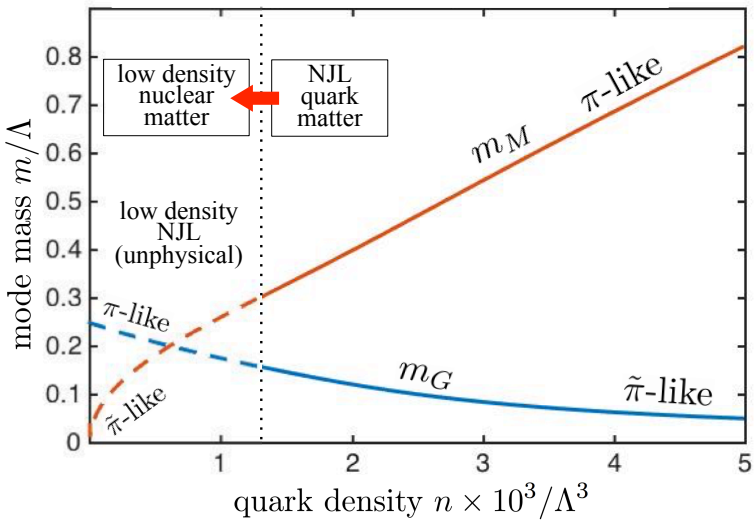


Figure 3.7: The perturbed masses of the NG mode, $m_G$, and of the heavy mode, $m_M$, as functions of quark density, $n$. Here we take $G = 11\Lambda^{-2}$, $H = 6\Lambda^{-2}$ and $m_q = 0.01\Lambda$. With decreasing density, $m_M$ rapidly decreases as the Fermi surface vanishes, eventually crossing the NG-mode mass $m_G$; this is an artifact of our simplified NJL model which does not take confinement into account. Realistically this low density regime is instead described by nuclear matter; the boundary of the transition from quark matter to nuclear matter drawn in the plot is only illustrative.

phases[10].

The persistence of the $\pi_G$ mode at all densities raises the possibility of a continuous Bose-Einstein condensation of the pions in dense quark matter. In the literature, homogeneous condensates of the pionic NG modes have been considered within NJL, in both the low density non-BCS (e.g., [79]) and high density BCS (e.g., [77]) limits. Our study here suggests that the pion condensation at the two limits could be smoothly connected, with no abrupt phase transitions in terms of the pion (or more generally, meson) condensation. Our present schematic model however cannot study such possibilities directly, since the pion condensation in this model will be trivial; the pion merely corresponds to a global axial $U(1)_A$ rotation of the system from the scalar state. In the chiral limit, the chiral symmetry is respected by the Lagrangian, and such rotation does not cost any free energy; the rotated system is energetically equivalent to the original scalar state. With a finite $m_q$ breaking chiral symmetry, the scalar state is the unique ground state with the lowest free energy, since there are no forces driving condensation, and homogeneous pion condensates are unstable.

To study in more detail the evolution of pion condensation at varying density, our model must be generalized into realistic $N_f = N_c = 3$ and quark masses, where driving factors of meson condensation emerge. For example, the mismatched Fermi surfaces of up and down quarks and an electric charge chemical potential translate directly into an effective chemical potential of the charged pions (see discussions of pion condensation in NJL models in [45, 78, 79, 80, 81, 82, 83, 84]). When the effective pion chemical potential overwhelms the pion mass, even homogeneous pion condensation can occur. Furthermore, as the pions directly couple to the quarks in the pseudoscalar $\bar{q}q$ and $qq$ channels as discussed in this section, more types of pionic condensates could be favored by the pion interacting with the quark matter medium at different densities, such as inhomogeneous meson condensates (e.g., [85, 86]) or condensation into states with finite momenta. Other exotic phases involving inhomogeneous chiral or diquark condensates (e.g., [87, 88]) could also affect pion condensation. These possibilities provide attractive future research opportunities.

Another direction worth pursuing from this study is the detailed realization of the meson mass reversal phenomenon [65] (where the mass ordering of the pseudoscalar mesons are reversed due to the diquarks forming $\bar{3}$ representations of flavor; as a result, diquark pions receive larger contributions from strange quarks and become heavier than the diquark kaons, which is totally opposite to the mass ordering of vacuum hadronic pions and kaons), again requiring generalization into $N_f = N_c = 3$. The masses and decay constants of the

[10] The 2SC phase is an exception, where the isospin component of the chiral symmetry is restored. It is an open question whether the 2SC phase actually appears in place of the CFL phase at intermediate densities with realistic strange quark masses [101]. Nevertheless, it has been found in NJL studies that the CFL phase remains more energetically favorable than the 2SC phase all the way down to nuclear matter density, as long as the diquark pairing attraction is strong enough to produce a CFL gap $\sim 100$ MeV in the chiral limit [52, 89, 90, 91, 92, 93].

generalized meson octet as functions of density can then be computed in the same way to study the the density-dependent meson mass spectrum throughout different phases, and how those mass curves depend on model parameters. Our schematic model provides an outline of calculating these meson properties.

We draw attention to the possible role of the $\hat{\phi}$ mode. This mode, discussed in Sec. 3.2.4, could also play a role in a realistic phase diagram (a possibility that has not received attention in present NJL studies). Although the $\hat{\phi}$ mode, not being a NG mode, is always massive, there may be density regions where its mass is significantly reduced. This observation comes from the fact that the $\hat{\phi}$ mode corresponds to a relative phase oscillation between the scalar diquark condensate $\Delta_s$ and the pseudoscalar $\Delta_{ps}$. Specifically, its stiffness term,

$$\frac{\partial^2\Omega}{\partial \sin^2\phi} = \frac{\Delta^4}{16}\sin^2 2\theta_d \sum_{\pm}\int_{\boldsymbol{p}} \frac{1}{\omega_{\pm}^3} > 0, \tag{3.127}$$

(calculated here, for simplicity, in the pure BCS limit with a finite $\theta_d$ chiral rotation from the scalar state in our model) can be made small if either the BCS gap $\Delta$ or the (homogeneous generalized pion condensation) $\theta_d$ is small. The possible role of the $\phi$ mode in the low energy physics of dense quark matter and its coupling to the pseudoscalar $\Delta_{ps}$ fluctuations and thus its coupling to the generalized pion can be explored in the future as well.

Our derivation of the generalized GMOR relation (3.123) is based on expanding the grand thermodynamic potential in terms of $m_q$ and bosonized fields. In the following sections 3.3 and 3.4, we develop a more general formalism for calculating the GMOR relation to arbitrary order, based on insertion of boson field vertices in quark loop diagrams. We demonstrate that this formalism yields the expected GMOR result to linear and quadratic order in $m_q$, and outline the strategy of calculating GMOR coefficients with the coexistence of chiral and diquark condensates.

Our formalism is presented in two parts. In Sec. 3.3 we first demonstrate how to self-consistently compute the meson inverse propagators in the general presence of multiple condensates (chiral and diquark); the resulting inverse propagators of different mesonic fields form a set of linear equations in terms of bubble diagrams. In Sec. 3.4 we develop a method of perturbing, using bare quark masses $m_q$, the bubble diagrams via vertex insertions self-consistently in the chirally broken state, constrained by gap equations. In turn, the perturbation to the meson inverse propagators by $m_q$ is obtained; solving for the zeros of the perturbed inverse propagators gives the perturbed energies of mesonic modes, and thus the mode masses as functions of $m_q$ – a generalized GMOR relation.

## 3.3 Self-consistent calculation of generalized meson inverse propagators

We first develop the self-consistent derivation of meson inverse propagators in this section; the method is based on Refs. [5] and [6], and an example of its application in cold atoms can be found in Ref. [94]. We start with a general Lagrangian

$$\mathcal{L} = \bar{\psi} S_0^{-1} \psi + \sum_\alpha g_\alpha \left(\bar{\psi}\Gamma_\alpha \psi\right)^\dagger \left(\bar{\psi}\Gamma_\alpha \psi\right); \tag{3.128}$$

here, $\psi$ can be the Nambu-Gorkov spinor or just the ordinary quark fields; the system has $g_\alpha$ couplings in the $\Gamma_\alpha$ channel. For example, in the NJL model, for the chiral $(\bar{q}q)^2$, $(\bar{q}i\gamma_5\tau_a)^2$ and diquark $|\bar{q}i\gamma_5\tau_A\lambda_A q^C|^2$ interactions, the vertices are

$$\Gamma_\sigma = 1,\ \Gamma_{\pi_a} = i\gamma_5\tau_a,\ \Gamma_{d_A} = 2\gamma_5\tau_A\lambda_A \begin{pmatrix} 0 & 0 \\ 1 & 0 \end{pmatrix}. \tag{3.129}$$

We define the composite operator

$$w_\alpha(x) \equiv \bar{\psi}(x)\Gamma_\alpha\psi(x), \tag{3.130}$$

which will serve as the interpolating field for the mesons, either NG or massive; its mean field expectation value is, in terms of the trace over the one particle correlation function of the fermion $S(1,2) \equiv -i\langle \mathcal{T}\psi(1)\bar{\psi}(2)\rangle$,

$$\langle w_\alpha(1)\rangle = -i\mathrm{tr}\left(S(1,1^+)\Gamma_\alpha\right), \tag{3.131}$$

where $1^+$ stands for $t_1' = t_1 + 0^+$ in the time component. The mean field Lagrangian is

$$\mathcal{L}_{MF} = \bar{\psi} S_0^{-1}\psi + \sum_\alpha g_\alpha \left[\langle w_\alpha\rangle^\dagger \bar{\psi}\Gamma_\alpha\psi + \langle w_\alpha\rangle \bar{\psi}\tilde{\Gamma}_\alpha\psi\right] - \sum_\alpha g_\alpha |\langle w_\alpha\rangle|^2, \tag{3.132}$$

where $\tilde{\Gamma}_\alpha \equiv \gamma^0\Gamma_\alpha^\dagger\gamma^0$; $\tilde{\Gamma}$ satisfying

$$\bar{\psi}\tilde{\Gamma}_\alpha\psi = (\bar{\psi}\Gamma_\alpha\psi)^\dagger. \tag{3.133}$$

Our goal is to compute the time-orderedmeson correlation function (the meson propagator),

$$D_{\alpha\beta}(1,2) \equiv -i\langle \mathcal{T} w_\alpha(1) w_\beta^\dagger(2)\rangle, \tag{3.134}$$

which is necessary to derive the meson dispersion relations.

To achieve this, we first add an external source perturbation to the mean

field Lagrangian,

$$\mathcal{L}_{\rm pert} = -\sum_\beta w_\beta(2) U_\beta(2) - \sum_\beta w^\dagger_\beta(2) U^\dagger_\beta(2), \tag{3.135}$$

making $S(1,2;U)$ a functional of the sources $U_\alpha$. The meson correlation functions can then be calculated using

$$D_{\alpha\beta}(1,2) = \left.\frac{\delta\langle w_\alpha(1)\rangle}{\delta U^\dagger_\beta(2)}\right|_{U=0} = \frac{1}{i}{\rm tr}\left[\frac{\delta S(1,1^+;U)}{\delta U^\dagger_\beta(2)}\Gamma_\alpha\right]. \tag{3.136}$$

After some algebra, we obtain

$$\begin{aligned} D_{\alpha\beta}(1,2) &= B_{\alpha\beta}(1,2) - \int_x \sum_\sigma B_{\alpha\sigma}(1,x) g_\sigma D_{\sigma\beta}(x,2) \\ &\quad - \int_x \sum_\sigma B_{\alpha\bar\sigma}(1,x) g_\sigma D_{\bar\sigma\beta}(x,2), \end{aligned} \tag{3.137}$$

where the bubbles and "anomalous" meson correlation functions are defined by

$$\begin{aligned} B_{\alpha\beta}(1,2) &= i{\rm tr}\left[S(1-2)\tilde\Gamma_\beta S(2-1^+)\Gamma_\alpha\right], \\ B_{\alpha\bar\beta}(1,2) &= i{\rm tr}\left[S(1-2)\Gamma_\beta S(2-1^+)\Gamma_\alpha\right], \\ D_{\bar\alpha\beta}(1,2) &= -i\langle T w^\dagger_\alpha(1) w^\dagger_\beta(2)\rangle. \end{aligned} \tag{3.138}$$

In compact form, we write

$$\boldsymbol{D} = -\boldsymbol{B} + \boldsymbol{B}\hat{g}\boldsymbol{D}, \tag{3.139}$$

where the correlation functions and bubbles are matrices with indices $\alpha, \beta, \tilde\alpha, \tilde\beta$ being channel labels, and $\hat g_{\alpha\beta} = \hat g_{\tilde\alpha\beta} = \hat g_{\alpha\tilde\beta} = \hat g_{\tilde\alpha\tilde\beta} = g_\alpha\delta_{\alpha\beta}$.

The matrix equation (3.139) is solved to compute $\boldsymbol{D}$ in terms of the bubbles $\boldsymbol{B}$; the poles of $\boldsymbol{D}$ encode the meson states. As a specific example, let us consider the application to a pure CFL phase pseudoscalar meson correlation functions.

We first work out the diquark meson vertices, which differ from the familiar vacuum meson vertices, e.g, for $\pi^-$,

$$\Gamma_{\pi^-} = \begin{pmatrix} i\gamma_5\frac{\tau_1+i\tau_2}{\sqrt{2}} & \\ & i\gamma_5\frac{\tau_1-i\tau_2}{\sqrt{2}} \end{pmatrix} \tag{3.140}$$

in the Nambu-Gorkov space, which can be derived by varying the chiral condensate with an infinitesimal transformation

$$\begin{aligned} &q \to \left[1 - i\gamma_5\theta_i\tau_i/2\right] q, \\ &\sigma = \bar q q \to \bar q\left[1 - i\gamma_5\theta_i\tau_i/2\right]\left[1 - i\gamma_5\theta_i\tau_i/2\right] q = \bar q q - \theta_i\bar q i\gamma_5\tau_i q. \end{aligned} \tag{3.141}$$

| charged meson | vaccum meson vertex | diquark meson vertex |
|---|---|---|
| $\pi^-(\sqrt{2}\bar{u}i\gamma_5 d)$ | $\begin{pmatrix} i\gamma_5\frac{\tau_1+i\tau_2}{\sqrt{2}} & \\ & i\gamma_5\frac{\tau_1-i\tau_2}{\sqrt{2}} \end{pmatrix}$ | $-\begin{pmatrix} & \sqrt{2}\tau_5\lambda_7 \\ \sqrt{2}\tau_7\lambda_5 & \end{pmatrix}$ |
| $\pi^+(\sqrt{2}\bar{d}i\gamma_5 u)$ | $\begin{pmatrix} i\gamma_5\frac{\tau_1-i\tau_2}{\sqrt{2}} & \\ & i\gamma_5\frac{\tau_1+i\tau_2}{\sqrt{2}} \end{pmatrix}$ | $-\begin{pmatrix} & \sqrt{2}\tau_7\lambda_5 \\ \sqrt{2}\tau_5\lambda_7 & \end{pmatrix}$ |
| $K^-(\sqrt{2}\bar{u}i\gamma_5 s)$ | $\begin{pmatrix} i\gamma_5\frac{\tau_4+i\tau_5}{\sqrt{2}} & \\ & i\gamma_5\frac{\tau_4-i\tau_5}{\sqrt{2}} \end{pmatrix}$ | $\begin{pmatrix} & \sqrt{2}\tau_2\lambda_7 \\ \sqrt{2}\tau_7\lambda_2 & \end{pmatrix}$ |
| $K^+(\sqrt{2}\bar{s}i\gamma_5 u)$ | $\begin{pmatrix} i\gamma_5\frac{\tau_4-i\tau_5}{\sqrt{2}} & \\ & i\gamma_5\frac{\tau_4+i\tau_5}{\sqrt{2}} \end{pmatrix}$ | $\begin{pmatrix} & \sqrt{2}\tau_7\lambda_2 \\ \sqrt{2}\tau_2\lambda_7 & \end{pmatrix}$ |
| $\bar{K}^0(\sqrt{2}\bar{d}i\gamma_5 s)$ | $\begin{pmatrix} i\gamma_5\frac{\tau_6+i\tau_7}{\sqrt{2}} & \\ & i\gamma_5\frac{\tau_6-i\tau_7}{\sqrt{2}} \end{pmatrix}$ | $-\begin{pmatrix} & \sqrt{2}\tau_2\lambda_5 \\ \sqrt{2}\tau_5\lambda_2 & \end{pmatrix}$ |
| $K^0(\sqrt{2}\bar{s}i\gamma_5 d)$ | $\begin{pmatrix} i\gamma_5\frac{\tau_6-i\tau_7}{\sqrt{2}} & \\ & i\gamma_5\frac{\tau_6+i\tau_7}{\sqrt{2}} \end{pmatrix}$ | $-\begin{pmatrix} & \sqrt{2}\tau_5\lambda_2 \\ \sqrt{2}\tau_2\lambda_5 & \end{pmatrix}$ |

Table 3.5: Vertices of the charged vacuum mesons and the diquark mesons.

However, the scalar diquark condensate, $d_j \equiv \bar{q}i\gamma_5\tau_j\lambda_j q^C$, transforms as

$$\begin{aligned} d_j &\rightarrow \bar{q}\left[1 - i\gamma_5\theta_i\tau_i/2\right] i\gamma_5\tau_j\lambda_j \left[1 - i\gamma_5\theta_i\tau_i^T/2\right] q^C \\ &= d_j + \bar{q}\theta_i\frac{1}{2}(\tau_i\tau_j + \tau_j\tau_i^T)\lambda_j q^C, \end{aligned} \tag{3.142}$$

where the additional term corresponds to pseudoscalar diquark condensates, as expected. Taking $j = 1, 2$ for charged pions, we find

$$\Gamma_{\pi^-} = -\begin{pmatrix} & \sqrt{2}\tau_5\lambda_7 \\ \sqrt{2}\tau_7\lambda_5 & \end{pmatrix}. \tag{3.143}$$

The vacuum meson in the non-paired phase and diquark meson vertices in the CFL phase are summarized in Table. 3.5. These vertices are used to construct the interpolating fields (composite operators) for the mesons, e.g., the interpolating field for $\pi^-$ will be given by $\bar{\psi}(x)\Gamma_{\pi^-}\psi(x)$, and so on.

We note that the interpolating fields $w_{\pi,K}$ of diquark mesons as given by the vertices in Table. 3.5 are linear combinations of the $qq$ and $\bar{q}\bar{q}$ fields; however, the diquark interaction term in the original Lagrangian is of the form $(qq)(\bar{q}\bar{q})$, which does not manifestly factorize into the form $|w_{\pi,K}|^2$. We have to work with intermediate interpolating fields $s_{ij}, p_{ij}$ that are not the meson interpolating fields themselves, given by writing the scalar and pseudoscalar diquark

interaction term as

$$
\begin{aligned}
& H\sum_{ij}\left(\bar{q}^C i\gamma_5\tau_i\lambda_j q\right)\cdot\left(\bar{q}i\gamma_5\tau_i\lambda_j q^C\right) \\
&= 4H\sum_{ij}\bar{\psi}\begin{pmatrix} & i\gamma_5\Gamma^{ij} \\ 0 & \end{pmatrix}\psi\cdot\bar{\psi}\begin{pmatrix} & 0 \\ i\gamma_5\Gamma^{ji} & \end{pmatrix}\psi \\
&\equiv H\sum_{ij}s_{ij}^\dagger s_{ij}, \\
& H\sum_{ij}\left(\bar{q}^C\tau_i\lambda_j q\right)\cdot\left(\bar{q}\tau_i\lambda_j q^C\right) = 4H\sum_{ij}\bar{\psi}\begin{pmatrix} & \Gamma^{ij} \\ 0 & \end{pmatrix}\psi\cdot\bar{\psi}\begin{pmatrix} & 0 \\ \Gamma^{ji} & \end{pmatrix}\psi \\
&\equiv H\sum_{ij}p_{ij}^\dagger p_{ij}.
\end{aligned}
\tag{3.144}
$$

By construction, the actual meson interpolating fields are linear combinations of $p_{ij}$:

$$
\begin{aligned}
\pi^- &: -\sqrt{2}i\left(p_{57}-p_{75}^\dagger\right), \\
\pi^+ &: \sqrt{2}i\left(p_{57}^\dagger-p_{75}\right), \\
K^- &: \sqrt{2}i\left(p_{27}-p_{72}^\dagger\right), \\
\bar{K}^0 &: -\sqrt{2}i\left(p_{25}-p_{52}^\dagger\right).
\end{aligned}
\tag{3.145}
$$

The mean field Lagrangian, in terms of the fields $s_{ij}, p_{ij}$, is

$$
\begin{aligned}
& \mathcal{L}_{MF} \\
&= \bar{\psi}S_0^{-1}\psi + 2H\sum_{ij}\left[\langle s_{ij}\rangle^\dagger\bar{\psi}i\gamma_5\begin{pmatrix} & 1 \\ 0 & \end{pmatrix}\Gamma_{ij}\psi + \langle s_{ij}\rangle\bar{\psi}i\gamma_5\begin{pmatrix} & 0 \\ 1 & \end{pmatrix}\tilde{\Gamma}_{ij}\psi\right] \\
&- H\sum_{ij}|\langle s_{ij}\rangle|^2 \\
&+ 2H\sum_{ij}\left[\langle p_{ij}\rangle^\dagger\bar{\psi}\begin{pmatrix} & 1 \\ 0 & \end{pmatrix}\Gamma_{ij}\psi + \langle p_{ij}\rangle\bar{\psi}\begin{pmatrix} & 0 \\ 1 & \end{pmatrix}\tilde{\Gamma}_{ij}\psi\right] - H\sum_{ij}|\langle p_{ij}\rangle|^2 \\
&- \sum_{ij}s_{ij}W_{ij} - \sum_{ij}s_{ij}^\dagger W_{ij}^\dagger - \sum_{ij}p_{ij}U_{ij} - \sum_{ij}p_{ij}^\dagger U_{ij}^\dagger,
\end{aligned}
\tag{3.146}
$$

where $W_{ij}$ and $U_{ij}$ are scalar and pseudoscalar external sources. To compute the meson correlation functions, we need to calculate correlation functions of the form

$$
-i\langle Tp_{ij}p_{mn}\rangle, -i\langle Tp_{ij}^\dagger p_{mn}^\dagger\rangle, -i\langle Tp_{ij}p_{mn}^\dagger\rangle \tag{3.147}
$$

according to (3.145). Using method demonstrated earlier this section, we com-

pute

$$-i\langle Tp_{ij}(1)p_{mn}(2)\rangle = \frac{\delta\langle p_{ij}(1)\rangle}{\delta U_{mn}(2)}|_{U,W=0} = \frac{1}{i}\mathrm{tr}\left[\frac{\delta S(1,1^+;UW)}{\delta U_{mn}(2)}\Gamma_{ij}\right]; \quad (3.148)$$

using the identity

$$\frac{\delta}{\delta U}1 = 0 = \frac{\delta S}{\delta U}S^{-1} + S\frac{\delta S^{-1}}{\delta U}, \quad (3.149)$$

to obtain

$$\begin{aligned}
&\frac{1}{i}\mathrm{tr}\left[\frac{\delta S(1,1^+;UW)}{\delta U_{mn}(2)}\Gamma_{ij}\right] \\
&= -\frac{1}{i}\int_{3,4}\mathrm{tr}\left[S(1,3;UW)\frac{\delta S^{-1}(3,4;UW)}{\delta U_{mn}(2)}S(4,1^+;UW)\Gamma_{ij}\right] \\
&= -\frac{1}{i}\int_{3,4}\mathrm{tr}\left[S(1,3;UW)\Big(-\Gamma_{mn}\delta_{34}\delta_{23} + 2H\sum_{kl}\Gamma_{kl}\frac{\delta\langle p^\dagger_{kl}\rangle(3)}{\delta U_{mn}(2)}\delta_{34}\right. \\
&\left.+2H\sum_{kl}\tilde{\Gamma}_{kl}\frac{\delta\langle p_{kl}\rangle(3)}{\delta U_{mn}(2)}\delta_{34}\Big) \times S(4,1^+;UW)\Gamma_{ij}\right] \\
&= -i\mathrm{tr}\left[S(1,2)\Gamma_{mn}S(2,1^+)\Gamma_{ij}\right] + 2H\sum_{kl} i\int_3 \mathrm{tr}\left[S(1,3)\Gamma_{kl}S(3,1)\Gamma_{ij}\right] \\
&\times\frac{1}{i}\langle Tp_{mn}(2)p^\dagger_{kl}(3)\rangle + 2H\sum_{kl} i\int_3 \mathrm{tr}\left[S(1,3)\tilde{\Gamma}_{kl}S(3,1)\Gamma_{ij}\right] \\
&\times\frac{1}{i}\langle Tp_{mn}(2)p_{kl}(3)\rangle \\
&= B(1_{ij},2_{mn}) - 2H\cdot B(1_{ij},3_{kl})\cdot\frac{1}{i}\langle Tp_{mn}(2)p^\dagger_{kl}(3)\rangle \\
&-2H\cdot B(1_{ij},\bar{3}_{kl})\cdot\frac{1}{i}\langle Tp_{mn}(2)p_{kl}(3)\rangle,
\end{aligned} \quad (3.150)$$

where the $\bar{3}_{ij}$ means we use the conjugate vertex $\tilde{\Gamma}_{ij}$ in the bubble definition as in (3.138).

Let us investigate the $\pi^-$ bubble. Using (3.145), the correlation function of $\pi^-$ interpolating field is

$$\begin{aligned}
D_{\pi^-} &= \frac{1}{2i}\langle\mathcal{T}(p_{57} - p^\dagger_{75})(p^\dagger_{57} - p_{75})\rangle \\
&= \frac{1}{2i}(-D_{57,75} + D_{57,57^\dagger} + D_{75^\dagger,75} - D_{75^\dagger,57}),
\end{aligned} \quad (3.151)$$

where

$$D_{ij,mn} = \frac{1}{i}\langle Tp_{ij}p_{mn}\rangle, D_{ij,mn^\dagger} = \frac{1}{i}\langle Tp_{ij}p^\dagger_{mn}\rangle. \quad (3.152)$$

Since only a few $B$ and $D$ appears in a closed set of equations as other charged mesons and the neutral mesons do not mix with $\pi^-$, we adopt a simplified

notation

| | simplified subscript |
|---|---|
| $57, 57^\dagger$ | 1 |
| $57, 75$ | 2 |
| $75^\dagger, 57^\dagger$ | 3 |
| $75^\dagger, 75$ | 4 |

(3.153)

In this notation, we have simply

$$D_{\pi^-} = \frac{1}{2i}\left(D_1 - D_2 - D_3 + D_4\right). \tag{3.154}$$

The self-consistent equation (3.150) can then be written as

$$\begin{aligned}(1+2H\mathcal{B})\begin{pmatrix} D_1 \\ D_3 \end{pmatrix} \equiv \begin{pmatrix} 1+2HB_1 & 2HB_2 \\ 2HB_3 & 1+2HB_4 \end{pmatrix}\begin{pmatrix} D_1 \\ D_3 \end{pmatrix} &= \begin{pmatrix} B_1 \\ B_3 \end{pmatrix}, \\ \begin{pmatrix} 1+2HB_1 & 2HB_2 \\ 2HB_3 & 1+2HB_4 \end{pmatrix}\begin{pmatrix} D_2 \\ D_4 \end{pmatrix} &= \begin{pmatrix} B_2 \\ B_4 \end{pmatrix},\end{aligned} \tag{3.155}$$

where the products between $B$s and $D$s are always understood in coordinate space as

$$(B_{ij}D_{jk})(1,2) = \int dx\, B_{ij}(1,x)D_{jk}(x,2). \tag{3.156}$$

The solution to (3.155) is

$$\begin{aligned} D_1 &= \frac{B_1 + 2H\det\mathcal{B}}{2H\mathcal{K}}, \\ D_2 &= \frac{B_2}{2H\mathcal{K}}, \\ D_3 &= \frac{B_3}{2H\mathcal{K}}, \\ D_4 &= \frac{B_4 + 2H\det\mathcal{B}}{2H\mathcal{K}}; \end{aligned} \tag{3.157}$$

where the common denominator is

$$\mathcal{K} = \frac{1}{2H} + B_1 + B_4 + 2H\det\mathcal{B}. \tag{3.158}$$

Thus, according to (3.154), the same goes for $D_{\pi^-}$. The dispersion relation for the diquark pion is thus solved by

$$0 = \mathcal{K} = \frac{1}{2H}\left[(1+2HB_1)(1+2HB_4) - 4H^2B_2B_3\right]. \tag{3.159}$$

To find the modes, we first note that that the bubbles have the following properties in momentum space:

$$B_1(k_0) = B_4(-k_0),\ B_2(k) = B_3(k); \tag{3.160}$$

$B_1$ and $B_4$ in particular can also be written in the form

$$B_1 = B_0(k) + A(k)k_0, B_4 = B_0(k) - A(k)k_0, \tag{3.161}$$

where $A(k)$ and $B_0(k)$ are

$$\begin{aligned} A(k) &= -2\int_{\boldsymbol{p}} \sum_{i,j=\pm} \frac{(\epsilon_i + \epsilon'_j)^2 - \boldsymbol{k}^2}{2\epsilon_i\epsilon'_j} \times \frac{(u_i^2 u_j'^2 - v_i^2 v_j'^2)}{(\omega_i + \omega'_j)^2 - k_0^2}, \\ B_0(k) &= -2\int_{\boldsymbol{p}} \sum_{i,j=\pm} \frac{(\epsilon_i + \epsilon_j)'^2 - \boldsymbol{k}^2}{2\epsilon_i\epsilon'_j} \times \frac{(u_i^2 u_j'^2 + v_i^2 v_j'^2)(\omega_i + \omega'_j)}{(\omega_i + \omega'_j)^2 - k_0^2}; \end{aligned} \tag{3.162}$$

here $\omega_\pm = ((\epsilon_\pm - \mu)^2 + \Delta_{\rm CFL}^2)^{1/2}$ are the positive quasiparticle energies, $u_\pm, v_\pm$ are the coherence functions corresponding to $\omega_\pm$ (cf. Eq. (3.39) and (3.41)), $\epsilon_\pm = \pm(M^2 + \boldsymbol{p}^2)^{1/2}$, and the primed quantities are functions of $\boldsymbol{p} - \boldsymbol{k}$ instead of $\boldsymbol{p}$, where $\boldsymbol{k}$ is the spatial component of the four-momentum $k$.

The dispersion equation then reads

$$0 = (1 + 2HB_0(k) - 2HB_2(k))(1 + 2HB_0(k) + 2HB_2(k)) - 4H^2A^2k_0^2. \tag{3.163}$$

The full calculation of obtaining GMOR relation by perturbing the bubbles in (3.163) is very involved and we leave it to future studies; however, the formalism and guidelines are very clear. Here we merely verify that in the chiral limit, Eq. (3.163) gives the correct massless NG mode. This can be done by proving that $k = 0$ is a solution of (3.163). In fact, one can explicitly calculate that, using the CFL gap equation,

$$\begin{aligned} B_0(0) - B_2(0) &= B_1(0) - B_2(0) \\ &= -\int \sum_{\pm} \left( \frac{16}{3} \frac{1}{\omega_{\pm,\Delta_{\rm CFL}}} + \frac{8}{3\omega_{\pm,2\Delta_{\rm CFL}}} \right) = -\frac{1}{2H}, \end{aligned} \tag{3.164}$$

thus indeed proving $k = 0$ is a solution; meanwhile, the non-vanishing terms $1+2HB_0+2HB_2$ and $4H^2A^2k_0^2$ will contribute to the renormalization constant.

## 3.4 Gell-Mann–Oakes–Renner relation: another perspective from loop diagrams

Having discussed how to derive the meson inverse propagator in terms of quark bubbles in Sec. 3.3, we now discuss how to perturb the bubbles with bare quark masses $m_q$ in order to derive the generalized GMOR relation from the perturbed inverse propagator. We demonstrate our method in Sec. 3.4.1 and 3.4.2 using a simple $N_f = N_c = 1$ example; in Sec. 3.4.3 we outline how to generalize to realistic $N_f, N_c > 1$ models.

### 3.4.1 $N_f = N_c = 1$ with no pairing

We illustrate our method in this simplest case, before briefly discussing the generalization scheme to realistic $N_f = N_c = 3$. We start with the (homogeneous) gap equations, in the form of traces over quark propagators

$$\begin{aligned} -\frac{M}{2G}\cos\theta = \sigma &= \frac{1}{i}\mathrm{Tr}S, \\ -\frac{M}{2G}\sin\theta = \pi &= \frac{1}{i}\mathrm{Tr}Si\gamma_5, \end{aligned} \tag{3.165}$$

where $S$ is the quark propagator, $M$ the dynamic quark mass, $G$ the four-quark chiral coupling strength, and $\theta$ is the chiral angle locating the ground state on the chiral circle $(\sigma, \pi)$. The grand trace Tr again runs over all degrees of freedom including four-momentum. The inverse of the quark propagator is given by

$$\begin{aligned} S^{-1} &= i\not{\partial} + 2G(\langle\sigma\rangle + i\gamma_5\langle\pi\rangle) + \gamma_0\mu \\ &= i\not{\partial} - M(\cos\theta + i\gamma_5\sin\theta) + \gamma_0\mu. \end{aligned} \tag{3.166}$$

Considering the derivative of $S$ with regard to $\theta$, corresponding to applying a chiral transformation on the system, we have

$$\frac{\partial S}{\partial\theta} = -S\frac{\partial S^{-1}}{\partial\theta}S = SM(-\sin\theta + i\gamma_5\cos\theta)S. \tag{3.167}$$

In particular, in the scalar state $\theta = 0$, we have $\partial S/\partial\theta = SMi\gamma_5 S$; the derivative becomes an insertion of a pion vertex $i\gamma_5$ on the quark line $S$. This is reasonable, since in the scalar state, the variation of $\theta$ corresponds exactly to the pseudoscalar pion.

Applying the derivative with regard to $\theta$ on the two gap equations (3.165), we obtain

$$\begin{aligned} \frac{M}{2G}\sin\theta &= \frac{1}{i}\mathrm{Tr}SM(-\sin\theta + i\gamma_5\cos\theta)S \\ &= M(-\sin\theta B_{\sigma\sigma} + \cos\theta B_{\pi\sigma}) \end{aligned} \tag{3.168}$$

and

$$-\frac{M}{2G}\cos\theta = M(-\sin\theta B_{\sigma\pi} + \cos\theta B_{\pi\pi}); \tag{3.169}$$

here the bubbles with no external momentum follow the usual definition

$$B_{xy} = \frac{1}{i}\mathrm{Tr}\left(S\Gamma_x S\Gamma_y\right), \ x, y = \sigma, \pi, \tag{3.170}$$

and the vertices in Dirac space are $\Gamma_\sigma = 1$ and $\Gamma_\pi = i\gamma_5$. In the scalar state $\theta = 0$, we retrieve the gap equation in bubble form from (3.169):

$$\frac{1}{2G} + B_{\pi\pi} = 0. \tag{3.171}$$

Differentiating the gap equations one more time, we have:

$$\begin{aligned}
\frac{1}{2G}\cos\theta &= -\cos\theta B_{\sigma\sigma} + \cos\theta\frac{1}{i}\frac{\partial}{\partial\theta}\mathrm{Tr}\left(S\Gamma_\pi S\Gamma_\sigma\right) \\
&= -\cos\theta B_{\sigma\sigma} + \cos\theta\frac{M}{i}\mathrm{Tr}\left(S\Gamma_\pi S\Gamma_\pi S\Gamma_\sigma + S\Gamma_\pi S\Gamma_\pi S\Gamma_\sigma\right) \\
&\equiv -\cos\theta B_{\sigma\sigma} + \cos\theta M T_{\pi\pi\sigma},
\end{aligned} \tag{3.172}$$

where the triangle (again with vanishing external momentum) is defined by

$$T_{\pi\pi\sigma} = \frac{2}{i}\mathrm{Tr}\left(S\Gamma_\pi S\Gamma_\pi S\Gamma_\sigma\right). \tag{3.173}$$

In the scalar state, the differentiated gap equations (3.172) reduce to

$$\frac{1}{2G} + B_{\sigma\sigma} = M T_{\pi\pi\sigma}, \tag{3.174}$$

relating the $\sigma$-$\sigma$ bubble to a triangle diagram with two pion vertices.

The diagram relation (3.174) is useful for deriving the GMOR relation via perturbing $S$ with a small bare quark mass $m_q$. To do so, we write $S$ as well as the effective mass $M$ as expansions in powers of $m_q$,

$$\begin{aligned}
S &= S_0 + m_q S_1 + \dots \\
M &= M_0 + m_q M_1 + \dots
\end{aligned} \tag{3.175}$$

The self-consistent gap equation (3.165) then becomes

$$\frac{M_0 + M_1 m_q + \dots}{2G} = -\tfrac{1}{i}\mathrm{Tr}\left(S_0 + S_1 m_q + \dots\right). \tag{3.176}$$

Meanwhile, we note that $S$ also has explicit dependence on $M$, therefore

$$S_1 = \frac{\partial S}{\partial m_q} + \frac{\partial S}{\partial M}\frac{\partial M}{\partial m_q} = \frac{\partial S}{\partial m_q} + \frac{\partial S}{\partial M}M_1 = S_0 S_0\left(1 + M_1\right); \tag{3.177}$$

together with the expansion (3.176), we obtain

$$\frac{M_1}{2G} = -\frac{1}{i}\mathrm{Tr}\left(S_0 S_0 + S_0 S_0 M_1\right) \to \left(\frac{1}{2G} + B_{\sigma\sigma}\right) M_1 = -B_{\sigma\sigma}, \tag{3.178}$$

a relation for the $\sigma$-$\sigma$ bubble $B_{\sigma\sigma}$. With Eqs. (3.174) and (3.178) together, we obtain further

$$M_1 + 1 = \frac{1}{1 + 2GB_{\sigma\sigma}} = \frac{1}{2GT_{\pi\pi\sigma}M}. \tag{3.179}$$

We are now ready to perturb the (unrenormalized) inverse propagator for the pion:

$$\begin{aligned}
\mathcal{D}^{-1}(k) &= \frac{1}{2G} + B_{\pi\pi}(k) \\
&= \frac{1}{2G} + B_{\pi\pi}(k; m_q = 0) + \frac{1}{i}\mathrm{Tr}\big(S_0(p)S_0(p)\Gamma_\pi S_0(p-k)\Gamma_\pi \\
&\quad + S_0(p)\Gamma_\pi S_0(p-k)S_0(p-k)\Gamma_\pi\big)(1+M_1)m_q + \mathcal{O}(m_q^2) \\
&\equiv \frac{1}{2G} + B_{\pi\pi}(k; m_q = 0) + T_{\pi\pi\sigma}(k)(1+M_1)m_q + \mathcal{O}(m_q^2) \\
&= \frac{1}{2G} + B_{\pi\pi}(k; m_q = 0) + T_{\pi\pi\sigma}(1+M_1)m_q \\
&\quad + \left[T_{\pi\pi\sigma}(k) - T_{\pi\pi\sigma}\right](1+M_1)m_q + \mathcal{O}(m_q^2),
\end{aligned} \tag{3.180}$$

where we use $T_{\pi\pi\sigma}(k)$ to denote the triangle diagrams with one external leg carrying four-momentum $k$. Using Eq. (3.179), we arrive at

$$\mathcal{D}^{-1}(k) = \frac{1}{2G} + B_{\pi\pi}(k; m_q = 0) + \frac{m_q}{2GM} + \mathcal{O}(k^2 m_q, m_q^2). \tag{3.181}$$

The non-perturbed part $1/2G + B_{\pi\pi}(k; m_q = 0)$, after applying the gap equation (3.171), reduces to

$$\frac{\partial^2 B_{\pi\pi}(k; m_q = 0)}{\partial k^2} k^2 + \cdots = g_\pi^{-2} k^2 + \ldots; \tag{3.182}$$

thus the pion squared mass term at linear order in $m_q$ is (also using the Goldberger-Treiman relation $g_\pi f_\pi = M$)

$$m_\pi^2 = \frac{g_\pi^2 m_q}{2GM} = \frac{\sigma m_q}{f_\pi^2}, \tag{3.183}$$

the expected GMOR relation.

### 3.4.2 $N_f = N_c = 1$ with pairing

We now include diquark pairing. We write in total

$$\begin{aligned}
\frac{M}{2G}\cos\theta &= -\frac{1}{i}\mathrm{Tr}S\Gamma_\sigma, \\
\frac{M}{2G}\sin\theta &= -\frac{1}{i}\mathrm{Tr}S\Gamma_\pi, \\
\frac{\Delta}{4H}\cos\theta &= \frac{1}{i}\mathrm{Tr}S\Gamma_d = -\frac{1}{i}\mathrm{Tr}S\Gamma_{d^\dagger}, \\
\frac{\Delta}{4H}\sin\theta &= -\frac{1}{i}\mathrm{Tr}S\Gamma_p = \frac{1}{i}\mathrm{Tr}S\Gamma_{p^\dagger};
\end{aligned} \tag{3.184}$$

we use "$d$" to denote scalar diquark and "$p$" to denote pseudoscalar diquark. The quark inverse propagator is then (in Nambu-Gorkov space)

$$\begin{aligned}
&S^{-1} \\
&= \begin{pmatrix} i\partial\!\!\!/ - M(\cos\theta + i\gamma_5\sin\theta) + \gamma_0\mu & i\gamma_5 d^\dagger + p^\dagger \\ i\gamma_5 d + p & i\partial\!\!\!/ - M(\cos\theta + i\gamma_5\sin\theta) - \gamma_0\mu \end{pmatrix} \\
&= \begin{pmatrix} i\partial\!\!\!/ - M(\cos\theta + i\gamma_5\sin\theta) + \gamma_0\mu & (-\gamma_5\cos\theta - i\sin\theta)\Delta \\ (\gamma_5\cos\theta + i\sin\theta)\Delta & i\partial\!\!\!/ - M(\cos\theta + i\gamma_5\sin\theta) - \gamma_0\mu \end{pmatrix}.
\end{aligned} \tag{3.185}$$

Differentiating $S$ with regard to $\theta$ we obtain

$$\begin{aligned}
&\frac{\partial S}{\partial\theta} = -S\frac{\partial S^{-1}}{\partial\theta}S \\
&= S\left[-M\sin\theta\Gamma_\sigma + M\cos\theta\Gamma_\pi - \Delta\sin\theta(\Gamma_d - \Gamma_{d^\dagger}) + \Delta\cos\theta(\Gamma_p - \Gamma_{p^\dagger})\right]S,
\end{aligned} \tag{3.186}$$

where the pseudoscalar diquark vertices are

$$\Gamma_p \equiv \begin{pmatrix} & i \\ 0 & \end{pmatrix},\ \Gamma_{p^\dagger} = \begin{pmatrix} & 0 \\ i & \end{pmatrix}. \tag{3.187}$$

Note that in the scalar state, this is equivalent to the insertion of the generalized pion vertex (3.113) as discussed in Sec. 3.2:

$$S\left[M\Gamma_\pi + \Delta(\Gamma_p - \Gamma_{p^\dagger})\right]S = S\left[M\Gamma_\pi + \Delta\Gamma_{\tilde{\pi}}\right]S = Sf_G\Gamma_G S. \tag{3.188}$$

Differentiating the gap equations (3.184), after some algebra we obtain

$$\begin{aligned}
-\sin\theta\frac{\Delta}{2H} &= -M\sin\theta B_{\tilde{\sigma}\sigma} + M\cos\theta B_{\tilde{\sigma}\pi} - \Delta\sin\theta B_{\tilde{\sigma}\tilde{\sigma}} + \Delta\cos\theta B_{\tilde{\sigma}\tilde{\pi}},\\
\cos\theta\frac{\Delta}{2H} &= M\sin\theta B_{\tilde{\pi}\sigma} - M\cos\theta B_{\tilde{\pi}\pi} + \Delta\sin\theta B_{\tilde{\pi}\tilde{\sigma}} - \Delta\cos\theta B_{\tilde{\pi}\tilde{\pi}},\\
-\sin\theta\frac{M}{2G} &= M\sin\theta B_{\sigma\sigma} - M\cos\theta B_{\sigma\pi} + \Delta\sin\theta B_{\sigma\tilde{\sigma}} - \Delta\cos\theta B_{\sigma\tilde{\pi}},\\
\cos\theta\frac{M}{2G} &= M\sin\theta B_{\pi\sigma} - M\cos\theta B_{\pi\pi} + \Delta\sin\theta B_{\pi\tilde{\sigma}} - \Delta\cos\theta B_{\pi\tilde{\pi}},
\end{aligned} \tag{3.189}$$

where we have analogously defined the diquark "$\sigma$" vertex:

$$\Gamma_{\tilde{\sigma}} = \Gamma_d - \Gamma_{d^\dagger},\ \Gamma_d = \begin{pmatrix} & \gamma_5 \\ 0 & \end{pmatrix},\ \Gamma_{d^\dagger} = \begin{pmatrix} & 0 \\ \gamma_5 & \end{pmatrix}. \tag{3.190}$$

In the scalar state, the above equations reduce to

$$\begin{aligned}
M\left(\frac{1}{2G} + B_{\pi\pi}\right) &= -\Delta(B_{\pi p} - B_{\pi p^\dagger})\\
\Delta\left(\frac{1}{4H} + B_{pp} - B_{pp^\dagger}\right) &= -MB_{p\pi}\\
\Delta\left(\frac{1}{4H} + B_{p^\dagger p^\dagger} - B_{p^\dagger p}\right) &= MB_{p^\dagger\pi},
\end{aligned} \tag{3.191}$$

or more compactly,

$$\begin{aligned}
-\Delta B_{\pi\tilde{\pi}} &= M\left(\frac{1}{2G} + B_{\pi\pi}\right),\\
-MB_{\tilde{\pi}\pi} &= \Delta\left(\frac{1}{2H} + B_{\tilde{\pi}\tilde{\pi}}\right);
\end{aligned} \tag{3.192}$$

they are tightly related to the two-by-two inverse pion propagator, linking $\pi$ and $\tilde{\pi}$, as confirmed by Eq. (3.77) in Sec. 3.2.6.

Differentiating the gap equations (3.189) again, we arrive at further scalar state relations

$$\begin{aligned}
-\frac{M}{2G} &= MB_{\sigma\sigma} - M\left(MT_{\pi\sigma\pi} + \Delta T_{\tilde{\pi}\sigma\pi}\right) + \Delta B_{\sigma\tilde{\sigma}} - \Delta(MT_{\pi\sigma\tilde{\pi}} + \Delta T_{\tilde{\pi}\sigma\tilde{\pi}}),\\
-\frac{\Delta}{2H} &= -MB_{\tilde{\sigma}\sigma} + M\left(MT_{\pi\tilde{\sigma}\pi} + \Delta T_{\tilde{\pi}\tilde{\sigma}\pi}\right) - \Delta B_{\tilde{\sigma}\tilde{\sigma}} + \Delta\left(MT_{\pi\tilde{\sigma}\tilde{\pi}} + \Delta T_{\tilde{\pi}\tilde{\sigma}\tilde{\pi}}\right),
\end{aligned} \tag{3.193}$$

the second equation of which becomes in the pure-pairing ($M = 0$) scalar state

$$\begin{aligned}
-\frac{1}{2H} &= -B_{\tilde{\sigma}\tilde{\sigma}} + \Delta T_{\tilde{\pi}\tilde{\pi}\tilde{\sigma}},\\
B_{\sigma\tilde{\sigma}} &= -\Delta T_{\tilde{\pi}\sigma\tilde{\pi}}.
\end{aligned} \tag{3.194}$$

Let us proceed to expand the quark propagator and the gaps $\Delta$ and $M$ in $m_q$:

$$\begin{aligned} M &= M_0 + M_1 m_q + \frac{1}{2} M_2 m_q^2 \dots \\ \Delta &= \Delta_0 + \Delta_1 m_q + \frac{1}{2} \Delta_2 m_q^2 + \dots \\ S &= S_0 + S_1 m_q + \frac{1}{2} S_2 m_q^2 + \dots \end{aligned} \tag{3.195}$$

Due to the diquark sector contribution to the pion mass starts with leading order $m_q^2$, we need to work up to at least $S_2, \Delta_2$ and $M_2$. To find out the analytic expression for $S_1$ and $S_2$, we write down the variation

$$\begin{aligned} S_1 \delta m_q &= \partial_{m_q} S \delta m_q + \partial_M S \delta M + \partial_\Delta S \delta \Delta \\ &= \partial_M S \cdot m_q + \partial_M S \left( M_1 \delta m_q + \frac{1}{2} M_2 \delta m_q^2 + ... \right) \\ &\quad + \partial_\Delta S \left( \Delta_1 \delta m_q + \frac{1}{2} \Delta_2 \delta m_q^2 + ... \right) \end{aligned} \tag{3.196}$$

and

$$\begin{aligned} S_2 \delta m_q^2 &= \frac{\partial^2 S}{\partial m_q^2} \delta m_q^2 + \frac{\partial^2 S}{\partial M^2} \delta M^2 + \frac{\partial^2 S}{\partial \Delta^2} \delta \Delta^2 \\ &\quad + 2 \left( \frac{\partial^2 S}{\partial m_q \partial M} \delta m_q \delta M + \frac{\partial^2 S}{\partial m_q \partial \Delta} \delta m_q \delta \Delta + \frac{\partial^2 S}{\partial \Delta \partial M} \delta \Delta \delta M \right); \end{aligned} \tag{3.197}$$

using

$$\begin{aligned} &\partial_{m_q} S \delta m_q + \partial_M S \delta M + \partial_\Delta S \delta \Delta \\ &\quad = \partial_M S \cdot m_q + \partial_M S \left( M_1 \delta m_q + \frac{1}{2} M_2 \delta m_q^2 + ... \right) \\ &\qquad + \partial_\Delta S \left( \Delta_1 \delta m_q + \frac{1}{2} \Delta_2 \delta m_q^2 + ... \right) \\ &\quad = \left[ S \Gamma_\sigma S (1 + M_1) + S \Gamma_{\tilde{\sigma}} S \Delta_1 \right] \delta m_q + \frac{1}{2} \left( S \Gamma_\sigma S M_2 + S \Gamma_{\tilde{\sigma}} S \Delta_2 \right) \delta m_q^2 + ... \end{aligned} \tag{3.198}$$

and

$$\begin{aligned} &\frac{1}{2} \Bigg[ \frac{\partial^2 S}{\partial m_q^2} \delta m_q^2 + \frac{\partial^2 S}{\partial M^2} \delta M^2 + \frac{\partial^2 S}{\partial \Delta^2} \delta \Delta^2 \\ &\qquad + 2 \left( \frac{\partial^2 S}{\partial m_q \partial M} \delta m_q \delta M + \frac{\partial^2 S}{\partial m_q \partial \Delta} \delta m_q \delta \Delta + \frac{\partial^2 S}{\partial \Delta \partial M} \delta \Delta \delta M \right) \Bigg] \\ &= S \Gamma_\sigma S \Gamma_\sigma S (1 + M_1)^2 \delta m_q^2, \end{aligned} \tag{3.199}$$

we finally obtain

$$\begin{aligned} S_1 &= S\Gamma_\sigma S(1+M_1) + S\Gamma_{\tilde{\sigma}} S\Delta_1, \\ S_2 &= S\Gamma_\sigma S M_2 + S\Gamma_{\tilde{\sigma}} S\Delta_2 + 2S\Gamma_\sigma S\Gamma_\sigma S(1+M_1)^2. \end{aligned} \tag{3.200}$$

All we need next is to calculate $\Delta_{1,2}$ and $M_{1,2}$. Applying the gap equations (3.184) again in terms of the expansion in powers of $m_q$; with the help of the insertions

$$\begin{aligned} \frac{\partial S}{\partial M} &= -S\frac{\partial S^{-1}}{\partial M}S = SS = S\Gamma_\sigma S, \\ \frac{\partial S}{\partial \Delta} &= S\left(\Gamma_d - \Gamma_{d^\dagger}\right)S = S\Gamma_{\tilde{\sigma}} S, \\ \frac{\partial S}{\partial m_q} &= S\Gamma_\sigma S, \end{aligned} \tag{3.201}$$

we end up with another set of self-consistent relations (in the scalar state)

$$\begin{aligned} \left(\frac{1}{2G} + B_{\sigma\sigma}\right) M_1 &= -B_{\sigma\sigma} + B_{\sigma\tilde{\sigma}}\Delta_1, \\ \left(\frac{1}{2H} - B_{\tilde{\sigma}\tilde{\sigma}}\right)\Delta_1 &= B_{\tilde{\sigma}\sigma} + B_{\tilde{\sigma}\sigma} M_1, \end{aligned} \tag{3.202}$$

the second of which indicates that $\Delta_1 = 0$ if $B_{\sigma\tilde{\sigma}} = 0$, which is true in the pure-pairing limit. For simplicity we consider this limit. Using the power expansions back in the gap equations (3.184) at second order, we obtain

$$\begin{aligned} \left(\frac{1}{2G} + B_{\sigma\sigma}\right) M_2 &= -2T_{\sigma\sigma\sigma}(1+M_1) - B_{\sigma\tilde{\sigma}}\Delta_2 = -2T_{\sigma\sigma\sigma}(1+M_1) \\ \left(\frac{1}{2H} - B_{\tilde{\sigma}\tilde{\sigma}}\right)\Delta_2 &= 2T_{\tilde{\sigma}\sigma\sigma}(1+M_1) + B_{\tilde{\sigma}\sigma} M_2 = 2T_{\tilde{\sigma}\sigma\sigma}(1+M_1) \end{aligned} \tag{3.203}$$

Therefore, we have

$$\begin{aligned} M_1 &= \frac{-B_{\sigma\sigma}}{\frac{1}{2G} + B_{\sigma\sigma}},\ \Delta_1 = 0, \\ M_2 &= \frac{-2T_{\sigma\sigma\sigma}(1+M_1)}{\frac{1}{2G} + B_{\sigma\sigma}},\ \Delta_2 = \frac{2T_{\tilde{\sigma}\sigma\sigma}(1+M_1)}{\frac{1}{2H} - B_{\tilde{\sigma}\tilde{\sigma}}}. \end{aligned} \tag{3.204}$$

If we ignore the wave function mixing from the small chiral condensate due to $m_q$, then the diquark pion's inverse propagator can be written, after some

algebra, as

$$\begin{aligned}\frac{1}{2H}+B_{\tilde{\pi}\tilde{\pi}}(k) &= \frac{1}{2H}+B_{\tilde{\pi}\tilde{\pi}}(k;m_q=0)\\ &+(1+M_1)\left(T_{\sigma\tilde{\pi},\tilde{\pi}}(k)+T_{\tilde{\pi},\sigma\tilde{\pi}}(k)\right)m_q\\ &+\Big[2(1+M_1)^2Q_{\sigma\tilde{\pi},\sigma\tilde{\pi}}(k)+M_2\left(T_{\sigma\tilde{\pi},\tilde{\pi}}(k)+T_{\tilde{\pi},\sigma\tilde{\pi}}(k)\right)\\ &+\Delta_2\left(T_{\tilde{\sigma}\tilde{\pi},\tilde{\pi}}(k)+T_{\tilde{\pi},\sigma\tilde{\pi}}(k)\right)\Big]\frac{m_q^2}{2}+\mathcal{O}(m_q^3),\end{aligned} \tag{3.205}$$

where the triangle and square diagrams with external legs of momenta $q$ are defined by

$$\begin{aligned}T_{AB,C}(q) &= \frac{1}{i}\mathrm{Tr}S(p)\Gamma_A S(p)\Gamma_B S(p-q)\Gamma_C,\\ T_{A,BC}(q) &= \frac{1}{i}\mathrm{Tr}S(p)\Gamma_A S(p-q)\Gamma_B S(p-q)\Gamma_C,\\ Q_{AB,CD}(q) &= \frac{1}{i}\mathrm{Tr}S(p)\Gamma_A S(p)\Gamma_B S(p-q)\Gamma_C S(p-q)\Gamma_D.\end{aligned} \tag{3.206}$$

The GMOR relation can thus be readily extracted as triangle and square diagrams. In particular, if we simply remove the chiral sector, the inverse propagator of the diquark pion' becomes

$$\frac{1}{2H}+B_{\tilde{\pi}\tilde{\pi}}(k)=\frac{1}{2H}+B_{\tilde{\pi}\tilde{\pi}}(k;m_q=0)\Delta_2 T_{\tilde{\sigma}\tilde{\pi},\tilde{\pi}}(k)\frac{m_q^2}{2}+\mathcal{O}(m_q^3) \tag{3.207}$$

as expected.

### 3.4.3 Generalization to realistic models

The generalization of this method to $N_f, N_c > 1$ models with more general condensates is straightforward; the outline can be summarized as follows:

(1) Write down the self-consistent gap equations for all the condensates (mean fields), including all configurations of the ground state related to each other by chiral rotations. In our previous $N_f = N_c = 1$ example, both the scalar and pseudoscalar condensates (e.g., $\sigma$ and $\pi$) must be taken into account, even if we want to focus on the scalar state (or any particular state) only.

(2) Differentiate the gap equations with regard to parametrized chiral rotation angles. This procedure can generate an infinite set of equations relating loop diagrams with different numbers of vertex insertions – it relates tadpoles to bubbles, bubbles to triangles, triangles to squares, and so on. These equations can be used later on to identify the GMOR relation in the inverse propagator of the mesons.

(3) Expand the mean field quark inverse propagator as well as the condensates themselves in power series of the explicit symmetry breaking perturbation

($m_q$ in our case); this is essentially computing the variation of the quark lines by the perturbation, while constrained by the gap equations to ensure self-consistency.

(4) Match the powers of the perturbation. This step will generate a set of linear equations relating the perturbation terms $S_{1,2,...}$ and $M_{1,2,...}$ etc. at each power of the perturbation, with loop diagrams (such as bubbles and triangles) being the coefficients of this linear system. Solving this linear system will yield the perturbation terms completely.

(5) Write down the meson inverse propagator using $S_{1,2,...}$ and $M_{1,2....}$ etc. as a power series in the perturbation ($m_q$); the GMOR relation, relating the NG meson mass to powers of $m_q$, becomes manifest at arbitrary orders in the perturbation $m_q$.

# Chapter 4

# Quark-hadron continuity: CFL dressing

In this Chapter we derive a low energy gauge-invariant effective description of QCD in the coexistence phase in the presence of color-flavor-locked (CFL) diquark and chiral condensates (CFL+$\chi$SB). We show that the Lagrangian of this effective description, constructed from symmetry and quarks and gluons dressed by both chiral and diquark condensates, takes the form of that of a baryon-meson theory, with an intuitive mapping between the quarks and gluons and the baryons and mesons. Our method is a sophisticated generalization of the effective theory of baryons in CFL quark matter constructed in Ref. [7].

Our effective theory of dressed quarks and gluons is analogous to the nonlinear sigma model in the presence of symmetry-breaking condensates. We discuss the physical implications of this description of QCD as a concrete realization of quark-hadron continuity, where the low energy spectrum of the CFL QCD is tightly connected to that of hadronic matter, with possibly modifications in coupling structures.

## 4.1 CFL diquark and chiral condensates using quark fields

Let $U_{L,R}$ be a flavor $SU(3)_{L,R}$ transformation, and $U_C$ of $SU(3)_C$. Then, the quark fields transform as

$$q_{L,R;ia} \to U^{ij}_{L,R} U^{ab}_C q_{L,R;jb} = U_{L,R} q_{L,R} U_C^T, \tag{4.1}$$

where in the final term we treat color and flavor indices on an equal footing; the usefulness of this notation comes from the fact that in diquark pairing phase, flavor and color are locked and maneuvers often involve summations over both indices. The chiral condensate matrix $M_{ij} = \bar{q}_{Rj} q_{Li}$ (up to a renormalization constant), which is a color singlet with flavor indices $i$ and $j$, transforms as

$$M_{ij} = \bar{q}_{Rj} q_{Li} \Rightarrow M_{ij} \to U_{Lim} U^\dagger_{Rnj} M_{ij} = U_L M U_R^\dagger. \tag{4.2}$$

The color indices of the quark fields are implicitly summed over, resulting in a color singlet $M$. Under an axial SU(3) transformation where $U_L = U_R^\dagger$, $M$

transforms as a nonet. A useful parametrization is

$$M = \Sigma_s + i\Pi_p, \tag{4.3}$$

where "s, p" stand for scalar and pseudoscalar. Here, $\Sigma_s = \sum_{a=0}^{8} \bar{q}\tau_a q$ is the scalar $\bar{q}q$ bilinear component of $M$, $\Pi_p = \sum_{a=0}^{8} \bar{q}i\gamma_5\tau_a q$ is the pseudoscalar component; their diagonal $a = 0$ (trace) part, $\bar{q}q$ and $\bar{q}i\gamma_5 q$, correspond to "1" of the respective nonet. $\tau_{a=0,\ldots,8}$ are the SU(3) Gell-Mann matrices, with $\tau_0 = \sqrt{2/3}\,\mathbf{1}$ included ($\mathbf{1}$ is the unit matrix).

We separate $M$ into its magnitude (which carries the same dimension as $M$) and a dimensionless SU(3) phase $Y$:

$$M_{ij} = |M|Y_{ij}; \tag{4.4}$$

all the transformation properties of $M$'s are exhibited by $Y$, and a finite $|M|$ characterizes a non-vanishing chiral condensate. The simplest interaction term between the quark field and the chiral field is

$$g|M|\bar{q}_L Y q_R + h.c., \tag{4.5}$$

which can also be formally obtained from the mean field approximation in the NJL model (see Chapter 2). The form of this interaction is strictly constrained by symmetry, and must be universal in all effective theories that respect chiral symmetry at order $M$.

It is convenient to generalize all the matrix operations to formally act on both color and flavor. We formally write the transpose $q^T_{ia} = q_{ai}$ for the quark field, or any field with flavor index $i$ and color index $a$; similarly, traces and determinants are performed by formally treating color and flavor indices on an equal footing. One however must be careful in tracking the flavor and color indices during these matrix operations to avoid mixing up the two physically distinct quantum numbers. On the other hand, products in Dirac space are always implied without causing confusion, e.g., $q\Gamma q$ in this Chapter means $q_m\Gamma_{mn}q_n$ ($\Gamma$ is some Dirac matrix), which corresponds to $q^T q$ and $q^T\Gamma q$ in the usual notation where the normal transpose does not act on flavor and color. With these generalized matrix operations, we can write the interaction term as

$$g|M|\mathrm{Tr}(\bar{q}_L Y q_R) + h.c. \tag{4.6}$$

Similar to $M$, we construct the diquark condensate matrix as (up to a renormalization constant)

$$d^\dagger_{L,Rai} = \epsilon_{ijk}\epsilon_{abc} q^T_{L,R;jb} C q_{L,R;kc}, \tag{4.7}$$

which is totally anti-symmetric in spin, color and flavor. We observe that $d^\dagger_{ai}$

transforms as $\bar{3}_f$ and $\bar{3}_c$. As a result, the bosonic $d_{ia}$ will transform like a quark in flavor and color space. we can compactly write

$$d^*_{L,Ria} \equiv d^\dagger_{L,R;ai};\ d^\dagger_{L,R} \to U^*_C d^\dagger_{L,R} U^\dagger_{L,R}. \tag{4.8}$$

Separating $d$ into its magnitude (which characterizes the CFL condensate) and a $SU(3)_{CFL}$ phase (which carries both flavor and color indices)

$$d_{ia} = |d| X_{ia}, \tag{4.9}$$

we have

$$X^\dagger_{L,R} \to U^*_C X^\dagger_{L,R} U^\dagger_{L,R},\ X_{L,R} \to U_{L,R} X_{L,R} U^T_C; \tag{4.10}$$

where $X_{L,R}$ transforms like a quark, but carries baryon number -2/3:

$$X_{L,R} \to e^{2i\theta_B/3} X_{L,R},\ \text{for } q \to e^{-i\theta_B} q; \tag{4.11}$$

$\theta_B$ is the $U(1)_B$ phase.

The interaction between scalar diquark condensates and the quarks at leading order in $|d|$ is

$$h\frac{|d|}{2}\left[\mathrm{Tr}X^\dagger_L q_L C X^\dagger_L q_L - (\mathrm{Tr}X^\dagger_L q_L) C (\mathrm{Tr}X^\dagger_L q_L) + h.c.\right] - (L \leftrightarrow R). \tag{4.12}$$

This interaction is a generalization of the four-quark pairing interaction of the form $|q^T C\tau_A \lambda_A \gamma_5 q|^2$ (cf. Chapter 3). Indeed, in the scalar ground state, $X_{ia} = \delta_{ia}$, so

$$\begin{aligned}
&[\mathrm{Tr}q_L C q_L - (\mathrm{Tr}q_L) C (\mathrm{Tr}q_L) - (L \to R)] \\
&\qquad = \left[\delta_{ia}\epsilon_{ijk}\epsilon_{abc} q^{jb}_L C q^{kc}_L - (L \to R)\right] \\
&\qquad = -\delta_{ia}\epsilon_{ijk}\epsilon_{abc} q^{jb} C\gamma_5 q^{kc} \propto \delta_{AB}(q^T C\tau_A \lambda_B q),
\end{aligned} \tag{4.13}$$

where we have used the following property of the Levi-Civita symbol

$$\varepsilon_{ijk}\varepsilon_{imn} = \delta_{jm}\delta_{kn} - \delta_{jn}\delta_{km}. \tag{4.14}$$

Altogether, to lowest order in $|d|$ and $|M|$, we can write the chiral Lagrangian of quarks interacting with the condensates

$$\begin{aligned}
\mathcal{L} \ &= \ \bar{q} i\partial\!\!\!/ q + g|M|\,(\bar{q}_L Y q_R + h.c.) \\
&\quad + h\frac{|d|}{2}\left(\left[\mathrm{Tr}X^\dagger_L q_L C X^\dagger_L q_L - (\mathrm{Tr}X^\dagger_L q_L) C (\mathrm{Tr}X^\dagger_L q_L) - (L \to R)\right] + h.c.\right).
\end{aligned} \tag{4.15}$$

At this step, the dynamics of the NG bosons, which are contained in the matrix

representations $X$ and $Y$, is not manifestly present. As $X$ and $Y$ are linearly independent phases, we must diagonalize the Lagrangian in their coupling to the quarks to distinguish the physical NG bosons and the massive modes.

## 4.2 Dressed quarks with diquark and chiral condensates

We now construct fermion fields by dressing quarks with the diquark and chiral condensates, analogous to the dressing of nucleons by the chiral condensate in non-linear sigma model.

As the first step, a gauge-invariant fermion field can be formed via

$$q_{Lia}X^{\dagger}_{Laj} = \psi_{Lij}, \tag{4.16}$$

which transforms as a color singlet but a flavor nonet:

$$\psi_{L,R} \to U_{L,R}\psi_{L,R}U^{\dagger}_{L,R}. \tag{4.17}$$

The reversal to the quark field is

$$\begin{aligned} q_{Lia} &= \psi_{Lij}X_{Lja}, \\ \bar{q}_{Lai} &= X^{\dagger}_{Laj}\bar{\psi}_{Lji}. \end{aligned} \tag{4.18}$$

In terms of the new flavor nonet $\psi$, the quark coupling to the chiral phase $Y$ is

$$\bar{q}_{Lia}Y_{ij}q_{Rja} = \bar{\psi}_{Lmi}Y_{ij}\psi_{Rjn}X_{Rna}X^{\dagger}_{Lam} \equiv \mathrm{Tr}\left(\bar{\psi}_L Y \psi_R \tilde{Y}^{\dagger}\right). \tag{4.19}$$

Here, the color-singlet object $\tilde{Y}^{\dagger}_{nm} \equiv X_{Rna}X^{\dagger}_{Lam}$ transforms as a flavor nonet just like the chiral phase $Y^{\dagger}$:

$$\tilde{Y}^{\dagger} \to U_R\tilde{Y}^{\dagger}U^{\dagger}_L;\ \tilde{Y} \to U_L\tilde{Y}U^{\dagger}_R; \tag{4.20}$$

it contains the same physical information as the original diquark phase $X$, but has the advantage of being gauge-invariant. Meanwhile, $X$s in the diquark-quark interaction term are completely transformed away after dressing quarks into $\psi$ fields, and thus the interaction no longer contains NG bosons or the massive modes:

$$\begin{aligned} &\mathrm{Tr}X^{\dagger}_L q_L C X^{\dagger}_L q_L - (\mathrm{Tr}X^{\dagger}_L q_L)C(\mathrm{Tr}X^{\dagger}_L q_L) - (L \leftrightarrow R) \\ &= \mathrm{Tr}\psi_L C \psi_L - (\mathrm{Tr}\psi_L)C(\mathrm{Tr}\psi_L) - (L \leftrightarrow R). \end{aligned} \tag{4.21}$$

To further decode the information of the NG bosons from Eq. (4.19), we

define "half" of the chiral phase, $\xi$, as

$$\xi^2 = Y. \tag{4.22}$$

The pseudoscalar mesons, corresponding to the fluctuations of $\xi$ (and thus $Y$), are given by the parametrization

$$\xi = \exp\left[i\sum_{a=1}^{8}\tau_a\pi_a/2f_\pi\right], \tag{4.23}$$

where $\tau_a$ are the Gell-Mann matrices for flavor, $\pi_a$ the eight real fields, and $f_\pi$ the pion decay constant. The transformation rule for $\xi$ derives from that of $Y$. Introducing the "compensator" field, $K$, which is a function of both $\xi$ itself and the $SU(3)_{L,R}$ transformations:

$$K = U_L\xi\sqrt{U_L\xi^2U_R}^\dagger; \tag{4.24}$$

one can show that

$$\xi \to U_L\xi K^\dagger = K\xi U_R^\dagger. \tag{4.25}$$

Using $\xi$ we can further dress the fermion fields. We define

$$\begin{aligned}\phi_L &= \xi^\dagger\psi_L\xi,\\ \phi_R &= \xi\psi_R\xi^\dagger;\end{aligned} \tag{4.26}$$

the new fermion fields transform as flavor nonet

$$\phi_{L,R} \to K\phi_{L,R}K^\dagger. \tag{4.27}$$

The chiral interaction term then becomes

$$\mathrm{Tr}\left(\bar{\psi}_L Y\psi_R\tilde{Y}^\dagger\right) = \mathrm{Tr}\left(\bar{\phi}_L\phi_R Y_M^\dagger\right), \tag{4.28}$$

where the chiral phase $Y_M$ is defined by

$$Y_M \equiv \xi^\dagger\tilde{Y}\xi^\dagger = \xi^\dagger X_L X_R^\dagger\xi^\dagger. \tag{4.29}$$

The "$M$" in the subscript means "massive", which we will clarify in a moment. The diquark interaction term remains invariant after this dressing:

$$\begin{aligned}&\mathrm{Tr}\psi_L C\psi_L - (\mathrm{Tr}\psi_L)C(\mathrm{Tr}\psi_L) - (L\leftrightarrow R)\\ &= \mathrm{Tr}\phi_L C\phi_L - (\mathrm{Tr}\phi_L)C(\mathrm{Tr}\phi_L) - (L\leftrightarrow R).\end{aligned} \tag{4.30}$$

So far we have rotated away some of the chiral phases in the interaction

terms by two successive redefinitions of the quark field. These redefinitions, or dressing, will introduce derivative terms from the kinetic energy $\bar{q}i\partial\!\!\!/ q$. Indeed, after first dressing $q \to \psi$, which we call the "diquark dressing,"

$$\bar{q}i\partial\!\!\!/ q = \mathrm{Tr}\bar{\psi}i\partial\!\!\!/\psi - \left[\mathrm{Tr}\bar{\psi}_L i\gamma^\mu\psi_L\left(X_L\partial_\mu X_L^\dagger\right) + (L \leftrightarrow R)\right], \tag{4.31}$$

where $X_{L,R}\partial X_{L,R}^\dagger$ are gauge-invariant left- and right- handed diquark phase currents. With the additional dressing $\psi \to \phi$, which we call the "chiral dressing," we obtain further

$$\begin{aligned}\bar{q}i\partial\!\!\!/ q &= \mathrm{Tr}\bar{\phi}i\gamma_\mu\partial^\mu\phi - \mathrm{Tr}\bar{\phi}\gamma^\mu\gamma^5\phi\tilde{a}_\mu + \mathrm{Tr}\bar{\phi}i\gamma^\mu\phi\tilde{v}_\mu \\ &\quad -\mathrm{Tr}\bar{\phi}\gamma^\mu\gamma^5[a_\mu,\phi] + \mathrm{Tr}\bar{\phi}i\gamma^\mu[v_\mu,\phi];\end{aligned} \tag{4.32}$$

here, the chiral axial and vector currents $a, v$ are defined by

$$\begin{aligned}a_\mu &= \tfrac{i}{2}\left(\xi^\dagger\partial_\mu\xi - \xi\partial_\mu\xi^\dagger\right), \\ v_\mu &= \tfrac{1}{2}\left(\xi^\dagger\partial_\mu\xi + \xi\partial_\mu\xi^\dagger\right)\end{aligned} \tag{4.33}$$

while the diquark axial and vector currents (dressed by chiral condensates) $\tilde{a}, \tilde{v}$ are

$$\begin{aligned}\tilde{a}_\mu &= -\tfrac{i}{2}\left[\xi^\dagger\left(X_L\partial_\mu X_L^\dagger\right)\xi - \xi\left(X_R\partial_\mu X_R^\dagger\right)\xi^\dagger\right], \\ \tilde{v}_\mu &= -\tfrac{1}{2}\left[\xi^\dagger\left(X_L\partial_\mu X_L^\dagger\right)\xi + \xi\left(X_R\partial_\mu X_R^\dagger\right)\xi^\dagger\right].\end{aligned} \tag{4.34}$$

Equation (4.32) indicates that the two currents, $a, v$ and $\tilde{a}, \tilde{v}$, couple to $\phi$ with different flavor structures, despite them sharing the same flavor $SU(3)$ transformation rules. Also, at this stage it is clear that the pseudoscalar mesons corresponding to the $Y_M$ phase are massive, while the other linearly independent modes are the NG bosons. The reason is that only the $Y_M$ mesons are coupled to $\phi$ in a non-derivative interaction, which results in non-zero self-energy through interacting with $\phi$, which becomes a mass at zero four-momentum. The NG mode only couples to $\phi$ with a derivative coupling, so it remains massless.

To find the currents corresponding to the NG modes and the massive modes, we analogously define "half" of the diquark chiral phase

$$\tilde{\xi}^2 = \tilde{Y},\ \tilde{\xi} = \exp\left[i\sum_{a=1}^{8}\tau_a\tilde{\pi}_a/2f_\pi\right], \tag{4.35}$$

where $\tilde{\pi}_a$ are the eight real pseudoscalar diquark mesons, which are gauge-invariant; in this formalism, one can easily see that they correspond to $\bar{q}\bar{q}qq$-type fluctuations since $\tilde{Y} \sim \bar{q}\bar{q}qq$. Physically they are equivalent to the $qq$-type fluctuations studied in Chapter 2; they are merely different but equivalent descriptions of the same physical pseudoscalar mesons. Indeed, Table 4.1 shows the operator correspondence of the two different descriptions; each pair trans-

| diquark phases | gauge-invariant description |
|---|---|
| $X_L X_R^\dagger$ | $\tilde{\xi}^2$ |
| $X_L \partial_\mu X_L^\dagger$ | $\tilde{\xi}\partial\tilde{\xi}^\dagger$ |
| $X_R \partial_\mu X_R^\dagger$ | $\tilde{\xi}^\dagger\partial\tilde{\xi}$ |

Table 4.1: The correspondence between composite diquark phase operators and that of the gauge-invariant field $\tilde{\xi}$.

form identically under $SU(3)_{L,R,C}$, and are physically indistinguishable.

In the gauge-invariant description which also takes advantage of the parametrization (4.35), the dressed diquark axial and vector currents are

$$\begin{aligned} \tilde{a}_\mu &= -\tfrac{i}{2}\left[\xi^\dagger\left(\tilde{\xi}\partial_\mu\tilde{\xi}^\dagger\right)\xi - \xi\left(\tilde{\xi}^\dagger\partial_\mu\tilde{\xi}\right)\xi^\dagger\right], \\ \tilde{v}_\mu &= -\tfrac{1}{2}\left[\xi^\dagger\left(\tilde{\xi}\partial_\mu\tilde{\xi}^\dagger\right)\xi + \xi\left(\tilde{\xi}^\dagger\partial_\mu\tilde{\xi}\right)\xi^\dagger\right]. \end{aligned} \tag{4.36}$$

At linear order in the meson fields,

$$Y_M = \xi^\dagger\tilde{\xi}^2\xi^\dagger \approx 1 + \sum_a \tau_a\left(\frac{\tilde{\pi}_a}{f_{\tilde{\pi}}} - \frac{\pi_a}{f_\pi}\right). \tag{4.37}$$

Thus, if we parametrize the meson fields contained in $Y_M$ in a similar fashion

$$Y_M = \exp\left[i\sum_{a=1}^{8}\tau_a\pi_a^M/f_\pi\right] = 1 + i\sum_a \tau_a\frac{\pi_a^M}{f_M} + \ldots, \tag{4.38}$$

then at the same linear order,

$$\frac{\pi_a^M}{f_M} = \frac{\tilde{\pi}_a}{f_{\tilde{\pi}}} - \frac{\pi_a}{f_\pi}, \tag{4.39}$$

confirming that $\pi_a^M$ is indeed the massive mode. The other linearly independent mode is

$$\frac{\pi_a^G}{f_G} = \frac{f_{\tilde{\pi}}\tilde{\pi}_a + f_\pi\pi_a}{f_G^2}, \tag{4.40}$$

with

$$f_M = \frac{f_\pi\tilde{f}_\pi}{\sqrt{f_\pi^2 + \tilde{f}_\pi^2}},\ f_G = \sqrt{f_\pi^2 + \tilde{f}_\pi^2}; \tag{4.41}$$

here, $f_M$ and $f_G$ are such that $\pi_a^{M,G}$ are normalized and obey the same commutation relations as $\pi$ and $\tilde{\pi}$; they agree with the form derived in Chapter 2.

To identify the currents associated with the NG modes and the massive

modes, we expand the currents (4.33) and (4.36):

$$a_\mu = -\frac{1}{2f_\pi}\partial_\mu\Phi + \mathcal{O}\left[\left(\frac{\Phi}{f_\pi}\right)^3\right],\ v_\mu = -\frac{\{\Phi,\partial_\mu\Phi\}}{8f_\pi^2} + \mathcal{O}\left[\left(\frac{\Phi}{f_\pi}\right)^4\right],$$
$$\tilde{a}_\mu = -\frac{1}{2f_{\tilde{\pi}}}\partial_\mu\tilde{\Phi} + \mathcal{O}\left[\left(\frac{\tilde{\Phi}}{f_{\tilde{\pi}}}\right)^3\right],\ \tilde{v}_\mu = \frac{\{\tilde{\Phi},\partial_\mu\tilde{\Phi}\}}{8f_{\tilde{\pi}}^2} + \mathcal{O}\left[\left(\frac{\tilde{\Phi}}{f_{\tilde{\pi}}}\right)^4\right]; \quad (4.42)$$

here, $\Phi \equiv \sum_a \tau_a\pi_a$ and $\tilde{\Phi} \equiv \sum_a \tau_a\tilde{\pi}_a$. For later use, we also write $\Phi_G \equiv \sum_a \tau_a\pi_a^G$ and $\Phi_M \equiv \sum_a \tau_a\pi_a^M$, and define the NG and massive currents up to leading order in meson fields:

$$\begin{aligned} a_\mu^{G,M} &= -\frac{1}{2f_{G,M}}\partial_\mu\Phi_{G,M} + \ldots, \\ v_\mu^{G,M} &= -\frac{\{\Phi_{G,M},\partial_\mu\Phi_{G,M}\}}{8f_{G,M}^2} + \ldots, \end{aligned} \quad (4.43)$$

where the "..." implies higher order terms in the meson fields; in general, those terms are more complicated when constructed from $\Phi$ and $\tilde{\Phi}$. With this definition, up to leading order in meson fields,

$$\begin{aligned} a_\mu &= a_\mu^G - \frac{f_{\tilde{\pi}}^2}{f_G^2}a_\mu^M, \\ v_\mu &= v_\mu^G + \frac{f_{\tilde{\pi}}^4}{f_G^4}v_\mu^M - \frac{f_\pi f_{\tilde{\pi}}\left(\{\Phi_G,\partial_\mu\Phi_M\}+\{\Phi_M,\partial_\mu\Phi_G\}\right)}{8f_\pi^2 f_G^2}, \\ \tilde{a}_\mu &= a_\mu^G + \frac{f_\pi^2}{f_G^2}a_\mu^M, \\ \tilde{v}_\mu &= -v_\mu^G - \frac{f_\pi^4}{f_G^4}v_\mu^M + \frac{f_\pi f_{\tilde{\pi}}\left(\{\Phi_G,\partial_\mu\Phi_M\}+\{\Phi_M,\partial_\mu\Phi_G\}\right)}{8f_{\tilde{\pi}}^2 f_G^2}. \end{aligned} \quad (4.44)$$

If we consider low energy, we can neglect all the massive modes and current; the system then involves only $\phi$ and the NG modes, and $Y_M = 1$. The full Lagrangian, with both the kinetic term (4.32) and the interaction terms (4.28) and (4.30), is then

$$\begin{aligned} \mathcal{L} = {} & \mathrm{Tr}\bar{\phi}i\gamma_\mu\partial^\mu\phi - g_F\mathrm{Tr}\bar{\phi}\gamma^\mu\gamma^5[a_\mu^G,\phi] - g_D\mathrm{Tr}\bar{\phi}\gamma^\mu\gamma^5\{a_\mu^G,\phi\} \\ & -g'_F\mathrm{Tr}\bar{\phi}i\gamma^\mu[v_\mu^G,\phi] - g'_D\mathrm{Tr}\bar{\phi}i\gamma^\mu\{v_\mu^G,\phi\} \\ & +g|M|\mathrm{Tr}\left(\bar{\phi}_L\phi_R\right) \\ & +h\frac{|d|}{2}\mathrm{Tr}\phi_L C\phi_L - (\mathrm{Tr}\phi_L)C(\mathrm{Tr}\phi_L) - (L\leftrightarrow R), \end{aligned} \quad (4.45)$$

where the couplings are $g_F = g_D = 1/2$, $g'_F = 1/2$ and $g'_D = -3/2$; intriguingly the vector currents have a different coupling structure in flavor space than the axial currents. In particular, the axial vector coupling constant, $g_A$, is given by $g_A \equiv g_F + g_D = 1$, as in the NJL model.

The Lagrangian (4.45) is valid in the coexistence phase of diquark and chiral condensates; if either vanishes, then the dressing procedure loses its physical meanings. When one applies (4.45) in the $|M|$ or $|d| \to 0$ limit, the massive modes and currents are important and can no longer be removed. For the axial vectors, one can show that, using (4.44 and (4.32), the coupling constants for the massive modes are

$$g'_F = -\frac{2f_{\tilde{\pi}}^2 + f_\pi^2}{2f_G^2},\ g'_D = \frac{f_\pi^2}{2f_G^2}, \tag{4.46}$$

which depend on $f_\pi$ and $f_{\tilde{\pi}}$ and thus the density. The couplings of the NG mode to the fermion field $\phi$ on the other hand are constant as long as we remain in the coexistence phase.

The dressing scheme (4.26) using the chiral phase $\xi$ is not the only way to realize the non-linear chiral Lagrangian (4.45). In fact, one can at this step choose to dress the fermion fields $\psi$ with the gauge-invariant diquark phases $\tilde{\xi}$ again:

$$\phi'_L = \tilde{\xi}^\dagger \psi_L \tilde{\xi},\ \phi'_R = \tilde{\xi} \psi_R \tilde{\xi}^\dagger. \tag{4.47}$$

This dressing scheme will result in no chiral currents $a_\mu, v_\mu$ in the manifest Lagrangian, but the chiral interaction will still take a form of $\mathrm{Tr}(\bar{\phi}'_L Y_M^\dagger \phi'_R)$, exposing the massive modes; the construction of NG and massive currents follows identically. The resulting NG pseudoscalar sector $F_A = F_D = 1/2$ is still the same; however, the massive pseudoscalar current coupling becomes

$$g'_F = g'_D = \frac{f_\pi^2}{2f_G^2}, \tag{4.48}$$

a different set than Eq. (4.46). The reason is that the dressed fields $\phi'$ differ from $\phi$ by a total dressing of the massive modes:

$$\phi_L = \xi^\dagger \tilde{\xi} \phi'_L \tilde{\xi}^\dagger \xi = \sqrt{Y_M}\, \phi'_L \sqrt{Y_M}^\dagger. \tag{4.49}$$

Thus, the difference between the dressing schemes (4.26) and (4.47) is another field dressing with massive pseudoscalar modes; it is natural that this absorption of some massive chiral phases (and thus the massive currents) into the fermion fields produces different $F - D$ couplings. The NG currents on the other hand are completely independent of the dressing schemes, which is expected since they should only depend on the symmetry breaking pattern itself.

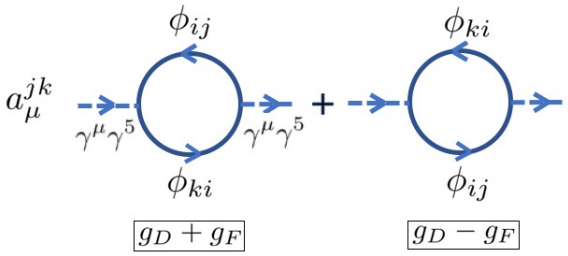


Figure 4.1: The bubble contribution to the self-energy of the axial current $a_\mu^{jk}$ of the NG bosons from both $g_D$ and $g_F$ coupling structures.

## 4.3 Meson kinetic energy and the non-linearity of the meson field transformation

We have worked out the quark-meson Lagrangian (4.45) at a basic level. To complete the effective theory where the NG bosons are long-lived particles with their own kinematics, we explicitly integrate out their self-energy given by bubble diagrams (see Eq. (4.50) and (4.52); the bubble contribution to self-energy is illustrated in Fig. 4.1). We consider the NG modes only.

The meson-fermion interaction from (4.45) has the general form

$$\mathcal{L}_{\pi_G-\phi} = -(g_F+g_D)\bar{\phi}_{ij}(\gamma^5\gamma^\mu)a_\mu^{jk}\phi_{ki} - (g_D-g_F)\bar{\phi}_{ki}(\gamma^5\gamma^\mu)\phi_{ij}a_\mu^{jk}; \quad (4.50)$$

here, the axial current $a_\mu$ can be that of the chiral mode, diquark mode, or the NG and massive modes; as they all share the same symmetry structure, it suffices to consider the chiral mode, whose calculation is simplest. For simply we assume free fermions $\phi$, such that their Green's functions obey

$$-i\langle T\phi_{ij}(1)\bar{\phi}_{ab}(2)\rangle = G(ij,ab)(1-2) = \delta_{ib}\delta_{ja}G(1-2). \quad (4.51)$$

After some algebra, the bubble connecting the two end axial current states $(a_\mu^G)^{jk}$ and $(a_\nu^G)^{mn}$ is

$$\begin{aligned} B_{\mu\nu}^{jk,mn}(k) &= 2\left\{\left(g_D^2+g_F^2\right)\delta_m^k\delta_n^j + \left(g_D^2-g_F^2\right)\delta_m^n\delta_j^k\right\}k^\mu k^\nu B_{\mu\nu}(k)\delta_m^k\delta_n^j, \\ B_{\mu\nu}(k) &\equiv 9i\int_p \mathrm{Tr}_\gamma\left[\gamma^5\gamma^\mu G_p\gamma^5\gamma^\nu G_{p-k}\right]. \end{aligned} \quad (4.52)$$

Similar to Chapter 2, we also write down the vacuum-to-meson transition amplitude parametrized in terms of $f_\pi$. The integration of such bubbles has been performed in [96] and the result is the standard kinetic energy

$$f_\pi^2\mathrm{Tr}a_\mu a^\mu = \frac{f_\pi^2}{4}\partial_\mu Y^\dagger\partial^\mu Y. \quad (4.53)$$

As $Y = \exp i\Phi/f_\pi$, up to quadratic order in $\Phi$, we simply have

$$\frac{f_\pi^2}{4}\partial_\mu Y^\dagger \partial^\mu Y \approx \frac{1}{4}\mathrm{Tr}\partial_\mu \Phi \partial^\mu \Phi = \frac{1}{4}\mathrm{Tr}\tau_a\tau_b \partial\pi_a \partial\pi_b = \frac{1}{2}\partial\pi_a\partial\pi_a, \tag{4.54}$$

the familiar form. The same kinetic energy form will exist for the diquark mesons, and thus the NG and massive mesons (after diagonalization) as well.

The meson kinetic energy form $(f_\pi^2/4)\partial_\mu Y^\dagger \partial^\mu Y$ has the advantage of $Y$ transforming linearly $Y \to U_L Y U_R^\dagger$, which is useful when considering the current algebra of this model. However, the transformation of $\Phi$ is highly non-linear.

Consider a pure left-hand $SU(3)$ transformation

$$U_L = e^{-i\tau_a\theta_a/2}, U_R = 1, \tag{4.55}$$

where $\theta_a$ parametrizes the transformation. We write the resulting transformation on $\Phi$ in a series:

$$\Phi \to \Phi' = \Phi + \theta_a A_a + \dots, \tag{4.56}$$

where $A_a$ are matrices; then

$$e^{i(\Phi + A_a\theta_a + \dots)/f_\pi} = e^{-\theta_a\lambda_a/2} e^{i\Phi/f_\pi}. \tag{4.57}$$

Expanding

$$\begin{aligned} e^{i(\Phi + A_a\theta_a + \dots)/f_\pi} &= 1 + \frac{i}{f_\pi}(\Phi + A_a\theta_a + \dots) + \frac{i^2}{2!f_\pi^2}(\Phi + A_a\theta_a + \dots)^2 + \dots \\ &\quad + \frac{i^n}{n!f_\pi^n}(\Phi + A_a\theta_a + \dots)^n + \dots, \end{aligned} \tag{4.58}$$

we obtain

$$\begin{aligned} e^{i(\Phi + A_a\theta_a + \dots)/f_\pi} &= e^{i\Phi/f_\pi} + \theta_a\Big[\frac{i}{f_\pi}A_a + \frac{i^2}{2f_\pi^2}\{\Phi, A_a\} \\ &\qquad + \frac{i^3}{3!f_\pi^3}(A_a\Phi\Phi + \Phi A_a\Phi + \Phi\Phi A_a) + \dots\Big] + \mathcal{O}(\theta^2) \\ &= e^{i\Phi/f_\pi} - \frac{i\theta_a\tau_a}{2}e^{i\Phi/f_\pi} + \mathcal{O}(\theta^2). \end{aligned} \tag{4.59}$$

The equation that determines $A_a$ is then

$$\begin{aligned} \frac{i}{f_\pi}A_a + \frac{i^2}{2f_\pi^2}\{\Phi, A_a\} + \frac{i^3}{3!f_\pi^3}(A_a\Phi\Phi + \Phi A_a\Phi + \Phi\Phi A_a) + \dots \\ = -i\frac{\tau_a}{2}(1 + \frac{i}{f_\pi}\Phi + \frac{i^2}{2f_\pi^2}\Phi^2 + \dots); \end{aligned} \tag{4.60}$$

unfortunately, $A_a$ does not have a simple form and depends on $\Phi$ itself, because of the non-linearity of $\Phi$ under an infinitesimal transformation.

## 4.4 Currents, symmetry and good quantum numbers: mapping to a baryon-meson theory

In this section we discuss the Noether currents resulting from the symmetry in terms of the dressed fermion fields as well as the meson fields, and show that they have a clear one-to-one correspondence in their quantum numbers. In the remainder of this section specifically, we neglect the massive modes altogether; whenever we mention the meson fields $Y$, $\pi_a$, $\Phi_a$ and the currents $a_\mu$ and $v_\mu$, we mean those of the NG modes. Based on last section, the NG bosons will contribute a kinetic energy to the Lagrangian

$$\frac{f_G^2}{4}\partial_\mu Y^\dagger \partial^\mu Y, \tag{4.61}$$

together with the derivative couplings to the fermions in the form of axial $a_\mu$ and vector $v_\mu$ currents.

The Noether current, corresponding to a global symmetry transformation parametrized by a set of angles $\theta_a$, is

$$J_\mu^a = \sum_i \frac{\delta \mathcal{L}}{\delta \partial^\mu O_i} \cdot \frac{\delta O_i}{\delta \theta_a}, \tag{4.62}$$

where $O_i$ are the fields in the Lagrangian; in our case they are the fermion and meson fields. Recall that the full QCD symmetry is

$$SU(3)_L \otimes SU(3)_R \otimes U(1)_B \otimes U(1)_A \otimes U(1)_{EM} \otimes SU(3)_C. \tag{4.63}$$

Denoting the left and right hand flavor transformation

$$U_L = e^{-i\theta_a^L \tau_a/2},\ U_R = e^{-i\theta_a^R \tau_a/2}; \tag{4.64}$$

under $U_{L,R}$ with an infinitesimal $\theta_a^{L,R}$, we see the quark fields transform as

$$\begin{aligned} q_L &\to q_L - \tfrac{i}{2}\theta_{La}\lambda_a q_L, \\ q_R &\to q_R - \tfrac{i}{2}\theta_{Ra}\lambda_a q_R, \end{aligned} \tag{4.65}$$

and the meson fields transform as

$$\begin{aligned} L: &\quad Y \to Y - \tfrac{i}{2}\theta_a^L \tau_a Y, \\ R: &\quad Y \to Y + \tfrac{i}{2}\theta_a^R Y \tau_a. \end{aligned} \tag{4.66}$$

Thus, the left and right hand currents, generated by both the fermions $\phi$ and

the mesons $Y$, are

$$\begin{aligned} J^L_{\mu,a} &= \frac{f_G^2}{4}\mathrm{Tr}\left[\partial_\mu Y^\dagger(-\frac{i}{2}\lambda_a Y)+\frac{i}{2}Y^\dagger\lambda_a\partial_\mu Y\right]=\frac{if_G^2}{4}\mathrm{Tr}\left[Y^\dagger\lambda_a\partial_\mu Y\right], \\ J^R_{\mu,a} &= \frac{f_G^2}{4}\mathrm{Tr}\left[\partial_\mu Y^\dagger(\frac{i}{2}Y\lambda_a)-\frac{i}{2}\lambda_a Y^\dagger\partial_\mu Y\right]=-\frac{if_G^2}{4}\mathrm{Tr}\left[\lambda_a Y^\dagger\partial_\mu Y\right]. \end{aligned} \tag{4.67}$$

The meson contribution to the vector and axial vector currents is then

$$\begin{aligned} J^{V,Y}_{\mu,a} &= J^L_{\mu,a}+J^R_{\mu,a}=\frac{if_G^2}{4}\mathrm{Tr}\left([Y^\dagger,\lambda_a]\partial_\mu Y\right)\approx -if_{abc}\pi_b\partial_\mu\pi_c, \\ J^{A,Y}_{\mu,a} &= -J^L_{\mu,a}+J^R_{\mu,a}=-\frac{if_G^2}{4}\mathrm{Tr}\left(\{Y^\dagger,\lambda_a\}\partial_\mu Y\right) \\ &\approx -\frac{if_G^2}{4}\mathrm{Tr}\frac{i}{f_G}\cdot 2\lambda_a\Phi=f_G\partial_\mu\pi_a. \end{aligned} \tag{4.68}$$

The fermion contribution to the currents is more easily worked out by writing the current in terms of the original quark fields first, and then in terms of $\phi$:

$$\begin{aligned} J^{L,q}_{\mu,a} &= \frac{1}{2}\bar{q}_L\gamma^\mu\tau_a q_L=\frac{1}{2}\mathrm{Tr}\bar{\phi}_L\gamma^\mu\xi^\dagger\tau_a\xi\phi_L \\ &= \frac{1}{2}\mathrm{Tr}\bar{\phi}_L\gamma^\mu\tau_a\phi_L+\frac{1}{2}\mathrm{Tr}\bar{\phi}_L\gamma^\mu[\tau_a,\frac{i\Phi}{2f_\pi}]\phi_L+\ldots, \\ J^{R,q}_{\mu,a} &= \frac{1}{2}\bar{q}_R\gamma^\mu\tau_a q_R=\frac{1}{2}\mathrm{Tr}\bar{\phi}_R\gamma^\mu\tau_a\phi_R-\frac{1}{2}\mathrm{Tr}\bar{\phi}_R\gamma^\mu[\tau_a,\frac{i\Phi}{2f_\pi}]\phi_R+\ldots \end{aligned} \tag{4.69}$$

Therefore, to leading order, the total axial and vector currents from the quark fields are

$$\begin{aligned} J^{V,q}_{\mu,a} &= J^{L,q}_{\mu,a}+J^{R,q}_{\mu,a}=\tfrac{1}{2}\mathrm{Tr}\bar{\phi}\gamma^\mu\tau_a\phi+\mathcal{O}(\bar{\phi}\phi\pi\pi), \\ J^{A,q}_{\mu,a} &= -J^{L,q}_{\mu,a}+J^{R,q}_{\mu,a}=\tfrac{1}{2}\mathrm{Tr}\bar{\phi}\gamma^\mu\gamma^5\tau_a\phi+\mathcal{O}(\bar{\phi}\phi\pi). \end{aligned} \tag{4.70}$$

The total axial and vector currents from (4.45) are then

$$\begin{aligned} J^V_{\mu,a} &= \tfrac{1}{2}\mathrm{Tr}\bar{\phi}\gamma_\mu\tau_a\phi-if_{abc}\pi_b\partial_\mu\pi_c+\mathcal{O}(\pi^4,\bar{\phi}\phi\pi\pi,\ldots), \\ J^A_{\mu,a} &= \tfrac{1}{2}\mathrm{Tr}\bar{\phi}\gamma_\mu\gamma^5\tau_a\phi+f_G\partial_\mu\pi_a+\mathcal{O}(\pi^3,\bar{\phi}\phi\pi,\ldots). \end{aligned} \tag{4.71}$$

In addition, the $U(1)_B$ current is simply

$$J^B_\mu=\frac{1}{2}\mathrm{Tr}\bar{\phi}\gamma_\mu\phi; \tag{4.72}$$

the mesons do not contribute as they carry no baryon number. In the paired phase, the baryon number and the electromagnetic $U(1)$ charge are not good quantum numbers, in the sense that the excitations are not eigenstates of baryon or electric charge numbers

Nevertheless, there exists an additional global $U(1)$ symmetry that is still respected in the CFL phase; its corresponding quantum number is called the generalized charge $\tilde{Q}$, as a counterpart to the electric charge $Q$ which is a good quantum number in non-pairing phases. The generalized charge is a special feature to $N_f = N_c = 3$ quark matter, where the electric charge matrix in flavor space,

$$Q = \mathrm{diag}(2/3, -1/3, -1/3), \tag{4.73}$$

has a similar structure to the 8th color charge matrix

$$Q_C^{(8)} = \mathrm{diag}(1, 1, -2)/\sqrt{3}, \tag{4.74}$$

where we use $R, G, B$ for the color index 1,2,3.

The generalized charge $\tilde{Q}$ is defined as

$$\tilde{Q} \equiv Q + Q_C^{(8)}/\sqrt{3}; \tag{4.75}$$

the resulting generalized charges for the quarks are summarized in Table 4.2 in comparison to the electric charge $Q$ of the baryon nonet. It can be seen that there is exact one-to-one mapping from the quark table to the baryon table in terms of the generalized charge to the electric charge. Furthermore, it can be shown that all CFL diquark condensates, which pair quarks in symmetric positions from the $\tilde{Q}$ quark table, carry zero $\tilde{Q}$ charge; thus, $\tilde{Q}$ is still a good quantum number even in CFL phase, while $Q$ is not. It also implies that the dressed fermion fields $\psi$ and $\phi$ share the same $\tilde{Q}$ table, since neither diquark condensates nor the chiral condensate carry $\tilde{Q}$ charge.

Table 4.4 also lists the $\tilde{Q}$ and $Q$ values of the pseudoscalar mesons calculated from the $\tilde{Q}$ table of the quarks. The mesons carry exactly the same $\tilde{Q}$ charge as their $Q$ charge; the former is useful in the CFL phase quark matter, while the latter is useful in the vacuum phase hadronic matter. This mapping inspires us to write the matrix elements of the $\phi$ field using baryon symbols as well:

$$\phi = \begin{pmatrix} \frac{1}{\sqrt{2}}\Sigma^0 + \frac{1}{\sqrt{6}}\Lambda + \Lambda' & \Sigma^+ & p^+ \\ \Sigma^- & -\frac{1}{\sqrt{2}}\Sigma^0 + \frac{1}{\sqrt{6}}\Lambda + \Lambda' & n^0 \\ \Xi^- & \Xi^0 & -\frac{2}{\sqrt{6}}\Lambda + \Lambda' \end{pmatrix}; \tag{4.76}$$

equivalently, we may describe $\phi$ as the effective baryons in CFL quark matter.

## 4.5 Color and electric charge densities in the mapped $\phi$ theory

So far we have mapped the basic quark Lagrangian into a gauge-invariant baryon Lagrangian, with exact mapping of their conserved charges. In quark matter,

| $\tilde{Q}$ | b | g | r |
|---|---|---|---|
| u | 0 | 1 | 1 |
| d | -1 | 0 | 0 |
| s | -1 | 0 | 0 |

| baryon notet | | |
|---|---|---|
| $\frac{1}{\sqrt{2}}\Sigma^0+\frac{1}{\sqrt{6}}\Lambda+\Lambda'$ | $\Sigma^+$ | $p^+$ |
| $\Sigma^-$ | $-\frac{1}{\sqrt{2}}\Sigma^0+\frac{1}{\sqrt{6}}\Lambda+\Lambda'$ | $n^0$ |
| $\Xi^-$ | $\Xi^0$ | $-\frac{2}{\sqrt{6}}\Lambda+\Lambda'$ |

Table 4.2: Generalized charge $\tilde{Q}$ for the quark fields, compared with the baryon nonet. Note the one-to-one correspondence of the generalized charges in the quark table to the electric charges in the baryon table.

| | $Q$ | $\tilde{Q}$ |
|---|---|---|
| $\pi^+=ud$ | +1 | +1 |
| $\pi^-=d\bar{u}$ | -1 | -1 |
| $\pi^0=\bar{u}u-dd$ | 0 | 0 |
| $K^+=u\bar{s}$ | +1 | +1 |
| $K^-=s\bar{u}$ | -1 | -1 |
| $K^0=d\bar{s}$ | 0 | 0 |
| $\eta$ | 0 | 0 |

Table 4.3: Generalized charge $\tilde{Q}$ and the electric charge $Q$ of the pseudoscalar mesons.

one often imposes the color neutrality and charge neutrality constraints, so the total color and electric charge densities $n_3=n_8=n_Q=0$ vanish in the bulk. We now show that these constrained electric and color densities, with the introduction of color and electric chemical potentials $\mu_{3,8,Q}$, translate into fermion densities in the $\phi$ theory, as well as $\phi$-meson interactions which take simple forms at leading order in the meson fields.

The color charge densities in the $\phi$ theory are

$$\begin{aligned} n_{3,8} &= q^\dagger_{Lai}\lambda^{ab}_{3,8}q_{Lib}+(L\leftrightarrow R)=X^\dagger_{Laj}\psi^\dagger_{Lji}\lambda^{ab}_{3,8}\psi_{Lik}X_{Lkb}+(L\leftrightarrow R)\\ &= \mathrm{Tr}\psi^\dagger_L\psi_L X_L\lambda_{3,8}X^\dagger_L+(L\leftrightarrow R)\\ &= \mathrm{Tr}\phi^\dagger_L\phi_L\xi^\dagger X_L\lambda_{3,8}X^\dagger_L\xi+\mathrm{Tr}\phi^\dagger_R\phi_R\xi X_R\lambda_{3,8}X^\dagger_R\xi^\dagger. \end{aligned} \tag{4.77}$$

In the gauge-invariant description, we replace $X_L, X_R$ with $\tilde{\xi},\tilde{\xi}^\dagger$, and $\lambda_{3,8}$ becomes essentially a flavor Gell-Mann matrix. At zeroth order in the meson fields $\Phi$ and $\tilde{\Phi}$, $n_{3,8}$ are simply specific $\phi$ baryon densities:

$$\begin{aligned} \mathrm{Tr}\phi^\dagger\phi\lambda_3 &= \Xi^{-\dagger}\Xi^--\Xi^{0\dagger}\Xi^0+\Sigma^{-\dagger}\Sigma^--\Sigma^{+\dagger}\Sigma^++\frac{1}{\sqrt{3}}\left(\Lambda^\dagger\Sigma^0+\Sigma^{0\dagger}\Lambda\right)\\ &\quad+\sqrt{\frac{2}{3}}\left(\Lambda'^\dagger\Sigma^0+\Sigma^{0\dagger}\Lambda'\right),\\ \mathrm{Tr}\phi^\dagger\phi\lambda_8 &= \frac{2}{\sqrt{3}}\Big(-n^\dagger n-p^\dagger p-\Lambda^\dagger\Lambda+\Xi^{0\dagger}\Xi^0+\Xi^{-\dagger}\Xi^-\\ &\quad+\Sigma^{+\dagger}\Sigma^++\Sigma^{-\dagger}\Sigma^-+\Sigma^{0\dagger}\Sigma^0\Big)+\sqrt{\frac{2}{3}}\left(\Lambda^\dagger\Lambda'+\Lambda'^\dagger\Lambda\right). \end{aligned} \tag{4.78}$$

At linear order in meson fields, $n_{3,8}$ has a commutator contribution

$$\mathrm{Tr}\phi^\dagger i\gamma_5\phi\left[\frac{\Phi}{2f_\pi}-\frac{\tilde{\Phi}}{2f_{\tilde{\pi}}},\lambda_{3,8}\right]; \tag{4.79}$$

this is an interaction of the $\phi$ baryons with the massive pseudoscalar mesons. This commutator picks out only off-diagonal mesons; thus, $\mu_{3,8}$ will translate into effective chemical potentials for the massive modes if the pseudoscalar densities $\langle\phi^\dagger\gamma^5\phi\rangle$ are non-vanishing. Neglecting massive modes is equivalent to keeping the (4.78) term only. Similarly, the electric charge density is

$$\begin{aligned} n_Q &= q^\dagger_{Lai}\begin{pmatrix} 2/3 & & \\ & -1/3 & \\ & & -1/3 \end{pmatrix}_{ij} q_{Lja}+(L\to R) \\ &\equiv q^\dagger_{Lai}Q_{ij}q_{Lja}+(L\to R) \\ &= X^\dagger_{Lam}\psi^\dagger_{Lmi}Q_{ij}\psi_{Ljn}X_{Lna}+(L\to R) \\ &= \mathrm{Tr}\psi^\dagger_L Q\psi_L X_L X^\dagger_L+(L\to R)=\mathrm{Tr}\phi^\dagger_L\xi^\dagger Q\xi\phi_L\xi^\dagger X_L X^\dagger_L\xi+(L\to R) \\ &= \mathrm{Tr}\phi^\dagger_L\xi^\dagger Q\xi\phi_L+\mathrm{Tr}\phi^\dagger_R\xi Q\xi^\dagger\phi_R. \end{aligned} \tag{4.80}$$

At zeroth order in meson fields, it contributes again a $\phi$ baryon density term; however, it does not correspond to the generalized charge $\tilde{Q}$ densities. This result is not intuitive, since one might expect the electric charge neutrality should directly translate into generalized charge neutrality, as the fermions and mesons carry the same generalized charge $\tilde{Q}$ and electric charge $Q$. However, this reasoning is wrong: although each $\phi$ fermion carries the same $\tilde{Q}$ as the $Q$ of its partner hadronic baryon, $\phi$ themselves do not carry the same $Q$ number as their $\tilde{Q}$, thus the $Q$ density of the $\phi$ baryons is not the same as their $\tilde{Q}$ density.

## 4.6 Dressed gluons

In this section we show that the same dressing scheme applies to gluons as well, mapping gluons into vector mesons in baryon-meson theories. We start with the quark-gluon and gluon tensor terms in QCD

$$\mathcal{L}=\bar{q}i\gamma^\mu D_\mu q-\frac{1}{4}F_{\mu\nu}F^{\mu\nu} \tag{4.81}$$

where the covariant derivative is

$$D_\mu=\partial_\mu-\frac{i}{2}g_s A^\alpha_\mu\lambda_\alpha \tag{4.82}$$

and the gluon tensor

$$F^\alpha_{\mu\nu} \quad =\partial_\mu A^\alpha_\nu-\partial_\nu A^\alpha_\mu+g_s f_{\alpha\beta\gamma}A^\beta_\mu A^\gamma_\nu. \tag{4.83}$$

The quark-gluon coupling preserves chirality, i.e., left-handed quarks are coupled to left-handed quarks, and right-handed quarks are coupled to right-handed quarks only. For left-handed quarks, the quark-gluon coupling in terms of the $\psi$ field (after diquark dressing) is

$$\begin{aligned}\frac{1}{2}\bar{q}_{Lai}\gamma^\mu A^\alpha_\mu \lambda^{ab}_\alpha q_{Lib} &= \frac{1}{2}X^\dagger_{Laj}\bar{\psi}_{Lji}\gamma^\mu A^\alpha_\mu \lambda^{ab}_\alpha \psi_{Lik}X_{Lkb} \\ &= \mathrm{Tr}\bar{\psi}_L\gamma^\mu\psi_L\left(\frac{1}{2}X_L\lambda_\alpha A^\alpha_\mu X^\dagger_L\right) \equiv \mathrm{Tr}\bar{\psi}_L\gamma^\mu\psi_L V^L_\mu\end{aligned} \tag{4.84}$$

and similarly for right-handed quarks. The gluons, losing colors by dressing via the CFL phases $X_{L,R}$, gain flavor and chirality instead, a defining feature of color-flavor-locking. Introducing the vector and pseudovector fields

$$2V_\mu = V^L_\mu + V^R_\mu,\ 2P_\mu = -V^L_\mu + V^R_\mu, \tag{4.85}$$

the quark-gluon coupling becomes

$$\begin{aligned}\mathrm{Tr}\bar{\psi}_L\gamma^\mu\psi_L V^L_\mu + (L\to R) &= \mathrm{Tr}\bar{\psi}_L\gamma^\mu\psi_L(V_\mu - P_\mu) + \mathrm{Tr}\bar{\psi}_R\gamma^\mu\psi_R(V_\mu + P_\mu) \\ &= \mathrm{Tr}\bar{\psi}\gamma^\mu\psi V_\mu + \mathrm{Tr}\bar{\psi}\gamma^\mu\gamma^5\psi P_\mu.\end{aligned} \tag{4.86}$$

This corresponds to a typical baryon–vector-meson interaction with $g_D = -g_F = 1/2$ (cf. Eq. (4.45)).

The next step of dressing via the chiral phases $\xi$ is straightforward. Define the further dressed vector mesons

$$W^L_\mu = \xi^\dagger V^L_\mu \xi,\ W^R_\mu = \xi V^R_\mu \xi^\dagger, \tag{4.87}$$

and $2W^V_\mu = W^L_\mu + W^R_\mu$, $2W^P_\mu = -W^L_\mu + W^R_\mu$; the fermion–vector-meson coupling simply becomes

$$\mathrm{Tr}\bar{\psi}\gamma^\mu\psi V_\mu + \mathrm{Tr}\bar{\psi}\gamma^\mu\gamma^5\psi P_\mu = \mathrm{Tr}\bar{\phi}\gamma^\mu\phi W^V_\mu + \mathrm{Tr}\bar{\phi}\gamma^\mu\gamma^5\phi W^P_\mu. \tag{4.88}$$

The gluon tensor term becomes slightly more complicated under the two steps of dressing. In terms of the dressed chiral and diquark axial and vector currents $a_\mu, v_\mu$ and $\tilde{a}_\mu, \tilde{v}_/mu$ from Eqs. (4.33) and (4.34), after some algebra one can show that the spatial derivatives of the dressed vector meson field are

$$\begin{aligned}2\partial_\mu W^L_\nu &= [W^L_\nu, \tilde{v}_\mu + i\tilde{a}_\mu] + [W^L_\nu, v_\mu - ia_\mu] + \xi^\dagger X_L\lambda_\alpha\partial_\mu A^\alpha_\nu X^\dagger_L\xi, \\ 2\partial_\mu W^R_\nu &= [W^R_\nu, \tilde{v}_\mu - i\tilde{a}_\mu] + [W^R_\nu, v_\mu + ia_\mu] + \xi X_R\lambda_\alpha\partial_\mu A^\alpha_\nu X^\dagger_R\xi^\dagger.\end{aligned} \tag{4.89}$$

To write down the gluon tensor term in terms of $W$, it is for later use to define the chiral covariant derivative, which acts differently on left- and right-handed

fields, by

$$\begin{aligned}\mathcal{D}_\mu W^L_\nu &\equiv \partial_\mu W^L_\nu + \frac{1}{2}[v_\mu + \tilde{v}_\mu + i(\tilde{a}_\mu - a_\mu), W^L_\nu],\\ \mathcal{D}_\mu W^R_\nu &\equiv \partial_\mu W^R_\nu + \frac{1}{2}[v_\mu + \tilde{v}_\mu - i(\tilde{a}_\mu - a_\mu), W^R_\nu];\end{aligned} \tag{4.90}$$

in addition, one can work out the following relations

$$\begin{aligned}\mathcal{D}_\mu W^L_\nu + \mathcal{D}_\mu W^R_\nu &= \partial_\mu W^V_\nu + \frac{1}{2}[v_\mu + \tilde{v}_\mu, W^V_\nu] - \frac{1}{2}[i(\tilde{a}_\mu - a_\mu), W^P_\nu],\\ -\mathcal{D}_\mu W^L_\nu + \mathcal{D}_\mu W^R_\nu &= \partial_\mu W^P_\nu + \frac{1}{2}[v_\mu + \tilde{v}_\mu, W^P_\nu] - \frac{1}{2}[i(\tilde{a}_\mu - a_\mu), W^V_\nu],\\ [W^L_\mu, W^L_\nu] + [W^R_\mu, W^R_\nu] &= \frac{1}{2}[W^V_\mu, W^V_\nu] + \frac{1}{2}[W^P_\mu, W^P_\nu],\\ -[W^L_\mu, W^L_\nu] + [W^R_\mu, W^R_\nu] &= \frac{1}{2}[W^P_\mu, W^V_\nu] + \frac{1}{2}[W^V_\mu, W^P_\nu].\end{aligned} \tag{4.91}$$

Using these relations, the left-handed dressed field tensor of the vector field, is then given by

$$\begin{aligned}&\frac{1}{2}\xi^\dagger X_L F^\alpha_{\mu\nu}\lambda_\alpha X^\dagger_L \xi\\ &= \partial_\mu W^L_\nu - \partial_\nu W^L_\mu - \frac{1}{2}\left([W^L_\nu, \tilde{v}_\mu + i\tilde{a}_\mu] + [W^L_\nu, v_\mu - ia_\mu] - (\mu \leftrightarrow \nu)\right)\\ &+\frac{1}{4}g_s X_L[\lambda_\beta, \lambda_\gamma]X^\dagger_L A^\beta_\mu A^\gamma_\nu\\ &= \partial_\mu W^L_\nu - \partial_\nu W^L_\mu - \frac{1}{2}\left([W^L_\nu, \tilde{v}_\mu + i\tilde{a}_\mu] + [W^L_\nu, v_\mu - ia_\mu] - (\mu \leftrightarrow \nu)\right)\\ &+g_s[W^L_\mu, W^L_\nu]\\ &\equiv \mathcal{D}_\mu W^L_\nu - \mathcal{D}_\nu W^L_\mu + g_s[W^L_\mu, W^L_\nu],\\ &\equiv W^L_{\mu\nu},\end{aligned} \tag{4.92}$$

and the right-handed $W^R_{\mu\nu}$ is defined similarly. The vector and pseudovector field tensors are defined by

$$\begin{aligned}W^V_{\mu\nu} &= W^L_{\mu\nu} + W^R_{\mu\nu}\\ &= \partial_\mu W^V_\nu + \frac{1}{2}[v_\mu + \tilde{v}_\mu, W^V_\nu] - \frac{i}{2}[\tilde{a}_\mu - a_\mu, W^P_\nu] - (\mu \leftrightarrow \nu)\\ &\quad +g_s\frac{[W^V_\mu, W^V_\nu] + [W^P_\mu, W^P_\nu]}{2},\\ W^P_{\mu\nu} &= -W^L_{\mu\nu} + W^R_{\mu\nu}\\ &= \partial_\mu W^P_\nu + \frac{1}{2}[v_\mu + \tilde{v}_\mu, W^P_\nu] - \frac{i}{2}[\tilde{a}_\mu - a_\mu, W^V_\nu] - (\mu \leftrightarrow \nu)\\ &\quad +g_s\frac{[W^P_\mu, W^V_\nu] + [W^V_\mu, W^P_\nu]}{2}.\end{aligned} \tag{4.93}$$

As a result, the original gluon tensor term becomes

$$\frac{1}{2}F_{\mu\nu}F^{\mu\nu} = 2\mathrm{Tr}W^L_{\mu\nu}W^{L\mu\nu} = 2\mathrm{Tr}W^R_{\mu\nu}W^{R\mu\nu}; \tag{4.94}$$

symmetrizing the left and right hand fields, we can write

$$\begin{aligned}\frac{1}{2}F_{\mu\nu}F^{\mu\nu} &= \frac{1}{4}\mathrm{Tr}(W^V - W^P)_{\mu\nu}(W^V - W^P)^{\mu\nu} \\ &\quad + \frac{1}{4}\mathrm{Tr}(W^V + W^P)_{\mu\nu}(W^V + W^P)^{\mu\nu} \\ &= \frac{1}{2}\mathrm{Tr}W^V_{\mu\nu}W^{V\mu\nu} + \frac{1}{2}\mathrm{Tr}W^P_{\mu\nu}W^{P\mu\nu}. \end{aligned} \tag{4.95}$$

*Combining (4.88) and (4.95), the quark-gluon Lagrangian (4.81) becomes completely transformed into a gauge-invariant interacting Lagrangian between $\phi$ baryons and a degenerate set of vector and pseudovector mesons $W^V_\mu$ and $W^P_\mu$.*

If a massive deformation term $m_g^2 A^\alpha_\mu A^\mu_\alpha$ is included in the quark-gluon Lagrangian (4.81), as in certain studies of infrared gluon dynamics [97, 98], it becomes a mass term for the dressed vector and pseudovector mesons. One can show that

$$\begin{aligned} m_g^2 A^\alpha_\mu A^\mu_\alpha &= m_g^2\left(\mathrm{Tr}W^L_\mu W^{L\mu} + \mathrm{Tr}W^R_\mu W^{\mu R}\right) \\ &= 2m_g^2\left(\mathrm{Tr}W^V_\mu W^{V\mu} + \mathrm{Tr}W^P_\mu W^{P\mu}\right). \end{aligned} \tag{4.96}$$

It is curious that the original eight gluons, after dressing in chiral and diquark condensates, become eight vector and eight pseudovector mesons; the doubling the degrees of freedom comes from the fact that both left and right hand condensates can dress the gluons on an equal footing. At this level, there is no mass splitting mechanism between the vector and pseudovector mesons.[1]

In the hadronic matter, vector mesons play an important role of mediating short range interactions between baryons. The physically observed vector mesons, $\rho^0, \rho^\pm(770)$, $\omega(782)$, $\phi(1020)$, $K^{*\pm}(891)$, and $K^{*0}(895)$, turn out to have masses of the same magnitude to that of infrared gluons $0.5 \pm 0.2$ GeV. However, the actual relation between the physical, long-lived vector mesons, the dressed gluon fields in our model, and the phenomenological vector fields in chiral baryon or quark Lagrangians is yet unclear. At the very least, these vector fields describe strong physics at a common energy scale $\lesssim 1$ GeV.

[1] The doubling of spin-1 bosons via the dressing of the gluons may seem to have troubling implications for the thermodynamics of the system from the perspective of hadrons transitioning into quarks and gluons: the specific heat would change significantly with the emergence of additional degrees of freedom, disfavoring a direct continuity between hadronic matter and quark matter. However, as we observe from the dressing schemes (4.84) and (4.87), the gluons are dressed by the massive modes in the gauge-invariant description. This immersion of the gluons in a cloud of the massive fluctuations should contribute to a gluon effective mass, in addition to gluon self-interactions. The resulting vector bosons should acquire significant masses. Since additional heavy particles do not notably alter the specific heat at low temperature, the mapping of eight gluons into sixteen vector bosons does not cause thermodynamic issues for quark-hadron continuity. We leave detailed discussion of this topic to future research.

## 4.7 $\phi$-baryon pairing, $\phi$-meson interaction and explicit chiral symmetry breaking

Having obtained an effective theory of the $\phi$-mesons from the gluons, we next discuss the pairing and $\phi$-meson coupling structures of the chiral Lagrangian (4.45). In flavor space, the pairing between $\phi$-baryons, corresponding to the original CFL pairing, is

$$\begin{aligned}\mathrm{Tr}\phi\phi - \mathrm{Tr}\phi\mathrm{Tr}\phi &= \left(p^+\Xi^- + \Xi^- p^+\right) + \left(n\Xi^0 + \Xi^0 n\right) + \left(\Sigma^+\Sigma^- + \Sigma^-\Sigma^+\right) \\ &\quad + \Lambda\Lambda + \Sigma^0\Sigma^0 - 2\Lambda'\Lambda' \\ &= [N\Xi]_{\mathrm{sym}} + [\Sigma\Sigma]_{\mathrm{sym}} + [\Lambda\Lambda]_{\mathrm{sym}} - 2[\Lambda'\Lambda']_{\mathrm{sym}}. \end{aligned} \tag{4.97}$$

The $\pm, 0$ charges here refer to the generalized charge, not the electric charge. The factor 2 in front of the singlet baryon $\Lambda'$ implies a single larger gap among the total nine gapped quasi-fermions in CFL pairing. In the $\phi$-baryon picture, all fermions pair with themselves, and thus form a much more convenient basis for computation.

This pairing pattern (excluding the largely gapped singlet) is structurally similar to that of the hadronic baryon-baryon pairing in $SU(3)$ flavor-symmetric matter. The pairing is most attractive in the flavor singlet channel for $N_f = 3$ [95]:

$$\sqrt{\frac{4}{8}}[N\Xi]_{\mathrm{sym}} + \sqrt{\frac{3}{8}}[\Sigma\Sigma]_{\mathrm{sym}} - \sqrt{\frac{1}{8}}[\Lambda\Lambda]_{\mathrm{sym}}; \tag{4.98}$$

nevertheless, the coefficients differ from Eq. (4.97), and neither pairing patterns are reflected in dense nuclear matter at $\sim 2n_0$, where only neutrons and protons are present. (It is unknown how the actual pairing pattern of nuclear matter will evolve at higher baryon density, with the possible generation of strangeness; this is again an intriguing future topic.)

The $\phi$-meson coupling, to leading order in $\Phi$ (the NG modes) with $g_F = g_D = 1/2$ is

$$\frac{1}{2f_G}\mathrm{Tr}\bar{\phi}\gamma^\mu\gamma^5[\partial_\mu\Phi,\phi] + \frac{1}{2f_G}\mathrm{Tr}\bar{\phi}\gamma^\mu\gamma^5\{\partial_\mu\Phi,\phi\} = \frac{1}{2f_G}\mathrm{Tr}\bar{\phi}\gamma^\mu\gamma^5(\partial_\mu\Phi)\phi. \tag{4.99}$$

Table 4.7 lists the detailed coupling of the mesons with the $\phi$ baryons, into both octet-only baryons and also the singlet baryon $\Lambda'$; this table is useful to compute meson-baryon scattering and meson self-energies, while making connections with the hadronic mesons in nuclear matter.

Finally let us consider the form of explicit chiral symmetry breaking terms in the $\phi$-baryon theory. The simplest explicit chiral symmetry breaking term

| | octet only contribution | singlet-involved |
|---|---|---|
| $\pi^+$ | $\bar{\Sigma}^-\Sigma^0 - \bar{\Sigma}^0\Sigma^+ + \sqrt{2}\bar{n}p + \frac{1}{\sqrt{3}}\left(\bar{\Sigma}^-\Lambda + \bar{\Lambda}\Sigma^+\right)$ | $\sqrt{\frac{2}{3}}\left(\bar{\Lambda}'\Sigma^+ + \bar{\Sigma}^+\Lambda'\right)$ |
| $\pi^-$ | $\bar{\Sigma}^0\Sigma^- - \bar{\Sigma}^+\Sigma^0 + \sqrt{2}\bar{p}n + \frac{1}{\sqrt{3}}\left(\bar{\Sigma}^+\Lambda + \bar{\Lambda}\Sigma^-\right)$ | $\sqrt{\frac{2}{3}}\left(\bar{\Lambda}'\Sigma^- + \bar{\Sigma}^-\Lambda'\right)$ |
| $\pi^0$ | $\bar{p}p - \bar{n}n + \bar{\Sigma}^-\Sigma^- + \bar{\Sigma}^+\Sigma^+ + \frac{1}{\sqrt{3}}\left(\bar{\Lambda}\Sigma^0 + \bar{\Sigma}^0\Lambda\right)$ | $\sqrt{\frac{2}{3}}\left(\bar{\Lambda}'\Sigma^0 + \bar{\Sigma}^0\Lambda'\right)$ |
| $K^+$ | $\bar{\Xi}^-\Sigma^0 + \sqrt{2}\bar{\Xi}^0\Sigma^+ + \frac{1}{\sqrt{3}}\left(\bar{\Xi}^-\Lambda - 2\bar{\Lambda}p\right)$ | $\sqrt{\frac{2}{3}}\left(\bar{\Xi}^-\Lambda' + \bar{\Lambda}'p\right)$ |
| $K^-$ | $\bar{\Sigma}^0\Xi^- + \sqrt{2}\bar{\Sigma}^+\Xi^0 + \frac{1}{\sqrt{3}}\left(\bar{\Lambda}\Xi^- - 2\bar{p}\Lambda\right)$ | $\sqrt{\frac{2}{3}}\left(\bar{\Lambda}'\Xi^- + \bar{p}\Lambda'\right)$ |
| $K^0$ | $-\bar{\Sigma}^0\Xi^0 + \sqrt{2}\bar{\Sigma}^-\Xi^- + \frac{1}{\sqrt{3}}\left(\bar{\Lambda}\Xi^0 - 2\bar{n}\Lambda\right)$ | $\sqrt{\frac{2}{3}}\left(\bar{\Lambda}'\Xi^0 + \bar{n}\Lambda'\right)$ |
| $\bar{K}^0$ | $-\bar{\Xi}^0\Sigma^0 + \sqrt{2}\bar{\Xi}^-\Sigma^- + \frac{1}{\sqrt{3}}\left(\bar{\Xi}^0\Lambda - 2\bar{\Lambda}n\right)$ | $\sqrt{\frac{2}{3}}\left(\bar{\Xi}^0\Lambda' + \bar{\Lambda}'n\right)$ |
| $\eta$ | $\frac{1}{\sqrt{3}}\left(\bar{n}n + \bar{p}p + \bar{\Lambda}\Lambda + \bar{\Sigma}^-\Sigma^- + \bar{\Sigma}^+\Sigma^+ + \bar{\Sigma}^0\Sigma^0 - 2\bar{\Xi}^0\Xi^0 - 2\bar{\Xi}^-\Xi^-\right)$ . | $\sqrt{\frac{2}{3}}\left(\bar{\Lambda}\Lambda' + \bar{\Lambda}'\Lambda\right)$ |

Table 4.4: Couplings between $\phi$-baryons and the pseudoscalar mesons from Eq. (4.99).

using the bare quark mass matrix is

$$\bar{q}_L \hat{m} q_R + h.c. = \bar{q}_{ai} \begin{pmatrix} m_u & & \\ & m_d & \\ & & m_s \end{pmatrix}_{ij} q_{ja} + h.c.; \tag{4.100}$$

after dressing, this mass term becomes

$$\begin{aligned} &\mathrm{Tr}\xi\bar{\phi}_L\xi^\dagger\hat{m}\xi^\dagger\phi_R\xi\tilde{Y}^\dagger + h.c. \\ &\quad\approx \mathrm{Tr}\bar{\phi}_L\hat{m}\phi_R - \frac{1}{4f_\pi^2}\mathrm{Tr}\bar{\phi}_L(\Phi^2\hat{m} + \Phi\hat{m}\Phi)\phi_R + h.c. \ldots \\ &\quad= \mathrm{Tr}\bar{\phi}_L\hat{m}\phi_R - \frac{1}{4f_G^2}\mathrm{Tr}\bar{\phi}_L(\Phi_G^2\hat{m} + \Phi_G\hat{m}\Phi_G)\phi_R + h.c. + \ldots \end{aligned} \tag{4.101}$$

where we again neglect the massive modes. Thus, in this non-linear realization, a bare quark mass matrix $\hat{m}$ not only induces a mass term for $\phi$-baryons, but also introduces corrections to the $\phi$-meson couplings. Most importantly, it produces a non-derivative coupling between the NG modes and the baryons. At quadratic order in meson fields, this coupling contributes a formal mass term $\sim \langle\bar{\phi}_L\phi_R\rangle\hat{m}^2/f_G^2$, which corresponds to the GMOR relation at linear order.

It should be noted that when the chiral condensate vanishes and the system is in purely diquark pairing phase, then we must apply the diquark-diquark dressing. In this case we still arrive at Eq. (4.101), but with $\Phi_G$ replaced by diquark meson matrix $\tilde{\Phi}$. At linear order in $\hat{m}$ this term no longer contributes to the meson self-energy because $\langle\bar{\phi}_L\phi_R\rangle = 0$; one must move to the next order, where the contribution will come from the bubble of the form $\sim \langle\phi_L\phi_L\rangle\langle\bar{\phi}_R\bar{\phi}_R\rangle \sim |\Delta|^2$; this corresponds to the GMOR relation at quadratic order in $\hat{m}$, agreeing with our demonstration in Chapter 3.

At linear order in $\hat{m}$ and mean field, assuming $m_u = m_d \ll m_s$ and $\langle\bar{\phi}_L\phi_R\rangle = \sigma 1/3$, the meson masses obtained from (4.101) are

$$m^2_{\pi^\pm,\pi_0} = \frac{(m_u+m_d)\sigma}{f_G^2},\ m^2_{K^\pm} = \frac{(m_u+m_s)\sigma}{f_G^2},\ m^2_{K^0,\bar{K}^0} = \frac{(m_d+m_s)\sigma}{f_G^2}; \tag{4.102}$$

the $\pi_8$ field, corresponding to the $\eta$ meson, will in general mix with flavor singlet $\eta'$ which corresponds to breaking of the $U(1)_A$; we leave their discussion to future studies as our $\phi$ theory has not included any prescription for the axial anomaly so far.

One can proceed to study higher order interaction terms in $\hat{m}$ generated by the (4.101) term; we leave it to a future project. In general, due to symmetry constraints, only the following combinations (at quadratic order in meson fields)

are allowed:

$$A\mathrm{Tr}\Phi\Phi\hat{m}\hat{m} + B\mathrm{Tr}\Phi\hat{m}\Phi\hat{m} + C\left(\mathrm{Tr}\Phi\hat{m}\right)^2, \tag{4.103}$$

where $A, B, C$ are constants proportional to $\sigma/f_G^2$. It is interesting that the term (4.101) can only produce a manifest chiral condensate contribution to the meson masses, while the diquark condensate contribution only comes from bubble diagrams (at one fermion-loop) containing anomalous Green's functions.

## 4.8 Alternative dressing scheme and coexistence of baryons formed by different diquark dressing

The dressed $\phi$ baryons constructed from past sections, despite having intuitive mapping to the hadronic baryons, actually have the wrong parity. This is because under parity transformation, $d_L \leftrightarrow -d_R$; as a result,

$$\phi_L \leftrightarrow -\phi_R. \tag{4.104}$$

In this section we show how this dilemma can be lifted by inclusion of an alternative dressing scheme, leading to an additional nonet of baryons. The coupling between the former and the new nonets via an explicit axial $U(1)$ symmetry breaking term as well as a direct mixing term can lift the degeneracy, retaining only positive parity baryons in the low energy spectrum. We dress the left(right) handed quark by a right(left) handed diquark instead:

$$\psi'_L = q_L X_R^\dagger,\ \psi'_R = q_R X_L^\dagger; \tag{4.105}$$

the resulting color-singlet fields transform as (compare with (4.17))

$$\psi'_L \to U_L \psi_L U_R^\dagger,\ \psi'_R \to U_R \psi_R^\dagger U_L^\dagger. \tag{4.106}$$

Similar to gluon dressing, as left and right handed diquarks are independent degrees of freedom, it is reasonable for the fermion sector to receive additional composite degrees of freedom under a different dressing scheme. The interaction term with chiral condensate and diquark pairing becomes

$$\mathrm{Tr}\bar{q}_L Y q_R = \mathrm{Tr}X_R^\dagger \bar{\psi}'_L Y \psi'_R X_L = \mathrm{Tr}\bar{\psi}'_L Y \psi'_R \tilde{Y}, \tag{4.107}$$

and

$$\begin{aligned} & \mathrm{Tr}X_L^\dagger q_L C X_L^\dagger q_L - \left(\mathrm{Tr}X_L^\dagger q_L\right) C \left(\mathrm{Tr}X_L^\dagger q_L\right) - (L \leftrightarrow R) \\ = \; & \mathrm{Tr}X_L^\dagger \psi'_L X_R C X_L^\dagger \psi'_L X_R - \left(\mathrm{Tr}X_L^\dagger \psi'_L X_R\right) C \left(\mathrm{Tr}X_L^\dagger \psi'_L X_R\right) - (L \leftrightarrow R) \\ = \; & \mathrm{Tr}\psi'_L C \tilde{Y}^\dagger \psi'_L \tilde{Y}^\dagger - \left(\mathrm{Tr}\psi'_L \tilde{Y}^\dagger\right) C \left(\mathrm{Tr}\psi'_L \tilde{Y}^\dagger\right) - (L \leftrightarrow R). \end{aligned} \tag{4.108}$$

Unlike the former dressing scheme, the diquark phases remain in the pairing interaction term. To transform them away, one must use the diquark-diquark dressing; that is, the next step is to dress $\psi'$ using gauge-invariant diquark phases

$$\begin{aligned} \phi'_L \quad &= \tilde{\xi}^\dagger \psi'_L \tilde{\xi}^\dagger, \; \phi'_L \to K \phi'_L K^\dagger, \\ \phi'_R \quad &= \tilde{\xi} \psi'_R \tilde{\xi}, \; \phi'_R \to K \phi'_R K^\dagger; \end{aligned} \tag{4.109}$$

they now transform identically as $\phi_{L,R}$, and the two interaction terms reduce to

$$\mathrm{Tr}\bar{\psi}'_L Y \psi'_R \tilde{Y} = \mathrm{Tr}\bar{\phi}'_L \tilde{\xi}^\dagger Y \tilde{\xi}^\dagger \phi'_R \equiv \mathrm{Tr}\bar{\phi}'_L Y'_M \phi'_R, \tag{4.110}$$

and

$$\mathrm{Tr}\psi'_L C \tilde{Y}^\dagger \psi'_L \tilde{Y}^\dagger - \left(\mathrm{Tr}\psi'_L \tilde{Y}^\dagger\right) C \left(\mathrm{Tr}\psi'_L \tilde{Y}^\dagger\right) - (L \leftrightarrow R) \tag{4.111}$$

$$= \; \mathrm{Tr}\phi'_L C \phi_L - \left(\mathrm{Tr}\phi'_L\right) C \left(\mathrm{Tr}\phi'_L\right) - (L \leftrightarrow R). \tag{4.112}$$

The meson field $Y'_M \equiv \tilde{\xi}^\dagger Y \tilde{\xi}^\dagger$ bears a similar structure to the original massive field $Y_M \equiv \xi^\dagger \tilde{Y} \xi^\dagger$; they coincide at leading order in $\Phi, \tilde{\Phi}$, but they do not commute at higher order due to the $SU(3)$ algebra. This feature is closely related to the fact that the NG modes are always the same, as they are directly given by the symmetry breaking pattern of the system. Under a chiral symmetry transformation, the phases rotate identically $\tilde{\xi} = \xi$, and one sees immediately that $Y_M = Y'_M = 0$. However, since all the condensates can rotate individually, the number of independent massive modes will be[2] $8 \times 8 \times 2 - 8 = 120$. Only when $N_f = N_c = 1$, are there just one massive mode and NG mode.

The huge amount of massive modes seem to contradict the fact that $Y_M$ and $Y'_M$ are only two $SU(3)$ matrices and cannot represent that many independent modes. One needs to realize that the mapping from $\xi, \tilde{\xi}$ to $Y_M$ and $Y'_M$ is surjective; any particular meson represented by the phases $Y_M$ and $Y'_M$ will correspond to a number of independent massive modes that are totally degenerate. In particular, there are at most 8 different masses for the massive modes,

[2]There are eight independent ways to rotate the chiral condensates and eight independent ways to rotate the diquark condensates; each pair of a chiral condensate rotation and a diquark condensate rotation has two linearly independent combinations. The total number of linearly independent fluctuations is thus $8 \times 8 \times 2 = 128$. Subtracting the eight massless NG modes, we end up with 120 massive modes.

as long as the chiral and diquark interactions we have been using are the only interaction terms in the theory. Since these massive modes are always unstable and will decay into the NG modes immediately, we do not pursue further details on their dynamics.

In order to construct effective baryons with positive parity, we return to the linear sigma model for the moment and start from the $\psi$ and $\psi'$ baryons. One can easily check that $\psi'$, thus the $\phi'$ baryons, also have negative parity. However, if we define linear combinations[3]

$$\begin{cases} \sqrt{2}\psi'_L = B'_L + B_L, & \psi'_L \to e^{-i\theta_B} e^{-i\theta_A} U_L \psi_L U_R^\dagger; \\ \sqrt{2}\psi'_R = B'_R - B_R, & \psi'_R \to e^{-i\theta_B} e^{i\theta_A} U_R \psi_R U_L^\dagger; \\ \sqrt{2}\psi_L = B'_L - B_L, & \psi_L \to e^{-i\theta_B} e^{3i\theta_A} U_L \phi_L U_L^\dagger; \\ \sqrt{2}\psi_R = B'_R + B_R, & \psi_R \to e^{-i\theta_B} e^{-3i\theta_A} U_R \phi_R U_R^\dagger; \end{cases} \tag{4.113}$$

with the transformation rules under $SU(3)_{L,R}$ and $U(1)_{B,A}$, then the $B, B'$ baryons transform under parity as

$$B \to B, \ B' \to -B'. \tag{4.114}$$

The $B$ baryons have the desired parity, but their partners $B'$ will naturally coexist since they are just another combination of the $\psi$ and $\psi'$ fields. Next we show that, starting from a chiral Lagrangian of coexisting $\psi$ and $\psi'$ (thus $B$ and $B'$) fields, we can eventually split the masses of $B$ and $B'$ baryons with the help of the axial anomaly and $\psi$-$\psi'$ mixing, resulting in heavier $B'$ baryons; they decay into the lighter $B$ baryons via emission of pseudoscalar mesons, and thus disappear in the low energy effective theory. The resulting effective Lagrangian contains only positive parity $B$ baryons, which neatly map to hadronic baryons.

We first construct the chiral Lagrangian in the presence of both $\psi$ and $\psi'$. With a chiral condensate $M = |M|Y$, the chiral interaction term (4.19), aside from admitting masses and meson-baryon couplings between $\psi$ and $\psi'$ baryons themselves, can also yield a direct mixing term between $\psi$ and $\psi'$ with diquark phases canceled out, via dressing one quark into $\psi$ but the other quark into $\psi'$:

$$\bar{q}_L M q_R = \mathrm{Tr}\bar{\psi}'_L M \psi_R. \tag{4.115}$$

We also consider the following interaction that explicitly violates axial $U(1)$, but still respecting chiral symmetry:

$$2g'\varepsilon_{ijk}\varepsilon_{lmn}\left[\bar{\psi}'_{Lil} M^\dagger_{jm} \psi'_{Rkn} + h.c.\right]; \tag{4.116}$$

Note that $M$ itself transforms as $M \to M \exp 2i\theta_A$ under axial $U(1)$. This interaction is only possible in terms of $\psi'$ fields; it forms a flavor singlet by totally

[3]The resulting $\psi$ and $\psi'$ fields are analogous to mirrored chiral assignment of baryon multiplets in construction of baryon chiral Lagrangians [99].

anti-symmetrizing left and right handed flavor indices. We will see shortly it plays an important role in splitting the masses of $B$ and $B'$ baryons.

For simplicity we ignore all meson field fluctuations at the moment and work on the baryon sector alone. Using

$$\varepsilon_{ijk}\varepsilon_{lmn} = \det \begin{pmatrix} \delta_{il} & \delta_{im} & \delta_{in} \\ \delta_{jl} & \delta_{jm} & \delta_{jn} \\ \delta_{kl} & \delta_{km} & \delta_{kn} \end{pmatrix}, \tag{4.117}$$

one can show that (4.116) can be written as

$$\begin{aligned} \varepsilon_{ijk}\varepsilon_{lmn}\bar{\psi}'_{Lil}M^\dagger_{jm}\psi'_{Rkn} &= \left(\mathrm{Tr}M^\dagger\,\mathrm{Tr}\psi'_R - \mathrm{Tr}M^\dagger\psi'_R\right)\mathrm{Tr}\bar{\psi}'_L - \mathrm{Tr}\bar{\psi}'_L M^\dagger\,\mathrm{Tr}\psi'_R \\ &\quad + \mathrm{Tr}\bar{\psi}_L\{M^\dagger,\psi'_R\} - \mathrm{Tr}M^\dagger\,\mathrm{Tr}\bar{\psi}'_L\psi'_R \\ &= \mathrm{Tr}\bar{\psi}'_L\{M^\dagger,\psi'_R\} - \mathrm{Tr}M^\dagger\,\mathrm{Tr}\bar{\psi}'_L\psi'_R + h.c. + \text{singlet}. \end{aligned} \tag{4.118}$$

In this study, we ignore the baryon singlet $\mathrm{Tr}\psi'$ (as it has a large gap). The total Lagrangian, without diquark pairing and meson currents for the moment, allowing possible different coupling strength with different dressed baryons, is

$$\begin{aligned} \mathcal{L} &= \mathrm{Tr}\bar{B}(i\partial\!\!\!/ - gM)B + \mathrm{Tr}\bar{B}'(i\partial\!\!\!/ + gM)B' && (4.119) \\ &\quad + g_{\mathrm{mix}}\left[\mathrm{Tr}(\bar{\psi}'_L M\psi_R) + \mathrm{Tr}(\bar{\psi}'_R M^\dagger\psi_L) + h.c.\right] && (4.120) \\ &\quad + 2g'\left[\mathrm{Tr}\bar{\psi}'_L\{M^\dagger,\psi'_R\} - \mathrm{Tr}M^\dagger\,\mathrm{Tr}\bar{\psi}'_L\psi'_R + h.c.\right], && (4.121) \end{aligned}$$

where we have already written the kinetic energy and the chiral interaction term (4.19) $\propto g$ in terms of the $B$ and $B'$ baryons. Note the different sign in the $g$ term for $B$ and $B'$. It is also convenient to break down $M$ in its hermitian (positive parity) and anti-hermitian (negative parity) parts

$$M = \Sigma + i\Pi; \tag{4.122}$$

in the following we also ignore the singlet $\mathrm{Tr}\Pi$. Further utilizing the relationships between $\phi, \phi'$ and $B, B'$, we have

$$\mathrm{Tr}(\bar{\psi}'_L M\psi_R) + \mathrm{Tr}(\bar{\psi}'_R M^\dagger\psi_L) + h.c. = \mathrm{Tr}\bar{B}(\Sigma + i\Pi\gamma_5)B + (B \leftrightarrow B'), \tag{4.123}$$

and

$$\begin{aligned} & 2\left(\mathrm{Tr}\bar{\psi}'_L\{M^\dagger,\psi'_R\} - \mathrm{Tr}M^\dagger\,\mathrm{Tr}\bar{\psi}'_L\psi'_R + h.c.\right) \\ = \;& \mathrm{Tr}\Sigma\,\mathrm{Tr}\bar{B}B - \mathrm{Tr}\bar{B}\{\Sigma,B\} + \mathrm{Tr}\bar{B}i\gamma_5\{\Pi,B\} - \mathrm{Tr}\bar{B}'\gamma_5\{\Sigma,B\} + \mathrm{Tr}\bar{B}'i\{\Pi,B\} \\ & -(B \leftrightarrow B'). \end{aligned} \tag{4.124}$$

At mean field, assuming $\langle\Sigma\rangle = \sigma\mathbf{1}$ and $\langle\Pi\rangle = 0$, the Lagrangian becomes

$$\mathcal{L}_{MF} = (\bar{B}, \bar{B}') \begin{pmatrix} \not{p} + (g_{\rm mix} - g)\sigma + g'\sigma & -g'\sigma\gamma_5 \\ g'\sigma\gamma_5 & \not{p} + (g_{\rm mix} + g)\sigma - g'\sigma \end{pmatrix} \begin{pmatrix} B \\ B' \end{pmatrix}. \tag{4.125}$$

This Lagrangian can be diagonalized by the transformation

$$\begin{pmatrix} B \\ B' \end{pmatrix} = \begin{pmatrix} \cos\theta & \gamma_5 \sin\theta \\ -\gamma_5 \sin\theta & \cos\theta \end{pmatrix} \begin{pmatrix} \beta \\ \beta' \end{pmatrix}, \tag{4.126}$$

where

$$\sin 2\theta = \frac{g'}{\sqrt{g_{\rm mix}^2 + g'^2}}, \ \cos 2\theta = \frac{g_{\rm mix}}{\sqrt{g_{\rm mix}^2 + g'^2}}. \tag{4.127}$$

The resulting two diagonal baryons, $\beta$ and $\beta'$, have masses

$$\begin{aligned} m &= -\sigma(\sqrt{g_{\rm mix}^2 + g'^2} - g + g'), \\ m' &= -\sigma(\sqrt{g_{\rm mix}^2 + g'^2} + g - g'). \end{aligned} \tag{4.128}$$

The chiral condensate $\sigma$ is negative. As $g_{\rm mix}$ and $g$ originate from the same chiral interaction (4.19), one can assume $g_{\rm mix} \sim g$ as a starting consideration. In this case, $0 < m < m'$ as long as $g > g'$; the $\beta$ baryons, carrying positive parity, will have lower masses. The $\beta'$ baryons become unstable and can decay into $\beta$ baryons by emission of a pseudoscalar meson, parametrized as $\Pi$ in this linear model.

In dense quark matter where the axial anomaly is suppressed by high baryon chemical potential, it is reasonable that $g_{\rm max} \sim g$ and $g > g'$. An interesting situation arises if $g' = 0$ and $g_{\rm max} = g$; then, the $\beta$ baryons are massless despite spontaneous chiral symmetry breaking, while $\beta'$ remain massive. However, one cannot simply conclude that the lowest lying baryons thus must be massless; there can be higher order terms in $M$ that contribute to the baryon masses as well.

We next study the interaction between $\beta$ baryons and pseudoscalar mesons in this linear realization. For simplicity we focus on the $g_{\rm mix}$ and $g'$ terms, which are new to the baryon-meson coupling we have considered so far:

$$\begin{aligned} \mathcal{L}_{\beta\Pi} &= g_{\rm mix}\left[{\rm Tr}\bar{B}i\gamma_5\Pi B + (B \leftrightarrow B')\right] \\ &\quad + g'\left[{\rm Tr}\bar{B}i\gamma_5\{\Pi, B\} + {\rm Tr}\bar{B}'i\{\Pi, B\} - (B \leftrightarrow B')\right]. \end{aligned} \tag{4.129}$$

In terms of $\beta$ and $\beta'$ baryons, together with the mass diagonalization, the total

baryon-meson Lagrangian reads

$$\begin{aligned}\mathcal{L} &= \mathrm{Tr}(\bar{\beta},\bar{\beta}')\begin{pmatrix} \not{p}-m & 0 \\ 0 & \not{p}-m' \end{pmatrix}\begin{pmatrix} \beta \\ \beta' \end{pmatrix} \\ &\quad +g_{\mathrm{mix}}\cos 2\theta\left[\mathrm{Tr}\bar{\beta}i\gamma_5\Pi\beta+\mathrm{Tr}\bar{\beta}'i\gamma_5\Pi\beta'\right] \\ &\quad +g'\left[(1+\sin 2\theta)\mathrm{Tr}\bar{\beta}i\gamma_5\{\Pi,\beta\}-(1-\sin 2\theta)\mathrm{Tr}\bar{\beta}'i\gamma_5\{\Pi,\beta'\}\right] \\ &\quad +g_{\mathrm{mix}}\sin 2\theta\left[\mathrm{Tr}\bar{\beta}i\Pi\beta'-\mathrm{Tr}\bar{\beta}'i\Pi\beta\right]-g'\left[\cos 2\theta\mathrm{Tr}\bar{\beta}i\{\Pi,\beta'\}-\mathrm{Tr}\bar{\beta}'i\{\Pi,\beta\}\right] \\ &\equiv \mathcal{L}_{kin}+\mathcal{L}_{\bar{\beta}\beta\Pi}+\mathcal{L}_{\bar{\beta}'\beta'\Pi}+\mathcal{L}_{\bar{\beta}\beta'\Pi}, \end{aligned} \tag{4.130}$$

where $\mathcal{L}_{\bar{\beta}\beta'\Pi}$ is responsible for $\beta'$ decaying into $\beta$ plus a pseudoscalar meson. The part only involving $\beta$ is

$$\mathcal{L}_\beta = \mathrm{Tr}\bar{\beta}(\not{p}-m)\beta+g'_D\mathrm{Tr}\bar{\beta}i\gamma_5\{\Pi,\beta\}+g'_F\mathrm{Tr}\bar{\beta}i\gamma_5[\Pi,\beta], \tag{4.131}$$

where (the $g'_{D,F}$ defined in this linear realization is different from those in non-linear realization as in previous sections)

$$g'_D=\frac{1}{2}g_{\mathrm{mix}}\cos 2\theta,\ g'_F=\frac{1}{2}g_{\mathrm{mix}}\cos 2\theta+g'(1+\sin 2\theta); \tag{4.132}$$

due to the mixing angle $\theta$, we no longer have $g_D = g_F$ as in the models with only one type of baryon. This is because the $g'$ term introduces different $g_{D,F}$ values in the baryon-meson couplings. To compute the total axial coupling, one needs to add the contribution from the $g$ term, whose sign is reversed for $\beta$ baryons:

$$g_D=g_F=-\frac{g}{2}; \tag{4.133}$$

as a result,

$$\begin{aligned} g_A &\equiv g_D+g_F+g'_D+g'_F=\frac{g_{\mathrm{mix}}^2}{\sqrt{g_{\mathrm{mix}}^2+g'^2}}+g'\left(1+\frac{g'}{\sqrt{g_{\mathrm{mix}}^2+g'^2}}\right)-g \\ &= \sqrt{g_{\mathrm{mix}}^2+g'^2}-g+g'=\frac{m}{-\sigma}, \end{aligned} \tag{4.134}$$

as expected.

## 4.9 Outlook

In this Chapter we have constructed in detail a mapping from the quarks and gluons into a gauge-invariant effective theory, which takes the form of color-singlet baryons and pseudoscalar, vector and pseudovector mesons. The dressing of the quarks using the CFL condensate and chiral condensate is central to the mapping, which is only possible for an $N_f = N_c = 3$ color superfluid. We have computed the masses and gaps of the effective baryons, and their couplings to the mesons. Our mapping scheme directly establishes quark-hadron continuity

in the case of complete flavor-symmetry.

In reality, our picture still faces challenges from realistic quark masses that explicitly break chiral symmetry. As a result, CFL pairing will be stressed at lower density, and possible 2SC pairing and inhomogeneous phases may form; in these more complicated phases, the dressing scheme and the mapping cannot be directly applied. Even in the high density limit, the mapping between dressed-quark baryons and hadronic baryons may face complications. It is known that realistic baryons are not simple representations of flavor $SU(3)$ groups, but a superposition of multiple different representations due to the breaking of flavor symmetry; in nuclear matter, flavor symmetry is relatively severely broken, and the generation of strangeness as a function of density in hadronic regime is still an open question. Nevertheless, the study of a chiral baryon-meson theory as an effective description of CFL quark matter is still meaningful. Even without a complete mapping, this theory could still differ from realistic baryon theories only by limited modification (e.g., of coupling constants, mass matrices etc.). Given the likelihood of a relatively smooth crossover from hadrons to quarks, it is useful to push this theory of quark-hadron mapping, which helps to advance our understanding of both nuclear matter and quark matter.

# Chapter 5

# Understanding vector repulsion from gluon exchange

In Chapter 4 we have mapped quark-gluon matter in the color-flavor-locked (CFL) phase to hadronic matter with baryons and mesons. We have also considered the possible connection between effective quark models and hadronic matter in Chapter 2 in terms of chiral symmetry breaking, and the light collective modes (pseudoscalar mesons) in particular, in both the $G$ and $H$ sectors. In this Chapter, we turn to the vector repulsion sector, $g_V$, and try to understand it from the perspective of QCD; such vector repulsion is a requirement to support two-solar mass neutron stars suggested by the QHC19 studies.

We find that non-perturbative single gluon exchange can produce enough positive energy density in the vector channel to explain an effective vector repulsion coupling $g_V \sim G$ as in the Nambu–Jona-Lasinio (NJL) model, when provided with dynamic gluon mass $m_g$ in the range 200 - 600 MeV and the QCD strong coupling $\alpha_s = 2$ - 6 in the sub-GeV energy scale.

We also estimate the effects of quark masses and a CFL pairing gap on the quark propagators. As it turns out, $g_V$ can be well approximated by a flavor-symmetric, decreasing function of density, and the flavor dependence of $g_V$ from the Fermi surfaces are well-suppressed by a gluon mass. We briefly discuss similar matchings for the isovector repulsion and for the pairing attraction, and compare the isovector energies in dense hadronic matter.

This Chapter is mainly based on Ref. [9] submitted for publication at the time of writing this thesis.

## 5.1 Phenomenological $g_V$ in the NJL model

Recall that the NJL model with point interactions in the scalar, diquark, and vector-isoscalar channels is described by the interaction Lagrangian schematically of the form [23]

$$\mathcal{L}_{\rm int} = G(\bar{q}q)^2 + H(\bar{q}\bar{q})(qq) - g_V(\bar{q}\gamma^\mu q)^2, \tag{5.1}$$

where the vector repulsion in the isoscalar channel [100] is needed for quark matter to support heavy neutron stars. The resultant energy density from the vector repulsion is $g_V n_q^2$, where $n_q = 3n_B$ is the quark number density.

As we stated before the scalar coupling $G$ and the ultraviolet cutoff $\Lambda_{\rm NJL}$

of the NJL model can be directly related to physical observables such as the properties of pseudoscalar mesons. However, the vector repulsion at present is constrained only by comparing the equation of state of matter with observations of neutron stars. Nevertheless, the QHC19 study provides strict constrains on its value; to support neutron stars of masses above two solar masses (including the recently measured neutron star mass, $2.17 \pm 0.1 M_\odot$ in the pulsar PSR J0740+6620 [17]) requires that $g_V$ be well in the range 0.6-1.3 $G_0$, and $H$ in the range 1.35-1.65 $G_0$ [29], where $G_0 = 1.835\Lambda_{\rm NJL}^{-2}$ with $\Lambda_{\rm NJL} = 631.4$, is the scalar coupling in the vacuum obtained by a fitting of pion observables [23].

The NJL model four-quark interactions are inspired by color-current–color-current interaction, $\sim (\bar{q}\gamma_\mu \lambda^\alpha q)^2$. A Fierz transformation of this interaction into the chiral, diquark and vector-isoscalar channels leads to NJL couplings (5.1) with the ratios $g_{V0}/G_0 = 1/2$ and $H_0/G_0 = 3/4$ (see Appendix) [23] where the "0" continues to indicate vacuum values. But in the fully interacting system, these ratios need not hold; as in QHC18 and QHC19 we focus on more general in-medium values of $g_V$ and $H$, studying here the density dependence of $g_V$ in particular.

The density dependence (or independence) of $g_V$ can be understood from dimensional arguments. Since $g_V$ has dimensions of mass$^{-2}$, at asymptotically large densities, where the only energy scale is the quark Fermi momentum $p_F$, $g_V$ should behave as $\sim \alpha_s/p_F^2$, where $\alpha_s$ is the QCD running coupling constant. On the other hand, in the highly non-perturbative vacuum at zero baryon density, the relevant scale is $\Lambda_{\rm QCD}$, and we expect $g_V \sim \alpha_s/\Lambda_{\rm QCD}^2$. Thus, the matter density dependence of $g_V$ can be ignored only when $p_F \ll \Lambda_{\rm QCD}$, provided that $\alpha_s$ also freezes at low energy [11]. To smoothly connect $g_V$ at low density with that at high density, we adopt a model of massive gluons [97, 98] which includes non-perturbative generation of the gluon mass $m_g$ as well as the freezing of $\alpha_s$ in the Landau gauge at low energies.

As we estimate, a gluon mass $m_g \sim 0.4$ GeV, and a moderately strong quark-gluon coupling $\alpha_s \sim 3$ at $5n_0$ (or similar values, shown in Fig. 5.3 below, with $\alpha_s/m_g^2$ roughly constant) can produce a strong enough $g_V \sim G_0$ to allow quark matter to support two-solar mass neutron stars.

At high density, where the matter tends to have equal population of up-, down-, and strange-quarks, flavor-singlet channels are much more important than non-singlet flavor channels. This allows us to focus on the flavor-singlet scalar and vector couplings as well as CFL-type diquark pairing [101], favored for equal flavor population. Flavor non-singlet interactions are nonetheless important at low densities, as we shall discuss in Sec. 5.6.

## 5.2 Weak coupling limit results

Before considering the highly non-perturbative properties of the system at $\sim 5n_0$, let us first consider the extrapolated results from the weak coupling limit

which is only valid at ultra high density. The energy density shift due to the quark-gluon interaction to leading order in $\alpha_s$ is

$$E_{\rm QCD} = -\frac{i\pi\alpha_s}{2}\int d^4x\,\langle J^\alpha_\mu(x)A^\mu_\alpha(x)J^\beta_\nu(0)A^\nu_\beta(0)\rangle, \tag{5.2}$$

where the expectation value is in a Fermi gas, $x=(t,\boldsymbol{x})$, and $t$ is integrated from 0 to $-i/T$ (with $T$ the temperature). The currents are $J^\alpha_\mu(x)\equiv\bar q(x)\gamma_\mu\lambda^\alpha q(x)$, where the $\lambda_\alpha$ are the color $SU(3)$ Gell-Mann matrices normalized to ${\rm tr}\lambda_\alpha\lambda_\beta = 2\delta_{\alpha\beta}$.

Without diquark pairing, Eq. (5.2) simply becomes the Fock term in terms of the two-quark interaction

$$E_{\rm QCD} \approx \frac{\pi\alpha_s}{2}\int_{p,p'} {\rm Tr}\,[S(p)\lambda_\alpha\gamma^\mu S(p')\lambda_\beta\gamma^\nu]\,D^{\alpha\beta}_{\mu\nu}(p-p'); \tag{5.3}$$

here the trace Tr runs over flavor, color, and Dirac indices, and the integrations over frequencies $p_0$ and $p_0'$ are understood as the fermion Matsubara frequency summations, $\int dp_0 f(p_0)\to 2\pi iT\sum_n f(i\omega_n)$, where $\omega_n = 2\pi Tn$, with $n=\pm1/2,\pm3/2,\ldots$. The time-ordered quark Green's function is

$$S^{ab}_{ij}(x-y) = -i\langle\mathcal{T}q^a_i(x)\bar q^b_j(y)\rangle \tag{5.4}$$

and are denoted by $S(p)$ in momentum space; here $a,b$ are color indices and $i,j$ flavor indices. The gluon Green's function is

$$D^{\alpha\beta}_{\mu\nu}(x-y) = -i\langle\mathcal{T}A^\alpha_\mu(x)A^\beta_\nu(y)\rangle. \tag{5.5}$$

With no medium modification of the gluons, $D$ in the Landau gauge takes the form in the momentum space,

$$D^{\alpha\beta}_{\mu\nu}(q) = -\delta^{\alpha\beta}\left(g_{\mu\nu}-\frac{q_\mu q_\nu}{q^2}\right)D(q). \tag{5.6}$$

The full calculation of the energy leads to divergent Dirac sea contributions involving antiparticles. Only the $g_{\mu\nu}$ term in $D^{\alpha\beta}_{\mu\nu}(q)$ contributes to the particle-particle exchange (Fock) energy, and we keep only this term.

Similar to local four-quark interactions, the traces in Eqs. (5.3) can be reorganized, via a Fierz transformation (see Appendix), into traces over quark Green's functions in the quark-antiquark channels. The NJL model contains two such channels: the scalar $\bar qq$ channel – which is used to characterize the spontaneous chiral symmetry breaking – and the vector-isoscalar $\bar q\gamma^\mu q$ channel. The energies corresponding to the scalar and vector channels, after the Fierz

expansion of Eqs. (5.3), denoted by $E^{\rm s}_{\rm QCD}$ and $E^{\rm v}_{\rm QCD}$, are

$$E^{\rm s}_{\rm QCD} = -\frac{8\pi\alpha_s}{27}\int_{p,p'} {\rm Tr}S(p)\,{\rm Tr}S(p')D(p-p'), \tag{5.7}$$

$$E^{\rm v}_{\rm QCD} = \frac{4\pi\alpha_s}{27}\int_{p,p'} {\rm Tr}[S(p)\gamma^\mu]{\rm Tr}[S(p')\gamma_\mu]D(p-p'). \tag{5.8}$$

To relate these Fierz results to the NJL $G$ and $g_V$, we consider two limiting extremes, low and high density, where the gluon propagator's momentum dependence can be simplified. Owing to the non-perturbative infrared cutoff of order $\Lambda_{\rm QCD}$, the gluon propagator has a finite limit $D(q\to 0)$ at low energy; thus at low densities we have

$$E^{\rm s,v}_{\rm QCD} = C_{\rm s,v}\alpha_s D(0)\left(\int_p {\rm Tr}\left[S(p)\Gamma_{\rm s,v}\right]\right)^2, \tag{5.9}$$

where $C_{\rm s} = -8\pi/27 = -2C_{\rm v}$ and $\Gamma_{\rm s} = 1$, and provided that $\int_p {\rm Tr}[S(p)\gamma_j] = 0$, $\Gamma_{\rm v} = \gamma^0$. In this form one can readily identify the NJL couplings as $G = 2g_V = C_{\rm s}\alpha_s D(0)$.

At higher densities however, we must keep the momentum dependence of the gluon propagators. With massless free quark and gluon propagators,

$$S^{0,ab}_{ij}(p) = \delta_{ab}\delta_{ij}\frac{\gamma_\mu p^\mu}{(p_0+\mu)^2-\boldsymbol{p}^2}, \tag{5.10}$$

$$D^0(p) = \frac{1}{p^2}, \tag{5.11}$$

where $\mu$ is the quark chemical potential, we find the perturbative result,[1]

$$E^{\rm v}_{\rm QCD} = 24\pi\alpha_s\left(\int\frac{d^3p}{(2\pi)^3}\frac{f(|\boldsymbol{p}|-\mu)}{|\boldsymbol{p}|}\right)^2, \tag{5.12}$$

where $f(z) = [\exp(z/T)+1]^{-1}$ is the Fermi distribution function; at zero temperature (5.12) reduces to

$$E^{\rm v}_{\rm QCD} = \frac{3\alpha_s p_F^4}{2\pi^3}. \tag{5.13}$$

This result is identical to the exchange energy of a highly relativistic electron

[1] While the full trace in Eq. (5.3) contains contributions from both particles and antiparticles, we focus only on modifications due to non-zero particle densities here.

gas to within flavor and color factors.[2,3]

Meanwhile, the vector repulsion contributes an energy density in the NJL model [29]

$$E^{\rm v}_{\rm NJL} = g_V n_q^2, \tag{5.15}$$

which we identify with $E^{\rm v}_{\rm QCD}$ in the matching density region $\sim$ 5-20 $n_0$ corresponding to $p_F \sim$ 0.4-0.6 GeV, one finds

$$g_V = \frac{\pi \alpha_s}{6 p_F^2}. \tag{5.16}$$

The solid line in Fig. 5.1 shows $g_V$ obtained using (5.16) and the two-loop running coupling constant $\alpha_s(\mu_q)$:

$$\alpha_s(\mu_q) = \frac{4\pi}{9 \ln \tilde{\mu}^2} \left( 1 - \frac{64 \ln \ln \tilde{\mu}^2}{81 \ln \tilde{\mu}^2} \right), \tag{5.17}$$

with $\tilde{\mu} \equiv \mu_q / \Lambda_{\rm QCD}$ and $\Lambda_{\rm QCD} = 340$ MeV [11]. The shaded horizontal band indicates the range of (constant) $g_V$ in QHC19 [29]. Although $g_V$ in Fig. 5.1 approaches the needed range below $20 n_0$, the factor $p_F^{-2}$ and the running $\alpha_s$ near the Landau pole at $\Lambda_{\rm QCD}$ already causes strongly divergent behavior of $g_V$ even at $5 n_0$ (corresponding to $p_F \sim 400$ MeV), in contrast to the simple treatment in NJL of $g_V$ as constant in this regime. However, extending the pQCD calculation down to $\Lambda_{\rm QCD}$ is not reliable. The solid line in Fig. 5.1 shows $g_V$ for $\alpha_s$ frozen at 3.0 at low energies [11]. Although the divergence from the Landau pole is removed in this case, $g_V$ still increases rapidly at low energy.

## 5.3 Non-perturbative $\alpha_s$ and massive gluons below one GeV

We now examine the consequences of the non-perturbative behavior of the strong coupling constant $\alpha_s$ and the gluon propagator below the 1 GeV scale. For reviews, see Refs. [11, 98] and references therein. In various non-perturbative approaches for the gluon sector (lattice gauge theory, Schwinger-Dyson equa-

[2] Equation (5.12) includes the interactions between quark number densities $\bar{q}\gamma_0 q$, as well as those between spatial currents, $\bar{q}\gamma_j q$. These contributions yield the matrix element, for on-shell momenta,

$$\mathrm{Tr}[S(p)\gamma^\mu]\,\mathrm{Tr}[S(p')\gamma_\mu] \;\propto\; \frac{|\boldsymbol{p}||\boldsymbol{p}'| - \boldsymbol{p}\cdot\boldsymbol{p}'}{2|\boldsymbol{p}||\boldsymbol{p}'|}\,, \tag{5.14}$$

whose numerator cancels the pole from the massless gluon propagator, giving Eq.(5.12).

[3] In deriving $E^{\rm v}_{\rm QCD}$ in Eq. (12) from Eq. (5.9) with a momentum-dependent gluon propagator, the correlation functions $\langle \bar{q}\vec{\gamma} q \rangle$ are as important as $\langle \bar{q}\gamma^0 q \rangle$; the former is not included in the NJL mean field description. Such deficiency in the NJL model can be compensated by absorbing the contribution from $\langle \bar{q}\vec{\gamma} q \rangle$ into the density dependence of $g_V$ itself; in this way, we can directly compare the NJL $g_V$ with the current definition of $g_V$ in terms of QCD parameters.

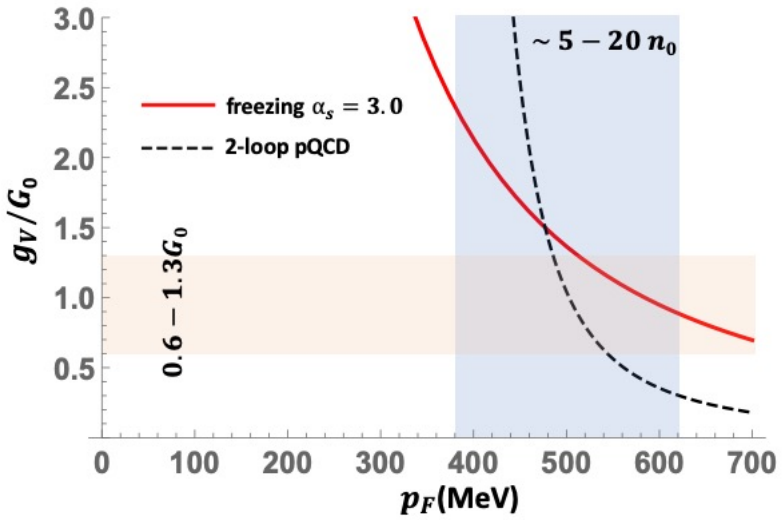


Figure 5.1: The dashed line indicates the single gluon exchange result for $g_V$ in perturbative QCD as a function of the quark matter Fermi momentum, $p_F$. The horizontal shaded region shows the range of $g_V$ in QHC19 [29], while the vertical shaded region shows the baryon density $\sim$ 5-20$n_0$. The solid line indicates the result for $\alpha_s$ frozen at 3.0 at low energies [11].

tions, and gauge/gravity duality) under gauge fixing, $\alpha_s$ is of order unity below one GeV (with freezing or decoupling behaviors in the deep infrared limit, $q \to 0$). Here we focus on gluons dynamically acquiring a mass, favored by the lattice results (and corresponding to the decoupling solution of the gluon Schwinger-Dyson equations in the Landau gauge),

$$D(p) = \frac{1}{p^2 - m_g^2}. \tag{5.18}$$

Estimates of $m_g$ tend to lie in the range $\sim 500 \pm 200$ MeV [97, 98].

Equation (5.18) regulates the divergent behavior of $g_V$ as $p_F \to 0$ in Fig. 5.1 and leads to

$$E^{\rm v}_{\rm QCD}(m_g) = E^{\rm v}_{\rm QCD}(0) + \delta E^{\rm v}_{\rm QCD}(m_g), \tag{5.19}$$

where (as in derivation of Eq. (5.12), $E^{\rm v}_{\rm QCD}(0)$ results from a cancellation between the massive gluon propagator with a part of quark matrix elements, while the remaining terms are proportional to $m_g^2$)

$$\begin{aligned} \delta E^{\rm v}_{\rm QCD}(m_g) &= -\frac{3\alpha_s m_g^2}{2\pi^3} \int_0^{p_F} \int_0^{p_F} dp\, dp'\, \ln\left(1 + \frac{4pp'}{m_g^2}\right) \\ &= \frac{3\alpha_s m_g^4}{8\pi^3} K(x), \end{aligned} \tag{5.20}$$

where $z \equiv (2p_F/m_g)^2$ and $K(z) \equiv 2z - (1+z)\ln(1+z) + {\rm Li}_2(-z)$ with ${\rm Li}_2(-z) \equiv$

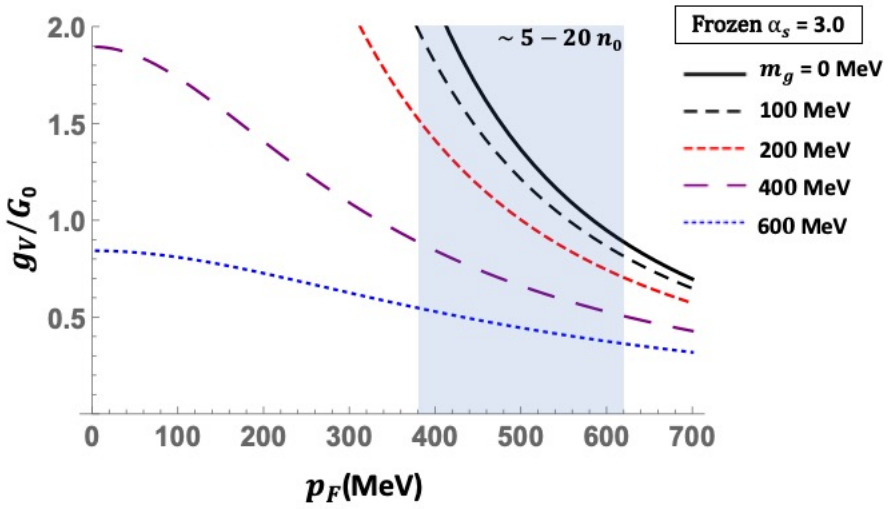


Figure 5.2: The vector coefficient $g_V$ as a function of quark Fermi momentum generated by a frozen $\alpha_s$ =3 below 1 GeV and different gluon masses $m_g$.

$\sum_{\ell=1}^{\infty}(-z)^\ell/\ell^2$ the polylogarithm function with $n = 2$. Thus one finds,

$$E^{\rm v}_{\rm QCD}(m_g) = \frac{3\alpha_s p_F^4}{2\pi^3}\left(1 + \frac{K(z)}{z^2}\right). \tag{5.21}$$

Note that for positive $z$, $0 \le 1 + K(z)/z^2 < 1$, implying that the finite gluon mass softens the repulsion while keeping the total vector energy positive.

Matching Eq. (5.15) with Eqs. (5.16) and (5.21) one finds

$$\begin{aligned} g_V(p_F; z \gg 1) \quad &\to \quad \frac{\pi\alpha_s}{6p_F^2}, \\ g_V(p_F; z \ll 1) \quad &\to \quad \frac{4\pi\alpha_s}{27m_g^2}. \end{aligned} \tag{5.22}$$

Figure 5.2 shows $g_V$ for different gluon masses $m_g$ with a typical value of the frozen $\alpha_s = 3.0$ at low energies $\lesssim 1$ GeV [11]. In the infrared $g_V$ is regulated by the gluon mass, $m_g$, so that there is no divergent behavior at $p_F = 0$.

Figure 5.3 gives contour plots of the resulting vector coefficient $g_V$ for given different $\alpha_s$ and gluon mass $m_g$, at $5n_0$ and $20n_0$. For the resulting $g_V/G_0$ to be in the interval 0.6-1.3 at $5n_0$ with $m_g = 400$ MeV, one needs a strong $\alpha_s \sim$ 2-4, within the range of possible quark-gluon coupling strengths at low energies [11]. Future theories of the quark-gluon vertex $\alpha_s$ together with detailed forms of gluon correlation functions below one GeV will be of interest as they can be directly related to effective quark models constrained by neutron star observations.

In the density range $\sim 5n_0$ in a neutron star, where the quark Fermi momentum lies well below one GeV, it is reasonable to assume an approximately

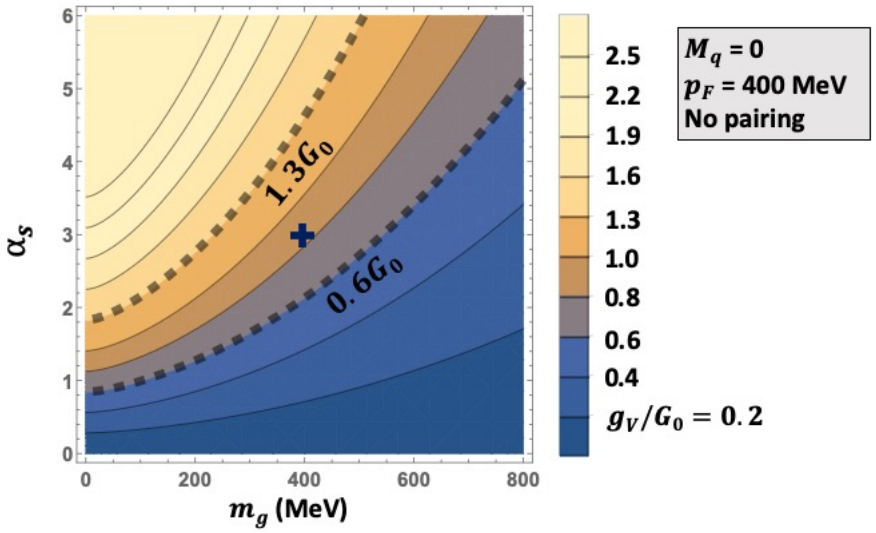


Figure 5.3: The vector coefficient $g_V$ generated by different constant $\alpha_s$ and gluon masses $m_g$, at $p_F = 400$ MeV ($\sim 5n_0$). The central cross indicates $\alpha_s = 3$ and $m_g = 400$ MeV.

constant $\alpha_s$ and $m_g$. The two limiting results, Eq. (5.22), thus suggest an approximate density-dependent parametrization of $g_V$ based on explicit single-gluon exchange

$$g_V(p_F; m_g) \simeq \frac{4\pi\alpha_s/3}{9m_g^2 + 8p_F^2}. \tag{5.23}$$

This parametrization is useful for including the density dependence of $g_V$ in the quark-hadron crossover equations of state.

## 5.4 Effect of finite quark mass

At high densities quark matter contains both a weak chiral condensate, $\sim \langle\bar{q}q\rangle$ as well as a diquark condensate $\sim \langle qq\rangle$, as a consequence of the six-quark Kobayashi-Maskawa-'t Hooft (KMT) effective interaction [102]. The quark effective mass, $M_q \sim \langle\bar{q}q\rangle$, is dynamically generated by the chiral condensate; in the NJL model, $M_q$ is the mean-field self-energy generated by the effective local four-quark interaction. At densities $\gtrsim 5n_0$, the chiral condensate enhanced by the KMT interaction could result in an effective mass $M_q \sim$ 50-70 MeV for the light quarks, and $\sim$ 250-300 MeV for the $s$ quark [10]. These masses are not small compared to the quark Fermi momentum at these densities, and must be taken into account in the exchange energy calculation.

Here we calculate the effects of $M_q$ on $g_V$ only by modifying the quark propagators in Eq. (5.9), and not further correcting the vertices. We recognize that this is not a self-consistent calculation; rather we aim here to get a sense

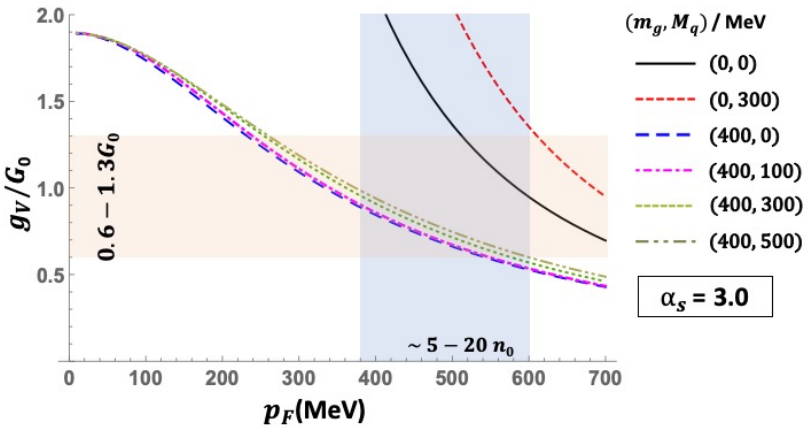


Figure 5.4: Vector repulsion coefficient $g_V$ for different values of $M_q$ with $m_g = 400$ MeV and $\alpha_s = 3$.

of the effects of a finite quark mass on the the vector channel of the matrix element (5.2), which is connected to perturbative QCD at asymptotic density. We take the quark Green's function to be

$$S_{ij}^{ab}(p) = \delta_{ab}\delta_{ij}\frac{\gamma_\mu p^\mu + M_q}{(p_0+\mu)^2 - \boldsymbol{p}^2 - M_q^2}, \tag{5.24}$$

and assume the same effective mass $M_q$ for all flavors.

With this $S$, we obtain after some algebra, with $\epsilon_p = (|\mathbf{p}|^2 + M_q^2)^{1/2}$,

$$\begin{aligned} E_{\rm QCD}^{\rm v} &= 24\pi\alpha_s\Bigg[\left(\int\frac{d^3p}{(2\pi)^3}\,\frac{f(\epsilon_p-\mu)}{\epsilon_p}\right)^2 \\ &\quad -(2M_q^2 - m_g^2)\int\frac{d^3p\,d^3p'}{(2\pi)^6}\frac{1}{\epsilon_p\epsilon_{p'}}\cdot\frac{f(\epsilon_p-\mu_q)f(\epsilon_{p'}-\mu_q)}{(\epsilon_p-\epsilon_{p'})^2 - |\boldsymbol{p}-\boldsymbol{p}'|^2 - m_g^2}\Bigg]. \end{aligned} \tag{5.25}$$

The asymptotic forms of Eq. (5.25) for $p_F \gg M_q$ and $m_g$, and for $p_F \ll M_q$ and $m_g$ can be readily found, with the result that $g_{_V}(p_F; m_g, M_q)$ agrees in these limits with Eq. (5.22). In particular, $g_V$ is independent of $M_q$ at $p_F = 0$ as long as $m_g$ is finite. The combined effects of $M_q$ and $m_g$ are shown in Fig. 5.4, which compares $g_{_V}$ at several different values of $M_q$ and $m_g = 400$ MeV. We find that the effect of $M_q$ on $g_{_V}$ is almost negligible. Thus the assumption that $g_{_V}$ is flavor independent is reasonable, despite flavor symmetry being significantly broken by the strange quark mass; the parametrization (5.23) is approximately useful independent of flavor.

## 5.5 Effect of diquark pairing

We next consider the effects on $E^{\rm v}_{\rm QCD}$ of scalar color-flavor-locked pairing among quarks through modification of the normal quark Green's function $S$ in Eq. (5.9).[4] In the CFL phase it is convenient to expand the quark field (with $SU(3)$ flavor and $SU(3)$ color indices), as $q_{ia} = \sum_{A=0}^{8} \lambda^A_{ia} q_A/\sqrt{2}$, in term of the Gell-Mann matrices, $\lambda^A$ ($A = 1, 2, ..., 8$), and $\lambda^0 = \mathbf{1}\sqrt{2/3}$. In this basis, the normal quark propagator becomes diagonal

$$S^{ab}_{ij}(x-y) = \sum_A \frac{1}{2} \lambda^A_{ia} \lambda^A_{bj} S_A(x-y). \tag{5.26}$$

With CFL pairing, the $S_{A=1,...,8}$ describe eight paired quark quasiparticles with the same gap $\Delta_{A=1,...,8}(p) = \Delta(p)$, and one quasiparticle $S_0$ with double the gap $\Delta_0(p) = 2\Delta(p)$.

For massless quarks ($\epsilon_p = |\mathbf{p}|$), one finds

$$\begin{aligned} E^{\rm v}_{\rm QCD} &= \frac{4\pi\alpha_s}{27} \sum_{A,B} \int_{pp'} {\rm tr}[S_A(p)\gamma^\mu]{\rm tr}[S_B(p')\gamma_\mu] \frac{1}{(p-p')^2 - m_g^2}, & (5.27) \\ &= \frac{\alpha_s}{54\pi^3} \sum_{A,B} \int_0^\infty dp\, dp'\, v^2_{Ap} v^2_{Bp'} \\ &\quad \times \left[ 4pp' - J_{AB}(p,p',m_g) \ln \left| 1 + \frac{4pp'}{J_{AB}(p,p',m_g)} \right| \right], & (5.28) \end{aligned}$$

with $v^2_{Ap} = \frac{1}{2}\left(1 - (\epsilon_p - \mu)/E^A_p\right)$, $E^A_p = [(\epsilon_p - \mu)^2 + \Delta^2_A]^{1/2}$, and $J_{AB}(p,p',m_g) = m_g^2 + (p-p')^2 - (E^A_p - E^B_{p'})^2$. Generalization to the case with finite quark mass $M_q$ is straightforward. Note that the total quark density is given by

$$n_q = 2 \sum_A \int \frac{d^3p}{(2\pi)^3} v^2_{Ap}. \tag{5.29}$$

The integral in Eq. (5.28) converges only with a momentum dependent gap. Following the numerical study in Ref. [103, 104], we approximate the spatial momentum dependence of $\Delta$ by

$$\Delta(p) = \frac{\Delta(\mu)}{(1 + b(p-\mu)^2/\mu^2)^\zeta}; \tag{5.30}$$

the constant $b > 0$ parametrizes how fast $\Delta(p)$ falls off away from the Fermi surface, and the exponent $\zeta > 0$ parametrizes the behavior of $\Delta(p)$ at high momenta (see Fig. 5.5). In the weak coupling limit, $\zeta = 1 + \mathcal{O}(\alpha_s)$ and $\Delta \sim \mu g^{-5} e^{-3\pi^2/\sqrt{2}g}$ [105, 106]. Here we simply vary the gap in the range, $\Delta(\mu) =$ 100-300 MeV, consistent with the QHC19 equation of state.

[4] The anomalous Green's function, $F^{ab}_{ij}(x-y) = -i\langle \mathcal{T} q^a_i(x)(q^T C)^j_b(y)\rangle$, leads as well to the familiar energy shift $E^{\rm pair}_{\rm QCD}$ proportional to the square of the pairing gap, an effect related to inferring the in-medium modification of $H$.

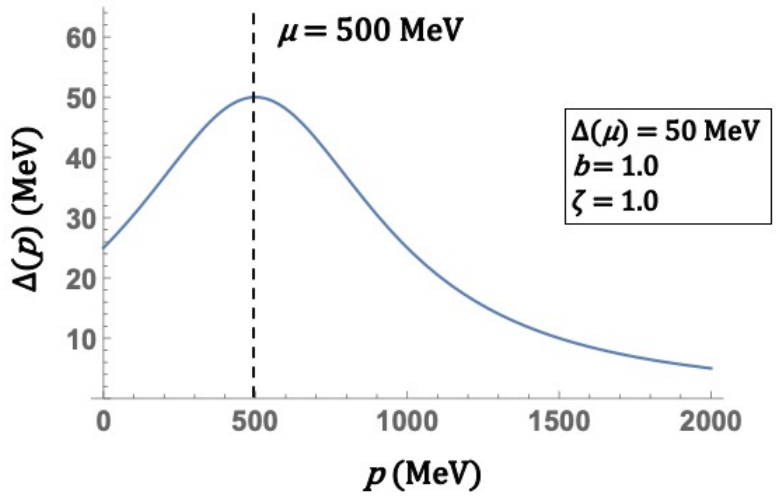


Figure 5.5: The parametrization (5.30) of the momentum dependence gap $\Delta(p)$ for $\mu = 500$ MeV, $b = 1.0$, $\Delta(\mu) = 50$ MeV, and $\zeta = 1.0$.

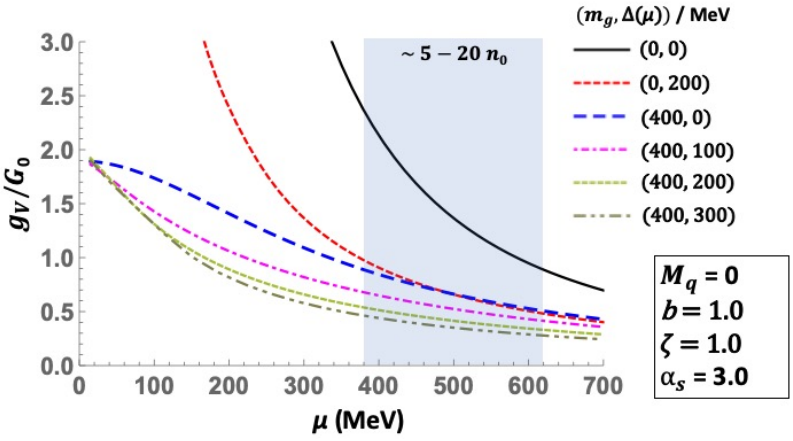


Figure 5.6: The vector repulsion coefficient $g_V$ for different $\Delta(\mu)$ with $m_g = 400$ MeV and $\alpha_s = 3$. The curves show how inclusion of pairing in the presence of a massive gluon has only a small effect on $g_V$.

As we see, a gap decreases $g_V$ at all densities, and the dependence of the gap is significant for massless gluons. For gluon masses $m_g \sim 400$ MeV, however, even a large variation of $\Delta$ from 0 to 300 MeV does not change the qualitative behavior of $g_V$. In comparison with the effects of $M_q$, a large gap $\Delta(\mu) = 200$ MeV (as in QHC19) still has a sizable impact: at $5n_0$, a 200 MeV CFL gap reduces $g_V$ from $\sim 0.9\,G_0$ to $\sim 0.55\,G_0$, even with $m_g = 400$ MeV.

The gluon propagator is also modified in a dense quark medium by Landau damping [105, 106, 107], and the Debye screening mass in the longitudinal sector, and in the presence of diquark pairing by Meissner masses in the transverse sector [89, 108], of order $\sqrt{\alpha_s}\,\mu$. The interplay of these modifications of the gluon propagator in the quark matter in neutron stars, and their effects on neutron star properties is an open question worthy of future research.

## 5.6 The vector-isovector channel and connection with nucleon-meson interactions

Our discussion has so far focused on the flavor symmetric case, where the isoscalar channel is the only non-vanishing contribution from single gluon exchange energy in the vector channel. However, for realistic constituent quark masses, the vector-isovector channel (denoted by $\tau$) also contributes to the single gluon exchange energy,

$$E_{\rm QCD}^{{\rm vec},\tau} = \frac{2\pi\alpha_s}{9}\int_{p,p'} {\rm Tr}[S(p)\gamma^\mu\tau_\alpha]{\rm Tr}[S(p')\gamma_\mu\tau_\alpha]D(p-p'), \tag{5.31}$$

where the $\tau_{\alpha=1,\ldots,8}$ are the eight Gell-Mann flavor matrices. This isovector channel corresponds to the interaction $g_\tau(\bar{q}\gamma^\mu\tau_\alpha q)^2$. In particular, the $\alpha = 3$ and 8 terms yield the exchange energy at low density of the form

$$g_\tau\left[(n_u - n_d)^2 + \frac{1}{3}(n_u + n_d - 2n_s)^2\right]. \tag{5.32}$$

This vector-isovector energy is analogous to the neutron-proton symmetry energy in nuclear matter. For the single gluon exchange, $g_\tau/g_V = 3/2$, indicating an vector-isovector energy comparable to the vector-isoscalar energy for significant differences in flavor densities. In this case, adding the isoscalar channel contribution $g_{_V}(n_u + u_d + n_s)^2$ with $g_\tau/g_{_V} = 3/2$, the total vector exchange energy reads

$$E_{\rm QCD}^{\rm vec} + E_{\rm QCD}^{{\rm vec},\tau} = 3g_{_V}(n_u^2 + n_d^2 + n_s^2), \tag{5.33}$$

reflecting the fact that the gluons carry no flavor quantum numbers.

It is instructive, in constructing quark-hadron crossover descriptions of dense

matter between the nucleonic and quark phases, to understand how the vector energy in the NJL model connects at low densities with the corresponding energy in nuclear matter, taking into account the isospin symmetry energy in both phases. In the chiral nucleon-meson model [109] treated at mean field, a phenomenological vector repulsion for nucleons in the isoscalar and isovector channels, mediated by massive vector boson exchange, is:

$$\begin{aligned} & G_V(n_p+n_n)^2 + G_\tau(n_p-n_n)^2 \\ &= \frac{G_V}{9}(n_u+n_d)^2 + \frac{G_\tau}{9}(n_u-n_d)^2, \end{aligned} \tag{5.34}$$

where $G_V$ is estimated to be $\simeq 5.12\,\mathrm{fm}^{-2}$ and $G_\tau$ to be $\simeq 1.07\,\mathrm{fm}^{-2}$. In the absence of strange quarks, the total vector energy in quark matter is

$$E_{\mathrm{QCD}}^{\mathrm{vec(total)}} = \left(g_{_V} + \frac{g_\tau}{3}\right)(n_u+n_d)^2 + g_\tau(n_u-n_d)^2, \tag{5.35}$$

where we assume the flavor symmetry $g_\tau^{(3)} = g_\tau^{(8)} = g_\tau$. Matching $G_V/9$ to $g_{_V} + g_\tau/3$ and $G_\tau/9$ to $g_\tau$, we would obtain

$$g_V = 2.93G,\ g_\tau = 0.66G, \tag{5.36}$$

where $g_V$ is about three times the suggested NJL value, and $g_\tau/g_V \approx 0.23$. The former result is incompatible with the estimates in QHC19, and the latter significantly deviates from the single gluon exchange prediction. However, with possible explicit flavor symmetry breaking $g_\tau^{(3)} \neq g_\tau^{(8)}$ (which is beyond the effects of single gluon exchange), the matching becomes

$$G_V/9 = g_V + g_\tau^{(8)}, \qquad G_\tau/9 = g_\tau^{(3)}. \tag{5.37}$$

Still $g_\tau^{(3)} = 0.66G$. For $g_V$ in the range 0.6-1.3$G$ as found in the QHC19 equation of state, we obtain

$$g_\tau^{(8)} \sim 1.9 - 2.6G \gg \frac{1}{3}g_\tau^{(3)}. \tag{5.38}$$

That is, to make a close connection of the vector energies in the NJL model to the nucleon-meson model at low density would require including a very strong explicit flavor symmetry breaking in the vector-isovector channel, in the form of a huge 'symmetry energy' between light and heavy quarks.

Including the $g_\tau^{(3)}$ and $g_\tau^{(8)}$ interactions in the NJL model would significantly impact the phase diagram in states with flavor asymmetry, if the above values from matching to the chiral nucleon-meson model (or indeed from single gluon exchange) are used. Such symmetry energies strongly favor equal densities in all flavors, suggesting that strange quarks would appear and the system would enter the CFL phase at relatively low densities. At least a moderate vector-isovector

interaction with coupling strength $\sim$ 1-2 $G$ should be explored in future NJL model studies of quark matter at $\gtrsim 5n_0$ as well.

In the remainder of this paper, we consider the vector-isoscalar energy only, since the strong diquark pairing strength $H \simeq 1.5G$ and vector-isoscalar repulsion $g_V \simeq 1.0G$ found in QHC19, would predict that quark matter at densities $\gtrsim 5n_0$ is already in the CFL phase with weak flavor asymmetry. Furthermore Ref. [110] argues that the equation of state of quark matter described by NJL without pairing is insensitive to the vector-isoscalar interaction for a moderate $g_V = 0.8G$. We defer more detailed studies of the impact of vector-isovector interactions on the NJL equation of state to the future.

## 5.7 Conclusion

We have computed the vector repulsion coefficient $g_V$ from the explicit gluon exchange energy in quark matter, modifying the quark and gluon Green's functions to account for a non-perturbative gluon mass $m_g$, chiral condensate and diquark pairing, and included as well a possible infrared-finite $\alpha_s$. In the density range $\sim$ 5-20$n_0$ with reasonable parameters for $\alpha_s$, gluon mass, quark mass and pairing gap, we can begin to understand the origin of a $g_V$ of order $\sim$ 0.6-1.3$G$. The parameters we have chosen, despite their uncertainties, lie within estimates from a variety of models and theoretical frameworks of sub-GeV QCD. Among the non-perturbative effects we have considered, the resulting $g_V$ is most sensitive to $\alpha_s$ and $m_g$, while $M_q$ and $\Delta$ induce only relatively small changes owing to suppression by a gluon mass. Thus, the parametrization (5.23) should be a good approximate description of the density dependence of $g_V$, to be included in the equation of state for neutron star matter with a strongly interacting quark phase.

Many open questions remain. The vector repulsion between quarks at densities $\gtrsim 5n_0$ may also come from non-perturbative QCD beyond the single gluon-exchange contribution treated in this paper; such uncertainty is not under control at present. As $\alpha_s$ could range anywhere from 0 to 10 (or even be divergent at low momentum scales), the assumption that the vector repulsion is dominated by a single gluon exchange with a fixed $\alpha_s$ and $m_g$ is overly simplified. Our treatment can be improved and extended in several directions. The first would be inclusion of more realistic quark and gluon propagators, including possible momentum dependence of masses and differences between transverse and longitudinal gluons. The second would be to include the non-perturbative running of $\alpha_s$. Including the density dependence of $g_V$, as in the parametrization (5.23), can have a significant effect on model studies of quark matter. In particular, corrections to the contributions from the light and heavy quarks could shift the phase boundaries and modify the equation of state. Including the density dependence of the diquark coupling, $H$, would have similar effect.

We note that relating the effective QCD vector couplings $g_V$ and $g_\tau^\alpha$ in

the NJL model of dense matter (an effective field theory for quarks) to nucleon-meson models (effective field theories for hadrons) would provide a further probe of quark-hadron continuity [102, 111]. If the transition from nuclear to quark matter is essentially smooth, one expects the vector repulsion from hadronic to quark matter to be similarly smooth, since in the quark-hadron continuity picture, the spectrum of light gluonic excitations is tightly connected to that of hadronic vector mesons [112], while quarks are mapped to the baryons in nuclear matter. Low energy quark-gluon matter treated in this way becomes an extension of the baryon-meson picture of nuclear matter, plausibly enabling a relatively smooth crossover and in turn mapping $g_V$ and $g_\tau^\alpha$ from the hadronic to quark phases.[5]

[5] One may ask how vector repulsions in the nucleon-meson description of nuclear matter, a gauge-invariant theory, can be mapped onto vector repulsions in the gauge-dependent theory of quarks and gluons, despite the vector repulsions in both being effective fermion-fermion interactions mediated by massive boson exchange. We have shown in Chapter 4 that including color charge screening by CFL diquark condensates [7, 113] leads to a low energy gauge-invariant description of quarks and gluons of the same form as a baryon-meson Lagrangian.

# Appendix

# Fierz transformation

The Fierz transformation is a re-arrangement of fermion operator products in the Dirac, flavor and color space using index-exchanging properties of the gamma and $SU(N)$ generator matrices. In the quark-antiquark channel, re-arrangement of the Dirac indices read

$$\begin{aligned}(\gamma^\mu)_{mn}(\gamma_\mu)_{m'n'} &= \mathbf{1}_{mn'}\mathbf{1}_{m'n} + (i\gamma_5)_{mn'}(i\gamma_5)_{mn'} \\ &\quad -\frac{1}{2}(\gamma^\mu)_{mn'}(\gamma_\mu)_{m'n} \\ &\quad -\frac{1}{2}(\gamma^\mu\gamma_5)_{mn'}(\gamma_\mu\gamma_5)_{m'n},\end{aligned} \tag{.1}$$

and those of the the flavor and color indices ($N_f = N_c = 3$) read

$$\begin{aligned}\mathbf{1}_{ij}\mathbf{1}_{kl} &= \frac{1}{3}\mathbf{1}_{il}\mathbf{1}_{kj} + \frac{1}{2}(\tau_a)_{il}(\tau_a)_{kj}, \\ \lambda^{ab}_\alpha\lambda^{a'b'}_\alpha &= \frac{16}{9}\mathbf{1}_{ab'}\mathbf{1}_{a'b} - \frac{1}{3}\lambda^{ab'}_\alpha\lambda^{a'b}_\alpha.\end{aligned} \tag{.2}$$

In the quark-quark channel,

$$\begin{aligned}(\gamma^\mu)_{mn}(\gamma_\mu)_{m'n'} &= (i\gamma^5 C)_{mm'}(i\gamma^5 C)_{nn'} + C_{mm'}C_{nn'} \\ &\quad -\frac{1}{2}(\gamma^\mu\gamma^5 C)_{mm'}(\gamma_\mu\gamma^5 C)_{nn'} \\ &\quad -\frac{1}{2}(\gamma^\mu C)_{mm'}(\gamma_\mu C)_{nn'},\end{aligned} \tag{.3}$$

and

$$\begin{aligned}\mathbf{1}_{ij}\mathbf{1}_{kl} &= \frac{1}{2}(\tau_S)_{ik}(\tau_S)_{lj} + \frac{1}{2}(\tau_A)_{ik}(\tau_A)_{lj}, \\ \lambda^{ab}_\alpha\lambda^{cd}_\alpha &= \frac{2}{3}\lambda^S_{ac}\lambda^S_{bd} - \frac{4}{3}\lambda^A_{ac}\lambda^A_{bd},\end{aligned} \tag{.4}$$

where $S$ and $A$ stand for symmetric and antisymmetric indices, and the $\tau_{\alpha=1,\ldots,8}$ are the eight Gell-Mann flavor matrices. Using these relations, one can transform a single trace into products of two traces, as done in e.g. Eq. (5.9):

$$\mathrm{Tr}[S(p)\Gamma^I S(p')\Gamma^I] = \sum_M g_M \mathrm{Tr}[S(p)\Gamma^M]\mathrm{Tr}[S(p')\Gamma^M], \tag{.5}$$

where $\Gamma^I$ are Dirac, flavor and color matrices.

# Bibliography


[1] Y. Nambu and G. Jona-Lasinio, Dynamical model of elementary particles based on an analogy with superconductivity. I, Phys. Rev. **122**, 345 (1961).

[2] Y. Nambu and G. Jona-Lasinio, ynamical model of elementary particles based on an analogy with superconductivity. II, Phys. Rev. **124**, 246 (1961).

[3] G. Baym, Neutron stars and the property of matter at high density, Copenhagen : Nordisk institut for teoretisk atomfysik (1977).

[4] M. Gell-Mann, R. J. Oakes, and B. Renner, Behavior of current divergences under $SU_3 \times SU_3$, Phys. Rev. **175** 2195 (1968).

[5] G. Baym and L.P. Kadanoff, Conservation laws and correlation functions, Phys. Rev. **124** 287 (1961).

[6] G. Baym, Self-consistent approximations in many-body systems, Phys. Rev. **127** 1391 (1962).

[7] A. Kryjevski and T. Schaefer, An effective theory for baryons in the CFL phase, Phys. Lett. B**606** 52(2005).

[8] Y. Song and G. Baym, Generalized Nambu-Goldstone pion in dense matter: a schematic NJL model, Phys. Rev. C**96** 025206 (2017).

[9] Y. Song, G. Baym, T. Hatsuda and T. Kojo, Effective repulsion in dense quark matter from non-perturbative gluon exchange, to be published (2019).

[10] G. Baym et al., From hadrons to quarks in neutron stars: a review, Rep. Prog. Phys. **81** 056902 (2018).

[11] A. Duer, S. J. Brodsky, and G. F. de Teramond, The QCD running coupling, Prog. Part. Nucl. Phys. **90** 1 (2016).

[12] C. Gattringer and C. B. Lang, Quantum chromodynamics on the lattice: an Introductory presentation, vol. 788 of Lecture Notes in Physics. Springer, 2010.

[13] S. Muroya, A. Nakamura, C. Nonaka, and T. Takaishi, Lattice QCD at finite density: an introductory review, Prog. Theor. Phys. **110** 615-668 (2003).

[14] W. Busza, K. Rajagopal and W. van der Schee, heavy ion collisions: the big picture and the big questions, Annual Review of Nuclear and Particle Science **68** 399 (2018).

[15] E. Fonseca et al., The NANOGrav nine-year data set: mass and geometric measurements of binary millisecond pulsars, Astrophys. J. **832** 167:1-22 (2016).

[16] J. Antoniadis, et al., A massive pulsar in a compact relativistic binary, Science **340** 1233232 (2013).

[17] H. T. Cromartie et al., A very massive neutron star: relativistic Shapiro delay measurements of PSR J0740+6620, arXiv:1904.06759 [astro-ph.HE] (2019).

[18] I. Bombaci, The hyperon puzzle in neutron stars, PS Conf. Proc. 17, 101002 (2017).

[19] L. Giusti, F. Rapuano, M. Talevi and A. Vladikas, The QCD chiral condensate from the lattice, Nucl. Phys. B**538** 249 (1999).

[20] M. Alford, K. Rajagopal and F. Wilczek, Color-flavor locking and chiral symmetry breaking in high density QCD, Nucl. Phys. B**537** 443 (1999).

[21] G. 't Hooft, Symmetry breaking through Bell-Jackiw anomalies, Phys. Rev. Lett. **37** 8-11 (1976).

[22] G. 't Hooft, How instantons solve the U (1) problem, Phys. Rep. **142**, 357 (1986).

[23] M. Buballa, NJL-model analysis of dense quark matter, Phys.Rept. **407**, 205 (2005).

[24] A. M. Polyakov, Thermal properties of gauge fields and quark liberation, Phys. Letters B**72** 477-80 (1978).

[25] L. Susskind, Lattice models of quark confinement at high temperature, Phys. Rev. D**20** 2610-8 (1979).

[26] P. M. Lo, B. Friman, and K. Redlich, Polyakov loop fluctuations and deconfinement in the limit of heavy quarks, Phys. Rev. D**90** 074035 (2014).

[27] K. Fukushima, Chiral effective model with the Polyakov loop, Phys. Letters B**591** 277-284 (2004).

[28] S. Rossner, C. Ratti, and W. Weise, Polyakov loop, diquarks and the two-flavour phase diagram, Phys. Rev. D**75** 034007 (2007).

[29] G. Baym, S. Furusawa, T. Hatsuda, T. Kojo, and H. Togashi, New Neutron Star Equation of State with Quark-Hadron Crossover, arXiv:1903:08963 [astro-ph.HE].

[30] M. Kobayashi and T. Maskawa, Chiral symmetry and eta-X mixing, Prog. Theor. Phys. **44** 1422-4 (1970).

[31] G. 't Hooft, How instantons solve the U(1) problem, Phys. Rept. **142** 357-387 (1986).

[32] T. Hatsuda and T. Kunihiro, QCD phenomenology based on a chiral effective Lagrangian, Phys. Rep. **247** 221-367 (1994).

[33] H. Togashi, K. Nakazato, Y. Takehara, S. Yamamuro, H. Suzuki, and M. Takano, Nuclear equation of state for core-collapse supernova simulations with realistic nuclear forces, Nucl. Phys. A**961** 78 (2017).

[34] R. C. Tolman, Static solutions of Einstein's field equations for spheres of fluid, Phys. Rev. **55** 364-73 (1939).

[35] J. Oppenheimer and G. Volkoff, On massive neutron cores, Phys. Rev. **55** 374-81 (1939).

[36] J. M. Lattimer and A, W. Steiner, Neutron star masses and radii from quiescent low-mass X-ray binaries, Astrophys. J, **784** 123-137 (2014).

[37] F. Özel, D. Psaltis, T. Guver, G. Baym, C. Heinke, and S. Guillot, The dense matter equation of state from neutron star radius and mass measurements, Astrophys. J. **820** 28:1-25 (2016).

[38] P. M. Fishbane, R. E. Norton, and T. N. Truong, Finely tuned Nambu–Jona-Lasinio and linear sigam models, Phys. Rev. D**46** 1768 (1992).

[39] H. Abuki, Y. Takeda, and M. Harada, Dual chiral density waves in nuclear matter, EPJ Web of Conferences **192** 00020 (2018).

[40] E. Nakano and T. Tatsumi, Chiral symmetry and density wave in quark matter, Phys. Rev. D**71** 114006 (2005).

[41] C. Y. Wong, T. A. Welton, and J. A. Maruhn, Dynamics of nuclear fluid. II. Normal sound, spin sound, isospin sound, and spin-isospin sound, Phys. Rev. C**15** 1558 (1977).

[42] V. Bernard, Remarks on dynamical breaking of chiral symmetry and pion properties in the Nambu and Jona-Lasinio model, Phys. Rev. D**34** 1601 (1986).

[43] D. Ebert, T. Feldmann, R. Friedrich, and H. Reinhardt, Effective meson Lagrangian with chiral and heavy quark symmetries from quark flavor dynamics, Nucl. Phys. B**434**, 619 (1995).

[44] M. Oertel, M. Buballa, and J. Wambach, Meson properties in the 1/Nc-corrected NJL model, Nucl. Phys. A**676**, 247 (2000).

[45] L. He, M. Jin, and P. Zhuang, Pion superfluidity and meson properties at finite isospin density, Phys. Rev. D**71**, 116001 (2005).

[46] H. Hansen, W. M. Alberico, A. Beraudo, A. Molinari, M. Nardi, and C. Ratti, Mesonic correlation functions at finite temperature and density in the Nambu–Jona-Lasinio model with a Polyakov loop, Phys. Rev. D**75**, 065004 (2007).

[47] V. Kleinhaus, M. Buballa, D. Nickel, and M. Oertel, Pseudoscalar Goldstone bosons in the color-flavor locked phase at moderate densities Phys. Rev. D**76**, 074024 (2007).

[48] M. Ruggieri, A diagrammatic derivation of the meson effective masses in the neutral color-flavor-locked phase of Quantum Chromodynamics, JHEP 0707, 031 (2007).

[49] D. Ebert, K.G. Klimenko, and V.L. Yudichev, Mass spectrum of diquarks and mesons in the color–flavor locked phase of dense quark matter, Eur. Phys. J. C**53**, 65 (2008).

[50] M. Rho, A. Wirzba, and I. Zahed, Generalized pions in dense QCD, Phys. Lett. B**473**, 126 (2000).

[51] K. Fukushima and T. Hatsuda, The phase diagram of dense QCD, Rept. Prog. Phys.**74**:014001(2011).

[52] D. Blaschke, S. Fredriksson, H. Grigorian, A. M. Öztaş, and F. Sandin, Phase diagram of three-flavor quark matter under compact star constraints, Phys. Rev. D**72**, 065020 (2005).

[53] T. Hatsuda and T. Kunihiro, QCD Phenomenology based on a Chiral Effective Lagrangian, Phys. Rep. **247**, 22 (1994).

[54] H. J. Warringa and D. Boer, Color superconductivity versus pseudoscalar condensation in a three-flavor Nambu–Jona-Lasinio model, Phys. Rev. D**72**, 014015 (2005).

[55] C.Ratti, M. A. Thaler, and W. Weise, Phases of QCD: Lattice thermodynamics and a field theoretical model, Phys. Rev. D**73**, 014019 (2006).

[56] S. Rößner, C. Ratti, and W. Weise, Polyakov loop, diquarks, and the two-flavor phase diagram, Phys. Rev. D**75**, 034007 (2007).

[57] H. Abuki, Polyakov-Nambu-Jona Lasinio Model and Color-Flavor-Locked Phase of QCD, Prog Theor Phys **174**: 66 (2008).

[58] H. Abuki, G. Baym, T. Hatsuda, and N. Yamamoto, Nambu–Jona-Lasinio model of dense three-flavor matter with axial anomaly: The low temperature critical point and BEC-BCS diquark crossover, Phys. Rev. D**81**, 125010 (2010).

[59] G. Y. Shao, M. Di Toro, V. Greco, M. Colonna, S. Plumari, B. Liu and Y. X. Liu, Phase diagrams in the hadron–Polyakov–Nambu–Jona-Lasinio model, Phys. Rev. D**84** 3, 034028, (2011).

[60] T. M. Schwarz, S. P. Klevansky, and G. Papp, Phase diagram and bulk thermodynamical quantities in the Nambu–Jona-Lasinio model at finite temperature and density, Phys. Rev. C**60**, 055205 (1999).

[61] P. D. Powell and G. Baym, Axial anomaly and the three-flavor Nambu–Jona-Lasinio model with confinement: Constructing the QCD phase diagram, Phys. Rev. D**85**, 074003 (2012).

[62] P. D. Powell and G. Baym, Asymmetric pairing of realistic mass quarks and color neutrality in the Polyakov–Nambu–Jona-Lasinio model of QCD, Phys. Rev. D**88**, 014012 (2013).

[63] P. D. Powell, Doctoral dissertation, University of Illinois at Urbana-Champaign, 2013.

[64] N. Yamamoto, M. Tachibana, T. Hatsuda and G. Baym, Phase structure, collective modes, and the axial anomaly in dense QCD, Phys. Rev. D**76**, 074001 (2007).

[65] D. T. Son and M. A. Stephanov, Inverse meson mass ordering in color-flavor-locking phase of high density QCD, Phys. Rev. D**61**, 074012 (2000).

[66] D. G. Yakovlev, A.D. Kaminker, O.Y. Gnedin, and P. Haensel, Neutrino emission from neutron stars, Phys. Rep. **354**, 1(2001).

[67] N. Bilić, K. Demeterfi and B. Petersson, Strong-coupling analysis of the chiral phase transition at finite chemical potential and finite temperature, Nucl. Phys. B**377**, 651 (1992).

[68] T. Eguchi, New approach to collective phenomena in superconductivity models, Phys. Rev. D**14**, 2755 (1976).

[69] M. K. Volkov, Meson Lagrangians in a superconductor quark model, Ann. Phys. **157**, 282 (1984).

[70] D. Ebert and M. K. Volkov, Composite-meson model with vector dominance based onU(2) invariant four-quark interactions, Z. Phys. C. Particles and Fields **16**, 205 (1983).

[71] S. Goda and D. Jido, Pion properties at finite nuclear density based on in-medium chiral perturbation theory, Prog. Theor. Exp. Phys. 033D03 (2014).

[72] M. Kobayashi and T. Maskawa, Chiral symmetry and eta–x mixing, Prog. Theor. Phys. **44**, 1422 (1970).

[73] R. Rapp, T. Schäfer, E. V. Shuryak, and M. Velkovsky, High-density QCD and instantons, Ann. Phys. (N.Y.) 280, 35 (2000).

[74] T. Schäfer, Instanton effects in QCD at high baryon density, Phys. Rev. D**65**, 094033 (2002).

[75] T. D. Cohen and W. Broniowski, Pseudo-Goldstone modes in isospin-asymmetric nuclear matter, Phys. Lett. B**348** 12 (1995).

[76] W. Broniowski and B. Hiller, Current algebra and soft pionic modes in asymmetric quark matter, Phys. Lett. **392** 267 (1997).

[77] M. Buballa, NJL-model description of Goldstone boson condensation in the color-flavor-locked phase, Phys. Lett. B**609**, 57 (2005).

[78] P.F. Bedaque and T. Schäfer, High-density quark matter under stress, Nucl. Phys. A**697**, 802 (2002).

[79] J. Anderson and L. Kyllingstad, Pion condensation in a two-flavour NJL model: the role of charge neutrality, J. Phys. G: Nucl. Part. Phys. **37** 015003 (2010).

[80] D. Ebert and K. G. Klimenko, Pion condensation in quark matter with finite baryon density, J. Phys. G: Nucl. Part. Phys. **32** 599 (2006).

[81] D. Ebert and K. G. Klimenko, Pion condensation in electrically neutral cold matter with finite baryon density, Eur. Phys. J. C**46** 771 (2006).

[82] X. Hao and P. Zhuang, Meson mixing in pion superfluid, Phys. Lett. B**652**, 275 (2007).

[83] H. Abuki, M. Ciminale, R. Gatto, N. D. Ippolito, G. Nardulli and M. Ruggier, Electrical neutrality and pion modes in the two flavor Polyakov–Nambu–Jona-Lasinio model, Phys. Rev. D**78** 014002 (2008).

[84] H. Abuki, R. Anglani, R. Gatto, M. Pellicoro, and M. Ruggier, Fate of pion condensation in quark matter: From the chiral limit to the physical pion mass, Phys. Rev. D**79** 034032 (2009).

[85] M. M. Forbes, Kaon condensation in a Nambu–Jona-Lasinio model at high density, Phys. Rev. D**72** 094032 (2005).

[86] N. V. Gubina, K. G. Klimenko, S. G. Kurbanov, and V. Ch. Zhukovsky, Inhomogeneous charged pion condensation phenomenon in the $NJL_2$ model with quark number and isospin chemical potentials, Phys. Rev. D**86** 085011 (2012).

[87] M. Buballa and S. Carignano, Inhomogeneous chiral condensates, Prog. Part. Nucl. Phys **81** 39 (2015).

[88] M. Alford, J. A. Bowers and K. Rajagopal, Crystalline color superconductivity, Phys. Rev. D**63** 074016 (2001).

[89] K. Fukushima, Analytical and numerical evaluation of the Debye and Meissner masses in dense neutral three-flavor quark matter, Phys. Rev. D**72** 074002 (2005).

[90] M. Alford and K. Rajagopal, Absence of two-flavor color-superconductivity in compact stars, J. High Energy Phys. **06** 031 (2002).

[91] M. Alford, C. Kouvaris and K. Rajagopal, Evaluating the gapless color-flavor locked phase, Phys. Rev. D**71** 054009 (2005).

[92] H. Abuki, M. Kitazawa, and T. Kunihiro, How do chiral condensates affect color superconducting quark matter under charge neutrality constraints, Phys. Lett. B**615** 102 (2005).

[93] S. B. Rüster, V. Werth, M. Buballa, I. A. Shovkovy, and D. H. Rischke, Phys. Rev. D**72** 034004 (2005).

[94] Z. Yu and G. Baym, Spin-correlation functions in ultracold paired atomic-fermion systems: sum rules, self-consistent approximations, and mean fields, Phys. Rev. A**73** 063601 (2007).

[95] T. Inoue, S. Aoki, T. Doi, T. Hatsuda, Y. Ikeda, N. Ishii, K. Murano, H. Nemura, and K. Sasaki, Two-baryon potentials and H-dibaryon from 3-flavor lattice QCD simulations, Nucl. Phys. A**881** 28 (2012).

[96] R. Casalbuoni and D. Gatto, Effective theory for color-flavor locking in high density QCD, Phys. Lett. B**464** 111 (1999).

[97] J. M. Cornwall, Dynamical mass generation in continuum quantum chromodynamics, Phys. Rev. D**26** 1453 (1982).

[98] A. C. Aguilar, D. Binosi and J. Papavassiliou, The gluon mass generation mechanism: A concise primer, Front. Phys. **11**(2) 111203 (2016).

[99] L. Olbrich, M Zetenyi, and F Giacosa, Three-flavor chiral effective model with four baryonic multiplets within the mirror assignment, Journal of Physics: Conference Series 742 01201 (2016), and the references therein.

[100] T. Kunihiro, Quark-number susceptibility and fluctuations in the vector channel at high temperatures, Phys. Lett. B**271** 395 (1991).

[101] M. Alford, A. Schmitt, K. Rajagopal and T. Schäfer, Color superconductivity in dense quark matter, Rev. Mod. Phys. **80** 4, 1455 (2008).

[102] T. Hatsuda, M. Tachibana, N. Yamamoto, and G. Baym, New critical point induced by the axial anomaly in dense QCD, Phys. Rev. Letters **97** 122001 (2006); N. Yamamoto, M. Tachibana, T. Hatsuda, and G. Baym, Phase structure, collective modes, and the axial anomaly in dense QCD, Phys. Rev. D**76** 074001 (2007); H. Abuki, G. Baym, T. Hatsuda, and N. Yamamoto, The NJL model of dense three flavor matter with axial anomaly: the low temperature critical point and BEC-BCS diquark crossover, Phys. Rev. D**81** 125010 (2010).

[103] M. Matsuzaki, Spatial structure of quark Cooper pairs in a color superconductor, Phys. Rev. D**62** 017501 (2000).

[104] H. Abuki, T. Hatsuda, and K. Itakura, Structural change of Cooper pairs and momentum-dependent gap in color superconductivity, Phys. Rev. D**65** 074014 (2002).

[105] D. T. Son, Superconductivity by long-range color magnetic interaction in high-density quark matter, Phys. Rev. D**59** 094019 (1999).

[106] R. D. Pisarski and D. H. Rischke, Proc. of the Judah Eisenberg Memorial Symposium, Tel Aviv, April 14 - 16; arXiv:nucl-th/9907094 (1999).

[107] G. Baym, C. J. Pethick, and H. Monien, Kinetics of quark-gluon plasmas, Nucl. Phys. **A**498 313c-322c (1989); G. Baym, H. Monien, C. J. Pethick and D. G. Ravenhall. Transverse interactions and transport in relativistic quark-gluon and electromagnetic plasmas, Phys. Rev. Lett. **64** 1867 (1990).

[108] D. H. Rischke, Debye screening and Meissner effect in a three-flavor color superconductor, Phys. Rev. D**62** 054017 (2000).

[109] M. Drews and W. Weise, Functional renormalization group studies of nuclear and neutron matter, Prog. Part. Nucl. Phys. 93, 69 (2017).

[110] P. C. Chu, X. Wang, L. W. Chen and M. Huang, Quark magnetar in three-flavor Nambu–Jona-Lasinio model with vector interaction and magnetized gluon potential, Phys. Rev. D**91** 023003 (2015).

[111] T. Schaefer and F. Wilczek, Continuity of quark and hadron matter, Phys. Rev. Lett. **82** 3956 (1999).

[112] T. Hatsuda, M. Tachibana, and N. Yamamoto, Spectral continuity in dense QCD, Phys. Rev. D**78**, 011501(R) (2008).

[113] Y. Song and G. Baym, in preparation.